Centrifuge modelling of piled foundations in swelling clays

UNIVERSITEIT VAN PRETORIA
UNIVERSITY OF PRETORIA
YUNIBESITHI YA PRETORIA

Tiago Alexandre Valentim Gaspar

Department of Civil Engineering

University of Pretoria

This thesis is submitted for the degree of

Philosophiae Doctor (Civil Engineering)

November 2020

DECLARATION

I, the undersigned hereby declare that:

- I understand what plagiarism is and I am aware of the University's policy in this regard;
- The work contained in this project report is my own original work;
- I did not refer to work of current or previous students, lecture notes, handbooks or any other study material without proper referencing;
- I have not allowed anyone to copy any part of my project report;
- I have not previously in its entirety or in part submitted this project report at any university for a degree.

Tiago Alexandre Valentim Gaspar
10096401
November 2020

ACKNOWLEDGEMENTS

While I do not believe any PhD gets completed without the help of others, I am of the opinion that I have been particularly fortunate with the support and guidance I have received over the last three years. For this reason, I apologise in advance if this section is slightly longer than is typical.

My supervisor, Professor Jacobsz, gave me the rare opportunity to work on such an incredibly interesting topic, through which I had the chance to interact with countless experienced researchers and practitioners in the field of geotechnical engineering. The reason these acknowledgements include such a diverse range of professionals is because of the opportunities with which Prof. Jacobsz has provided me. In addition to the financial support offered, I also believe that his supervision throughout my masters and doctoral degrees have taught me to be a meticulous and critical thinker. To any students I may supervise in the future who get annoyed with my reviews, my apologies, it's how I was trained, and it's for your own good!

Professor Heymann is known to have contributed significantly to the geotechnical engineering community in South Africa. However, I feel it necessary to highlight here that no number of awards, honours or recognitions will do his contributions justice. As my undergraduate soil mechanics lecturer, Prof. Heymann is, quite frankly, the reason I decided to pursue geotechnical engineering to this extent (and I know many engineers in SA who would share the same sentiment). Despite not 'officially' being my supervisor, our countless discussions on various aspects of this thesis were invaluable to the final product. If I am ever able to inspire young engineers to a fraction of the degree that Prof. Heymann has, I will consider myself lucky.

Working on the Wind Africa research project allowed me to work alongside Dr. Gerrit Smit. It is difficult to properly acknowledge Gerrit in one paragraph, because his contributions to this project covered so many facets. Technically, Gerrit somehow manages to combine the dexterity of an experienced craftsman with an understanding of soils, on par with the top practitioners in the field. Furthermore, I am certain that calmly dealing with many of my

late-night neurotic episodes in the laboratory has granted him sainthood. Following many hours working side-by-side, I have learnt a tremendous amount from Gerrit (including but certainly not limited to geotechnical engineering), and the work presented in this thesis most definitely benefited from his vast expertise. In addition to the professional assistance offered by Gerrit, I am also lucky to have made such a good friend.

Having worked on such an extensively collaborative project, I was fortunate enough to have interacted with a number of researchers from a range of institutions, all of whom contributed to this project. While it is not possible to state their individual contributions here, I would like to express my gratitude to Prof. E. Kearsley, Dr T. Charlton, Prof. A. S. Osman, Prof. D. G. Toll, and Prof. A. Gens. I would also like to thank the following friends and colleagues who proofread parts of this thesis and/or assisted with some laboratory work: Rick Vandoorne, Dr Phia Smit, Hendrik Louw, Paul le Roux and Frans van der Merwe.

I would also like to thank the following friends who offered invaluable moral support throughout this research project: Kim Blakey, Chantel Niebuhr, Tiaan Bosman, Stuart Hofmeyr, Mario Schulz-Poblete, Warren Condon, Bryan Brett, Tyron & Liana Wessels, Dawie Marx, Anton du Preez, Serena Bruni, Michaela Tafani, Kim Wessels, Nikita Andrews, Daniellé Gianico, Jessica Rushton, Miguel Sanches, Sonia Manku, Richard Botha, Shaun Cramer, Megan Weyers, Micia de Wet, André Broekman, Deidre Coghlan and Melanie van Zyl.

Last and foremost, I must thank my mother. My education is always something she has prioritised well above any of her own needs/wants. She has encouraged me throughout my studies and provided me with the moral and financial support necessary to get me to this point. Any work ethic or tenacity I have managed to muster over the past few years, are without a doubt, traits I have learnt from her. I believe this achievement is as much hers as it is mine, and as a result, I am eternally grateful.

Summary

Centrifuge modelling of piled foundations in swelling clays

Tiago Alexandre Valentim Gaspar

Supervisor: Prof. S.W. Jacobsz
Department: Civil Engineering
University: University of Pretoria
Degree: Philosophiae Doctor (Civil Engineering)

In geotechnical engineering, the soil type which has had some of the most severe economic implications is that of swelling clays. Swelling or expansive clays form a subgroup within the field of unsaturated soils which exhibit large volumetric changes upon wetting and drying, thereby causing severe distress to structures. The aim of this study was to use a combination of element testing and centrifuge modelling to investigate certain aspects affecting the behaviour of piled foundations.

To perform the necessary centrifuge modelling, a sample preparation procedure was developed whereby the aim was to prepare samples which retained some degree of fissuring. Samples with such a fabric type facilitate a more rapid ingress of moisture. Element testing was then carried out to investigate any difference in the mechanical or soil water retention properties of the laboratory compacted specimens and undisturbed intact samples. The mechanical properties of primary interest were the pressure required to prevent swell, as well as the clay's heave potential at various applied stresses. The results of the element testing conducted illustrated that the properties of interest remained, for all practical purposes, unchanged between statically compacted and intact undisturbed samples.

Consolidation testing was also performed on various statically compacted and undisturbed samples. Additionally, the intrinsic clay properties were established from a test on a reconstituted specimen and were found to conform well to the framework outlined by Burland (1990). Comparisons of the consolidation tests on statically compacted and undisturbed samples with the reconstituted specimen allowed for soil structure and swell induced-softening to be analysed. This analysis revealed that only undisturbed samples which were inundated at relatively high stresses existed in structure permitted space upon further loading. This result illustrated the effect of swelling on soil structure and highlighted how, for the stress range applicable to this

study, both undisturbed and statically compacted samples exist in permissible stress states after swelling. Furthermore, for samples which had undergone swell, yielding was found to occur at significantly lower stresses than what would be predicted for unstructured soils. More specifically, yielding occurred well within permissible stress space, rather than on the intrinsic compression line defined by the reconstituted consolidation test. This finding is consistent with the swell-induced softening described by the constitutive framework considered in this study.

The centrifuge modelling conducted illustrated that the sample and preparation procedure utilised, facilitated the ingress of moisture, such that a significant magnitude of swell could be achieved within a practical time frame. This allowed for various aspects affecting the performance of piled foundations to be evaluated before (at the clay's in-situ moisture content) and after a targeted value of swell was achieved. A series of 'pull-out' tests were conducted to evaluate the shaft capacity of short length piles at various depths in a clay profile, before and after achieving the targeted swell. The piles used for this evaluation were bored piles manufactured from rapid hardening grout. From this series of testing it was found that on average, the shaft capacity of piles reduced after achieving the targeted magnitude of swell. Exceptions to this trend were found at greater depths in the profile where shaft resistances increased.

A final centrifuge model was conducted to evaluate the development of lateral pressure against a pile throughout a swell process. This test included an aluminium pile anchored at its base, instrumented with lateral load cells. The development of lateral pressures was monitored up until the targeted magnitude of swell was achieved. This test illustrated a distinct initial increase in lateral pressure, followed by a more gradual reduction in pressure as swell progressed. This result helps clarify some discrepancies in the literature on the effect of soil swell on the shaft capacity of piled foundations. If testing is performed fairly early in the swell process where lateral pressures are increasing, it is possible that an increase in shaft capacity will be measured. However, if shaft capacity is assessed at relatively large magnitudes of heave (as was done in this study), reductions in shaft capacity are likely to be measured.

TABLE OF CONTENTS

LIST OF FIGURES

LIST OF TABLES

NOMENCLATURE

Roman Symbols

$\bar{p}$	net-mean stress
$\bar{p}_m$	microstructural net-mean stress
$\bar{p}_o$	net-mean yield stress at suction greater than zero
$\bar{p}_o^*$	net-mean yield stress at suction equal to zero
C_c	compression index
C_c^*	intrinsic compression index
C_e	expansion index
e	void ratio
e_L	void ratio at liquid limit
e_{1000}^*	intrinsic void ratio at 1000 kPa
e_{100}^*	intrinsic void ratio at 100 kPa
F	factor to account for overburden pressure, moisture content and other factors
g	gravitational acceleration at the surface of the earth
h	unit heave
h_m	modified unit heave
K_o	coefficient of lateral earth pressure at rest
N	model scale factor

q	deviatoric stress
R	radius of curvature in simplified Young-Laplace equation
r_1 & r_2	radii of curvature along two orthogonal directions
r_e	effective radius
s	matric suction
S^*	swell
s_m	microstuctural matric suction
s_o	osmotic suction
s_t	total suction
t	thickness of expansive clay layer
T_s	surface tension
u_a	pore air-pressure
u_w	pore water-pressure
w	gravimetric moisture content
W_{LL}	weighted liquid limit
w_L	liquid limit

Greek Symbols

α	contact angle
χ	empirical factor related to degree of saturation and soil type
$\dot{\theta}$	angular velocity
ε_m	microstructural strain
ε_{vm}	microstructural volumetric strain
ε_{VT}	total volumetric strain
ρ_b	bulk density

ρ_d dry density

σ^* Bishop effective stress

σ_v total vertical (overburden) stress

σ'_{vy} effective vertical yield stress

Acronyms / Abbreviations

LC load-collapse yield curve

NL neutral line

PI plasticity index

SI suction-increase yield curve

SWRC soil water retention curve

CHAPTER 1

INTRODUCTION

"The class of unsaturated soil problems involving negative pore-water pressures that has received the most attention is that of swelling or expansive clays."

(Fredlund et al., 2012)

Starting in 1957 with the First Symposium on Expansive Clays held in South Africa, a number of conferences was subsequently held to specifically address the difficulties associated with this problem soil. With the emergence of unsaturated soil mechanics, expansive clays have remained a key topic at conferences held around the world to this day. While unlikely to cause loss of life, the substantial economic implications associated with expansive soils highlights its necessity as an ongoing topic of research. Furthermore, and perhaps more importantly, there is a general need for the outcomes of research to provide practical guidelines to engineers in industry (Day, 2017). The aim of this research is to investigate the performance of piled foundations in swelling clays by means of element testing and centrifuge modelling.

1.1 Background

The presence of swelling clays across the world has had catastrophic economic consequences. Jones & Holtz (1973) stated how in the United States, the damage to infrastructure caused by swelling clays amounts to $2.3 billion each year, more than twice that caused by hurricanes, tornadoes and earthquakes combined. More recent sources have placed this annual expenditure at $13 billion (Puppala & Cerato, 2009) and $15 billion (Jones & Jefferson, 2012). Moving to other regions of the world, similar accounts have been made. In China, annual expenses of $15

billion are incurred due to swelling clay related damages (Miao et al., 2012). Jones & Jefferson (2012) stated how the adverse effect of swelling/shrinking clays is the most damaging geohazard in Britain today. The literature goes on to show how this problem soil has been encountered in almost every continent on earth, as illustrated by Figure 1 and Table 1. The different colours used in Figure 1 are simply to make the different countries more easily distinguishable.

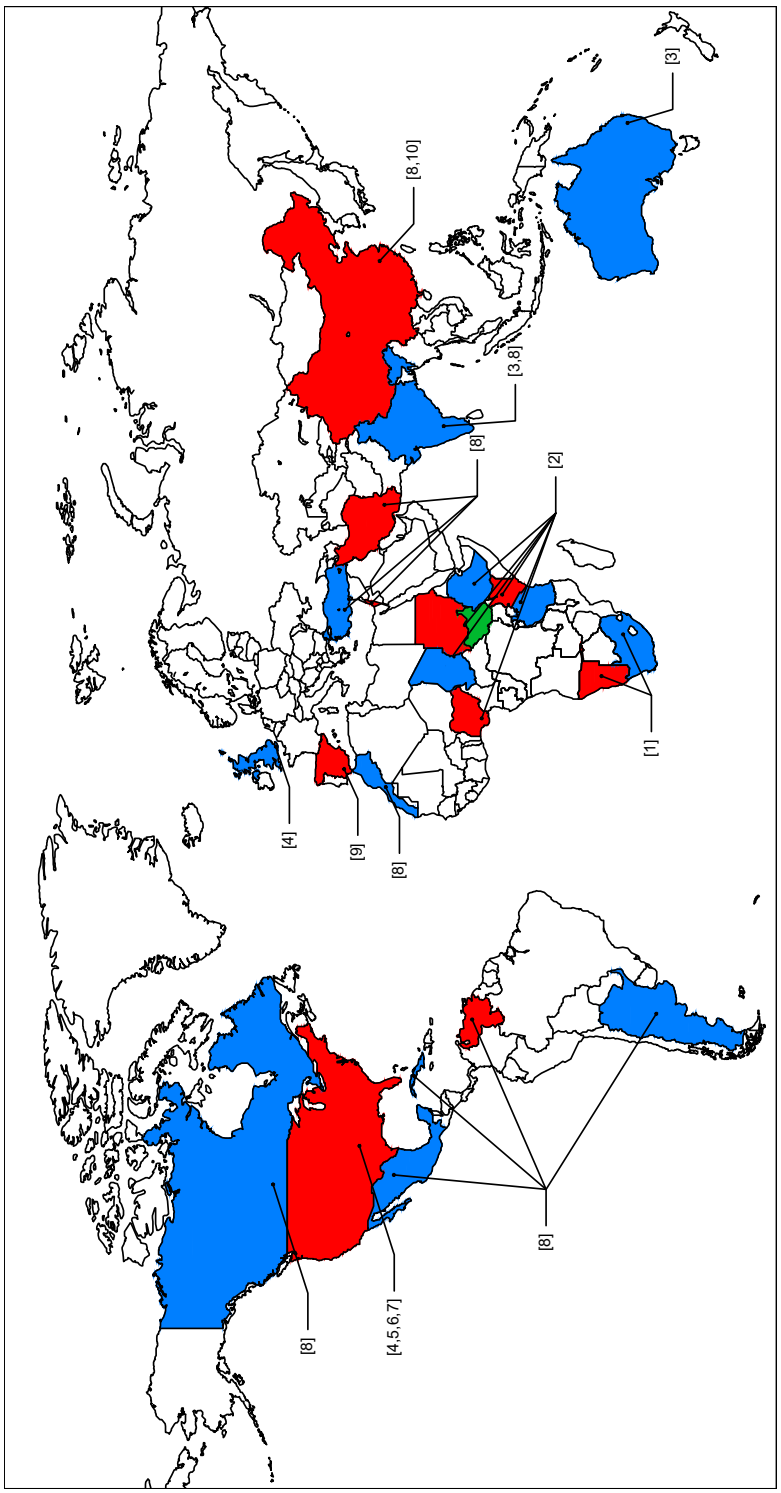

Figure 1: Distribution of expansive clays across the world

Table 1: Worldwide reported occurrences of swelling clays

Label	Reference	Countries
[1]	Williams et al. (1985)	South Africa, Namibia
[2]	Morin (1971)	Central Sudan,[1] Kenya, Tanzania, Chad, Nigeria, Ethiopia, Australia, India, China
[3]	Li et al. (2014)	Australia, India, China
[4]	Jones & Jefferson (2012)	UK, USA
[5]	Puppala & Cerato (2009)	USA
[6]	Jones & Holtz (1973)	USA
[7]	Armstrong & Zornberg (2017)	USA
[8]	Fredlund & Rahardjo (1993)	Canada, China, Cuba, Ghana, India, Iran, Israel, Kenya, Mexico, Morocco, Turkey, Venezuela, Argentina
[9]	Justo et al. (1984)	Spain
[10]	Gu et al. (2010)	China

[1] Now the southern part of Sudan and the Northern part of South Sudan

The world map produced in Figure 1 provides an indication of reported occurrences of swelling clays across the world. While this figure does not indicate the area of coverage within each region, it emphasises how widespread this problem soil is. The references listed in Table 1 present more detailed accounts of these occurrences, however, common to all regions are the severe economic implications of this problem soil.

Proper investigation on the behaviour of swelling clays is however particularly problematic. One difficulty encountered when studying expansive clays is that they tend to occur in a highly fissured state in-situ. For this reason, element testing becomes troublesome since samples which are highly fissured tend to break apart either during sampling on-site, or during extraction in the laboratory. This presents a natural bias towards the testing of stronger, less fissured samples (Thorne, 1984). In addition to soil strength, the hydraulic conductivity of a mass-fissured profile on site will be significantly greater than what is measured in the laboratory. For example, this was observed by Clayton et al. (1995) who noted that gross underestimations of the coefficient of consolidation were obtained from the laboratory testing of fissured clays in comparison to field testing.

For this reason, it can be seen why large-scale field testing for fissured expansive clays is performed (Blight, 1984*a*,*b*; Brackley & Sanders, 1992; Meintjes, 1991; Meintjes & Pellissier, 1994). However, such studies are both costly and time consuming, with some lasting many years. A particularly extreme example of such a full-scale test was reported by Williams (1991) where heave continued for a period of 10 years. Centrifuge modelling provides geotechnical researchers with a compromise between the carefully controlled boundary conditions possible in element testing, and the ability to model large-scale problems which are more typical of that encountered in practice. Furthermore, centrifuge modelling allows for seepage and diffusion processes (e.g. consolidation and swelling) to be investigated in a significantly shorter time-frame than what would be required for the corresponding full-scale test. While geotechnical modelling is an area of research where substantial developments have taken place over the last several decades, its applicability to expansive clays have not been fully exploited. This statement is supported by the fact that, at the last three International Conferences on Physical Modelling in Geotechnics (ICPMGs), a mere three publications investigated swelling clays despite the economic implications of this problem soil.

When designing foundations on expansive soils, arguably the most commonly adopted engineering solution for foundation design are stiffened raft foundations (Byrne et al., 2019; Charlie et al., 1985; Li et al., 2014; Pellissier, 1997). Such foundation types are typically used for lighter structures and in cases where a certain degree of foundation movement is tolerable. However, for major structures, or in cases where it is critical to restrict ground movement, piled foundations are utilised. Examples include certain structures in coal power stations (Blight, 1984*a*) or wind turbines. There are however discrepancies in the literature as to the effect of soil swell on the shaft capacity of piled foundations. Blight (1984*a*) found an increase in shaft capacity after swell and attributed this finding to an increase in lateral pressure. Conversely, Elsharief et al. (2007) found a reduction in shaft capacity after prolonged wetting.

It is therefore the aim of this study to utilise element testing, the principles of unsaturated soil mechanics and centrifuge modelling to investigate certain factors affecting the behaviour of piled foundations.

1.2 Study objectives

While there are many design approaches which can be utilised for construction on swelling clays, the primary aim of this thesis can be stated as follows.

Investigate factors affecting the performance of piled foundations by means of physical modelling in a geotechnical centrifuge, with specific emphasis on factors such as shaft capacity and lateral induced swell pressures.

This aim of this study can be subdivided into the following objectives.

- Develop a sample preparation procedure that can be used to produce closely fissured samples for use in centrifuge modelling.
  - The preparation procedure should produce samples which possess similar swell characteristics in comparison to undisturbed specimens.
- Evaluate the effect of the swelling process on the pull-out (shaft) capacity of piled foundations.
- Determine whether there is a dependency of pile depth on the measured shaft capacity after achieving a targeted amount of swell.
- Gain a better understanding of the mechanisms controlling the shaft capacity of piled foundations throughout the swell process.

1.3 Scope of work

The aim of this study was to investigate certain factors affecting the behaviour of piled foundations in swelling clays. This was achieved by a combination of element testing and centrifuge modelling. The scope of this study can be outlined as follows:

- Element testing carried out was aimed at quantifying the following parameters for statically compacted and undisturbed specimens.
  - Swell magnitude at various applied stresses.
  - The magnitude of pressure required to prevent swell (i.e. the swelling pressure).
  - The soil water retention properties of the soil.
  - The differences in soil structure between compacted and undisturbed samples.
- For all centrifuge modelling, initial sample properties (i.e. moisture content and void ratio) were targeted to be representative of field conditions. Furthermore, for all instances

where features were investigated after allowing swell to occur, the same amount of swell was targeted. The targeted amount of swell was that predicted by Van der Merwe (1964) for a clay of *very high potential expansiveness*. By keeping initial and 'swelled' conditions consistent between tests, meaningful comparisons could be made. The centrifuge modelling performed was aimed at addressing the following aspects:

  - Soil swell in the geotechnical centrifuge under greenfield conditions.
  - Change in pull-out capacity of piles at the clay's initial 'in-situ' moisture content and after achieving the targeted swell.
  - The variability in pull-out capacity at various depths was investigated both under in-situ conditions and after reaching the targeted swell.
  - The change in lateral pressure against a pile throughout the swell process.

The limitations of this study can be stated as follows:

- Only one clay type was considered.
- For all centrifuge testing, swell was induced by flooding the soil profile from the bottom of the model. Infiltration from the top of the profile to simulate infiltration due to precipitation was not considered.

1.4 Methodology

The approach followed for this study is outlined below.

- A literature review was conducted to examine the current state of knowledge on unsaturated soils, expansive clays and centrifuge modelling.
- Element testing was used to evaluate various properties of the compacted fissured material.
  - The purpose of the element testing was to evaluate any differences in swell magnitude, swell pressure, soil water retention properties, or soil structure between the laboratory prepared specimens and undisturbed samples.

- Centrifuge modelling was conducted at a centrifugal acceleration of 30 g to assess the following aspects.
  - Swell in the geotechnical centrifuge under greenfield conditions
  - The shaft capacity of piles was assessed by conducting pile pull-out tests. These tests were conducted on short length piles installed at various depths, both at the soil's in-situ moisture content and after achieving the targeted swell.
  - The variation in lateral pressure against a pile shaft was investigated using an aluminium pile instrumented for this purpose.
- The element testing and centrifuge modelling conducted were jointly interpreted using the principles of unsaturated soil mechanics and a constitutive framework for expansive clays developed by Gens & Alonso (1992).

1.5 Layout of thesis

The layout of this thesis is as follows:

- Chapter 1 provides an introduction to this thesis.
- Chapter 2 presents a background on the fundamentals of unsaturated soil mechanics and the measurement of soil suction.
- Chapter 3 presents a background on expansive clays as a subgroup of the larger field defined by unsaturated soils. The chapter begins by addressing the mineralogical mechanisms which characterise swelling clays. A conceptual background is provided on a constitutive framework used for the numerical modelling of swelling clays. The chapter goes on to describe conventional testing procedures for swelling clays as well as empirical approaches used to estimate heave in geotechnical practice. The chapter is then concluded with a brief description of various construction methods employed when swelling clays are present.
- Chapter 4 presents a background of centrifuge modelling.
- Chapter 5 describes the experimental procedure followed.
- Chapter 6 presents a discussion of the results of the element testing performed.

- Chapter 7 presents a discussion of the results from the centrifuge modelling.
- Chapter 8 contains the conclusions of the study as well as recommendations, both for further research and for the practising engineering community.

CHAPTER 2

BACKGROUND ON UNSATURATED SOIL MECHANICS

Within the study of soil mechanics, the oldest and most well understood field is that relating to saturated soils. However, over the past few decades it has become increasingly recognised that the assumption of a soil to be fully saturated in practice, is very often not applicable. This has led to a surge in the research of unsaturated soil mechanics. Unsaturated soils are associated with many behavioural complexities and pose many difficulties in the measurement of the necessary stress-state variables, both in-situ and in the laboratory. With technological advancements and the development of specialised measuring equipment, a better understanding of unsaturated soils has been gained over the years. The understanding of the hydraulic and mechanical behaviour of unsaturated soils does however, not approach that achieved for saturated soils, leaving considerable scope for research.

The aim of this chapter is to provide a review of past and present research on unsaturated soils. The chapter begins with a background on some fundamental properties, namely surface tension and soil suction. This is followed by a description of one of the most fundamental relationships in unsaturated soil mechanics, namely, the soil water retention curve (SWRC). The SWRC describes the relationship between soil suction and moisture content. A discussion is then presented on the stress state variables necessary to fully describe the behaviour of partially saturated soils. The chapter concludes with a description of various methods that can be used to measure soil suction.

2.1 Surface tension and soil suction

Whilst it is certainly possible for soil suction and surface tension to be present when a soil is fully saturated, as will be discussed later in this chapter, these two phenomena are more typically associated with partially saturated soils. In this case of partially saturated soils, free air and water exist simultaneously in the soil matrix. The purpose of this section is to provide an overview of the mechanisms associated with surface tension and total soil suction, where total suction is the sum of matric and osmotic suction as illustrated by Equation 1. The nomenclature used in this equation follows that proposed by Gens (2007).

$$s_t = s + s_o \tag{1}$$

Where:

s_t = total suction (kPa)
s = matric suction (kPa)
s_o = osmotic suction (kPa)

2.1.1 Surface tension

To understand the concept of surface tension, it is useful to consider the air-water interface at a molecular level. At the meniscus, mechanical equilibrium is achieved through a balance of intermolecular forces in the air phase, intermolecular forces in the water phase and an additional component referred to as surface tension (Lu & Likos, 2004). Surface tension is often defined as the maximum energy level a fluid can store without breaking apart (Lu & Likos, 2004). As a result, surface tension is often defined by units of joules per square metre (J/m^2), or by a force per unit length i.e. Newtons per metre (N/m) with the two units being equivalent.

A rigorous explanation of how surface tension manifests itself at the molecular level was provided by Sophocleous (2010). A brief summary of this explanation is provided in the following paragraph and in Figure 2. Firstly, it should be recognised that molecules in a fluid experience equal attractive and repulsive forces in all directions, with attractive forces predominating. As a result, a molecule within the bulk of a fluid (Molecule A in Figure 2) will have a potential energy of zero (Sophocleous, 2010). At an air-water interface however, molecules in the meniscus (Molecule B) will have fewer neighbouring molecules in the gaseous phase above it. This is due to the fact that the density of air is substantially less than that of

water. For this reason, a molecule in the meniscus will experience a net downward pull towards the bulk of the fluid. For mechanical equilibrium to be achieved, this force is balanced by the presence of surface tension.

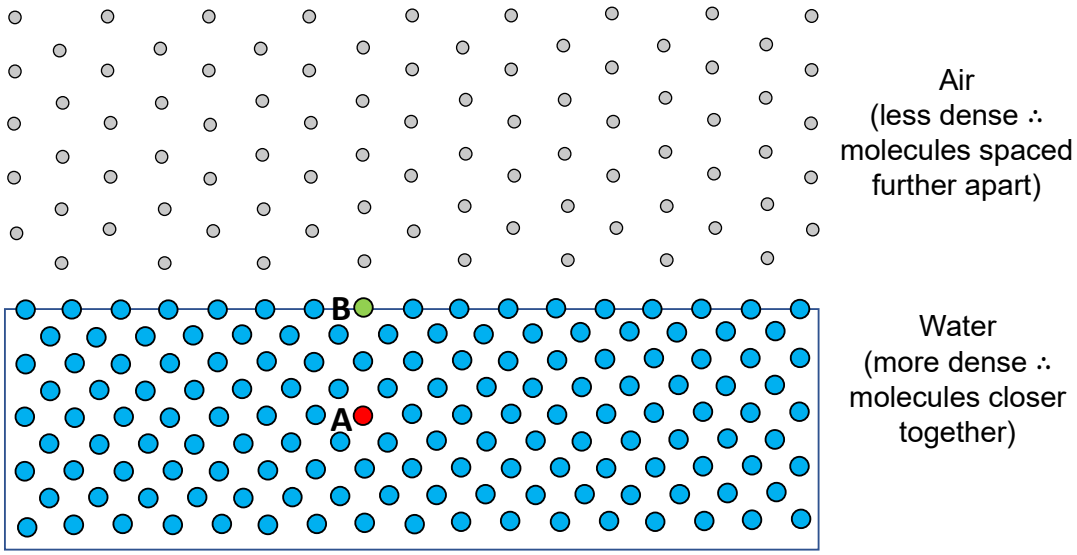

Figure 2: Interaction between liquid and gaseous phases

2.1.2 Matric suction

In the previous section it was stated how the difference in pressure across the air-water interface is related to the surface tension of the meniscus. While the term matric suction is sometimes extended to include the effects of short-range adsorption (Lu & Likos, 2004), it is more common to simply define matric suction as the difference between pore-air and pore-water pressure as illustrated in Equation 2.

$$s = u_a - u_w \tag{2}$$

Where:

s = matric suction (kPa)
u_a = pore-air pressure (kPa)
u_w = pore-water pressure (kPa)

The magnitude of matric suction is directly related to the geometry of the air-water interface. This relationship is defined by the Young-Laplace equation for a three-dimensional meniscus as illustrated in Equation 3.

$$(u_a - u_w) = T_s \cdot cos\alpha \cdot \left(\frac{1}{r_1} + \frac{1}{r_2}\right) \tag{3}$$

Where:

T_s = surface tension (N/m)
α = contact angle (°)
r_1 & r_2 = the radii of curvature along two orthogonal directions (m)

For unsaturated soils, the contact angle represents the angle through the liquid phase between a line tangent to the air-water interface and a line defined by the water-solid interface as illustrated in Figure 3 (Lu & Likos, 2004). From Equation 3 it can be seen that the radius of curvature is inversely proportional to the magnitude of suction. Therefore, for a value of $s = 0$, the radius of curvature will tend towards infinity, corresponding to a perfectly flat air-water interface.

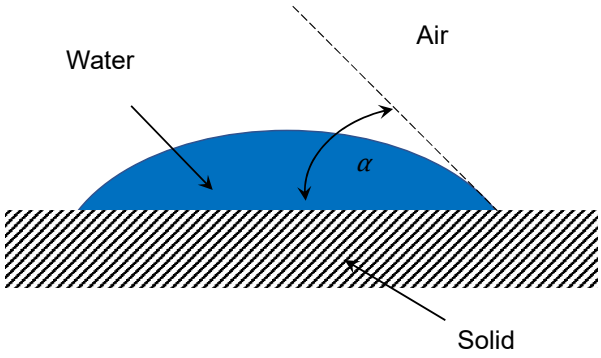

Figure 3: Graphical illustration of the contact angle between an air-water-solid system

In describing the effect of pore size on the magnitude of matric suction in unsaturated soils, it is useful to consider pores as capillary tubes. The height of water rise within the capillary tube is then taken to be analogous to the magnitude of matric suction. This is commonly known as capillary theory and can be represented by a simplified version of the Young-Laplace equation where $r_1 = r_2 = R$, and the contact angle is assumed equal to zero as illustrated in Equation 4 (Toll, 2012).

$$(u_a - u_w) = \frac{2T_s}{R} \tag{4}$$

The assumption of contact angle equal to zero is generally valid for a soil undergoing drying. However, for a wetting interaction most soils exhibit contact angles considerably greater than zero (Lu & Likos, 2004). Despite this limiting assumption, capillary theory is useful in illustrating how the magnitude of matric suction that can be sustained in an unsaturated soil increases as pore sizes reduce. Figure 4 illustrates the values of matric suction predicted by capillary theory, along with measured values of suction. The data points included in Figure 4 have been taken from a study reported by Jones & Kohnke (1952).

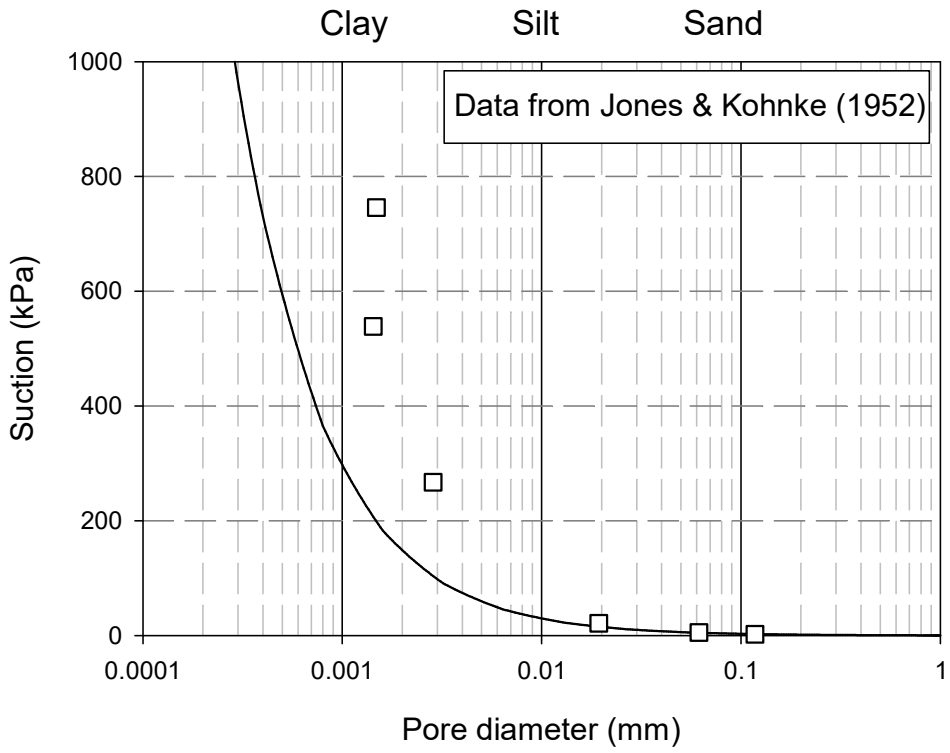

Figure 4: Relationship between pore size and matric suction (after Toll, 2012)

2.1.3 Osmotic suction

While matric suction arises due to the difference in pressure across the air-water interface, osmotic suction is driven by the difference in salt concentrations within soil water. Considering that water is attracted to dissolved solutes, soil-water tends to move from a position of low ion concentration to an area of high ion concentration (Radcliffe & Šimůnek, 2010). This property can be illustrated by considering two sections of a container separated by a semipermeable membrane, allowing only pure water to pass through it as shown in Figure 5.

In Figure 5, the right side of the container is filled with pure water while the left side contains dissolved salts. The presence of the semipermeable membrane in the centre of the container facilitates pure water to pass through it, but restricts movement of salts. As a result, the attraction of pure water to dissolved salts will cause a migration of pure water to the left side of the container, ultimately resulting in an increase in pressure denoted by the change in hydraulic head, h. This pressure build-up is referred to as osmotic pressure.

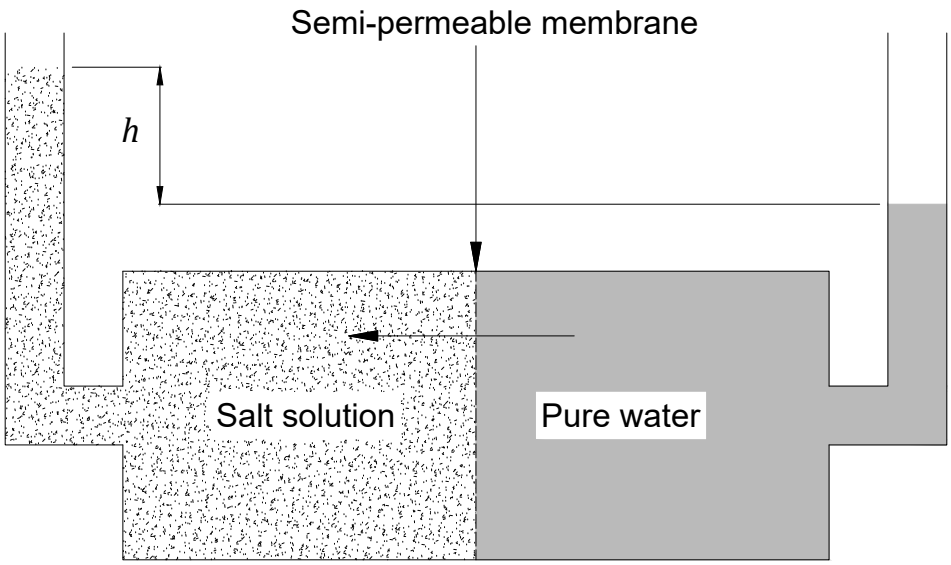

Figure 5: Graphical illustration of osmotic suction (after Radcliffe & Šimůnek, 2010)

2.2 Soil water retention curve (SWRC)

Perhaps the most useful tool in the description and implementation of unsaturated soil mechanics is the SWRC. In simple terms the SWRC provides the relationship between soil suction and soil moisture content. While this relationship is sometimes referred to as the soil water characteristic curve (SWCC), the relationship is dependent on factors such as initial void ratio. For this reason, the relationship is not characteristic of the soil and as such, the term SWRC is preferred (Toll, 2012). In a series of honorary and special lectures over the past few decades, Professor Delwyn Fredlund, a respected figure in the field of unsaturated soil mechanics has emphasised its importance. Below are references to the aforementioned lectures, along with some key quotations.

17th Jennings Lecture - The 17th African Regional Conference on Soil Mechanics and Geotechnical Engineering (2019)

Determination of unsaturated soil property functions for engineering practice

"...key to its [unsaturated soil mechanics] implementation... based on the soil-water characteristic curve"

Special lecture: The 7th International Conference on Unsaturated Soils (2018)

Role of the soil-water characteristic curve in unsaturated soil mechanics

"... SWCC, has been referred to as the key to the implementation of unsaturated soil mechanics into geotechnical engineering practice."

The R.M. Hardy Lecture (2000)
The implementation of unsaturated soil mechanics into geotechnical engineering
"... use of the soil-water characteristic curve has been shown to be the key to the implementation of unsaturated soil mechanics."

The Fourth Spencer Buchanan Lecture (1996)
The emergence of unsaturated soil mechanics
"The soil-water characteristic curve has been shown to be a key soil function which can be used to approximate the behaviour of unsaturated soils."

As can be seen from the above references, it becomes clear that a wealth of information is held in the relationship between moisture content and soil suction. Figure 6 illustrates a typical example of the soil water retention curve (SWRC). It is worth noting that osmotic suction should remain constant across the full range of degrees of saturation provided that the concentration of dissolved solutes remains constant within the soil water (Lu & Likos, 2004). It is also common to plot values of total and matric suction on the same set of axes as has been described by Fredlund (2019). For this reason, the general term 'soil suction' has been used to denote the horizontal axis on Figure 6.

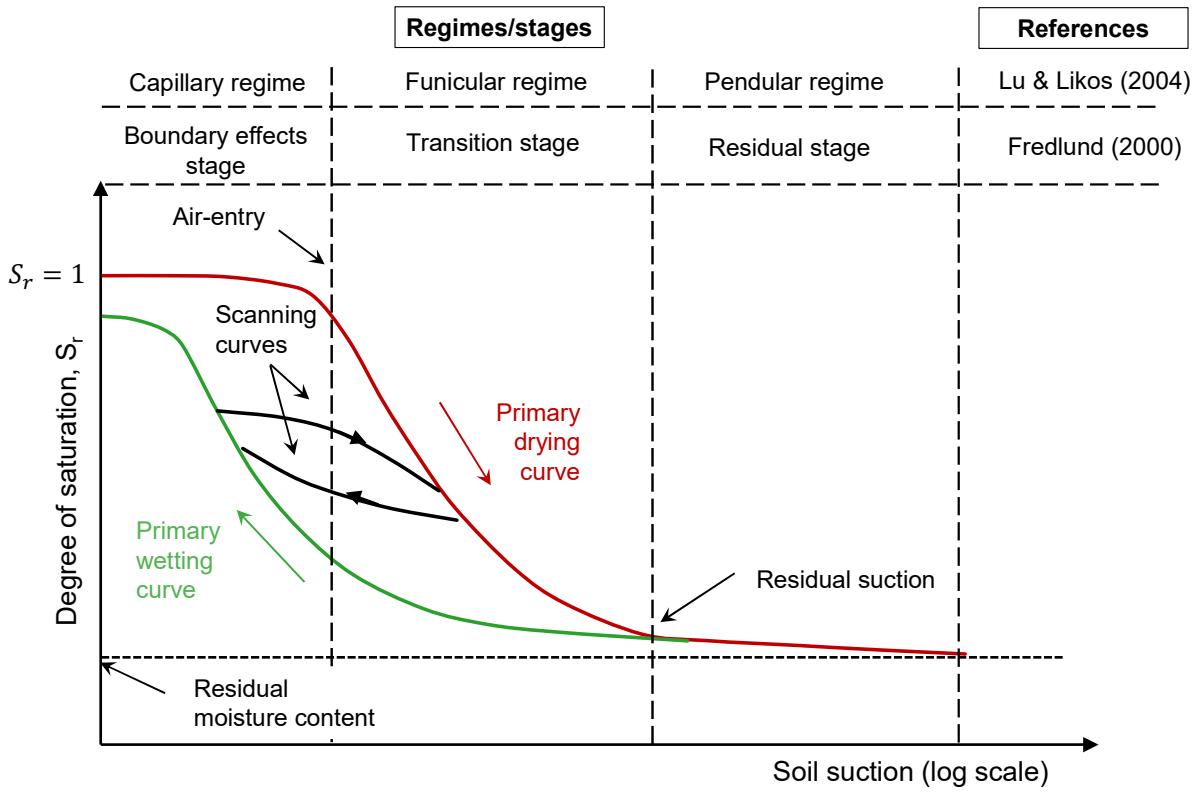

Figure 6: Typical soil water retention curve

If a sample (originally at $S_r = 1$) with no suction is allowed to dry out, it will initially experience an increase in suction without decreasing saturation. The point at which air begins to enter the soil matrix is defined as the air-entry value. Following air-entry, the soil will begin to desaturate until the residual moisture content and residual suction of the soil are achieved. This is a point on the SWRC where the measured curve will approach an asymptotic value of saturation. In this region, a small change in moisture content will lead to disproportionately large changes in suction. If a soil is wetted from its residual moisture content, a primary wetting curve will be observed. While the shape of the primary wetting curve is similar to the drying curve, it plots below the primary drying curve illustrating how, for a given value of moisture content, suction will be less in a soil undergoing wetting. Furthermore, it can be seen that the sample often does not reach full saturation again. This can be attributed to air-entrapment or to irrecoverable shrinkage of the soil (Toll, 2012).

Provided measurements are conducted on a reconstituted sample, the bounding primary drying and wetting curves define an envelope of possible states within which a soil can exist (Toll, 2012). However, if a wetting or drying process is stopped and reversed partway, a

scanning curve (at a flatter slope) will be followed until the corresponding bounding curve is reached (Al Haj & Standing, 2016; Toll, 2012). Examples of scanning curves are included in Figure 6. It should be noted that for the majority of cases, soils encountered in practice lie on one of these scanning curves.

It is also common to divide the SWRC into different regimes or states, depending on the state of soil water within the matrix. Definitions provided by different authors have been illustrated in Figure 6, but for this thesis, those proposed by Lu & Likos (2004) will be used. The capillary regime refers to the portion of the SWRC where suction is developed at, or close to, full saturation. Within this regime, the effects of surface tension are predominantly present at the boundary of the soil mass.

Once air enters the soil matrix, it transitions into the funicular regime. In the funicular regime, liquid bridges can connect adjacent particles resulting in both suction and surface tension contributing to interparticle attraction (Schubert, 1975). Another useful characteristic of this portion of the curve is that it is related to the particle size distribution of the soil. For a fairly uniformly graded soil, the slope will tend towards verticality with a change in moisture content leaving the magnitude of suction almost unaffected. For a well-graded soil, the slope of the funicular regime will reduce (Lu & Likos, 2004).

As the soil proceeds into the pendular regime at the residual moisture content of the soil, the water phase becomes discontinuous except for thin films surrounding individual soil particles (Kim & Hwang, 2003; Lu & Likos, 2004). The dominant mechanism of suction around its residual moisture content is the short-range adsorption effects between the discontinuous water phase and the surfaces of soil solids (Lu & Likos, 2004). A graphical illustration of the soil matrix at different moisture regimes is provided in Figure 7. This figure was produced on the assumption of spherical particles.

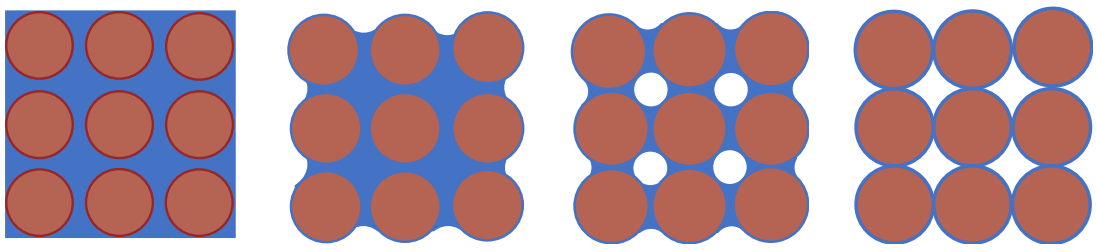

(a) (b) (c) (d)

Figure 7: Graphical illustration of different moisture regimes where a) $s = 0$ in the capillary regime, b) $s > 0$ in the capillary regime, c) the funicular regime and d) the pendular regime

In Figure 7 a), the soil is fully saturated with suction equal to zero, as is evident by the perfectly flat menisci. In Figure 7 b), curvature begins to develop in the menisci along the boundaries of the soil mass indicating that the pore water pressure has become negative. Thereafter, air-entry occurs, and the soil moves to the funicular and pendular regime in Figure 7 c) and d) respectively.

What is particularly interesting about the SWRC is that it illustrates how negative pore pressures can still be present in a soil before it begins to desaturate. This has led to recent publications (Fredlund, 2019) arguing that unsaturated soils should be defined in terms of stress state (i.e. the presence of negative pore-water pressure) rather than the amount of air or water existing in the voids.

However, an argument can be made that the original definition of an unsaturated soil to include the presence of free air within the soil matrix is more linguistically intuitive. The prefix "un", in the phrase unsaturated soils implies that the soil is *not* saturated. The same is true of the other commonly used term, *partially* saturated. Considering that the definition of soil saturation has been well established in the field of soil mechanics over the last century, this change in definition could lead to unnecessary confusion. Furthermore, it is also possible for positive pore water pressure to be present in a soil containing both water and air in its matrix. This is the basic concept used in the commonly used axis translation technique. It is therefore rather proposed that practitioners and researchers are aware that negative pore pressures can exist at full saturation. It can also be seen from Figure 6 that across the full spectrum of possible soil states, full saturation constitutes only a small portion. For this reason, it is proposed that the concepts relating to saturated soil mechanics be considered a special and simplified case of soil mechanics as a whole. This is in contrast to the prevailing view that unsaturated soils are the exception within the greater field of soil mechanics.

An argument for the SWRC being the cornerstone to the implementation of unsaturated soil mechanics is that from it, many soil parameters can be estimated as a function of soil suction. Fredlund (2019) gave practical guidelines on how to derive functions relating, hydraulic conductivity, water holding capacity and shear strength, to soil suction. It should be noted that while shear strength is often the soil parameter most emphasised by practitioners, the hydraulic conductivity of a soil can drop several orders of magnitude as it begins to desaturate, as illustrated by Fredlund (2019). Its relation to all these soil parameters is due to the fact that matric suction is an important stress state variable which largely governs the behaviour of unsaturated soils.

2.3 Stress state variables for unsaturated soils

The principle of effective stress as defined by Terzaghi (1936) lies at the foundation of most modern soil mechanics theory and practice (Jennings & Burland, 1962). It has also been regarded as the single most valuable contribution to the understanding of saturated soil mechanics (Atkinson & Bransby, 1978). Being more than just an indication of saturated soil strength, the concept of effective stress allows the behaviour of a soil to be fully defined in terms of one stress variable. In his original publication, Terzaghi (1936) stated how:

"All measurable effects of a change in stress, such as compression, distortion and a change of shearing resistance, are exclusively due to changes in effective stress".

This elegant stress state variable provided the impetus for researchers of unsaturated soils to adopt a similar concept which could fully define the behaviour of unsaturated soils. Jennings (1957), Croney et al. (1958), Bishop (1959) and Aitchison (1960) were some of the first to investigate such an approach. However, following a discussion between researchers at the Conference on Pore Pressure and Suction in Soils (1960), it was agreed that the model proposed by Bishop (1959) was the most general, owing to the inclusion of a term for the pressure in the gas phase (Jennings & Burland, 1962). The expression proposed by Bishop (1959) is provided in Equation 5.

$$\sigma^* = \sigma + \chi(u_a - u_w) - u_a \tag{5}$$

Where:

σ^* = Bishop effective stress (kPa)
σ = Total normal stress (kPa)
u_a = Pore-air pressure (kPa)
u_w = Pore-water pressure (kPa)
χ = Empirical factor related to degree of saturation and soil type (Bishop & Blight, 1963)

Soon after its publication, the Bishop stress approach was scrutinised. Standing (2012) stated how Bishop himself recognised some of the shortcomings of Equation 5 as an effective

stress principle after a series of experimental programmes (Bishop et al., 1960). However, a publication by Jennings & Burland (1962) conclusively illustrated how Equation 5 failed to predict volume change (particularly collapse) relationships for unsaturated soils. In this publication, a series of oedometer tests were presented. One set involved soaking a sample in the oedometer under a constant applied stress. In such cases, a reduction in suction would have taken place, thus reducing the Bishop or 'effective stress', and according to effective stress theory, an increase in volume should have been observed. Conversely, collapse of specimens was measured during this process, directly contradicting the predictions of the effective stress principle.

A second set of tests were conducted where a partially saturated sample was placed in an oedometer and soaked. An effort was then made to keep the volume of the sample constant by adjusting the applied vertical stress. According to effective stress theory, a reduction in matric suction would have necessitated an increase in applied pressure to maintain constant volume. It was however observed that a *decrease* in applied vertical pressure was required, again directly contradicting predictions made by effective stress theory.

In a follow up publication by Bishop & Blight (1963) it was recognised that two stress paths relating to net stress $(\sigma - u_a)$ and matric suction $(u_a - u_w)$ need to be accounted for separately. The importance of accounting for these two stress state variables was particularly emphasised for the predictions of stress-volume changes. Conversely, it was found that the 'effective' or Bishop stress approach was more accurate in the prediction of shear strength. Its usefulness in this regard has led to more recent publications replacing the χ parameter with degree of saturation (Bolzon et al., 1996) or the ratio of air-entry value to matric suction (Khalili & Khabbaz, 1998). In doing so, the aforementioned authors have avoided the use of the difficulties associated with the χ parameter.

Bishop & Blight (1963) recognised how the empirical factor χ was different for shear strength and volumetric change, further illustrating limitations in the use of a single 'effective stress' approach for unsaturated soils. Further work by Fredlund & Morgenstern (1977) stated how such a parameter was "essentially impossible" to determine uniquely and provided a theoretical justification for the use of the two stress state variables (net stress and matric suction). It is on the basis of these two stress state variables that the most progress in the constitutive modelling of unsaturated soils has taken place over the last few decades (Standing, 2012).

2.4 Measurement of soil suction

The testing of unsaturated soils is substantially more complex compared to the testing of saturated soils. This can be attributed to two factors, firstly, the soil-water pressure in unsaturated soils is generally negative, which is significantly more difficult to measure than positive pore-water pressure (Standing, 2012). Additionally, due to the inclusion of free-air in the soil matrix, volumetric measurements become problematic. This can be attributed to the fact that the change in volume of a sample is no longer simply due to migration of water into or out of the sample, but also to the compressibility of air (Standing, 2012). Volumetric measurements of unsaturated soils require innovative solutions particularly for triaxial testing.

The aim of this section is to discuss the measurement equipment and techniques that can be used to measure and control soil suction. Details are only provided for techniques used in this study. Considering that the quantification of soil strength was not within the scope of this thesis, no background has been provided on triaxial testing.

2.4.1 General approaches to the measurement of soil suction

In both Sections 2.2 and 2.3, the importance of soil suction on the behaviour of unsaturated soils was emphasised. While Section 2.3 (discussion on stress state variables) specifically emphasised matric suction, it is common to measure total suction in the high suction range and plot the two components on a single SWRC as the general term soil suction. This is due to the fact that new technology makes it significantly easier to measure total suction in the high suction range. The inconsistency of plotting two different components of soil suction on an SWRC does not appear to create significant difficulties in geotechnical engineering (Fredlund, 2019). Furthermore, at lower moisture contents the effects of osmotic suction are said to be small (ASTM D6836–16, 2016). Figure 8 illustrates various types of measurement techniques that are commonly used to measure soil suction. The figure was taken from Toll (2012). However, where measurement ranges have been modified, and where instrumentation has been added, additional references have been included. These references have been provided in Table 2.

When considering Figure 8, it should be borne in mind that the material considered in this study was a highly expansive clay with a high montmorillonite content. Such a soil has the potential to sustain high values of suction in-situ, thus making many of the commonly used methods mentioned above unusable. Following site investigations, after both the wet and dry seasons, suction measurements conducted using the filter paper technique revealed that the

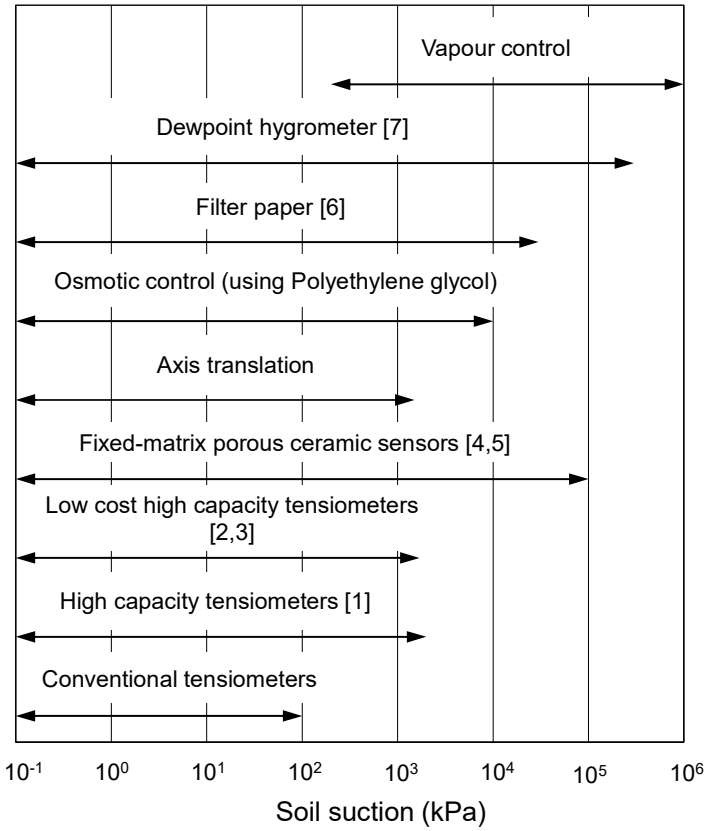

Figure 8: Various suction measurement techniques and their associated measurement ranges (after Toll, 2012)

Table 2: Reference list for suction measurement devices

Reference number	Reference
[1]	Lourenço et al. (2006)
[2]	Jacobsz (2018)
[3]	Jacobsz (2019)
[4]	Metergroup (2017*a*)
[5]	Tripathy et al. (2016)
[6]	Al Haj & Standing (2016)
[7]	Metergroup (2017*b*)

average matric suction of undisturbed samples was approximately 2.5 MPa. It can be seen from the outset that this magnitude of suction rules out many of the commonly used options listed in Figure 8. For this reason, only the measurement techniques used in this study are discussed in the sections that follow, namely the filter paper method, the dewpoint hygrometer and the fixed

matrix porous sensor. Other approaches, and practical combinations of techniques to measure SWRCs across the full range of suction are provided by Gaspar et al. (2019*a*).

2.4.2 The filter paper method

Arguably the oldest and simplest approach to the measurement of soil suction is the filter paper approach. Developed in the agricultural field by Gardner (1937), the technique allows both matric and total suction to be measured. The basic concept of this technique is that moisture is allowed to transfer between the soil sample and a piece of calibrated filter paper. Once suction equilibrium is achieved, the moisture content of the filter paper is related to soil suction based on calibration curves previously established in the literature (ASTM D5298–16, 2016; Chandler & Gutierrez, 1986; Hamblin, 1981) or by a batch specific calibration performed by the user. In this study, Whatman No. 42 filter paper was used.

If the hydraulic equilibrium between the sample and filter paper occurs through the liquid phase via direct contact between the soil sample and filter paper, matric suction is measured. If however, hydraulic equilibrium occurs through the vapour phase (non-contact approach) then total suction will be measured. In either case, the soil specimen and filter paper are kept inside a sealed environment to avoid moisture loss, as illustrated in Figure 9. Once either the matric or total suction has been measured, the sample can be weighed, and its moisture content calculated. This will need to be repeated several times at different moisture contents to obtain a complete SWRC.

While this technique is useful and has a wide measurement range, one drawback of the approach is the time taken for one measurement. ASTM D5298–16 (2016) recommends a period of 7 days for the equilibration period. If suction is to be measured at a range of different moisture contents, this approach can become cumbersome and time consuming. For this reason, filter paper measurements were only used in this study in two cases:

1. To determine the in-situ matric suction of block samples after wet and dry seasons.
2. To determine the initial matric suction of centrifuge specimens prior to testing.

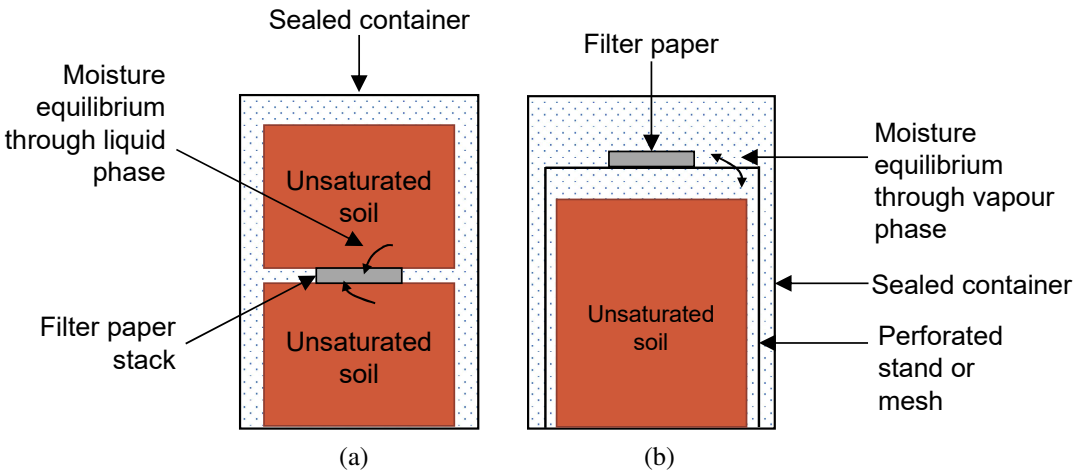

Figure 9: Graphical illustration of the a) contact and b) non contact filter paper method

2.4.3 Dewpoint hygrometer

The dewpoint hygrometer, or chilled mirror hygrometer as it is sometimes referred to, provides an advantage over the filter paper method since it allows a single reading to be taken within a matter of minutes (≈15 minutes). While the approach can only measure total suction, it has a practical working range of 300 MPa (10 times that of the filter paper approach). The method is based on the concept of the thermodynamic relationship between total suction and relative humidity. The method involves placing a small specimen inside a sealed chamber with an exposed mirror inside it. The temperature of the mirror is slowly lowered until such point that condensation occurs on the mirror. The dewpoint and temperature in the chamber at that instant is then used to determine the relative humidity above the sample which, at temperature equilibrium, is a direct measurement of soil suction (Metergroup, 2017*b*). As for the filter paper approach, mass readings will need to be carried out for each suction reading to determine the corresponding moisture content.

One issue with this approach is the small sample size utilised (≈ 10 cm^3). The use of such a small sample becomes problematic since any loss of solids during the measurement of an SWRC will significantly affect the calculated moisture content. This is particularly a concern when volumetric readings need to be taken of the sample (discussed by Gaspar et al. 2019*a*). The importance of recording volumetric changes in soil samples during the measurement of an SWRC was emphasised by Toll et al. (2015). Despite this limitation, given meticulous implementation, the method is still useful owing to its short measurement time and wide measurement range. For this study, the dewpoint hygrometer approach was used to measure the primary drying and wetting curves for several SWRCs.

2.4.4 The fixed-matrix porous ceramic sensor

Of the measurement techniques listed in Figure 10, this is perhaps the newest commercially available sensor. To the author's knowledge, at the time of writing, there are only two publications investigating its usage (Karagoly et al., 2018; Tripathy et al., 2016). The sensor operates on the principle of hydraulic equilibrium. If two materials are initially at different energy states, i.e. different pressure heads or water potentials, water will flow from the material with the highest energy state to that of the lowest (Fredlund et al., 2012). This will occur until equilibrium is achieved. At equilibrium, the water potential (or suction) will be the same in both materials. For this reason, if a material with known water retention properties is placed in contact with soil, after equilibrium has been reached, the suction can be measured. This is a concept that has been employed for many years in electrical conductivity sensors, moisture blocks and thermal conductivity sensors (Tripathy et al., 2016).

For the fixed-matrix porous ceramic sensor depicted in Figure 10, the ceramic discs have known water retention properties and a dielectric constant of 5 (Metergroup, 2017*a*)[1]. When placed in contact with a soil, moisture will be transferred between the soil and the discs until equilibrium is achieved. The change in moisture content of the ceramics resulting from this transfer of water will act to change the dielectric permittivity of the discs. This change will allow the moisture content of the discs to be ascertained, and then, through a predetermined SWRC on the ceramic discs, a value of matric suction can be inferred. It was decided that this sensor would be used for centrifuge testing, owing largely to its wide measurement range (9 kPa–100 000 kPa) (Metergroup, 2017*a*). Since it is the relationship between suction and water content that is important in the understanding of unsaturated soil mechanics, this suction sensor was used in conjunction with a volumetric water content sensor based on capacitance/frequency domain technology. This technology is well established in the field of geotechnical engineering and agricultural sciences. As such, it is not described further in this thesis. Details of installation procedures have however been provided in Section 5.4.

[1]This is the date when the sensor was purchased and the "Teros 21 integrator guide" downloaded. No date is however mentioned in this documentation

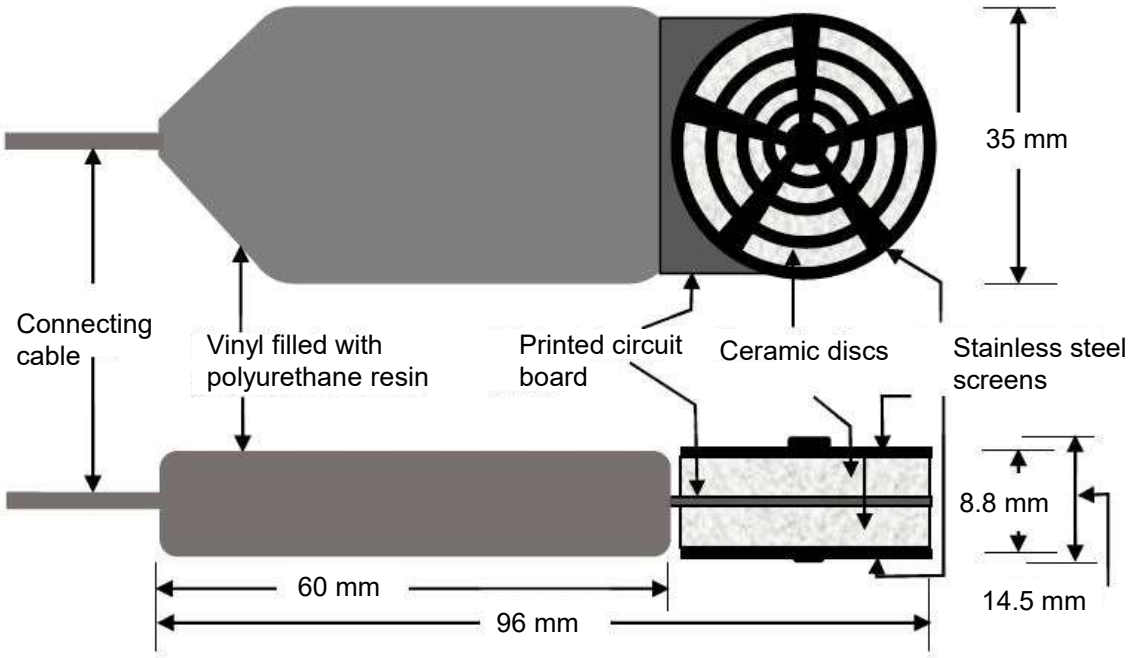

Figure 10: Fixed-matrix porous ceramic sensor (after Tripathy et al., 2016)

2.5 Summary

As highlighted in this chapter, significant developments in the field of unsaturated soil mechanics have been made over the past few decades. With the technological advancements that have taken place regarding the measurement of soil suction, a deeper understanding of the mechanisms and stress state variables governing the behaviour of unsaturated soils has been gained. This understanding has highlighted the importance of the soil water retention curve in describing the behaviour of unsaturated soils. Using the technological advancements and development of knowledge in this field, a better understanding can be attained of the subgroup of unsaturated soils referred to as swelling or expansive clays.

CHAPTER 3

BACKGROUND ON EXPANSIVE CLAYS

At the beginning of Chapter 2, it was stated how partially saturated soils form a subgroup of soil mechanics that is significantly less well understood than that of saturated soil mechanics. Schreiner (1988*b*) pointed out how, within the field of unsaturated soil mechanics, there lies the narrower and arguably less well understood field of expansive soils. Whereas soil chemistry is generally disregarded in geotechnical engineering, it is essentially chemical interactions which govern the intrinsic volumetric properties of swelling clays.

Soil fabric is also particularly important for expansive clays. Since these soils tend to occur in a highly fissured state in the field, laboratory testing becomes problematic. In retrieving an undisturbed sample of expansive clay, what will ultimately be obtained is an intact block of clay which avoids any adjacent fissures. In reviewing the coefficient of consolidation, both in-situ and in the laboratory, Clayton et al. (1995) reported how gross underestimations of this parameter were obtained from laboratory testing, particularly for soils occurring in a highly fissured state in-situ.

Despite the aforementioned difficulties associated with this soil, as technological advancements arise, more information and a better understanding of this problem soil can be acquired. The aim of this chapter is to provide the reader with a background of the fundamental properties of swelling clays, beginning at a chemical level. Thereafter, a conceptual description of the Barcelona Basic Model (BBM) and the extended Barcelona Basic Model for expansive clays (BExM) is provided. While no numerical modelling was conducted in this study, the framework set out by the BExM constitutive model provides a framework within which experimental data can be analysed. Conventional testing methods for expansive clays are then discussed and their limitations highlighted. While most conventional testing methods for expansive clays have

significant limitations, the reality is that practising engineers quite often resort to empirical prediction methods of heave. These approaches are typically based on basic soil properties such as Atterberg limits and grading analyses. A discussion of five of these approaches is included in Section 3.4 The chapter is then concluded with a brief description of some commonly employed design approaches for foundations on this problem soil.

3.1 Mineralogical aspects

The formation of soils, or pedogenesis, occurs when a parent rock is weathered either by mechanical or chemical effects. Chemical weathering can result in mineralogical changes from the parent rock to form crystalline particles of colloidal size referred to as clay minerals (Caenn et al., 2017; Knappet & Craig, 2012). Clay minerals are usually of a plate-like form. A single clay platelet is referred to as a unit layer and comprises a single octahedral sheet combined with one or two tetrahedral sheets. Unit layers can then be combined to form a crystal lattice (Caenn et al., 2017). Basal spacing is a term used to describe the distance between a plane in one layer and the corresponding plane in the next (Caenn et al., 2017). This distance has been highlighted in the figures presented in this section when discussing the various clay minerals.

Tetrahedral sheets generally consist of a central silicon atom coordinated with four oxygen atoms. Octahedral sheets conventionally consist of a central aluminium atom, in octahedral coordination with the oxygen atoms of hydroxyl ions. Such a configuration is referred to as a gibbsite sheet. These structures are illustrated in Figure 11 with simplified representations of the sheets presented in Figure 12.

Through the sharing of common oxygen atoms, these two sheets are bonded together (Caenn et al., 2017). In clay minerals where only one silica sheet is bound to one gibbsite sheet, it is referred to as a 1:1 or two-layer clay mineral (Knappet & Craig, 2012). When a single gibbsite sheet is sandwiched between two silica sheets, the resulting clay structure is referred to as a 2:1 clay mineral (Knappet & Craig, 2012; Mitchell & Soga, 2005) or a 3-layer Hofmann structure (Hofmann et al., 1933).

The basic sheet structures described above can be arranged in many different ways, creating dozens of different clay minerals (Holtz & Kovacs, 1981). However, in the context of engineering there are three types of minerals which are generally highlighted, namely kaolinite, illite and montmorillonite (Knappet & Craig, 2012; Nelson & Miller, 1992). A brief description of these minerals has been provided in the sections that follow.

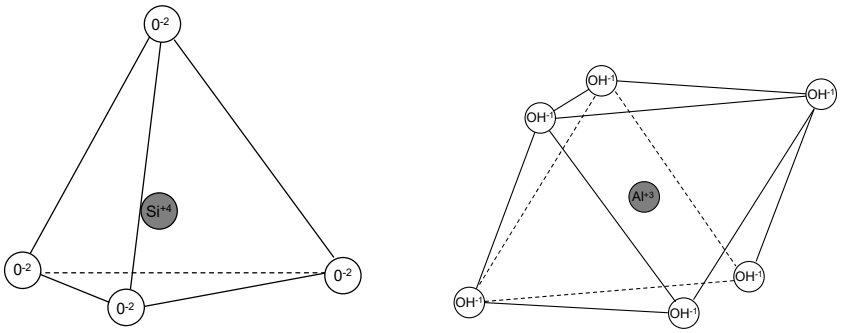

(a) (b)

Figure 11: Schematic of a) silica-oxygen tetrahedron and b) aluminium hydroxyl octahedron (after Knappet & Craig, 2012)

(a) (b)

Figure 12: Schematic of a) silica and b) gibbsite sheet (after Knappet & Craig, 2012)

3.1.1 Kaolinite

In its simplest form, kaolinite is a 1:1 clay mineral with a unit layer consisting of 1 silica sheet and 1 gibbsite sheet, with a basal spacing of 0.72 nm (Caenn et al., 2017; Holtz & Kovacs, 1981; Mitchell & Soga, 2005). Figure 13 illustrates the basic structure of kaolinite. In reality however, kaolinite crystals (or particles) consist of several unit layers stacked upon each other, bonded together by hydrogen bonds. Since hydrogen bonds are extremely strong, they prevent hydration between unit layers (Holtz & Kovacs, 1981). This allows crystal thicknesses to range from 50 nm to about 2000 nm (Caenn et al., 2017; Mitchell & Soga, 2005).

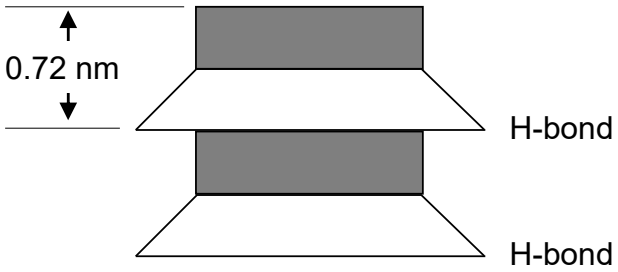

Figure 13: Basic structure of Kaolinite

3.1.2 Illite

In contrast to kaolinite, illite is a 2:1 mineral whereby the unit layer comprises one gibbsite sheet sandwiched between two silica sheets as illustrated in Figure 14. The unit layers are bonded together by strong potassium bonds, which, as with kaolinite, only permits hydration on the exterior surfaces of the crystal (Caenn et al., 2017). The basal spacing of this mineral is of the order of 0.96 nm (Holtz & Kovacs, 1981) to 1 nm (Mitchell & Soga, 2005). Owing to the strong potassium bonds between unit layers, illite crystals can be in the order of 72 nm thick (Caenn et al., 2017).

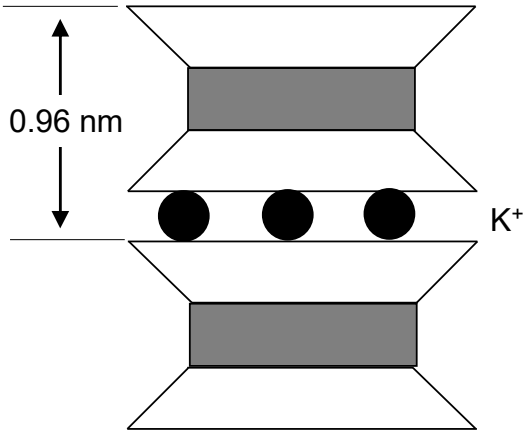

Figure 14: Basic structure of Illite

3.1.3 Montmorillonite

Montmorillonite is a member of the smectite group which, as with illite, has a 2:1 structure with two silica sheets and one gibbsite sheet. However, the behaviour of montmorillonite differs substantially from that of illite because unit layers are bound by weak Van der Waals forces (Mitchell & Soga, 2005). This weak bonding allows water to enter between the unit layers and increase basal spacing from around 0.96 nm to complete separation of unit layers (i.e. a montmorillonite particle can consist of one unit layer) (Mitchell & Soga, 2005). This feature of montmorillonite gives it an expansive lattice (Caenn et al., 2017) and as a result it is this clay mineral that is generally at the root of troublesome ‘swelling clays’ dealt with by geotechnical engineers (Holtz & Kovacs, 1981; Knappet & Craig, 2012; Nelson & Miller, 1992). The basic structure of montmorillonite is illustrated in Figure 15. It should be noted that the basal spacing illustrated in this figure is only applicable before hydration has occurred between the unit layers.

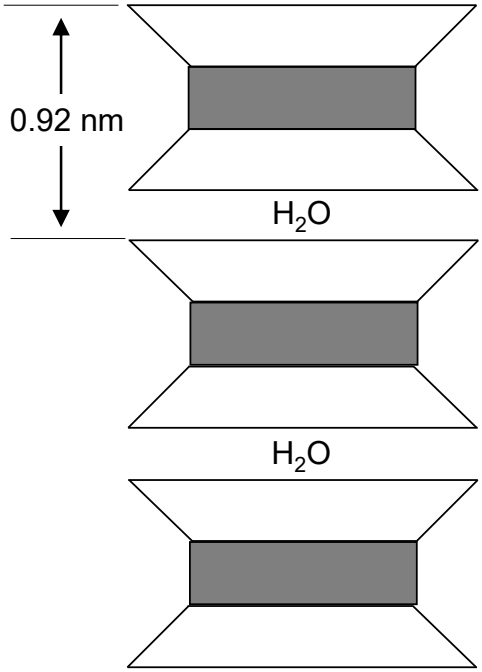

Figure 15: Basic structure of Montmorillinite

One characteristic that is common to all clay minerals discussed, is that they are associated with a negative surface charge. This can be attributed to two factors. Firstly, the edge of silica sheets comprises negatively charged oxygen ions, while the edge of the aluminium octahedra are made up of the negatively charged hydroxyl ions. These negative charges are not balanced by the internal Si or Al atom in the silica and gibbsite sheet respectively. This charge imbalance can be further enhanced by a process known as *isomorphic substitution*. As the name suggests, isomorphic substitution involves the replacement (or substitution) of similarly sized (isomorphic) ions without changing the fundamental structure of the mineral. These substitutions can occur in the central atoms of either the tetrahedral or octahedral sheets and can act to make the surface charges of the clay minerals more negative. For example, a common substitution in the octahedral sheet is the central Al^{+3} for an Mg^{+2} ion (Caenn et al., 2017; Mitchell & Soga, 2005). This would result in a charge deficiency of -1. Similarly, in the tetrahedral sheet, Si^{+4} can be substituted with Mg^{+2} (Caenn et al., 2017; Mitchell & Soga, 2005) resulting in a change in net charge of -2.

Regardless of the precise surface charge, these imbalances are compensated for by the adsorption of cations (Caenn et al., 2017). The layer of cations that exist at the surface of the clay mineral is termed the *Stern layer* (Caenn et al., 2017). However, some ions are not tightly held by the surface and tend to form a diffuse ‘cloud’ of ions around the clay surface,

some of which will be positively charged and attracted to the clay surface, while others will be negatively charged and repelled by the clay surface (Caenn et al., 2017). The negative charge of the particle surface along with the diffused layer of cations is commonly referred to as the *diffuse double layer* (Bolt, 1956). In the presence of water, these cations can be replaced with different cations in the water and are therefore referred to as exchangeable cations (Caenn et al., 2017).

Clay minerals are also commonly surrounded by water molecules. Since water molecules are dipolar, the positive end of a water molecule will be attracted to the negative surface of a clay platelet and form an adsorbed layer. This adsorbed layer can also form due to hydrogen bonding (Knappet & Craig, 2012). The adsorbed layer is tightly bound to the clay surface. However, subsequent layers of water molecules will experience less attraction to the clay as the distance of the water molecule from the surface increases to that of 'free water'. A schematic illustration of the relationship between a clay surface, its exchangeable cations and its interaction with water has been presented in Figure 16. In this figure, provision has been made in the Stern layer for both the positively charged end of water molecules, as well as for other cations.

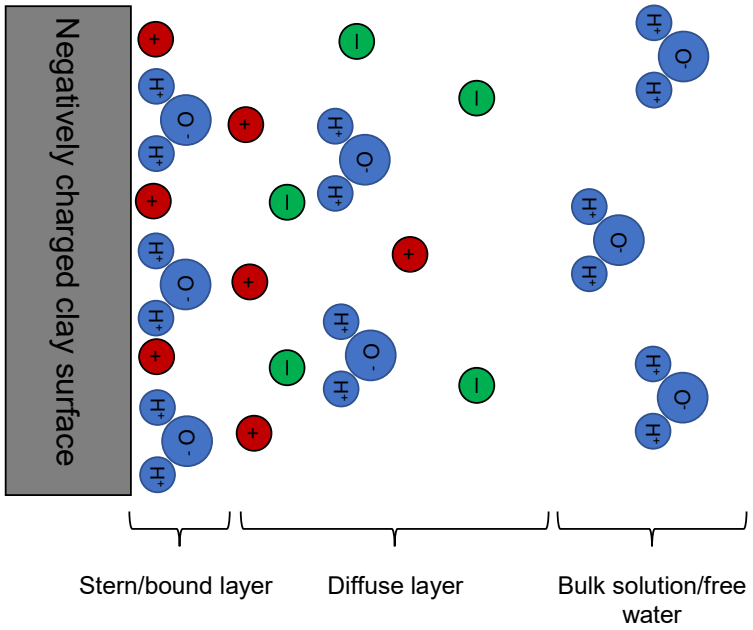

Figure 16: Interaction between clay surface, adsorbed ions, exchangeable cations and bulk water

Using the concept of the diffuse double layer, the most widely used approach to relate clay compressibility to basic particle-water-cation interaction, is the Gouy-Chapman double

layer theory (Chapman, 1913; Gouy, 1910). While the precise details of this theory lie outside the scope of this study, it should be recognised that this theory has been extensively used to predict certain properties of expansive clays (Olson & Mesri, 1970; Sridharan & Jayadeva, 1982; Tripathy et al., 2004). Although this theory is not without its limitations, it has been shown to adequately predict microscopic behaviour of swelling clays. Through the use of the extended framework of the Barcelona basic model (BExM) for expansive clays, this microscopic behaviour can be related to macroscopic behaviour to describe the engineering characteristics of expansive clays. Overviews of the BBM and BExM are provided in the following section.

3.2 Constitutive modelling of unsaturated expansive soils

For any material, the use of a constitutive framework is essential for describing/predicting the stress-strain behaviour of that material. In the field of saturated soil mechanics, during the late 1950s and 1960s, researchers at Cambridge University developed the elasto-plastic model which came to be known as Cam-Clay (Poorooshasb & Roscoe, 1961; Roscoe & Poorooshasb, 1963; Roscoe et al., 1958, 1965; Schofield & Wroth, 1968). Cam-Clay was then modified by Roscoe & Burland (1968) to develop the Modified Cam-Clay (MCC) model. These constitutive relationships are perhaps the best-known soil models to date and form the basis for many other more complex frameworks.

The development of a similar constitutive model for partially saturated soils was met with great difficulty for many years owing largely to one factor. While the behaviour of saturated soils can be fully defined by one stress state variable, namely, effective stress, unsaturated soils require two, net stress $(\sigma_n - u_a)$ and matric suction $(u_a - u_w)$, as discussed in Section 2.3.

Using net stress and matric suction as stress variables, Alonso et al. (1990) were the first to develop a complete elasto-plastic model for unsaturated soils which came to be known as the Barcelona Basic Model (BBM). One limitation of this framework is that it was intended for soils which are slightly or moderately expansive (Alonso et al., 1990), and consequently would not be applicable to the highly expansive material described in this study. To address this limitation Gens & Alonso (1992) extended the BBM to account for expansive clays. This extended framework will be referred to in this study as the BExM.

Since this study is experimental in nature rather than numerical, the descriptions that follow will be primarily conceptual, with mathematical descriptions limited as far as possible. It should be noted that while the terms “preconsolidation pressure” and “apparent preconsolidation pressure” are used in the original publications cited, namely Alonso et al. (1990) and Gens &

Alonso (1992), the more general term "yield stress" will be used in this study. The justification for the use of this terminology stems from recommendations provided by Burland (1990) who stated how the term "preconsolidation pressure" should be reserved for situations where the magnitude of such pressure can be established by geological means. In cases where this is not possible, Burland (1990) suggested that the term "yield stress" rather be used. It will be seen later in this chapter that this terminology is more appropriate, since the yield stress of unsaturated soils is dependent on suction magnitude and, in the case of expansive clays, the amount of swell allowed prior to testing. Recognising these factors, the yield stress of an unsaturated soil can change, whereas the preconsolidation pressure, defined as the maximum effective vertical stress that has acted on the soil in the past (Knappet & Craig, 2012), has remained the same.

3.2.1 Barcelona Basic Model

When developing the BBM, one of the priorities of Alonso et al. (1990) was simplicity. As such, the model used well established theories for hardening and plasticity, and reduces to a critical state model (Modified Cam Clay) at full saturation. Furthermore, the model assumes that the behaviour of soils is controlled by the two stress state variables, net stress and matric suction. Many of the volume change characteristics of unsaturated soils can be adequately represented in $(\bar{p}, s)$ space, where $\bar{p}$ is the net mean stress and s is the matric suction. The same stress space can be used to discuss oedometer testing by making $\bar{p}$ equal to the net vertical stress (Gens & Alonso, 1992). It should be noted that the symbol s referred to in this thesis should not be confused with the stress invariant for plane strain conditions commonly used in saturated soil mechanics (i.e. $\frac{1}{2}(\sigma_1 + \sigma_3)$).

A key aspect of the BBM was the introduction of the load-collapse (LC) yield curve. The benefit of this yield curve is that it simultaneously captures two aspects which are known to occur in unsaturated soils.

1. An increase in suction can result in an increase in the yield stress of a soil (Dudley, 1970).
2. When dealing with a soil that has an open structure, whether due to depositional processes or compaction methods, a reduction in suction can cause an irreversible reduction in volume (i.e. wetting induced collapse). This is an aspect which has received widespread attention in the field of unsaturated soil mechanics (Jennings & Knight, 1975; Rust et al., 2005; Schwartz, 1985).

To illustrate the basic consequences of the LC yield curve, consider Figure 17 and Figure 18 which illustrate loading and wetting paths respectively. If the stress path L_1 in Figure 17 is considered, the following behaviour will be observed. If the sample is loaded at a constant value of suction (s_1), deformations will remain elastic until the LC yield curve is reached. After this point, plastic deformations will occur. Looking at stress paths denoted by L_2 and L_3 which have increasingly lower values of suction (i.e. $s_3 < s_2 < s_1$), yielding will occur at progressively lower stresses as suction is reduced. One additional factor worth noting is that the post-yielding stiffness will increase with an increase in suction (Gens & Alonso, 1992).

For Figure 18, three wetting paths at various mean stresses are observed. For load path C_1, taking place at a relatively small mean stress, the soil remains in the elastic zone as suction is reduced (wetting), which results in small recoverable swelling strains. Load path C_2 takes place at a slightly higher mean stress. For this load path, as suction is reduced, small recoverable swelling will occur whilst the stress path remains in the elastic region. However, after the LC yield curve is reached, irrecoverable collapse will occur. Load path C_3, saturated at a relatively high stress begins very near the LC yield curve and, as a result, very little swelling is observed before large collapse strains occur (Gens & Alonso, 1992).

Figure 17 and Figure 18 illustrate how the LC yield curve elegantly describes two important behavioural aspects of unsaturated soils. A point of interest however may be the shape of this curve. The shape of the LC curve presented in Figures 17 and 18 was chosen arbitrarily to illustrate the effect of suction and net-stress on the volumetric behaviour of an unsaturated soil. The shape of this yield curve is however not fixed and can change for different soil types.

For a material where the LC has a relatively large amount of curvature, the position of that soil's yield stress will be highly dependent on suction. This would be true particularly in the low suction range where for a given change in suction, say Δs, the corresponding change in yield stress will be relatively large. However, at higher values of suction where the LC curve tends towards verticality, Δs will result in a much smaller change in the yield stress. A yield curve of this shape could perhaps be associated with a clay or silty clay. This feature of the LC curve highlights the diminishing contribution of suction to the position of the yield stress in a soil. This characteristic is similar to that captured by the χ parameter in Bishop's effective stress (discussed in Section 2.3) which highlights a diminishing contribution of suction to soil strength, as suction is increased. For a case where the LC yield curve is near vertical, there will be a much smaller dependency of yield stress on suction across the full suction range. Furthermore, such a material would not be particularly susceptible to wetting induced collapse.

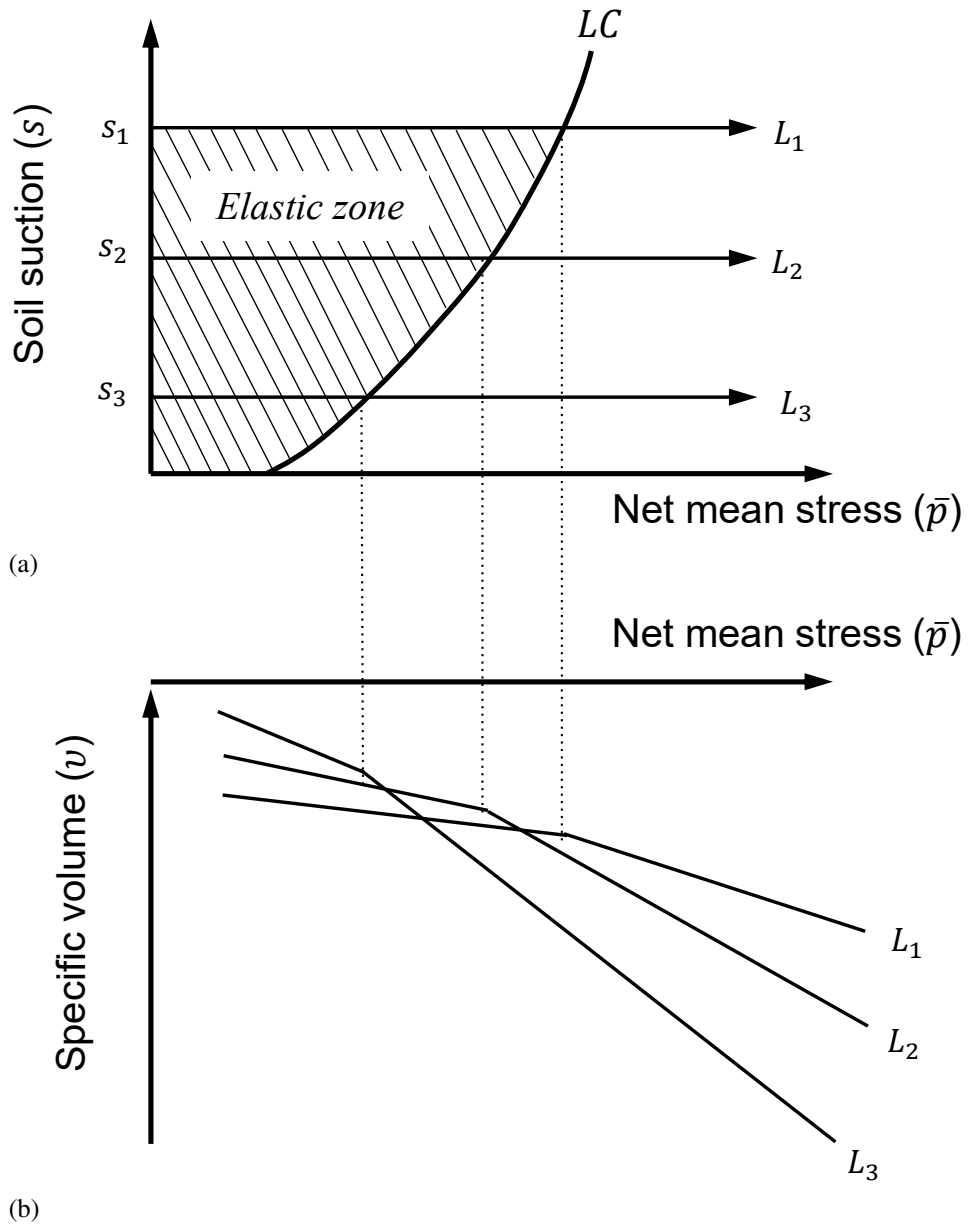

Figure 17: The effect of suction on the loading deformation of an unsaturated soil illustrated as a) a stress path in $\bar{p} - s$ space and b) volume change during compression (after Gens & Alonso, 1992)

A yield curve of this shape could perhaps be associated with a clean dense sand (without the presence of clay material providing some degree of suction bonding between particles).

In addition to the LC yield curve, there is literature to suggest that an increase in suction can result in irreversible volumetric strains (Josa et al., 1987; Yong et al., 1971). To deal

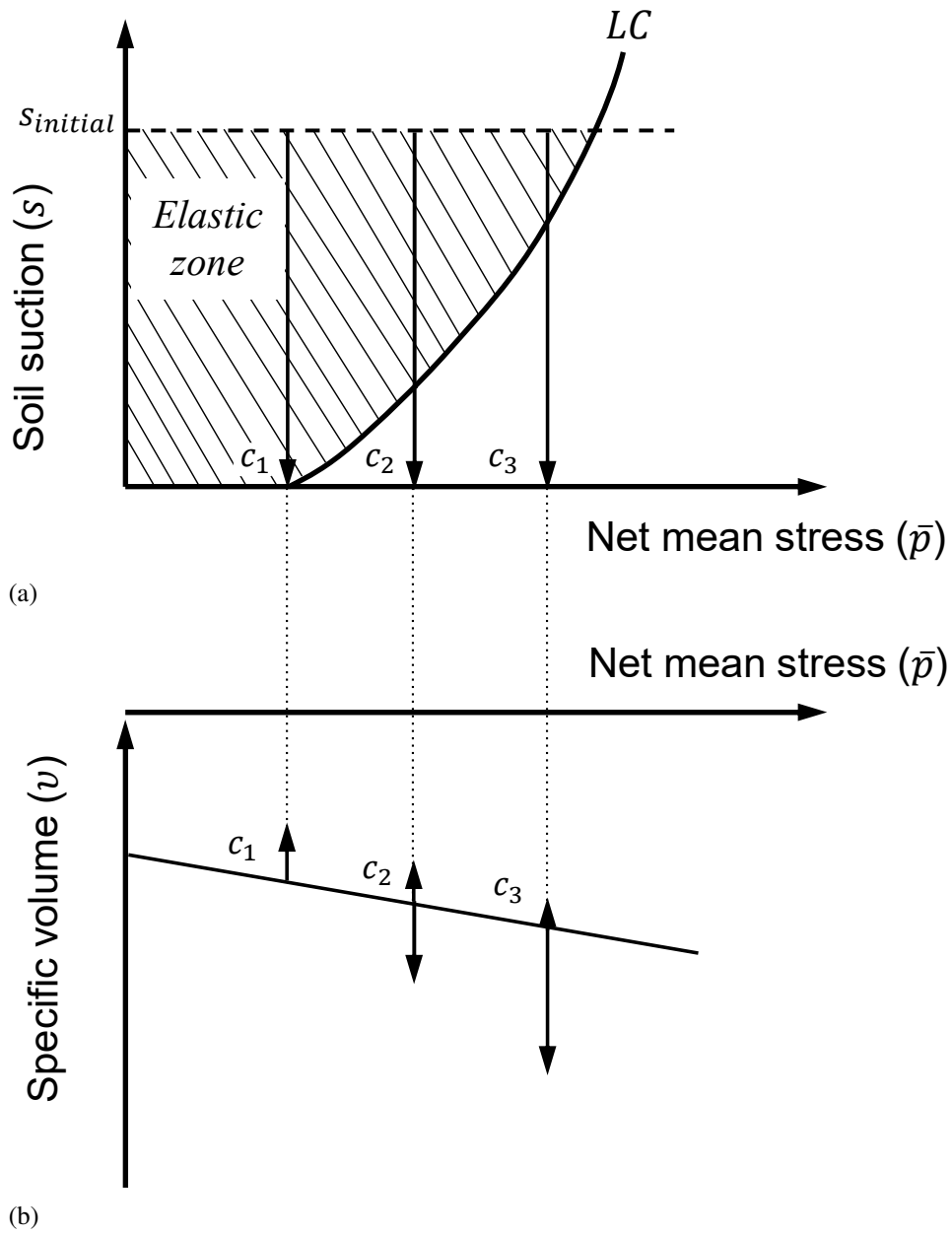

Figure 18: The effect of net mean stress on wetting-induced deformations on an unsaturated soil illustrated as a) a stress path in $\bar{p} - s$ space and b) volume change upon wetting (after Gens & Alonso, 1992)

with this aspect, Alonso et al. (1990) put forth a proposition whereby, if a soil exceeds its maximum previously attained suction (s_{max}), irreversible strains will begin to occur. On this basis, the concept of the suction increase (SI) yield curve was established. In the absence of more experimental evidence, Alonso et al. (1990) assumed this yield curve to be a constant

value equal to s_{max}. Together, the LC and SI yield curves bound an elastic region in the $(\bar{p}, s)$ plane as illustrated in Figure 19. Based on experimental evidence by Josa et al. (1987), the BBM framework assumes a coupling between the SI and LC yield loci, i.e. an increase in suction past s_{max}, will not only move the SI yield curve upwards, but will also move the LC yield curve to the right.

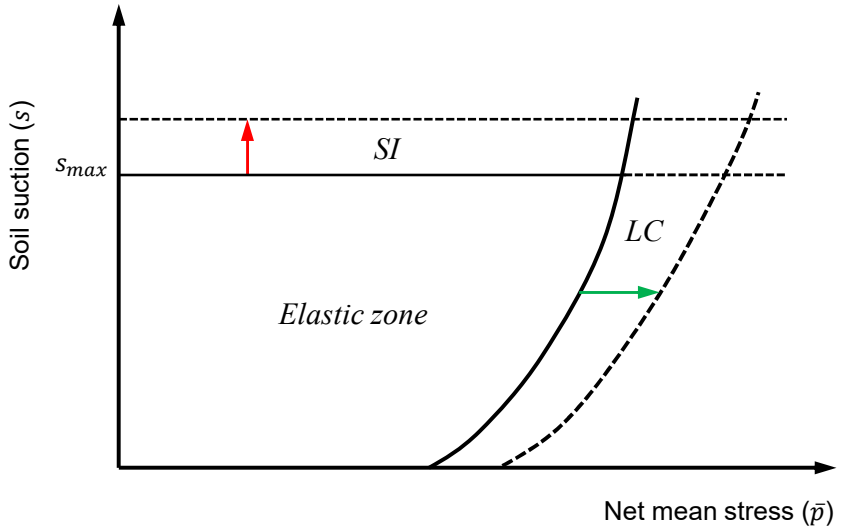

Figure 19: Loading collapse and suction increase yield curves (after Gens & Alonso, 1992)

The framework can then be extended to triaxial stress space by incorporating deviatoric stress (q) and assuming a critical state type model for the saturated case. As mentioned at the start of this section, the Modified Cam-Clay model (MCC) is assumed for a value of $s = 0$. Failure states are specified by the assumption that the slope of the critical state line remains constant. Finally, it is assumed that the SI yield curve rises vertically upwards with an increase in q (Alonso et al., 1990; Gens & Alonso, 1992). Figure 20 illustrates the yield curves in $\bar{p} - q - s$ space with the complete yield surface shown in Figure 21. It should be noted that in Figure 20, $\bar{p}_o^*$ and $\bar{p}_o$ denote the yield stress for the saturated case and for suction greater than zero respectively.

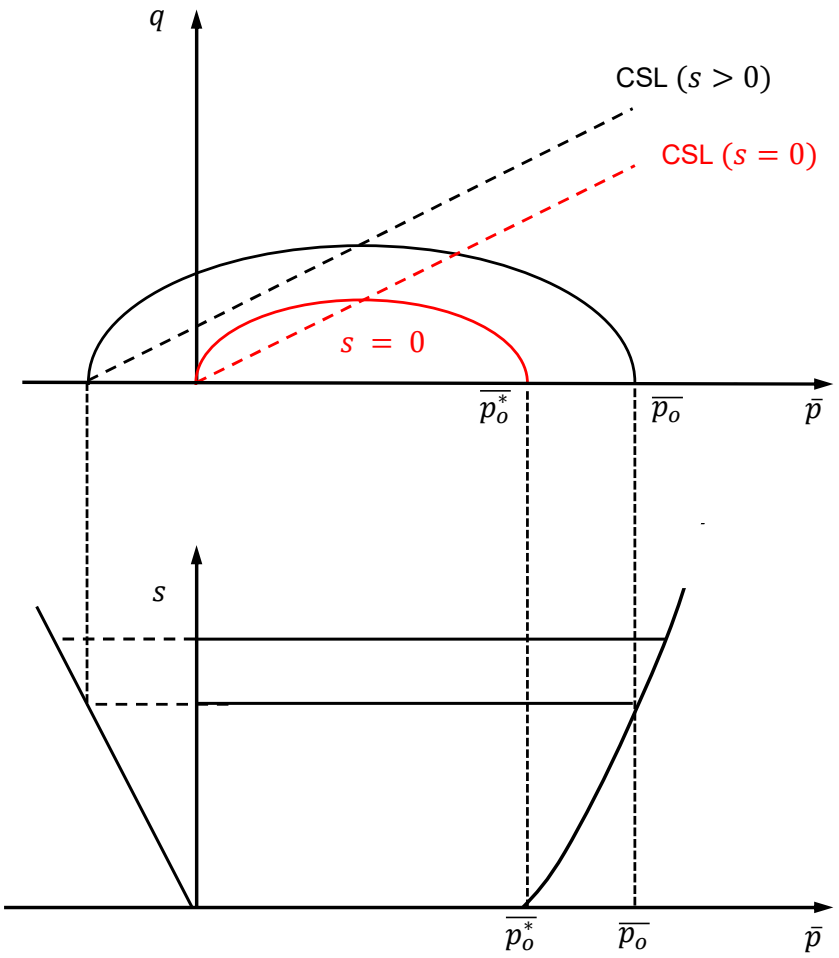

Figure 20: Yield curves in $\bar{p} - q - s$ space (after Gens & Alonso, 1992)

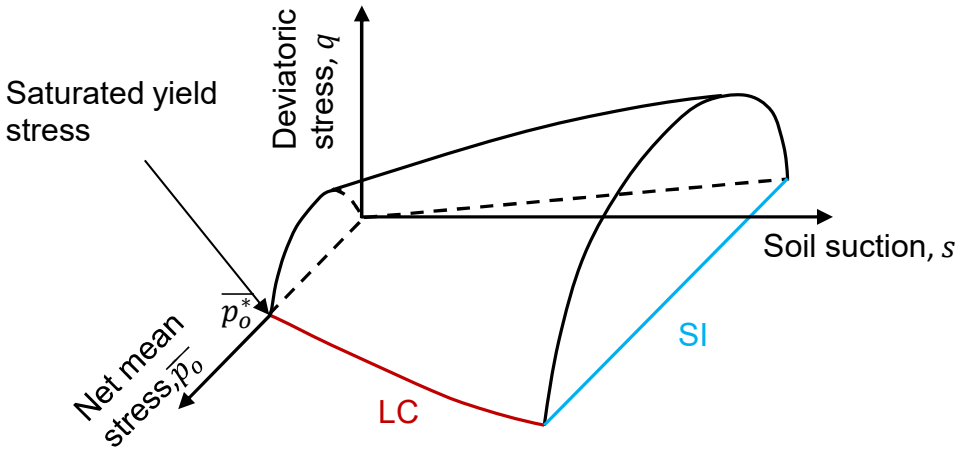

Figure 21: Three-dimensional view of the yield surface (after Alonso et al., 1990)

3.2.2 Extended framework for the behaviour of expansive clays

While the model proposed by Alonso et al. (1990) was shown to compare well with suction controlled laboratory testing, the framework was intended for slightly and moderately expansive soils. As such, it allows for only small reversible swelling strains. While it is true that all clays can swell to some extent, the term 'swelling' or 'expansive' clays is generally reserved for soils that can exhibit significant volumetric deformations which can be largely irreversible (Gens & Alonso, 1992).

In Section 3.1.3, it was described how the clay mineral montmorillonite is one of the most common highly expansive clay minerals. It was also mentioned that, through understanding of the chemistry of clay mineralogy, swell magnitude and pressure can be predicted using, for example, the double layer theory. While such a theory is capable of making predictions at a particulate level or for a relatively continuous matrix of clay aggregations, it is necessary to relate these predictions to the bulk behaviour of a soil element. For this reason, the BExM (Gens & Alonso, 1992) is founded on the consideration of two structural levels:

1. A microstructural level which refers to the active clay minerals and their vicinity.
2. A macrostructural level which accounts for the larger scale structure of the soil.

In the formulation of the framework, Gens & Alonso (1992) outlined the following basic assumptions.

- The deformation of the microstructure is controlled by physicochemical interactions at particle level and as such, the microstructure is assumed to be independent of macrostructural effects. However, deformations of the microstructure are able to affect the macrostructure.
- The microstructure is assumed to be fully saturated at all times, even when the soil mass as a whole is unsaturated.

McGown & Collins (1975) and Collins (1984) provided descriptions on microfabric forms based on SEM observations of natural soils. Figure 22 illustrates soil fabrics typical for expansive clays. For a swelling clay, the elementary particle will consist of a grouping of approximately parallel clay platelets (Figure 22 c)). These elementary particles can either join

to form aggregations or ‘packets’ (Figure 22 b)), or they can form a relatively continuous matrix (Figure 22 a)).

Whatever the arrangement of elementary particles, they will typically be interspersed with silt or sand grains. Provided that the clay minerals are expansive in nature, the continuous matrix illustrated in Figure 22 a) will result in an expansive soil whereas the fabric illustrated in Figure 22 b) may result in either swell or collapse (Gens & Alonso, 1992).

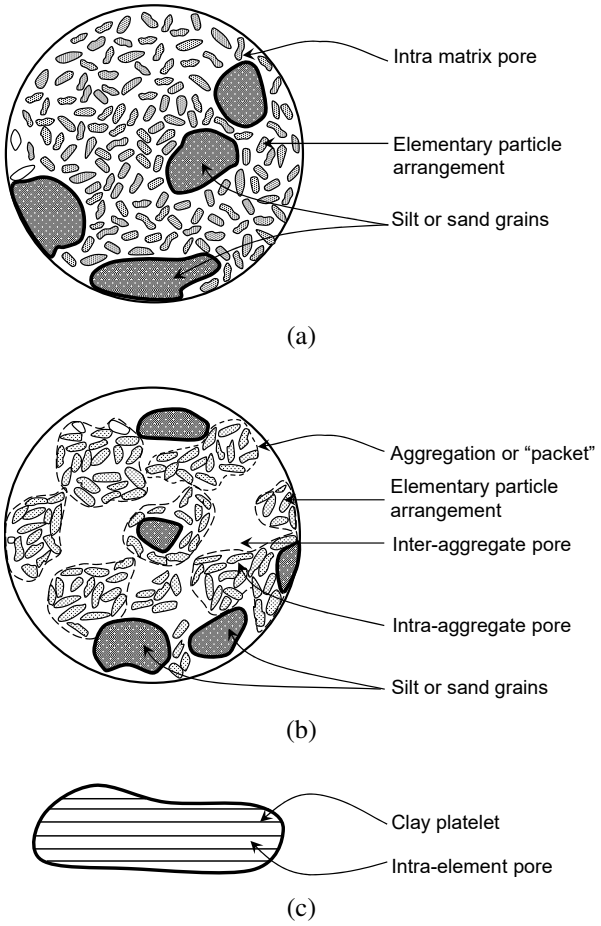

Figure 22: Fabric types for an expansive clay illustrating a) a microfabric predominantly consisting of a continuous matrix of elementary clay particles, b) a microfabric consisting of a number of ‘packets’ of elementary clay particles and c) an elementary particle arrangement consisting of a number of clay parallel clay platelets (after Gens & Alonso, 1992)

The BExM framework was intended to account for both fabric types a) and b) presented in Figure 22. For the microfabric type illustrated in Figure 22 b), macrostructural effects predominate and so, adequate description of the macrostructural behaviour and the relationship between the two levels is necessary. In contrast, for soils with the microfabric presented in

Figure 22 a), it is more critical for modelling purposes to provide an adequate description of the microstructural level, with the macrostructural level being of secondary importance (Gens & Alonso, 1992). Recognising the roles played by different fabric types, the BExM was aimed to include definition of:

1. The behaviour at the macrostructural level.
2. The behaviour at the microstructural level.
3. The coupling between the two structural levels.

The behaviour at the macrostructural level is assumed to be covered by the initial BBM framework. The basic mechanisms of soil expansion associated with the microstructural level can however be considered a field of research in its own right.

As alluded to in Section 3.1.3, the most widely used theory to relate particle-water-cation interaction is the Gouy-Chapman double layer theory (Chapman, 1913; Gouy, 1910, 1917). The double layer theory can provide a relationship between the distance between two adjacent clay particles, and the concentration of cations along the central plane between those particles (Bolt, 1956). The effective osmotic pressure on that midplane can then be determined by the concentration of ions along the plane (Verwey & Overbeek, 1948). According to osmotic theory, swelling pressure arises from the tendency of the liquid phase to re-enter the system as a result of this excess osmotic pressure. The concepts described above have been used reasonably successfully to predict volume change for expansive clay minerals. Successful applications of double-layer concepts include Olson & Mesri (1970), Mitchell (1976), Sridharan & Rao (1973) and Tripathy et al. (2004). Despite its successful use in a number of studies, the theory is not without its limitations, which has led to the development of a number of alternative theories to address various shortcomings (Kjellander, 1991; Low, 1980; Yong et al., 1984).

The formulation of the BExM allows the freedom to adopt any theory in the determination of microstructural swelling. However, to maintain simplicity in the framework, microstructural swelling is assumed to be reversible and independent of the macrostructure (Gens & Alonso, 1992). Furthermore, since the microstructure is assumed to remain saturated, in accordance with the principles of effective stress, changes in pore-water pressure or total stress are equivalent

as far as mechanical behaviour is concerned (Burland, 1965). As such, the microstructural approach adopted should take the form of Equation 6.

$$\varepsilon_m = f(s + \bar{p}, otherfactors) \tag{6}$$

Where:

ε_m = microstructural strains

The fact that microstructural swelling is predominantly governed by particle-water-cation interaction, the assumption of the microstructure being independent of macrostructural effects was made in the original BExM framework (Gens & Alonso, 1992). However, more recent publications on the use of the BExM (Alonso et al., 1999; Sánchez et al., 2005) highlighted the assumption of mechanical and hydraulic equilibrium between the two levels of structure. This assumption greatly simplifies the model in that the stress variables $\bar{p}$ and s, used to describe macrostructural phenomena in the original BBM, can be used in the description of microstructural volumetric strains.

In Figure 23, line x-y defines stress states where the value of $(s + \bar{p})$ remains constant. Any stress paths along this line (e.g. OA or OB) will result in no microstructural deformations and is hence referred to as the neutral line. The neutral line separates stress paths which will result in swelling (e.g. OC and OD) from those which will result in compression (OE and OF). The inclination of this line may vary depending on the microstructural theory adopted, however, in the original formulation of the BExM, Gens & Alonso (1992) assumed an inclination of 45°. Regardless of the microstructural theory adopted, there is agreement on the general trends regarding the effects of suction and net mean stress on microstructural swelling. Figure 24 illustrates the relevant relationships.

The results presented in Figure 24 a) illustrate the effect of suction variation at constant net stress on microstructural swelling strains. This schematic illustrates that, at a given level of net mean stress, reduction of suction from a higher value will result in more swell. Furthermore, the rate of swell with respect to suction increases at lower values of suction (Gens & Alonso, 1992). Similarly, Figure 24 b) highlights the influence that a variation in net stress will have on microstructural swelling, if suction is kept constant. Figure 24 b) shows how, if net mean stress is reduced from a higher value, a larger amount of microstructural swelling will occur. Another

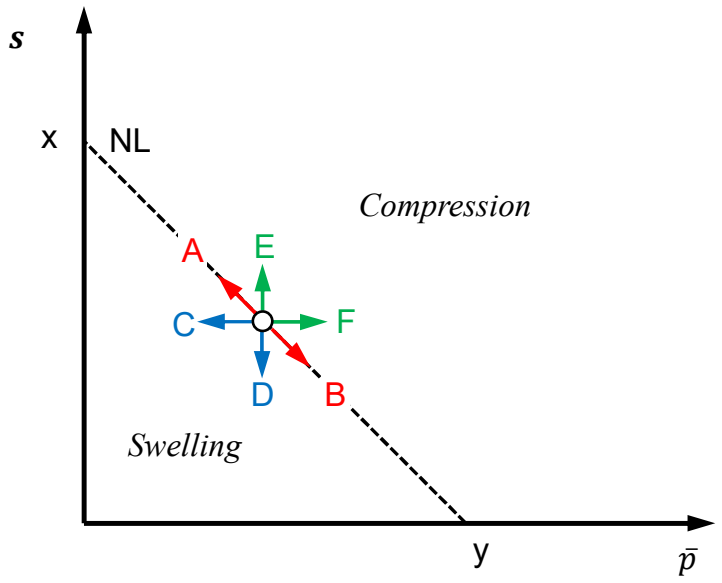

Figure 23: Microstructural behaviour described in $\bar{p} - s$ space (after Gens & Alonso, 1992)

characteristic captured by this figure is that the rate of swell with respect to net mean stress will increase at lower levels of net mean stress (Gens & Alonso, 1992). Finally, Figure 24 c) shows that microstructural swelling due to a reduction in suction will be smaller for larger values of net stress (Gens & Alonso, 1992).

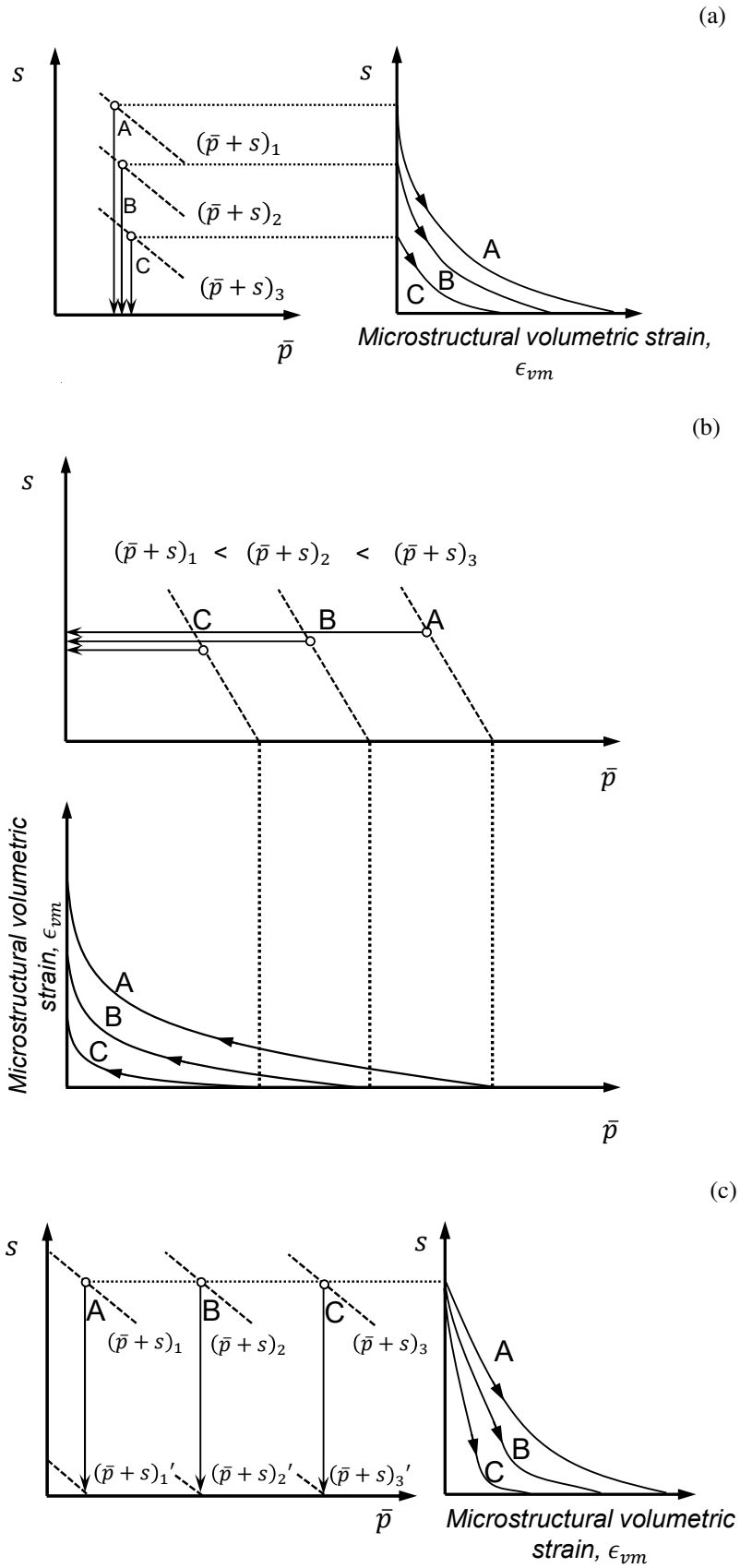

Figure 24: Description of the dependency of microstructural behaviour on a) suction variation at constant net stress, b) net-stress variation at constant suction and c) suction variation at various values of net-stress (after Gens & Alonso, 1992)

The final aim of the BExM was to couple the effects of the two structural levels, or more specifically, to illustrate the effect of microstructural swelling on the macrostructure of the soil. To illustrate this relationship, consider Figure 25. In this figure it can be seen that if the suction in a sample, originally at Point A is reduced to Point B, the microstructural swelling that would result would ultimately increase the macroscopic void ratio of the soil. This macroscopic volumetric change will result in softening of the clay which is represented by movement of the LC yield curve to the left (Gens & Alonso, 1992). If this reduction in suction is continued to $s = 0$, the LC curve will move further to the left. However, if the stress path is stopped at B and suction is increased to A, the LC yield curve will remain fixed and not return to its original position (Gens & Alonso, 1992).

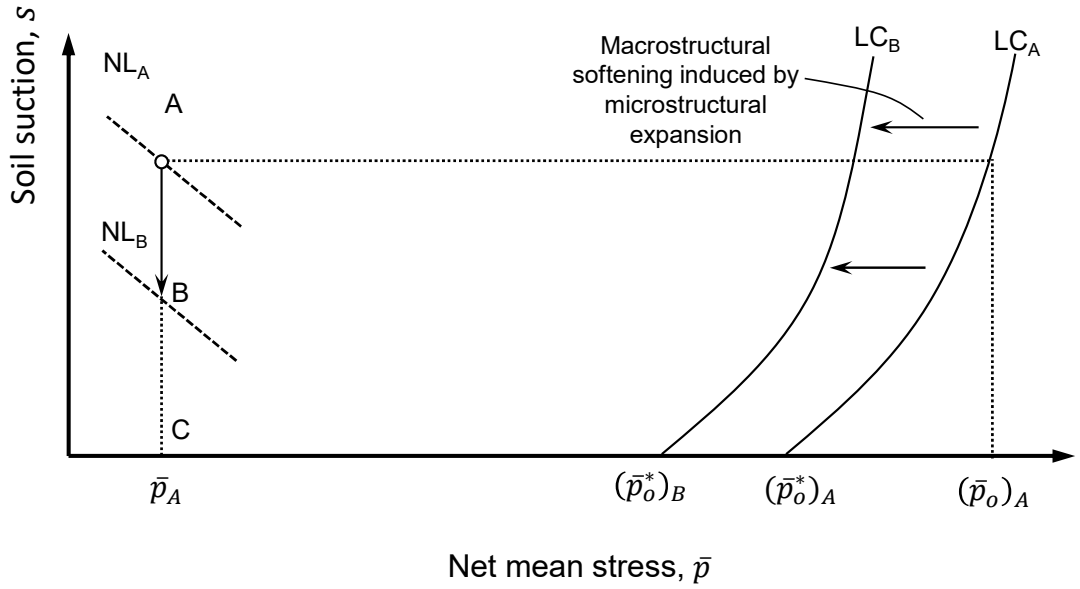

Figure 25: Coupling between microstructural deformation and macrostructural LC yield curve (after Gens & Alonso, 1992)

The results presented in Figure 25, illustrate the effect of microstructural swelling on the macrostructure. The extent to which microscopic strains affect the macrostructure is dependent on the relative position between the stress state in the soil and its LC yield curve. The coupling between the two structural levels is assumed to be dependent on the value of $\bar{p}/\bar{p}_o$, where $\bar{p}$ is the current value of net stress and $\bar{p}_o$ is the yield stress of the soil at the current value of suction. This relationship is illustrated graphically in Figure 26 with $\bar{p}/\bar{p}_o = 1$ corresponding to a fairly open macrostructure. For a value of $\bar{p}/\bar{p}_o \approx 1$ the soil is close to its LC yield curve and is thus potentially collapsible. A reduction of $\bar{p}/\bar{p}_o$ less than 1 corresponds to an increasingly denser macrostructure with higher potential for macrostructural swelling (Gens & Alonso, 1992; Gens et al., 2011). The effect of this relationship can be seen by the stress paths presented

in Figure 27. In this figure it is assumed that Samples A and B are at the same initial stress state, with different initial LC curves labelled LC_{Ai} and LC_{Bi} respectively. The same then applies for samples A' and B' with the only difference in these samples being a higher initial net stress.

If Sample A and B are compared, Sample B will swell more upon saturation. Despite the fact that both samples will experience the same amount of microstructural swelling, Sample B is further away from its initial yield curve, resulting in larger macroscopic expansion (Gens & Alonso, 1992). In the context of Figure 26, this is explained by the fact that $\frac{\bar{p}_1}{\bar{p}_{oB}} < \frac{\bar{p}_1}{\bar{p}_{oA}}$. In comparing Samples A and A', Sample A will experience larger macrostructural volumetric strains for two reasons. Firstly, the microstructural swelling of A will be greater than that of A' due to its lower net stress. Furthermore, A is further away from its LC yield curve than A' which means that the macrostructural swelling induced by microscopic swelling will be greater (Gens & Alonso, 1992). This can again be seen in the context of Figure 26 since $\frac{\bar{p}_1}{\bar{p}_{oA}} < \frac{\bar{p}_2}{\bar{p}_{oA}}$.

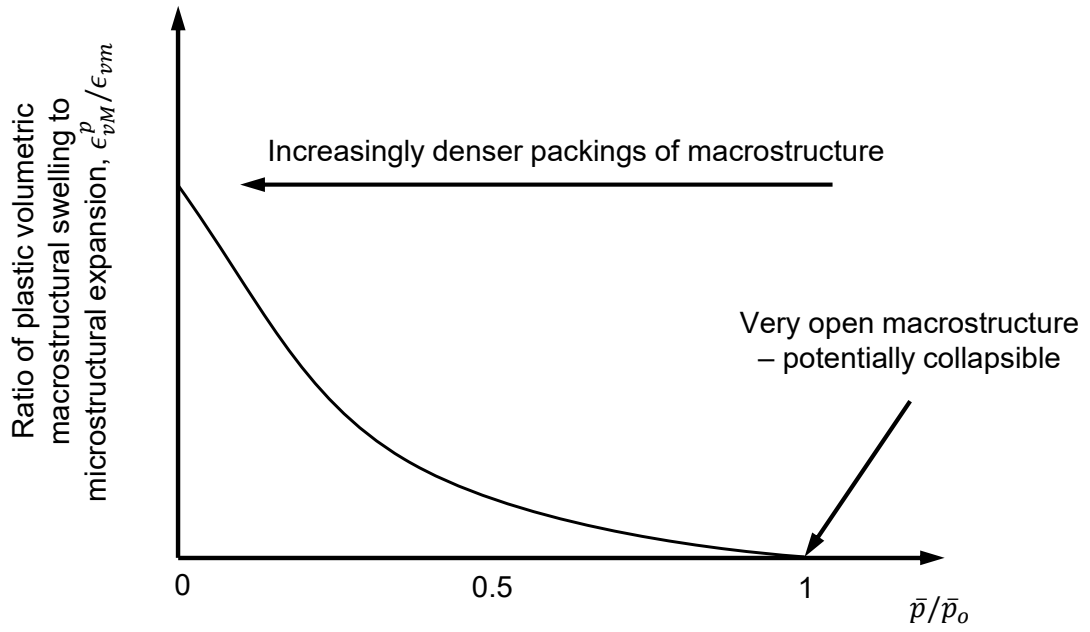

Figure 26: Dependence on the ratio between irreversible volumetric macrostructural deformation and microstructural swelling on the value of $\bar{p}/\bar{p}_o$ (after Gens & Alonso, 1992)

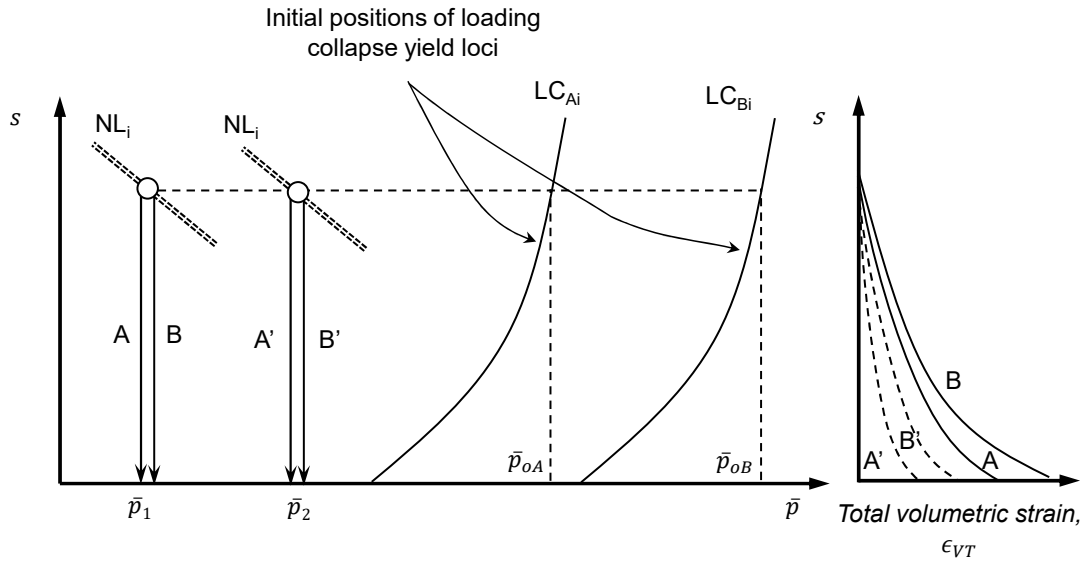

Figure 27: Effect of relative position on LC yield curve on the magnitude of swelling (after Gens & Alonso, 1992)

The BExM framework described in this section has been predominantly based on the original formulation put forth by Gens & Alonso (1992) and has been kept purely conceptual. While it is known that the model has since been described mathematically, applied to various scenarios and even altered slightly (Alonso et al., 1999; Gens et al., 2011; Sánchez et al., 2005) the purpose of the background given here is to provide a basis for the interpretation of experimental data, similar to what was done in the original publication. Such a description was deemed sufficient for the purposes of this study.

3.3 Laboratory testing of unsaturated expansive clays

When considering the problems associated with swelling clays, the two aspects which are arguably the most useful to a design engineer is the magnitude of swell to be expected, referred to as swell potential, and the amount of pressure required to completely prevent swell, a term defined as *swell pressure*. There are generally three tests which can be undertaken to determine these quantities, all of which take place in either a conventional or modified oedometer apparatus.

In conventional oedometer testing (generally available to the practising engineer), there is no control of suction or moisture intake. Additionally, only the vertical applied stress is known. Such an approach has severe limitations as highlighted by Schreiner (1988*b*) since they consider the worst-case scenario whereby the sample is wetted to a point of zero suction.

Additionally, since changes in suction and lateral stresses are not measured throughout testing, only the end point of the test can be accurately analysed. Furthermore, even at the end of testing, lateral stresses of the sample are not known and as such, limited information can be obtained from such tests. It is also true that some of these tests may not follow a stress path relevant to field conditions.

Recognising these limitations, modified oedometer apparatus have been developed which can measure/control suction (Delage et al., 1992), measure lateral stresses (Komornik & Zeitlen, 1965; Offer & Blight, 1985), or do both (Dineen, 1997; Dineen & Burland, 1995; Schreiner, 1988*b*). While being both time consuming and expensive to perform, tests conducted with these modified oedometer apparatus have provided invaluable insights into the behaviour of expansive clays and the limitations of conventional testing procedures.

Since the focus of this thesis is on the centrifuge modelling of expansive clays, it was decided that only conventional oedometer tests (available to the practising engineer) would be carried out. As a result, the basic concepts of each of the three procedures is described first. The section is then concluded with a discussion on the limitations and applicability of each test method, as highlighted by studies performed with the more sophisticated oedometer apparatus.

3.3.1 Swell followed by consolidation

To the author's knowledge, the earliest publication of this approach was the double-oedometer test proposed by Jennings & Knight (1957) as a method to determine swell potential. It would seem however that this test method was primarily for the study of collapse in unsaturated soils (Schreiner, 1988*b*), a plausible assertion considering the topic of Ken Knight's doctoral thesis on the collapse structure of sandy soils. That being said, the approach was later modified by Jennings et al. (1973) to a 'single oedometer' test.

While many variations of the test have been published in the literature, the concept can be described by Figure 28. A sample is placed in the oedometer at its in-situ moisture content and allowed to swell under a small seating stress, as illustrated by stress path AB (different authors have reported different seating pressures, e.g. 1 kPa (Jennings & Knight, 1957) and 6 kPa (Sridharan et al., 1986). Once the sample has been allowed to swell and reached equilibrium, the sample is consolidated in the conventional way (BC). If the conventional double oedometer approach is followed, a second sample under the same initial conditions is subjected to the same loading sequence as the sample that was allowed to undergo swell (this has not been illustrated in Figure 28). This sample would be sealed to ensure no moisture loss during the loading

process. The estimated swell at any applied vertical stress is then taken as the difference in void ratio between the saturated sample and the sample loaded at its in-situ moisture content.

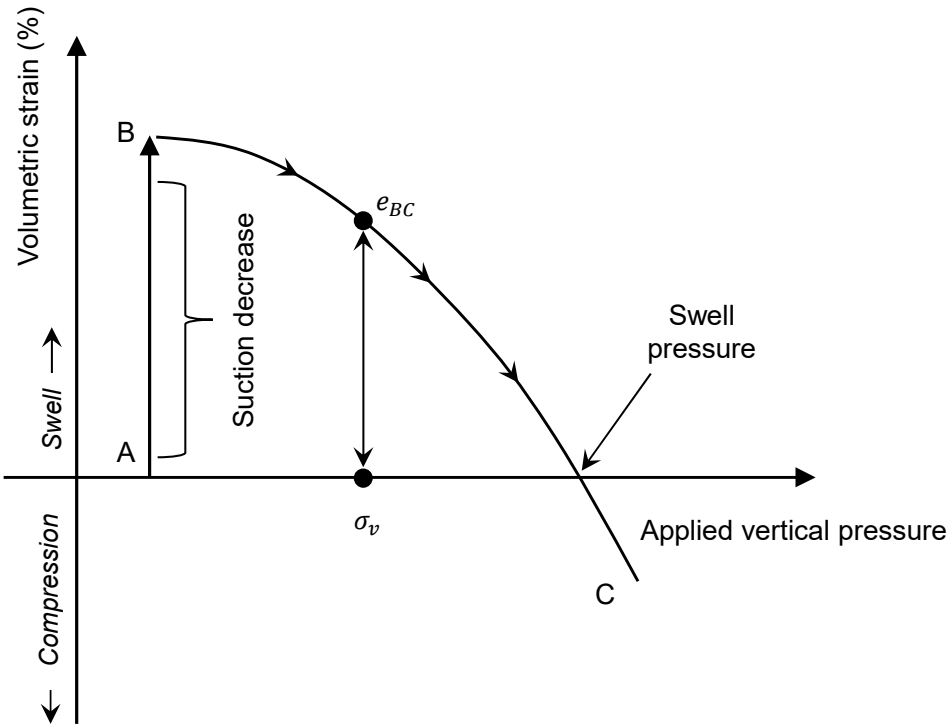

Figure 28: Swell followed by consolidation

The conventional double oedometer test requires constructions to be performed such that the two test results coincide at various points, as described by Jennings & Knight (1957). However, in recent publications it has become more common to simply apply the single oedometer approach whereby the estimated heave is taken as the difference between the void ratio on the consolidation curve at a given applied vertical stress, and the initial void ratio of the sample. Another advantage of this test is that the swell pressure can be interpreted as the intersection of the consolidation curve with the horizontal line at 0% volumetric strain (i.e. e_o).

3.3.2 Swell under constant load

The swell under constant load test first proposed by (Holtz & Gibbs, 1956) is illustrated graphically in Figure 29. The basic concept of this test is that a sample is placed in an oedometer at its in-situ moisture content. A load, equivalent to the anticipated field stress (overburden or overburden plus foundation stress), is then applied (AB). At this point the sample is inundated and brought to a state of zero suction (Path BC). Once equilibrium has been reached at Point C, the amount of potential heave can be estimated.

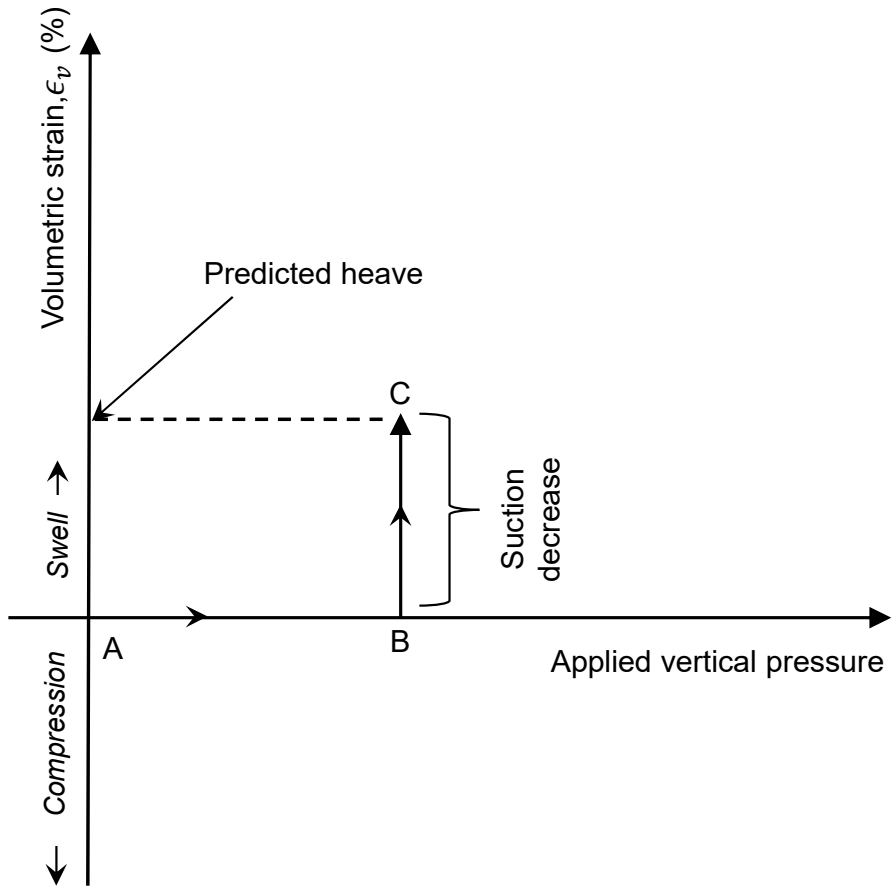

Figure 29: Swell under constant load test

If this test is to be repeated for a number of different applied vertical stresses, a soaking under load curve can be obtained as illustrated in Figure 30. From this test result an estimation of heave can be obtained at any overburden stress. Furthermore, the swell pressure of the clay can be obtained where the soaking under load curve intersects the horizontal axis. While this approach to the determination of swell pressure requires the meticulous preparation of several identical samples, it has been found to give repeatable results (Fourie, 1991). It should be noted that in Figure 30, a linear relationship is illustrated between volumetric strain and applied vertical strain. This relationship was observed by Fourie (1991) but has also been reported to be linear by other researchers. Vanapalli (2012) describes a linear relationship between void ratio and the net normal stress and, in doing so, cites the work of three other publications namely Fredlund (1983), Dhowian (1990) and Nelson et al. (2006). There have however been studies which report a non-linear relationship between void ratio (or volumetric strain) and applied vertical stress. Examples of such studies include Al Haj & Standing (2015) and Justo et al. (1984). Possible explanations for these different relationships include the range of stresses

considered, mineralogical differences between the various materials tested, soil fabric, and whether or not the samples in the various studies were in fact brought to a state of zero suction. The possibilities for the reported discrepancies listed are however merely suggestions since examination of this relationship, in detail, lies outside the scope of this study.

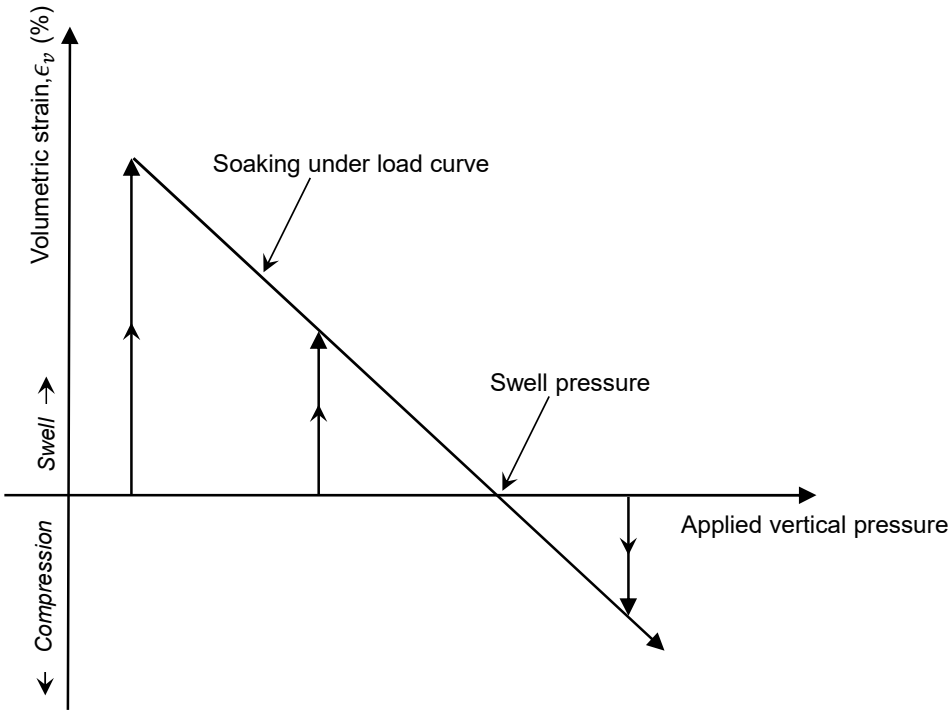

Figure 30: Soaking under load curve

3.3.3 Constant volume

To determine swell potential, the constant volume swell test, followed by rebound was proposed by Sullivan & McClelland (1969). The stress paths followed using this approach are illustrated in Figure 31. After placing a sample in the oedometer at its in-situ moisture content, the sample is inundated with water. During this process the volume of the sample is kept constant by incrementally increasing the applied vertical stress. The point where this process reaches equilibrium (i.e. no more stress is required to prevent swell) is the swelling pressure of that clay. However, Sullivan & McClelland (1969) suggested that if the sample is unloaded after this point (or volume change is no longer restricted), the potential heave can be estimated from the rebound curve (BC).

While the original version of this test involved having to manually increase the applied vertical stress in response to very slight volumetric changes, Brackley (1975*b*) developed an

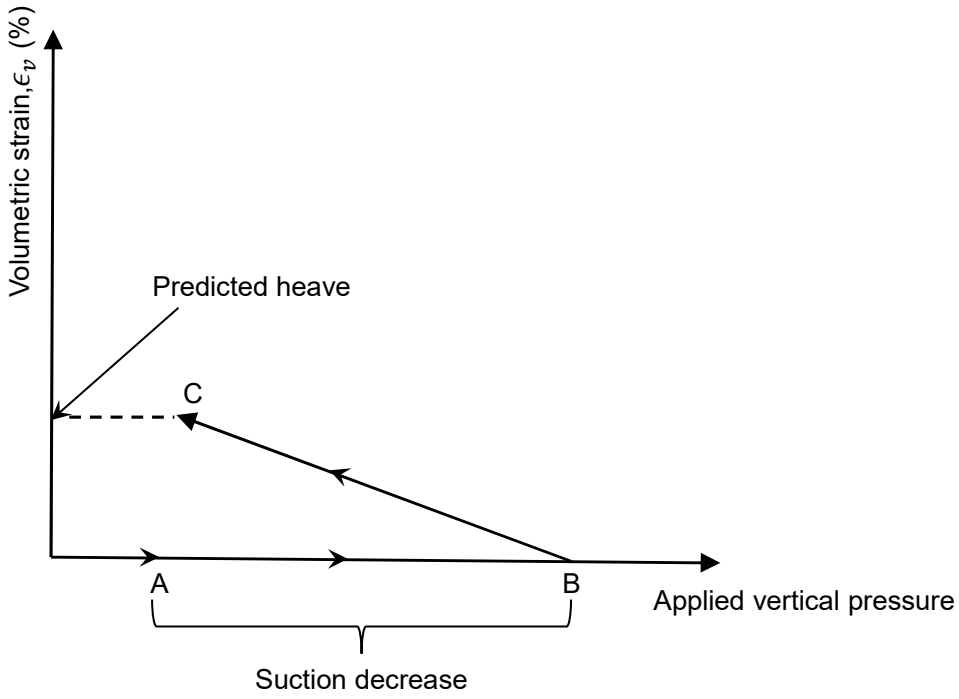

Figure 31: Constant volume test

apparatus which utilised a stiff load cell to keep the volume of the sample essentially constant, while measuring changes in swell pressure. Similar approaches appear to be used in recent publications (Manca et al., 2016), although commercially available automatic oedometers now exist where the increase in applied stress is performed automatically in response to minute changes in volume via a feedback loop system. A great advantage of the constant volume test is that the development of pressure can be monitored as suction is reduced. Such testing has provided much useful information on the behaviour of sand/bentonite mixtures which are increasingly being proposed as a containing material for radioactive waste. Some typical qualitative results obtained by various researchers (Ferrari et al., 2018; Ghiadistri et al., 2018; Mantikos et al., 2018; Ye et al., 2018) have been provided in Figure 32. Figure 32 illustrates how the development of swell pressure as suction is reduced, does not follow a single trend and can be dependent on the fabric of material being investigated.

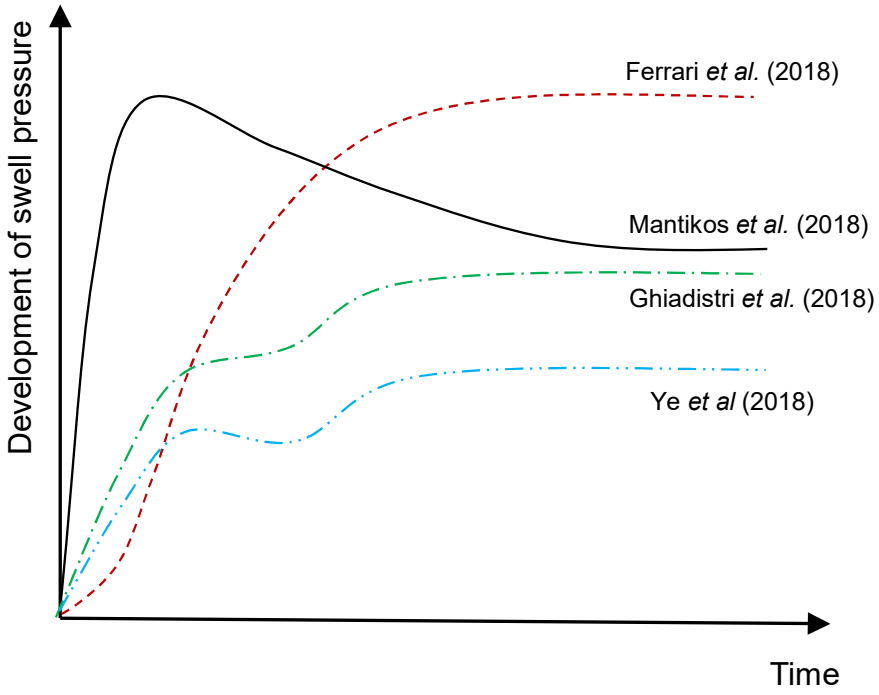

Figure 32: Qualitative illustration of the development of swell pressure in sand-bentonite mixtures

3.3.4 Limitations and applicability of various test methods

Perhaps the most apparent limitation of all the above-mentioned conventional methods is the fact that there is no control of suction or moisture intake, i.e. samples are wetted to a point of zero suction. This is sometimes erroneously described as being wetted to full saturation (Schreiner, 1988*b*). While it is possible that soils in practice may be wetted to a point of zero suction, this may not correspond to full saturation. As illustrated in Figure 6, although a wetting process of an unsaturated soil may well reduce suction to zero, it frequently does not achieve full saturation again. Such tests therefore provide an indication of the 'worst case scenario'.

Another issue of concern is whether the stress paths undertaken during any of these conventional oedometer tests represent field conditions. Schreiner & Burland (1991) compared the results of the three different test procedures and stated how the swell under constant load test was a stress path most representative of what would happen in practice. Such a situation would be one where a structure is erected while the soil is at its in-situ moisture content, and wetting of the soil only occurs after construction. The swell followed by consolidation test was also deemed to be a representative stress path if the 'pre-wetting' approach to construction

was taken. This approach, briefly discussed by Templer (1957), involves soaking the soil and allowing swell to occur before construction takes place.

Schreiner & Burland (1991) describe how if the soaking process is effective, little swell will occur after construction and settlement of the structure can be determined using consolidation theory from the data obtained from the loading part of the test. Schreiner & Burland (1991) went on to state that the constant volume test was unlikely to be relevant to most typical engineering applications. It should be noted that this publication was written in the context of estimating swell potential. It is the author's opinion, however, that useful information on the development of swell pressure during a wetting process can still be obtained from constant volume swell tests, as discussed in Section 3.3.3.

The third and perhaps most limiting aspect of conventional oedometer tests is the lack of radial stress measurements throughout a test. While all three tests can be used to determine vertical swelling pressures, lateral swell pressures are of particular importance for many geotechnical engineering problems, such as buried pipelines (Kassif & Zeitlen, 1962) retaining walls (Katti et al., 1983; Richards & Kurzeme, 1973), tunnels (Liu & Vanapalli, 2007) and piled foundations (Liu & Vanapalli, 2007). Of the studies listed above, all were specifically directed at swelling clays, and in the studies performed by Richards & Kurzeme (1973) and Katti et al. (1983) it was shown how lateral pressures were significantly larger than the corresponding vertical stresses.

The work of Schreiner & Burland (1991) help shed light on this issue where tests were conducted using a stress path oedometer developed at Imperial College, London. In this publication the results of swell tests using the three methods discussed in previous sections were tabulated. Some of these results have been reproduced in this section to highlight some key aspects relating to lateral induced swell pressures. The reproduced data has been plotted in such a way as to be comparable with conventional interpretation of swell tests. However, since the oedometer used by Schreiner & Burland (1991) allowed for soil suction to be measured, more detailed descriptions of the soil behaviour can be obtained from the original publication.

As stated previously, the swell under constant load test represents a stress path most likely to be encountered in practice. It is also representative of the centrifuge tests conducted in this study, which are described later. For this reason, it is this test result that has been reproduced in Figure 33. Figure 33 a) presents a similar relationship to what was described in Section 3.3.2. A sample at its compacted moisture content was placed in the oedometer at Point A, after which a vertical stress of 50 kPa was applied (Path AB). Suction in the sample was then reduced to

0 kPa along Path BC, resulting in the observed increase in void ratio. From this result, two important aspects should be recognised.

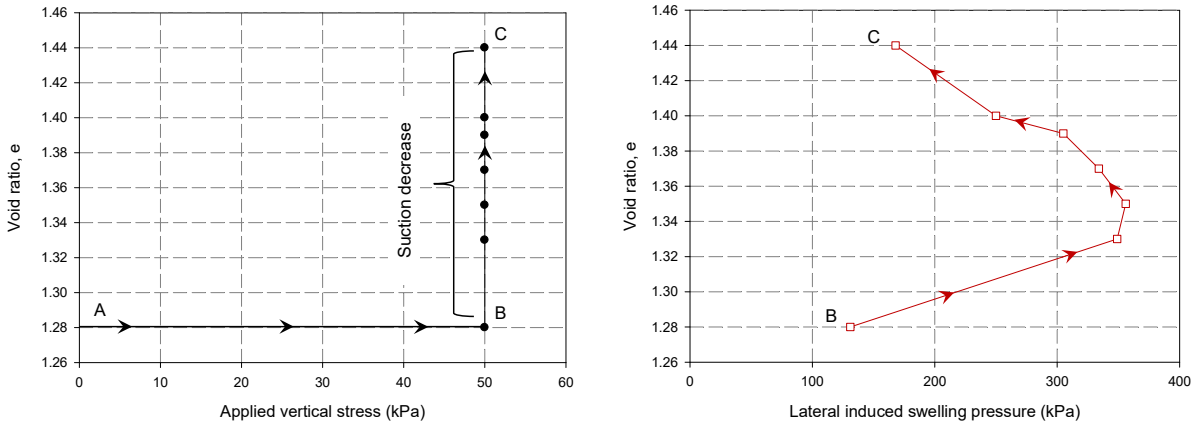

(a) (b)

Figure 33: Results of swell under constant load tests illustrating a) the relationship between void ratio and applied vertical stress and b) the swell induced lateral stresses upon wetting (reproduced by data from Schreiner & Burland, 1991)

1. K_o does not remain constant during a swelling process.
2. The highest lateral induced swelling pressure occurs early on in the swelling process.

Similar results for tests conducted in the same stress path oedometer are presented by Schreiner & Burland (1987). Robertson & Wagener (1975) investigated the development of lateral stresses upon soaking of a fill for the design of an abutment. In this study it was found that the maximum lateral stress measured, occurred before wetting was completed. Taking the lateral induced pressure at the end of a wetting process as the basis of a design may therefore not be adequate.

Similar to the soaking under load curve obtained by several swell under constant load tests, as described in Section 3.3.2, Fourie (1991) investigated the use of a lateral strain belt used in a triaxial apparatus to measure the lateral swelling pressure. In his study, Fourie (1991) performed several tests whereby a sample was soaked and allowed to swell (or compress) under constant isotropic stresses (this is analogous to the oedometer results presented in Figure 30). During the soaking process, lateral strains were measured using a lateral strain belt. Fourie (1991) found how the lateral swell pressure was double the vertical swell pressure determined from a soaking under load curve as illustrated in Figure 34. This finding is in agreement with

Schreiner & Burland (1991) who noted that the lateral pressures induced during a swell process can be many times greater than the applied vertical pressure. An additional interesting finding from the study conducted by Fourie (1991) was the effect of allowing a finite amount of strain on the measured swell pressure. This result is reproduced in Figure 35 and is useful since it demonstrates how a structure can be designed for a significantly lower lateral stress, if it is anticipated that some degree of lateral strain will be allowed.

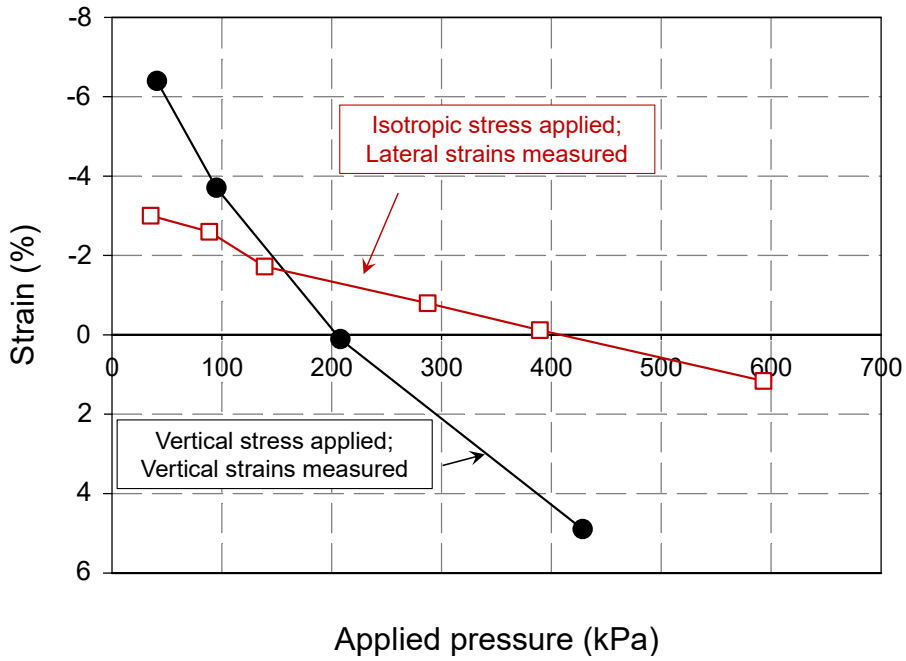

Figure 34: Comparison of vertical and lateral induced swelling pressure (after Fourie, 1991)

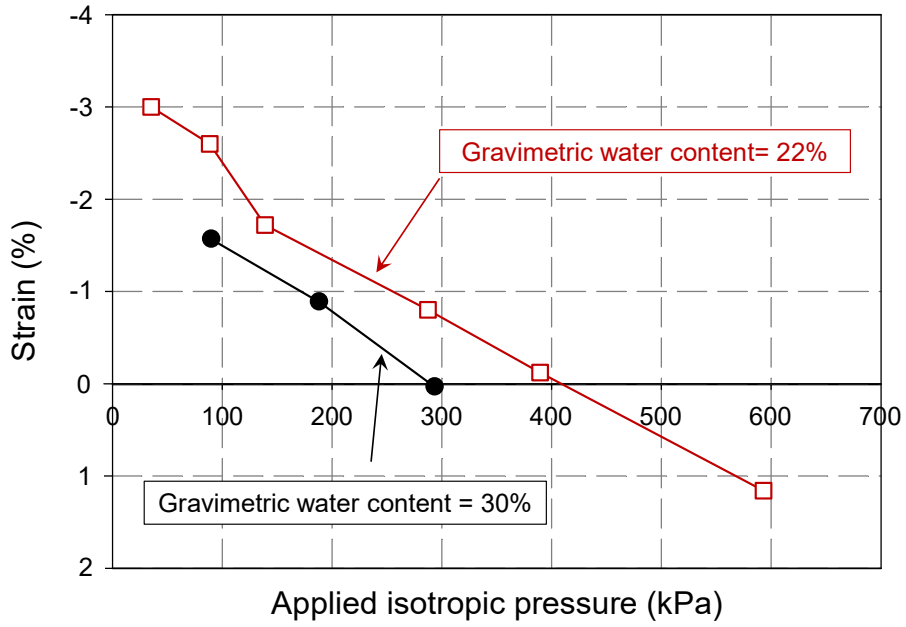

Figure 35: Variation of final measured lateral strain with applied cell pressure (after Fourie, 1991)

3.3.5 Concluding remarks on the testing of expansive clays

The benefit of using stress path controlled oedometers are vital to the understanding of the highly complex geotechnical problems associated with expansive soils. Such equipment is invaluable to the advancement of the understanding of swelling clays. It should however be noted that such equipment will rarely be readily accessible to the practising engineer. In light of this, the limitations of conventional testing should be recognised by the design engineer and emphasised by researchers for whom sophisticated testing equipment is readily available.

3.4 Determination of heave from empirical approaches

In addition to the aforementioned laboratory tests discussed in previous sections, many empirical prediction methods are often employed to ascertain the magnitude of heave to be expected. If these predictions illustrate severely problematic soils, further testing, such as those mentioned in the previous sections *should* be carried out. While there are a vast number of prediction methods available in the literature (see Vanapalli (2012) for an extensive review of prediction methods), there are “too many methods and the range of field conditions too great for a single method to be universally acceptable” - (Schreiner, 1988*a*). For this reason, only five prediction methods commonly used in Southern Africa (and throughout the African continent) are presented.

As discussed by Schreiner (1988*a*), there are two broad categories of prediction methods.

1. Those using classification data only to qualitatively assess the intrinsic expansiveness of the soil, i.e. Atterberg limits and clay fraction.
2. Those incorporating one or more other soil variables such as moisture content, stress and density, in addition to classification data.

Of the methods described in the section that follows, one falls into the first category requiring only classification data for its implementation. The rest of the approaches described incorporate one or more additional variables. The section is concluded by applying all of the above-mentioned methods to a 7.5 m profile of the material conducted in this study to illustrate the range of predicted heave that can be expected using the different applied methods. The reasoning for considering a profile that is 7.5 m deep is that this was the depth considered in the centrifuge modelling of this study. This depth is also representative of formation from which material was sampled.

3.4.1 Van der Merwe (1964)

The Van der Merwe (1964) method was based on observations of heave of buildings in the Free State province of South Africa. The attractiveness of this approach and its continued usage 56 years after publication is likely due to the ease with which it can be implemented. The only parameters required for this prediction method are the Atterberg limits and the percentage of clay in the soil profile. Surface heave prediction is then carried out as follows.

1. According to the Plasticity Index (PI) of the whole sample and its clay fraction, the soil is classified as having a low, medium, high or very high potential expansiveness. The PI required for this classification is that measured on the 'whole sample' rather than that measured only on the portion passing the 0.425 mm sieve as is typically specified by testing standards (ASTM D4318–17e1, 2017). These divisions have been illustrated in Figure 36.
2. According to its classification, the soil is assigned a unit heave based on the correlation provided by Jennings & Kerrich (1962) illustrated in Table 3.

3. A factor is included in the calculation to decrease the amount of predicted heave with depth. This reduction factor is "due to increases in weight of overlying soil, and due to decreases in changes in moisture content and other factors" (Van der Merwe, 1964).

4. The swell of a particular expansive layer is then calculated using Equation 7.

$$S^* = t \times h \times F \tag{7}$$

Where:

S^* = swell (m)
t = thickness of expansive layer (m)
h = unit heave (m/m)
F = factor to account for overburden pressure, moisture content and other factors

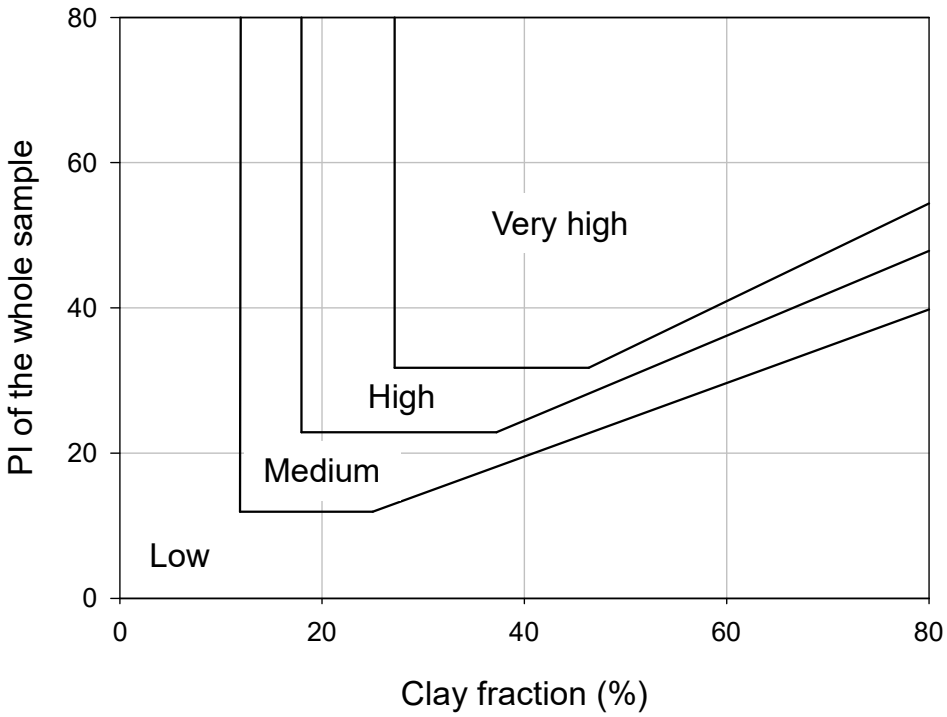

Figure 36: Expansiveness classification

Table 3: Classes of potential expansiveness

Class	Unit heave m/m
Very high	0.08
High	0.04
Medium	0.02
Low	0.00

Some limitations specific to this prediction model is that it does not account for the in-situ moisture content, soil suction or density of the soil. It has also been observed that this method can overpredict the observed swell (Jones et al., 2016). Furthermore, the factor introduced to reduce heave with depth is a function of depth, rather than unit weight or overburden pressure, both of which are more fundamental parameters and would make the approach more widely applicable.

3.4.2 Jones (2017)

The method proposed by Jones (2017) incorporates a simple modification to the Van der Merwe (1964) approach such that it allows for changes in moisture content to be accounted for. This simple modification changed only the unit heave (presented in Table 3) to a modified unit heave as illustrated in Table 4 as strain per percentage change in moisture content.

Table 4: Modified unit heave

Class	Unit heave ($m/m/\Delta w$)
Very high	0.0050
High	0.0025
Medium	0.0013
Low	0.0000

The modified unit heave requires an estimate to be made of the change in moisture content. The in-situ moisture content of the clay can be easily determined by conventional means, but the degree to which it changes will need to be estimated. In citing Weston (1980), Jones (2017) stated how the equilibrium moisture content of a soil can be estimated as half of the soil's liquid limit. This moisture content change can however also be made based on engineering judgement

and knowledge of the local site conditions. The calculation of swell for a particular expansive layer is performed using Equation 8.

$$S^* = t \times h_m \times F \tag{8}$$

Where:

S^* = swell (m)
t = thickness of expansive layer (m)
h_m = modified unit heave ($m/m/\Delta w$)

While this modification does account for changes in moisture content, it still suffers from the other drawback of the Van der Merwe (1964) approach in that it does not account for soil density. Furthermore, as with the Van der Merwe (1964) method, the empirical factor used is based on depth in the soil profile rather than unit weight or overburden pressure.

3.4.3 Weston (1980)

Weston (1980) proposed an empirical relationship for the prediction of heave which accounts for the initial moisture content, overburden pressure and the weighted liquid limit of the soil. The relationship was based on the results of 41 oedometer swell tests from samples taken along the national roadway (N_1) between the provinces of Gauteng and Limpopo in South Africa. The empirical equation was then found to compare well with the measured heave beneath a roadbed. The proposed prediction method has been illustrated in Equation 9.

$$S = 0.000411 \cdot (W_{LL})^{4.17} \cdot (\sigma_v)^{-0.386} \cdot {w_i}^{-2.33} \tag{9}$$

Where:

S = swell potential (%)
w_L = liquid limit (%)
W_{LL} = weighted liquid limit = LL×(% passing 0.425 mm)
σ_v = total vertical (overburden) pressure (kPa)

w_i = initial moisture content (%)

This approach has the benefit of accounting for overburden pressure and initial moisture content, in addition to the weighted liquid limit which provides an indication of the soil's intrinsic expansiveness. One drawback of this approach is that the weighted liquid limit is raised to the power of 4.17. Placing this much emphasis on a single parameter should be done cautiously, especially when the parameter in question is problematic to quantify repeatably. A study by Jacobsz & Day (2008) investigated the differences in basic soil properties reported by 4 different commercial laboratories in South Africa. The study revealed a variation in measured liquid limit of between 53–78%, with all tests being conducted on the same material. Gaspar (2019) illustrated how Weston's approach predicted significantly higher values of swell as compared to the Van der Merwe (1964) method, despite accounting for initial moisture conditions. This study also investigated the variation in predicted heave by varying the liquid limit $\pm$ 5%. It should therefore be borne in mind that while Weston's approach does make provisions for initial moisture content, it should be used with caution, particularly for soils with high liquid limits.

3.4.4 Brackley (1975*a*)

This approach is based on extensive laboratory testing on samples obtained in and around the province of Gauteng in South Africa. The benefit of this approach over the others presented in this section, is the fact that it accounts for the initial void ratio of the sample. The empirical prediction model is presented in Equation 10.

$$S = \left(5.3 - \left(\frac{147 \cdot e_o}{PI}\right) - \log_{10}\sigma_v\right) \times (0.525 \cdot PI + 4.1 - 0.85 w_i) \tag{10}$$

Where:

S = swell potential (%)
e_o = initial void ratio
**all other variables defined in previous equations*

By accounting for the most soil properties of the methods presented it could be argued that this prediction model is the most rigorous. However, the approach proposed by Brackley

(1975*a*), like the other relationships presented, is empirical and should therefore be used cautiously.

3.4.5 Brackley (1980)

What sets the approach by Brackley (1980) apart from the others presented in this section is that it accounts for soil suction. Soil suction, unlike moisture content is a more rational parameter to consider since it is independent of soil type (Williams et al., 1985). Brackley's (1980) prediction method is presented in Equation 11.

$$S = \left(\frac{PI - 10}{10}\right) \times \log_{10} \cdot \frac{s}{\sigma_v} \tag{11}$$

Where:

S = swell potential (%)
s = matric suction (kPa)
**all other parameters defined in previous equations*

A characteristic of an expansive clay profile in the field is that it can often be highly fissured. In such a profile, the exposed surfaces along the fissures will be drier than the centre of an intact mass of soil, thus having substantially higher suctions. Consider the soil element presented in Figure 37.

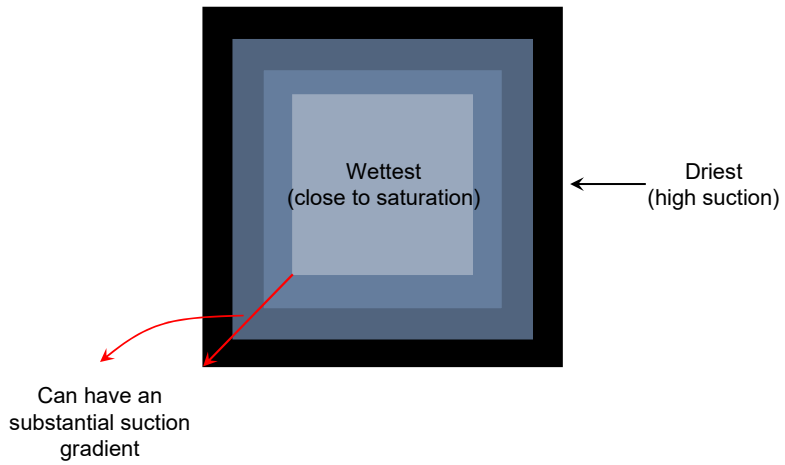

Figure 37: Variation in moisture content for an element of intact expansive clay

Figure 37 provides a graphical illustration of a likely distribution of suction within an intact mass of expansive clay. In such a scenario, suction measured on the outer surface may be too high, while a measurement from the centre may be too low. This raises the question as to what a 'representative' value of suction will be to accurately predict the heave of an expansive profile in the field, or indeed to model it using some constitutive relationship. To the author's knowledge, there is no such published guidance on how this 'representative' value of suction should be established.

3.4.6 Comparison between methods

Figure 38 illustrates the predicted heave for each of the methods discussed for a 7.5 m profile (the depth that was simulated in the centrifuge modelling of this study). Table 5 summarises the predicted heave for each of the approaches. The predictions were made for the clay type used in this study which was adequately characterised for these predictions. For both the Van der Merwe (1964) and Jones (2017) approach, the soil classifies as having a *very high potential expansiveness*.

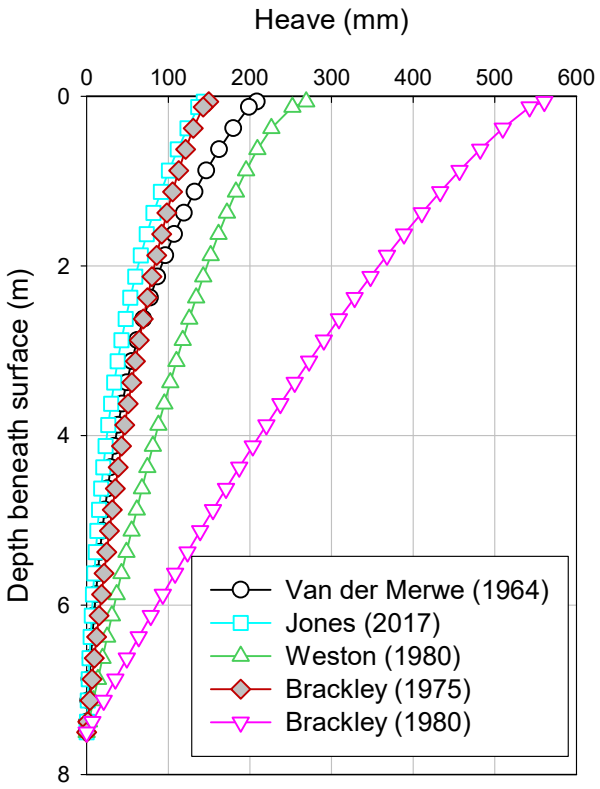

Figure 38: Heave profiles predicted using the estimation methods discussed

Table 5: Predicted surface heave from each of the methods described

Prediction method	Surface heave(mm)
Van der Merwe (1964)	208
Jones (2017)	143
Weston (1980)	269
Brackley (1975*a*)	150
Brackley (1980)	561

Being all empirically derived methods, the vast range of predictions made is perhaps not surprising. What is arguably more noteworthy is that it is not enough to simply regard one method as being more accurate due to the number of soil parameters it accounts for. The simplest of the methods described above (Van der Merwe, 1964) has been said to overpredict heave in comparison to field observations (Jones et al., 2016). Figure 38 illustrates that this approach predicted far less heave than both the Weston (1980) and Brackley (1980) methods. Possible explanations for these substantially higher predictions are due to the limitations discussed in Sections 3.4.3 and 3.4.5. A positive feature of the results presented in Figure 38 is that, with the exception of the method proposed by Brackley (1980), all predictions follow a similar trend, becoming increasingly non-linear towards the soil surface. Since many of these methods have been seen to compare well with field observations, it would seem that such a trend is characteristic of expansive soil profiles. This is in contrast to observations for swell under load tests (discussed in Section 3.3.2) which have been shown by several researchers to predict a linear relationship. This discrepancy perhaps illustrates that there are some mechanisms occurring at full scale which are not captured in oedometer testing.

In a discussion of expansive clays, Sparks & Pigeon (2011) stated how “It is a most disconcerting fact that certain soils have not ‘read’ the published theories”. The personification made in this statement, while not abiding to conventional scientific language, does well to emphasise a valid point. It should not be forgotten that the approaches described above were all derived for a particular class of soils under specific conditions. While these methods are useful in providing a first estimate of soil heave, they are by no means quantitative predictions applicable to all situations which might be encountered. The usefulness and limitations of each approach should always be borne in mind by the engineer, with further testing being done where applicable.

3.5 Construction on swelling clays

Since the problems associated with swelling clays have long been recognised, it should come as no surprise that a number of approaches have been developed and implemented over the years for the design of foundations on expansive clays. Broadly speaking, the design approaches carried out across the world can be subdivided into the following categories. A brief description of the various methods is provided in this section. The methods that are discussed have been listed below.

1. Soil treatment or replacement.
2. Construction directly on an expansive profile.
3. Isolation of superstructure from expansive soil.

3.5.1 Soil treatment or replacement

Removal and replacement of expansive clays are generally economical solutions when the depth of the profile is shallow (approximately 2 m deep), and when suitable inert material is readily available (Byrne et al., 2019). Alternatively, the soil can be 'treated' by pre-wetting the profile such that swell occurs before construction, thus limiting structural distress. Drawbacks of this approach include the time taken for the soil to reach an equilibrium moisture content, and the uncertainty of future changes in moisture throughout the lifetime of the structure (Byrne et al., 2019). It is however, a method that has been shown to work satisfactorily in road construction (Weston, 1980). Alternatively, the use of lime in the stabilisation of expansive clays has also been recognised as an alternative method of soil treatment (Charlie et al., 1985; Jones & Jefferson, 2012).

3.5.2 Construction directly on an expansive profile

Such methods allow for a certain amount of heave but attempt to keep differential foundation movements within tolerable limits. Arguably the most popular use of this approach is the utilisation of stiffened raft foundations (Byrne et al., 2019; Charlie et al., 1985; Li et al., 2014; Pellissier, 1997). In reviewing common practices for the design of stiffened raft foundations on swelling clays in South Africa, Day (2013) stated how the different design methods can be divided into the "plate-on-mound" or the "swell-under-load" approach. The "plate-on-mound" approach assumes that the raft is placed on a mound that already exists. A stiffened raft is then

designed to resist the bending moments resulting due to the 'cantilever' sections of the raft. In contrast, the "swell-under-load" approach attempts to predict distortions of the foundation resulting from moisture fluctuations in and around the stiffened raft after construction. Of the two methods, the "plate-on-mound" approach is far simpler to apply and generally results in a conservative design (Day, 2013). Other more innovative raft designs are described by Day (2013) but have not been included in this discussion. Figure 39 schematically illustrates how the use of a stiffened raft foundation would act to reduce differential heave such that distress on the superstructure is minimised.

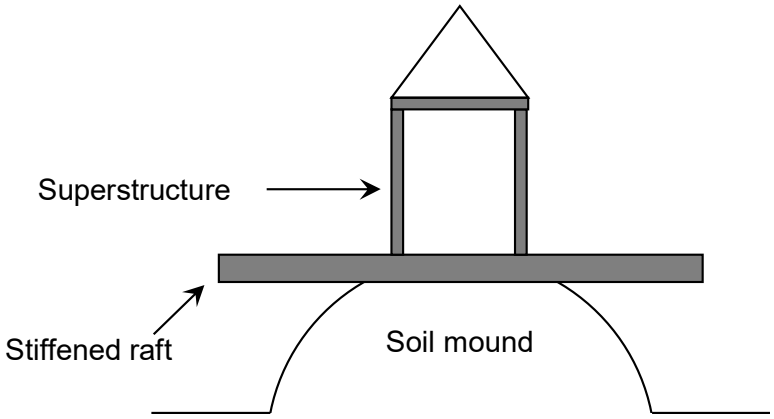

Figure 39: Conceptual illustration of a stiffened raft foundation on swelling clays

Another design method which falls under this category is one where conventional foundations are used with an articulated superstructure (Byrne et al., 2019), i.e. joints are provided such that different sections of the superstructure can move independently, thereby eliminating structural distress. Byrne et al. (2019) suggests that this method should only be used where the estimated total heave values do not exceed 25 mm.

3.5.3 Isolation of superstructure from expansive profile

Of the methods described thus far, isolation from the superstructure is the most expensive to implement. The approach generally involves piled foundations, extending either to bedrock where they can be socketed, or enlarged base piles founded on or within a stable soil horizon (Byrne et al., 2019). These piles are then used to provide a 'suspended' foundation which is completely isolated from the expansive profile. The gap provided between the suspended foundation and the ground level provides space for the soil to swell into, without affecting the superstructure. This approach to design on expansive clays has also been briefly mentioned by Fleming et al. (2009). Piles used in this construction method can be subjected to large uplift

forces due to heaving soil around the pile. To ensure cracking of the piles does not occur, they can either be adequately reinforced, 'sleeved' (provided with a slip layer) or a combination of these measures can be implemented (Fleming et al., 2009). Figure 40 provides a simple conceptual schematic on how this foundation type would be intended to operate. Figure 41 provides some specific details on the pile designs.

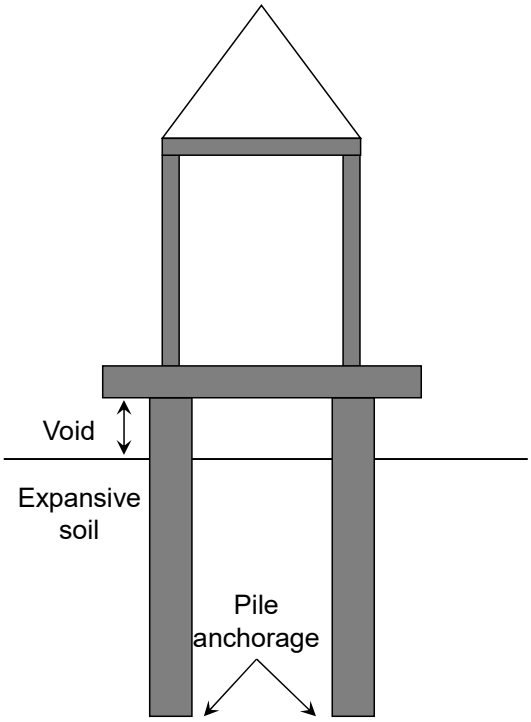

Figure 40: Basic concept of isolation of superstructure from underlying expansive clay

In Figure 41 a) it can be seen that the pile has extended to bedrock where it has been anchored by cementing it into position. Figure 41 b) illustrates a situation where perhaps the depth to bedrock was too great, making it uneconomical to drill to such depths. In such a situation, the pile can be anchored in a stable soil horizon using an enlarged base to counter the uplift forces. In this instance the term "stable soil horizon" is used to refer to a zone where no swelling takes place, either due to a lack in moisture content change, due to large overburden stresses acting to prevent swell, or a combination of both factors. As stated earlier, either design would require the pile to be adequately reinforced so as to reduce tensile cracking caused by heave of the expansive profile. Another measure illustrated in Figure 41 b) was the use of a sleeve which is free to move along the length of the pile, thus reducing uplift forces.

There are situations where an expansive profile can be extremely deep, thus making either of the above design approaches uneconomical. In Kimberley, South Africa, expansive profiles

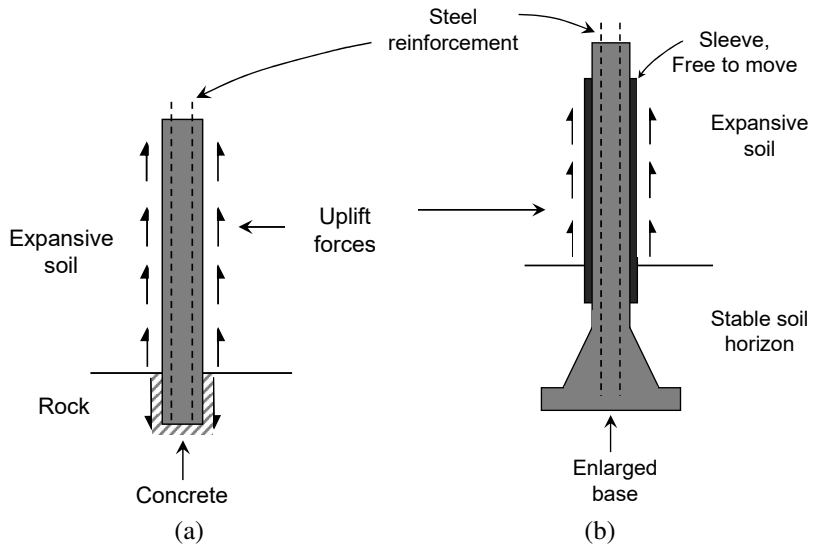

Figure 41: Detailed illustration of different piling options: a) rock socketed pile and b) enlarged base pile with a sleeved shaft

have been found to extend to a depth of up to 30 m (Byrne et al., 2019). Other instances of deep expansive profiles are have also been reported in Sudan, where it is not uncommon to have expansive profiles extending to greater than 10 m (Elsharief, 2012). In such situations, recommendations are made to have a minimum pile length of 7 – 8 m, twice the depth of seasonal moisture fluctuations (Charlie et al., 1985). Such provisions together with others described by Charlie et al. (1985) have been shown to perform adequately. It should however be noted that the piles themselves, have been shown to provide a flow path for water such that heave can be observed even beneath the base of the pile (Pellissier, 1991).

The use of such design approaches can result in doubling the cost of construction in comparison to a conventional strip footing foundation (Jennings & Kerrich, 1962) but, if applied correctly, can result in almost no foundation movements. It should therefore only be used where foundation movements are critical to design. However, while the design may seem like a fail-safe approach, it is not without its problems.

A case study in South Africa reports where such a design was used for various buildings at a thermal power plant. While the initial heave calculated for this site was in the order of 120 mm (Blight, 1984*a*), this was a gross underestimation of what was observed. Prior to construction, the land consisted of Eucalyptus (blue gum) plantations which have tremendous water demands and can lower the water table to significant depths (Day, 2017). Felling of the trees prior to construction resulted in rising of the water table, causing far greater heave than

what was initially estimated. As a result, remedial measures had to be taken. Such measures included isolation of the pile shaft from the surrounding material, additional reinforcement of the shafts to resist uplift forces and voids between the expansive clay and the suspended slabs were increased to 300 mm. It has been noted that beneath some of the buildings at the power plant, this gap has swelled completely closed requiring removal of soil below the pile caps (Day, 2017).

This particular case study led to a number of useful investigations on this method of construction on swelling clays. Blight (1984*a*) conducted pull-out tests on short length piles before and after wetting the profile for a period of 3–4 weeks. His results indicated that an increase in pile pull-out (shaft) capacity was observed after wetting. This finding was in direct contradiction with a study conducted by (Elsharief et al., 2007) for pile load tests conducted in Sudan. A study by Offer & Blight (1985) found how measurements of lateral stresses in an oedometer were far greater than what was back calculated from the pull-out tests reported by Blight (1984*a*). Offer & Blight (1985) attributed these differences by failure of oedometer samples to capture the fissured structure present in the field, which lead to an apparent high lateral compressibility of the clay.

Another case study where such a design approach resulted in structural damage was reported by (Meintjes, 1991). The study reported the results of severe structural distress experienced at a primary school in Vryburg, South Africa. The structural damage occurred despite the foundation being designed to have a void of 150 mm between the grade beam and pile cap, and under-reamed/enlarged base piles extending to a depth of 7.7 m. This case study also led to a number of additional investigations which will not be discussed in this thesis. However, in reviewing these case studies, it becomes clear that much remains to be understood regarding the implementation of this foundation type on swelling clays.

The element testing described in Section 3.3 is invaluable in highlighting a number of fundamental aspects associated with swelling clays since tests can be performed on samples where the stress state can be fully defined. Site investigations such as those reported by Offer & Blight (1985), Blight (1984*a*), Meintjes (1991) illustrate the importance of capturing the macroscopic fissured structure typical of expansive clays. Centrifuge modelling is an investigative tool which lies somewhere in between these two extremes, allowing larger samples to be tested and for the stress state of the soil to be better defined than what would be possible in the field. For this reason, centrifuge modelling was ultimately the focus of this thesis.

3.6 Summary

A review of the literature of unsaturated expansive soils presented in this chapter highlights the complexity of this problem soil. From the studies referred to, it can be seen that the majority of investigations done on this soil type occurred between the late 1950s to the early 1990s. During this period, many important contributions were made to the understanding of swelling clays. However, due to the limitations in the available measuring techniques, studies considering the effects of soil suction and the mechanisms governing unsaturated soils were limited. As a result, many empirical prediction methods were developed to guide geotechnical engineers in design. As discussed in Section 3.5, there are several approaches to construction which can be implemented when this problem soil is encountered. The focus of this study is however to investigate aspects of piled foundations in swelling clays. By making use of the technological developments and advancements in the understanding of unsaturated soil mechanics, this investigation aims to add to the pioneering research of previous generations. In doing so, a more comprehensive description of the behaviour of this problem soil can be provided.

CHAPTER 4

CENTRIFUGE MODELLING IN GEOTECHNICS

One of the main benefits for using a centrifuge in geotechnical testing is due to the fact that the stress-strain behaviour of soil is highly non-linear (Madabhushi, 2015) and dependent on self-weight. For this reason, testing a scaled model of a full-scale structure (referred to as the prototype) will lead to erroneous stress-strain behaviour. To emphasise this point, consider Figure 42 and Figure 43. Figure 42 illustrates a graph commonly used in many undergraduate textbooks to describe the behaviour of a loose sand. Figure 43 illustrates a prototype soil profile, and the corresponding test model scaled down by a factor of $N = 10$ respectively.

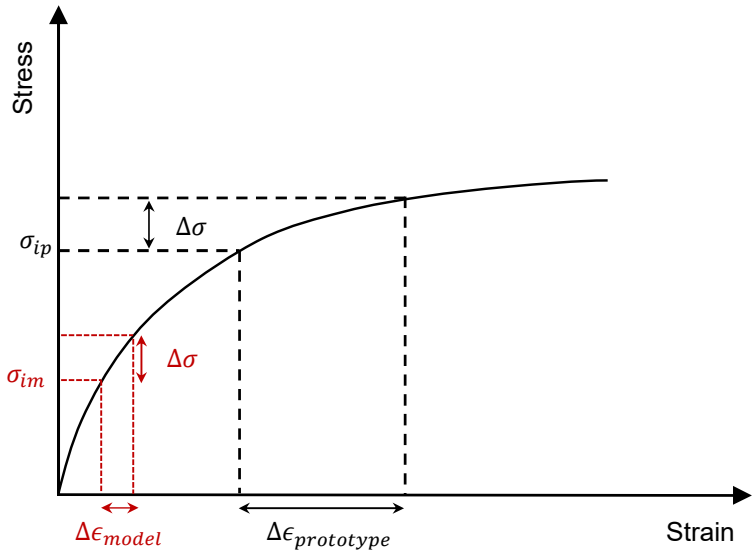

Figure 42: Non-linear stress-strain behaviour of soils

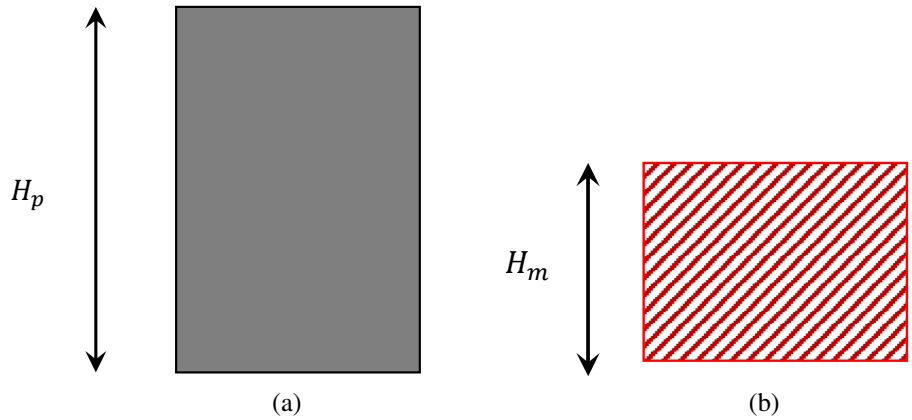

Figure 43: Illustration of a soil profile at a) prototype scale and b) model scale

If one was to calculate the total vertical stress midway through the profile, this could be done for either profile by using Equation 12.

$$\sigma_v = \rho_b \cdot g \cdot \left(\frac{H}{2}\right) \tag{12}$$

Where:

σ_v = total vertical stress (Pa)
ρ_b = bulk density (kg/m^3)
g = gravitational acceleration at the surface of the earth (m/s^2)
H = profile depth (m)

Considering that the scaled model is a factor of 10 smaller, the resulting stress calculated at this point would intuitively also be scaled down 10 times. This can be visualised in Figure 42 where the initial stress states in both the model and prototype profiles are denoted by σ_{im} and σ_{ip} respectively. If the stress on either profile were to be increased by the same amount, for example, due to foundation loading ($\Delta\sigma$), the corresponding change in strains for the model and prototype would be vastly different, as illustrated by $\Delta\varepsilon_{model}$ and $\Delta\varepsilon_{prototype}$. This illustrates how the behaviour of the scaled model would be completely unrepresentative of the true field conditions. Centrifuge modelling corrects for these behavioural differences by increasing the acceleration acting perpendicular to the scaled model by a factor of N. By doing so for the

profile presented in Figure 43 b), the total stress calculated midway through the profile would be calculated by Equation 13.

$$\sigma_v = \rho_b \cdot N \cdot g \cdot \left(\frac{H}{2}\right) \tag{13}$$

Where:

σ_v = total vertical stress (Pa)
ρ_b = bulk density (kg/m^3)
N = model scale factor
g = gravitational acceleration at the surface of the earth (m/s^2)
H = profile depth (m)

From this example it can be seen how the use of centrifuge modelling can, in certain instances, replicate field conditions thus eliminating the need for full scale testing, saving both time and money. While centrifuge modelling has become increasingly popular in the geotechnical community over the past few decades, it is a concept which has been recognised for nearly a century.

In the South African context, the first known usage of a centrifuge to study geomaterials occurred in the 1960s. The machine was designed by Dr. Evert Hoek during his time at the Council for Scientific and Industrial Research (CSIR) with the intention of testing intact rock, an idea he got from Professor Boskov at Columbia University, New York in 1961 (Hoek, 2020). Figure 44 illustrates the centrifuge, which was designed to operate at 1000 g, carrying packages of up to 100 *lb* (Hoek, 2020).

However, a more a comprehensive review of the early developments of centrifuge modelling in geotechnics can be found in the 20th Rankine Lecture presented by Schofield (1980). This publication provides an overview of the work carried out at Cambridge University since 1973.

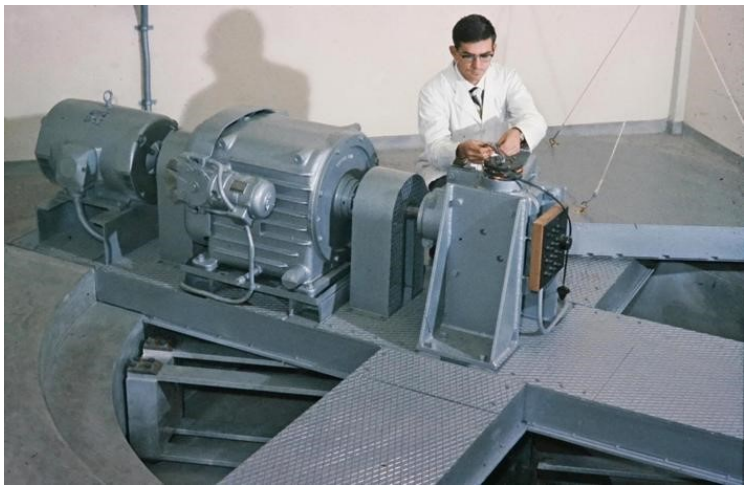

Figure 44: Centrifuge at the CSIR South Africa, designed by Dr. Hoek (Hoek, 2020)

4.1 Basic operational principles

The basic layout of the beam centrifuge used at the University of Pretoria (Jacobsz et al., 2014) is illustrated in Figure 45. The layout of the alternative drum centrifuge is not discussed in this section.

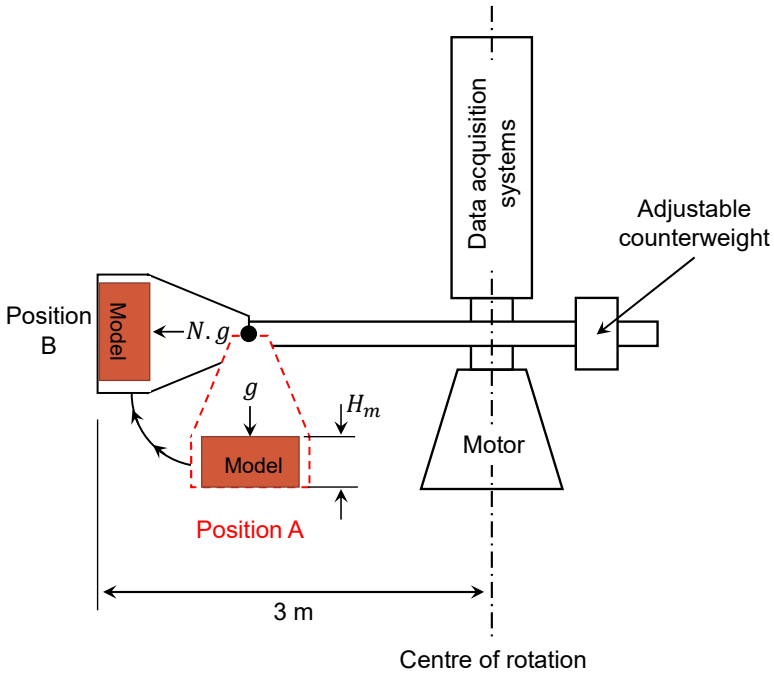

Figure 45: Basic layout of the beam centrifuge at the University of Pretoria

Originally, the $1/N$ scaled model is put onto the centrifuge swing at Position A. At this point the model merely experiences earth's gravitational acceleration, g. To achieve the enhanced acceleration on the model such that prototype stresses are achieved, the beam is rotated at an angular velocity of $\dot{\theta}$. After achieving the desired angular velocity, the model will be at Position B. The enhanced acceleration experienced perpendicular to the model is dependent not only on $\dot{\theta}$, but on the distance from a specific point on the model from the centre of rotation defined as r. This relationship is provided in Equation 14.

$$N \cdot g = r \cdot \dot{\theta}^2 \tag{14}$$

Where:

N = model scale factor (dimensionless)
g = gravitational acceleration at the surface of the earth ($\mathrm{m/s^2}$)
$\dot{\theta}$ = angular velocity ($1/\mathrm{s}$)

The angular velocity is set such that the desired centrifugal acceleration of $N \times g$ is experienced at the centre of gravity of the model (occurring at two thirds from the model's base). The distance between the centre of rotation and the centre of gravity of the model can be referred to as the effective radius (r_e). The relationship presented in Equation 14 illustrates the dependency of the enhanced gravitational acceleration on the distance from the centre of rotation of the centrifuge. This relationship results in some spatial errors regarding the stresses experienced at various positions in the model. These errors/limitations are discussed in the following section.

4.2 Errors and limitations of centrifuge modelling

The gravitational acceleration experienced at the surface of the earth is commonly accepted to be g =9.81 $\mathrm{m/s^2}$. For all practical civil engineering purposes, this value is constant regardless of how tall or deep a building or foundation might be respectively. In the geotechnical centrifuge however, this value is not constant and varies with depth throughout the model as illustrated in Equation 14. Figure 46 illustrates the variation in model stress with depth.

Since the angular rotation is set such that an acceleration of $N \cdot g$ is experienced at $\frac{2}{3} \cdot H_m$ from the base of the model where H_m is the total model depth, any point above or below this centre of gravity will be under and overstressed respectively. The maximum under-stress will

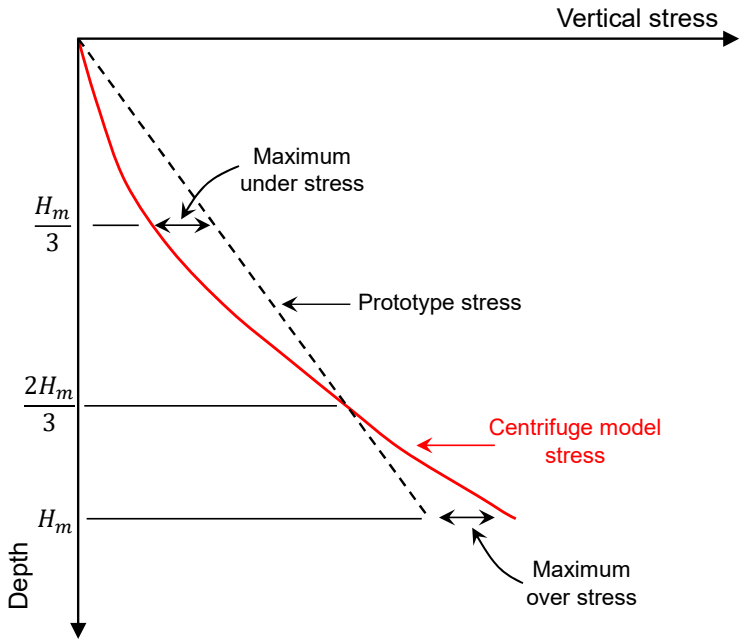

Figure 46: Under and over stresses in a centrifuge model (after Madabhushi, 2015)

be experienced at $\frac{H_m}{3}$ whereas the maximum over stress will be experienced at the bottom of the model, both errors being equal in magnitude. The under and over stress errors are equal in magnitude due to the effective radius of the model (r_e) being taken at $\frac{2}{3} \cdot H_m$ from the base of the model. The maximum error due to the vertical variation in stress within the model is given by Equation 15.

$$Error_{vertical} = \frac{H_m}{6 \cdot r_e} \tag{15}$$

Where:

H_m = total model depth (m)
r_e = effective radius (m)

The centrifuge at the University of Pretoria has a radius of 3 m from the centre of rotation to base of the payload platform. Considering that models were placed on a base that was approximately 150 mm thick, the maximum error along the depth of the profile was approximately 1.6%.

In addition to variability in stresses along the vertical axis, there is also an error induced along the width of the model. This error is again due to the different radii from the centre of rotation to a point in the model along the centre line, and from the centre of rotation to the same depth at a different horizontal location. Figure 47 illustrates the different radii to the base of the platform at the centre line and edge of the model respectively. This error can be calculated using Equation 16.

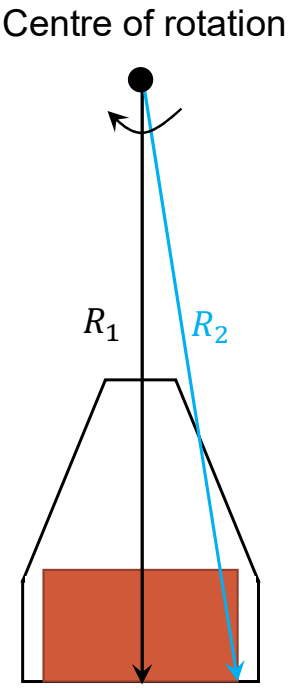

Figure 47: Radial variation in stresses

$$Error_{radial} = \left(1 - \frac{R_1}{R_2}\right) \tag{16}$$

For one of the tests performed in this study, the width of the model was 525 mm which corresponded to an error of 0.41%. This error was reduced to 0.16% in all subsequent models which measured 335 mm in width. While insignificant in the current study, the errors caused by radial variations in acceleration may be significant in some cases, and as such, has led to some researchers designing their models to be curved (Madabhushi, 2015). It is also for this reason that the main features of a model are typically placed at its centre.

4.3 Scaling laws

When increasing the gravitational acceleration acting perpendicular to a scaled model in the centrifuge, there are a number of scaling laws which apply. These scaling laws can then be used to relate various aspects of the model to an equivalent prototype. A list of basic scaling laws has been provided in Table 6.

Table 6: Centrifuge scaling laws

Parameter	Scaling factor (Prototype/model)
Length	N
Area	N^2
Volume	N^3
Mass	N^3
Stress	1
Strain	1
Force	N^2
Seepage velocity	N
Consolidation time	N^2

The scaling law for time relating to swelling processes is generally accepted to be equivalent to the time scaling law for consolidation presented in Table 6. Since consolidation is a diffusion process (Madabhushi, 2015), it is sensible to assume that swell caused by unloading (while the soil is in a saturated state) would simply be the reverse of this process and therefore follow the same time scaling law. To the author's knowledge, research into the time scaling factor for swelling clays from an unsaturated state is limited. However, a study conducted by Caicedo et al. (2006) concluded that the time scaling law used for consolidation was also applicable to this form of swell.

4.4 Modelling of expansive clays in the geotechnical centrifuge

Despite the advantages of centrifuge modelling, few centrifuge studies have been conducted on expansive clays. In the past three International Conferences on Physical Modelling in Geotechnics (ICPMGs) there were three publications investigating swelling soils by centrifuge modelling, namely, Laporte et al. (2018), Plaisted & Zornberg (2010) and Gu et al. (2010). In the discussion of these publications, prototype dimensions will be referred to as the various tests were conducted at different accelerations.

Laporte et al. (2018) conducted a study to investigate roads constructed on swelling clays. In this publication, a 90/10 mixture of kaolinite and bentonite was used, and wetting of the profile was induced in-flight (at 40 *g*) using misting nozzles. Laporte et al. (2018) reported results of heave over time across the width of the profile for several positions in the model, all at a depth of 0.52 m from the soil surface. While moisture content readings below this depth were not reported, in light of the other studies presented in this section, it is unlikely that moisture changes occurred much further beyond this depth.

Plaisted & Zornberg (2010) reported results from a study conducted with a 'miniature' centrifuge, where the distance from the centre of rotation to sample base was reported as 16.5 cm. While this use of centrifuge technology has proven valuable to characterise various aspects of swelling clays (Plaisted & Zornberg, 2011), its intended usage was to accelerate flow processes rather than reproduce the response of earth structure prototypes (Zornberg & McCartney, 2010).

Gu et al. (2010) investigated the lateral stresses induced on a retaining wall due to swelling clays. In this study the moisture content of the soil was increased in-flight in two ways, the first was by ponding water onto the surface of the expansive clay profile. The second approach was to use augered holes to simulate fissuring such that infiltration could be accelerated. For tests where water was ponded onto the soil surface, moisture changes were observed up to a depth of 2 m, whereas for tests conducted with the augered holes, moisture variations extended to the depth of the holes (5 m). The time of the wetting process was not discussed in this publication. An illustration of the model setup used is shown in Figure 48.

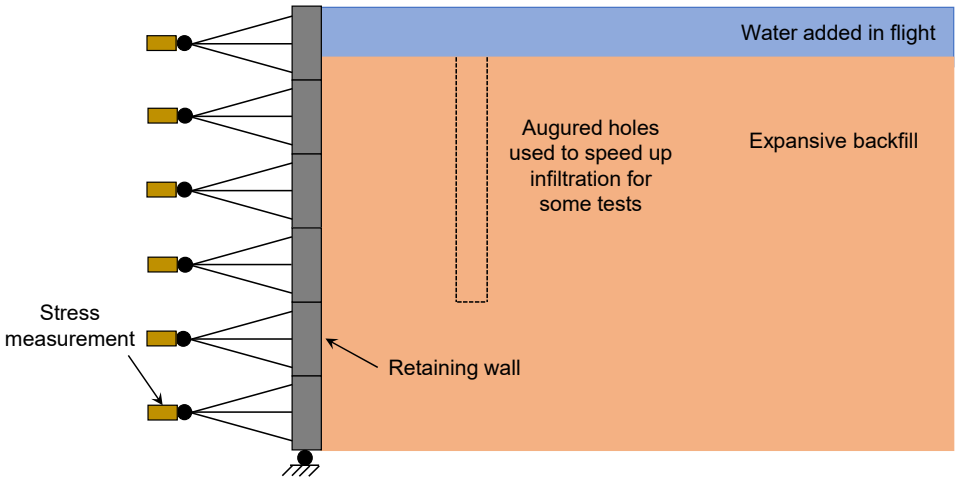

Figure 48: Centrifuge model implemented by Gu et al. (2010)

Another investigation, not presented at an ICPMG was performed by Chen et al. (2017). The purpose of this study was to investigate the stability of slopes comprising swelling clays. In these tests, wetting was not induced in flight, but was performed from the surface using sprayer units to create artificial rainfall. In all tests performed, the wetting processes took between 6–8 hours to reach a steady state condition. It was stated in this study that increases in moisture content were mostly confined to the upper portion of the profile. However, following a few drying and rewetting cycles, the depth of moisture infiltration was increased due to the presence of desiccation cracks.

Recognising the aforementioned studies, an argument can be made that the reason centrifuge modelling has not been extensively carried out on expansive clays, is primarily due to the time required to perform such tests. Expansive clays generally comprise some proportion of smectite minerals in their composition, and are therefore highly impervious. An aspect common to all tests described above is the sample preparation procedure. For all of the above tests, dried clay was mixed with a predetermined quantity of water, allowed to equilibrate and then compacted to a target density. A drawback of this approach is that it results in a fabric with macropores which are relatively isolated. This is in contrast to the fabric type more commonly associated with expansive clays which has a series of interconnected pores (i.e. fissures) that more easily facilitate the ingress of water. For this reason, it has been reported that when moisture is induced from the surface, the wetting front does not extend particularly deep. An explanation for this is that once an increase in moisture content is achieved at the surface, swelling occurs, and the body of the profile is effectively cut off from any simulated precipitation that follows.

This hypothesis is supported by Gu et al. (2010) who found that the use of boreholes increased the depth to which moisture could be increased. It is also supported by Chen et al. (2017) who observed that the depth of moisture variation increased after desiccation cracking was allowed to occur. Since swelling clays most susceptible to an increase in volume are typically in a fissured or desiccated state, this study is invaluable in illustrating the importance of fabric in expansive clays. Inducing this type of fabric through drying processes could however prove difficult to perform in a repeatable manner for comparative tests.

Another common theme from the above tests are that moisture has always been introduced from the surface. It could be argued that this is the most common method by which the moisture content of a soil is increased. However, as was discussed in previous sections, an increase in moisture content can also occur from beneath the structure after construction, when evaporation from the profile is cut off. Furthermore, removal of vegetation prior to construction can also contribute to rising of the water table, which may continue for years, causing severe structural

damage. Finally, it has also been seen that when piling foundations are used, care must be taken to ensure that the piles themselves do not serve as an entry point for moisture as was observed by Pellissier (1991) thereby causing heave at great depths.

4.5 Summary

In this chapter, the basic principles and benefits of centrifuge modelling are highlighted. This addition to geotechnical research provides an alternative to full-scale testing which is both cost effective and less time consuming. It also facilitates the control over boundary conditions and allows for various types of instrumentation to be utilised. In this way, it provides a compromise between carefully controlled element testing and the true behavioural aspects present at full-scale. Furthermore, it was also highlighted how this technological development has not been fully exploited to investigate the behaviour of swelling clays. It is therefore the aim of this study to combine the benefits of element testing and the advancements in unsaturated soil mechanics with the capabilities of centrifuge modelling. This will allow for aspects governing the design of piled foundations in swelling clays to be investigated.

CHAPTER 5

EXPERIMENTAL METHOD

The primary focus of this study was to investigate the use of piled foundations in swelling clays, both under in-situ and swelled states. However, due to the high montmorillonite content of these soils, they are associated with an extremely low hydraulic conductivity. In the field, it is predominantly the highly fissured nature of the material which facilitates the ingress of moisture, ultimately producing the observed heave during the lifetime of a structure. For this reason, the first part of this study was aimed at the development of a closely fissured clay which could be used for centrifuge modelling. Beginning with a general description of the tested soil, this chapter describes the development and preparation method of the closely fissured clay used for centrifuge modelling. Various element testing is then described. This element testing was carried out to investigate any discrepancies in the mechanical and water retention characteristics between the developed and intact clay samples. Following from the element testing, a description of the general layout of all centrifuge tests is provided. The chapter is then concluded with details of all specialised equipment developed for this study.

5.1 Material description

The soil used in this study was sampled from a bentonite mine located in the Limpopo province of South Africa, approximately 350 km northeast of Pretoria. Initial site investigations were carried out to determine the profile of the soil deposit. Figure 49 illustrates the profile description as performed by Day (2020) from the test pit where material was sampled. Tests presented in this thesis were conducted on samples collected from the upper 1.5 m portion of the profile.

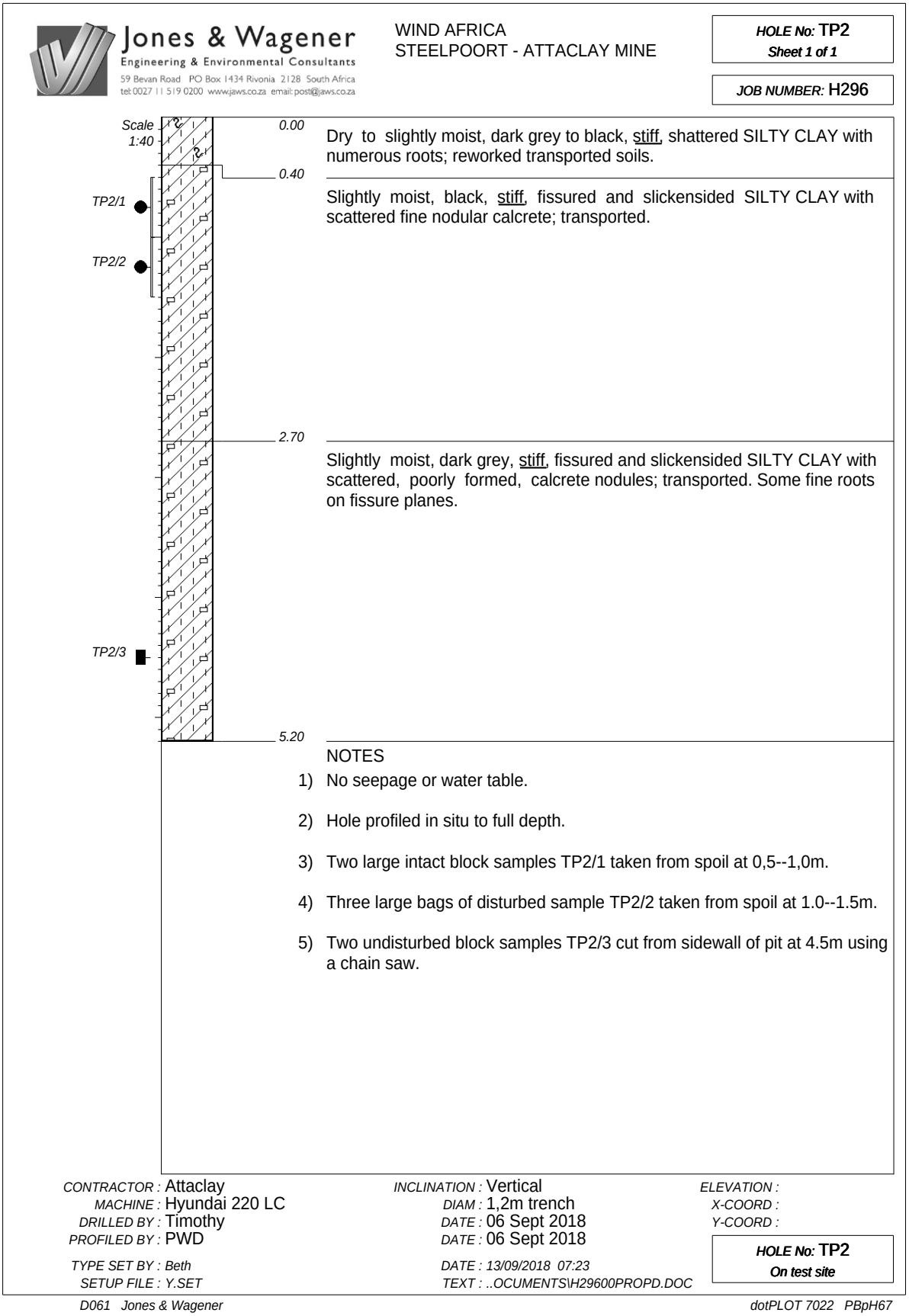

Figure 49: Test pit profiling

Various site visits were subsequently undertaken after the wet and dry seasons to determine the practical range of moisture content and suction that the clay will undergo during an annual cycle. These visits illustrated that the gravimetric moisture content varied between approximately 30 – 40 % at a matric suction of 4 – 2.5 MPa respectively (these measurements of matric suction were taken using the filter paper technique in accordance with ASTM D5298–16 (2016). It was also of interest to quantify the in-situ densities of the clay. The results of wax density measurements have been summarised in Table 7. Following determination of in-situ soil properties, a suite of benchmark laboratory tests was undertaken which included Atterberg limits and specific gravity, particle size distribution and X-ray diffraction tests. These results have been summarised in Table 8, Figure 50 and Table 9 respectively.

Table 7: Various in-situ properties of the clay following wet and dry seasons

Sample number	Depth (m)	Description	w (%)	$\rho_b(kg/m^3)$	$\rho_d(kg/m^3)$	e	S_r
1	1–1.5	Black clay	33.9	1832	1367	0.938	96
2	1–1.5	Black clay	31.8	1766	1340	0.977	86
3	1–1.5	Black clay	31.8	1792	1360	0.949	89
4	1–1.5	Black clay	40.3	1806	1371	0.933	90
5	1–1.5	Black clay	34.4	1743	1297	1.043	87
6	1–1.5	Black clay	32.6	1924	1451	0.827	105
7	1–1.5	Black clay	38.8	1768	1274	1.080	95

Table 8: Basic soil properties

Liquid limit	92
Plasticity index	55
Linear shrinkage (%)	25.5
Activity	0.8
Specific gravity	2.65
Unified soil classification	CH

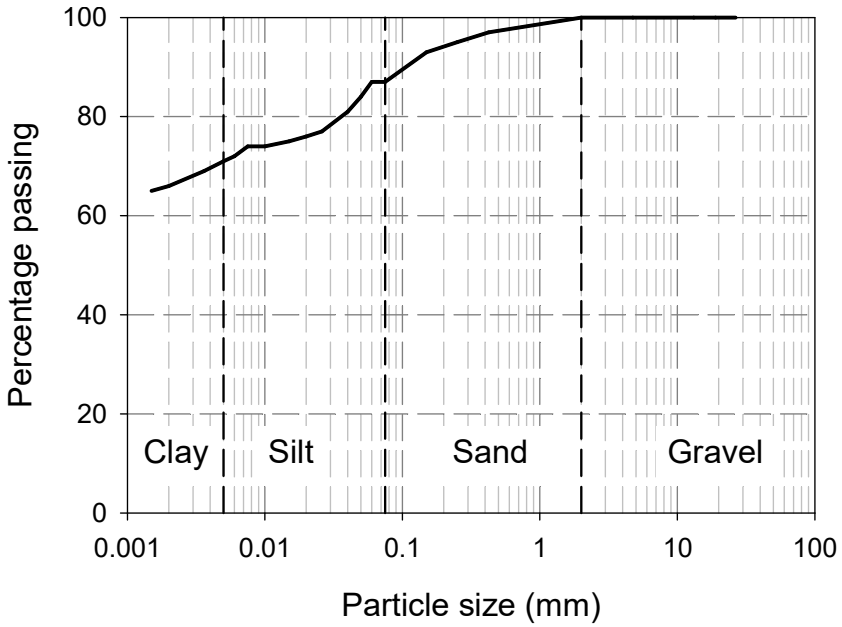

Figure 50: Particle size distribution curve

Table 9: X-ray diffraction results (after Moses, 2008)

Mineral	Composition (%)
Smectite	58
Palygorskite	19
Calcite	5
Plagioclase	5
Quartz	4
Enstatite	4
Kaolinite	3
Diopside	2

5.2 Sample preparation

As described at the start of this chapter, it was necessary to develop a material with a closely fissured structure that could be used for centrifuge modelling. The rationale behind this approach was to facilitate the rapid ingress of moisture such that a significant amount of heave could be achieved in the geotechnical centrifuge in a practical time frame. This was achieved by grating intact block samples at their in-situ moisture content, followed by statically compacting the gratings to the measured average bulk density of the in-situ material ($\rho_b = 1805 kg/m^3$). Specific details of the static compaction apparatus used are provided in Section 5.5.1. Figure 51

presents the sequence taken to prepare samples for both oedometer testing and centrifuge modelling.

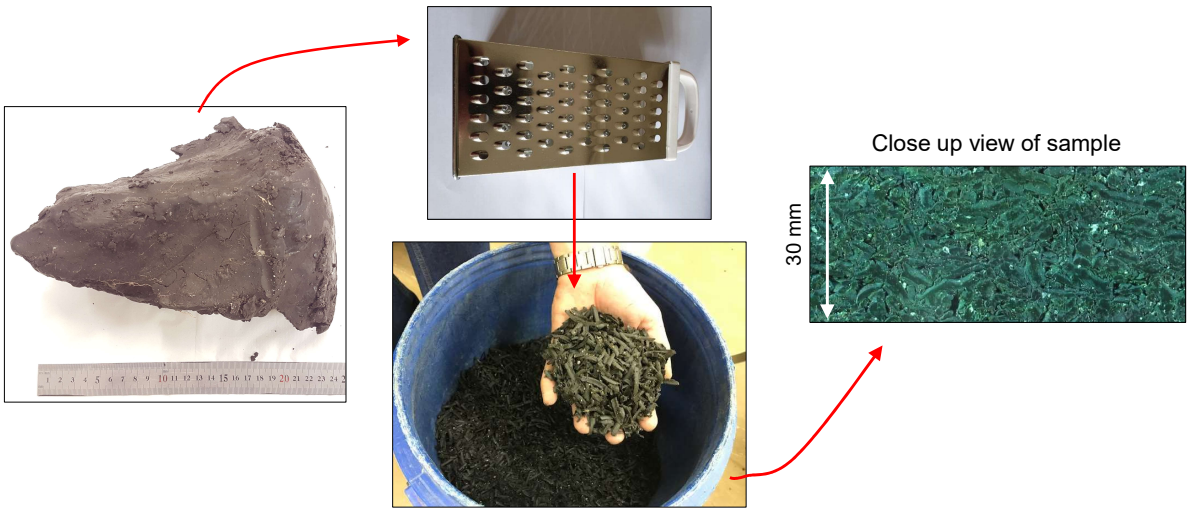

Figure 51: Flow diagram illustrating the sample preparation procedure implemented for all testing

5.3 Soil element testing

Due to the development/processing of the fissured specimens described in Section 5.2, it was necessary to evaluate any possible changes in mechanical or water retention characteristics in comparison to the undisturbed samples. The material properties of particular interest for the design of foundations on swelling clays are the potential magnitude of swell, as well as the swell pressure of the clay. It was also of interest to characterise the intrinsic parameters of the clay used such that it could be interpreted and compared with similar testing presented by previous researchers. Furthermore, since swelling clays are fundamentally an unsaturated soil mechanics problem, the soil water retention curves (SWRCs) were also measured. All tests described in the following sections were repeated for both the undisturbed and statically compacted samples.

5.3.1 Swell and consolidation tests

To determine the magnitude of swell which could be expected, a series of swell under load, or *wetting after loading* tests were performed in accordance with ASTM D4546–14 (2014). Such tests involve placing a sample in the oedometer apparatus at its in-situ moisture content, applying a specific vertical stress on the specimen and then flooding the oedometer housing

with distilled water. During the flooding process, the sample was allowed to absorb water and change in volume. The purpose for repeating the test under various applied vertical stresses is twofold. Firstly, the different applied stresses will correlate to different positions in the soil profile, thus giving an indication on the amount of swell that can be expected at various depths. Additionally, at some applied vertical stress the sample will undergo close to no change in volume. The stress at which no volume change occurs is termed the swell pressure. Starting with an applied vertical stress of 12.5 kPa, these tests were repeated at increasing stresses until such point that no swell occurred, or until compression of the sample was observed. All oedometer testing was performed on samples approximately 19 mm and 75 mm in height and diameter respectively.

Following the series of swell tests, the same samples were subjected to conventional one-dimensional consolidation tests. For the samples which underwent swell during the first phase of testing, the specimens were consolidated until such point that the volumetric strain reached or surpassed 0 % (i.e. the initial volume of the sample prior to flooding). Performing this series of consolidation tests provided information on yield stresses and the slopes of normal consolidation and swelling lines. Additionally, the stress at which 0 % volumetric strain occurred also served as a check on the swelling pressure of the clay (ASTM D4546–14, 2014). Following consolidation, these samples were subsequently unloaded until only the mass of the top cap and porous disc remained on the specimens. For samples which underwent compression after the flooding process, no additional stresses were added and, as for the other samples, the stress was incrementally removed. A separate consolidation test was also performed on a sample reconstituted at 1.1 times the soil's liquid limit. This test allowed the intrinsic soil properties to be quantified (Burland, 1990). Furthermore, it allowed the effects of structure to be evaluated for both the undisturbed and compressed samples.

Once samples were completely unloaded, they were left in the oedometer housing full of water and strains were monitored. Once changes in sample height stopped or became negligible, the samples were removed and used to measure a series of SWRCs. The purpose of the waiting period following the unloading phase was so that any values of suction measured on the sample after removal were due to the loss of moisture, with limited effects due to unloading obscuring the SWRC results. To summarise the purpose of the testing sequence followed, Figure 52 qualitatively provides a graphical illustration of the stress paths undergone for all oedometer samples apart for that which was used to determine the soil's intrinsic parameters, i.e. the sample reconstituted at $1.1w_L$. Table 10 then highlights the purpose of each stage of testing and the parameters attained from each stage. Table11 illustrates the initial properties of each

specimen. The term ‘initial’ is used to denote the state of each sample prior to the first stage of testing, i.e. the wetting after load tests.

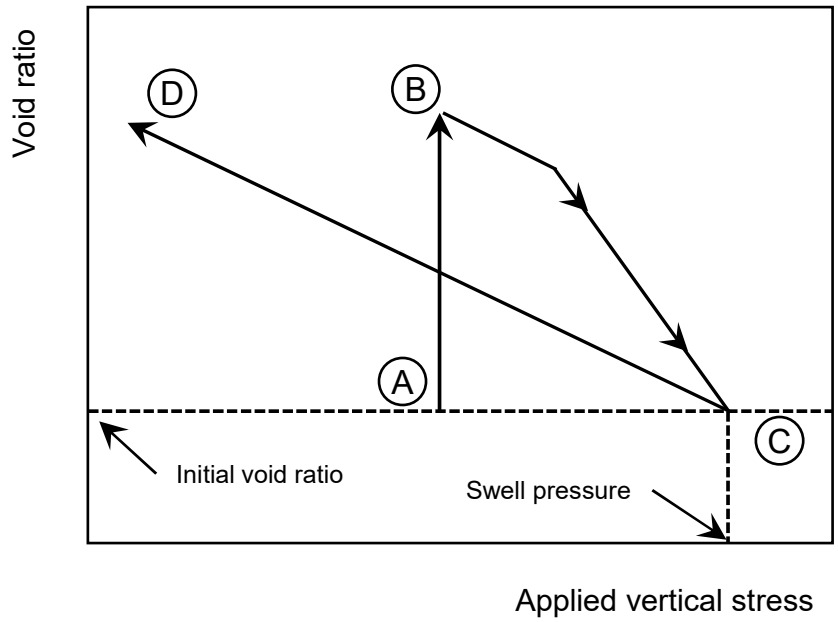

Figure 52: Stress paths undertaken for all samples besides the reconstituted sample

Table 10: Stress paths undergone and the purpose of each path

Stress path	Purpose
AB (soaking)	To determine the magnitude of swell which could be expected at a specific applied stress (this path was repeated at various applied stresses).
BC (loading)	To determine: • The pressure required to reduce the sample to its original volume (determination of swell pressure). • The slope of the virgin compression line. • The yield stresses of the various samples.
CD (unloading)	To determine the slope of the unloading line.
After Point D	Saturated samples were trimmed and had their respective primary drying and wetting curves measured.
For samples which underwent compression upon soaking (i.e. Path AB travelled downward), only path CD is relevant.	

Table 11: Initial sample properties

Description	Soaking stress (kPa)	Void ratio, e_i	Gravimetric moisture content, w_i (%)	Degree of saturation, Sr_i (%)
Compacted	12.5	1.253	33.59	71.9
Compacted	25	1.188	33.59	75.8
Compacted	50	1.120	30.34	72.6
Compacted	100	1.132	32.20	76.2
Compacted	200	1.053	34.65	88.2
Compacted	300	1.066	34.65	87.1
Compacted	400	1.025	34.65	90.6
Undisturbed	12.5	1.162	31.53	72.7
Undisturbed	25	1.082	30.32	75.1
Undisturbed	50	0.986	29.46	80.0
Undisturbed	100	1.028	30.24	78.9
Undisturbed	200	0.971	29.87	82.4
Undisturbed	300	1.097	30.32	74.1
Undisturbed	400	1.073	32.02	80.0
Undisturbed	500	1.007	30.77	81.9
Reconstituted	NA	2.521	98.5	104.7[1]

[1] This value can possibly be attributed to a slight error in the measured particle density

5.3.2 Measurement of soil water retention curves (SWRCs)

Measurement of SWRCs were performed on all samples mentioned in Section 5.3.1. These samples were prepared by trimming a portion of the main oedometer sample to a height and

diameter of approximately 9.5 mm and 37 mm respectively. Owing to the high values of suction anticipated for this clay, measurements were taken using the dewpoint hygrometer (WP4-C from Metergroup). This instrument measures total suction and has a reported maximum capacity of 300 MPa. Once removed from the oedometer, calculations indicated that all samples were fully saturated. The samples were then allowed to dry under ambient conditions in a temperature-controlled room (22 °C ± 1 °C) with suction measurements being taken periodically. After each suction measurement, volumetric readings were taken with a Vernier calliper and the sample mass was recorded with a high precision balance.

Drying under ambient conditions only allowed the samples to be dried out to a degree of saturation of approximately 65%. To dry the samples further, rather than placing them in the oven at an elevated temperature which is known to affect certain tropical soil properties (Schnaid & Haut, 2012), they were placed in a desiccator chamber for increasing periods of time. This was repeated until such point where samples showed no reduction in moisture content after remaining in the desiccator chamber for a period of 2 weeks. After this period, samples had a gravimetric moisture content of approximately 5 %. At this state it was assumed that the samples were in the pendular regime (at residual moisture content) with the water phase being discontinuous. It should be noted that while samples were dried to their residual moisture contents, the capacity of 300 MPa of the dewpoint hygrometer was reached at $S_r \approx 30$ %. The SWRCs presented therefore only extend to this point, even though the samples were dried out further. The shrinkage curves presented do however illustrate the full range of moisture contents.

Once primary drying curves were measured, samples were wetted up by placing them in a sealed chamber, partially filled with distilled water which would theoretically produce a relative humidity of 100 %. As soon as the suction of these samples began to fall within the capacity of the dewpoint hygrometer, the primary wetting curves were measured for all samples.

Difficulties associated with the SWRC measurement were encountered when taking volumetric readings of the undisturbed samples. The undisturbed specimens had a large quantity of calcrete nodules in their matrix. These nodules appeared to have increased the intensity of desiccation cracking, making accurate volumetric measurements problematic. This appeared to be less of a concern for the statically compacted samples as the grating process removed a substantial amount of the calcrete nodules present in the undisturbed samples.

5.4 Centrifuge modelling

For the purpose of this study, seven tests were conducted in the 150 g-ton geotechnical centrifuge at the University of Pretoria (Jacobsz et al., 2014). While the precise layout of each test did differ, there are certain details which were kept constant throughout. Aspects which were common to all tests are discussed first, with details specific to each individual test discussed in subsequent sections. It should be noted that Greenfield Test 1 and the Pile pull-out test served as preliminary tests, the results of which were presented by Gaspar et al. (2019*b*) and Smit et al. (2019) respectively. The results of these tests were presented in detail in the aforementioned publications but are discussed briefly in this study as they guided minor modifications made to all other tests presented.

The seven tests performed can be listed as follows:

1. Greenfield Test 1.
2. Greenfield Test 2.
3. Pile pull-out test.
4. Plug[2] pull-out tests (in-situ moisture conditions).
5. Plug pull-out tests (swelled state with unsupported holes).
6. Plug pull-out tests (swelled state with supported holes).
7. Instrumented pile test.

Each centrifuge test presented in this thesis consisted of five clay slabs statically compacted to a target height and bulk density of 50 mm and 1805 kg/m^3 respectively. While details of the press used for static compaction is provided in Section 5.5.1, the basic concept of the preparation was as follows. Static compaction was performed by placing clay gratings inside a mould measuring 710 mm in length and 152 mm in width (spacers were used to achieve the targeted height). The compressed slab was then cut to the desired size and offcuts were used to measure the initial moisture content and suction of each slab. When placed in the strongbox, the slabs were separated by layers of needle punched, non-woven geotextiles to facilitate the ingress of moisture. Adjacent to the clay slabs were two water wells manufactured from perforated steel plates covered with the same geotextile used to separate the clay layers. Upon reaching

[2] "Plug" refers to a short length pile

the desired centrifugal acceleration, the centrifuge strongbox was flooded from the bottom to induce swell. As the water level rose in the adjacent water wells, moisture was allowed to infiltrate the profile from the sides, as well as through the geotextile layers separating each of the clay slabs. For all tests with the exception of Greenfield Test 1, targeted slab dimensions were $50 \times 152 \times 335$ mm. For Greenfield Test 1, the targeted length was 525 mm rather than 335 mm. Throughout the descriptions that follow, the term 'swelled state' has been used. It should be noted that this refers to the amount of swell predicted by Van der Merwe (1964) for a clay of *very high potential expansiveness*, as discussed in Section 3.4.1. All tests performed under a 'swelled' state were conducted at this level of swell such that results between tests could be comparable. Finally, all tests presented in this thesis were performed at a centrifugal acceleration of 30 g. For each test, average values of certain variables of the five slabs have been provided in Table 12.

Table 12: Average initial soil properties for all centrifuge tests

Test	ρ_b (kg/m^3)	w (%)	Matric suction (MPa)
Greenfield test 1	1700	29.9	3.4
Greenfield test 2	1785	31.2	3.0
Pile pull-out test	1840	27.0	4.0
Plug pull-out test (in-situ moisture conditions)	1752	33.1	3.6
Plug pull-out test (swelled state with unsupported holes)	1698	33.1	3.2
Plug pull-out test (swelled state with supported holes)	1777	31.7	3.3
Instrumented pile test	1762	29.7	3.2

For two of the tests listed above, penetration tests were performed in flight at in-situ moisture conditions and after the target swell was achieved. Space restrictions in the other tests did not facilitate the use of the penetrometer. During preparation of the models where penetration tests were performed, holes were cut in the geotextiles to ensure that only the penetration resistance of the clay was measured. Results from these two tests are provided in Figure 53. For the results in Figure 53, 'GF 2' and 'IP' refer to the second greenfield test and instrumented pile test respectively.

The two extreme values encircled in red are points where the penetrometer punched through the geotextile (missing the pre-cut hole). Figure 54 shows the hole that was punched through the geotextile. Apart from those two anomalies, the peaks in penetration resistance correspond to the centres of each slab, while the troughs correspond to the transition points between slabs.

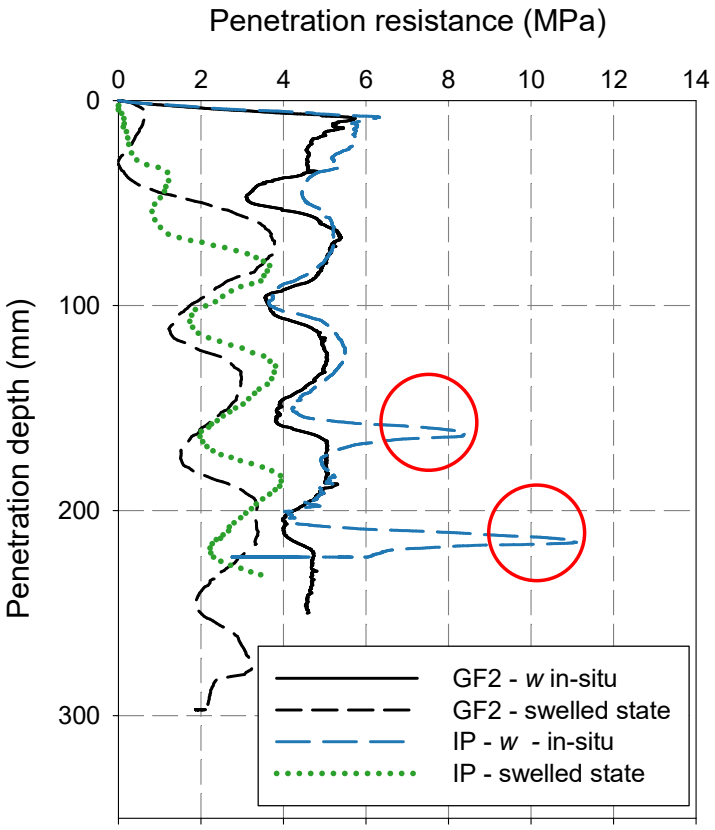

Figure 53: Penetration resistance measured in flight for two centrifuge tests

From the penetration results performed at the in-situ moisture content of the clay (w in-situ), it can be seen that a consistent penetration resistance of approximately 5 MPa was achieved throughout. This provides confidence in the repeatability of the sample preparation procedure implemented. Furthermore, it can be seen that after allowing for swell to occur, the slabs all softened to similar values with greater reductions occurring at the surface.

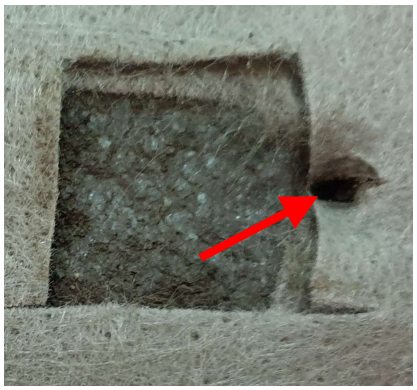

Figure 54: Penetrometer punching through geotextile

5.4.1 Greenfield Test 1

Greenfield Test 1 served as a preliminary test to illustrate that the developed fissured material could achieve the targeted swell within a reasonable time frame. Detailed results of this test can be found in the publication by Gaspar et al. (2019*b*). Figure 55 illustrates the general layout of this test.

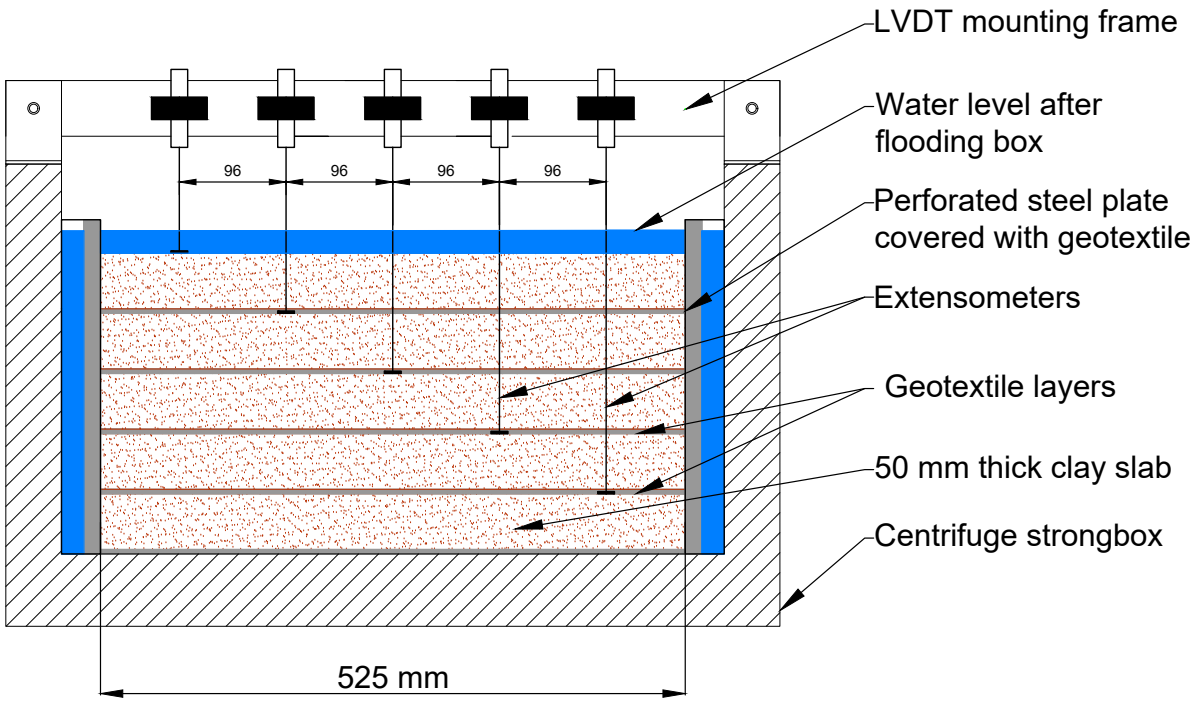

Figure 55: Test layout for Greenfield Test 1

The test involved accelerating the model illustrated in Figure 55 to 30 *g*. The strongbox was then flooded with water until approximately 20 mm of free water was observed above the top slab. In doing so, the profile was allowed to swell, and heave measurements were taken for each slab. While the test did highlight that the targeted swell could be achieved in a reasonably short time frame, there was room for improvement for a second greenfield test to be performed. One limitation of the test is that surface swell was only measured at one point on the top clay slab. Since a series of tests were planned to be conducted at a consistent magnitude of surface swell (i.e. Van der Merwe (1964) swell), this parameter was deemed critical to ensure meaningful comparisons between tests. For this reason, it was felt that redundancies in the measurement of surface swell were warranted. Secondly, the initial test did not incorporate any measurement of soil strength or moisture and suction changes. All these refinements and additions were implemented in Greenfield Test 2 presented in the following section.

5.4.2 Greenfield Test 2

While being conceptually very similar to Greenfield Test 1, Greenfield Test 2 incorporated the following additional instrumentation.

- Volumetric moisture content sensors (5TM probe by Metergroup).
- Fixed matrix porous sensors for the measurement of matric suction (Teros 21 sensor by Metergroup).
- Cone penetrometer.

A diagram of the test layout is provided in Figure 56, with photographs of the moisture content and suction sensors provided in Figure 57. Schematics and design principles of the penetrometer have been provided in Section 5.5.2.

To install the moisture content and suction sensors in the clay slabs, static compaction of the clay was performed with void formers in the desired positions of these sensors. Following compaction, the void formers were removed leaving a space for the sensors to be installed. Clay gratings were then moulded around the sensors prior to installation and any space behind them was backfilled with the same material. Figure 58 illustrates a flow chart of this process. For the moisture content sensors, the response time of readings appeared to be almost instantaneous and could therefore be installed immediately after the moulding of the clay. In contrast, the suction sensors have been shown to have a slow initial equilibration period and so these sensors

had to be prepared in advance. Furthermore, research by Tripathy et al. (2016) illustrated how different suction measurements could be obtained depending on whether the sensors were installed in a wet or dry state. For this reason, an additional study was carried out on the suction sensors prior to being used in centrifuge testing.

To determine a preparation procedure for the suction sensors prior to centrifuge testing, the following aspects needed to be investigated:

1. The response time of the sensors.
2. The potential difference in measured suction depending on the initial state of the sensor.

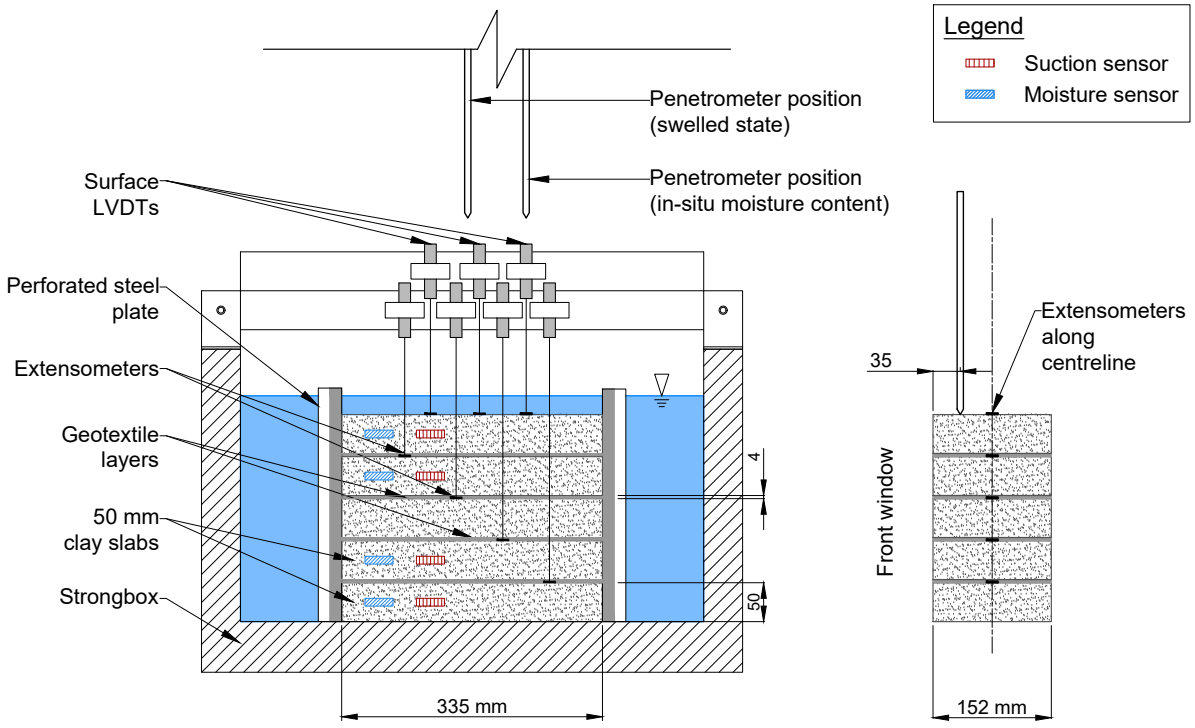

Figure 56: Test layout for Greenfield Test 2

(a) (b)

Figure 57: Photograph of the a) volumetric moisture content and b) matric suction sensors

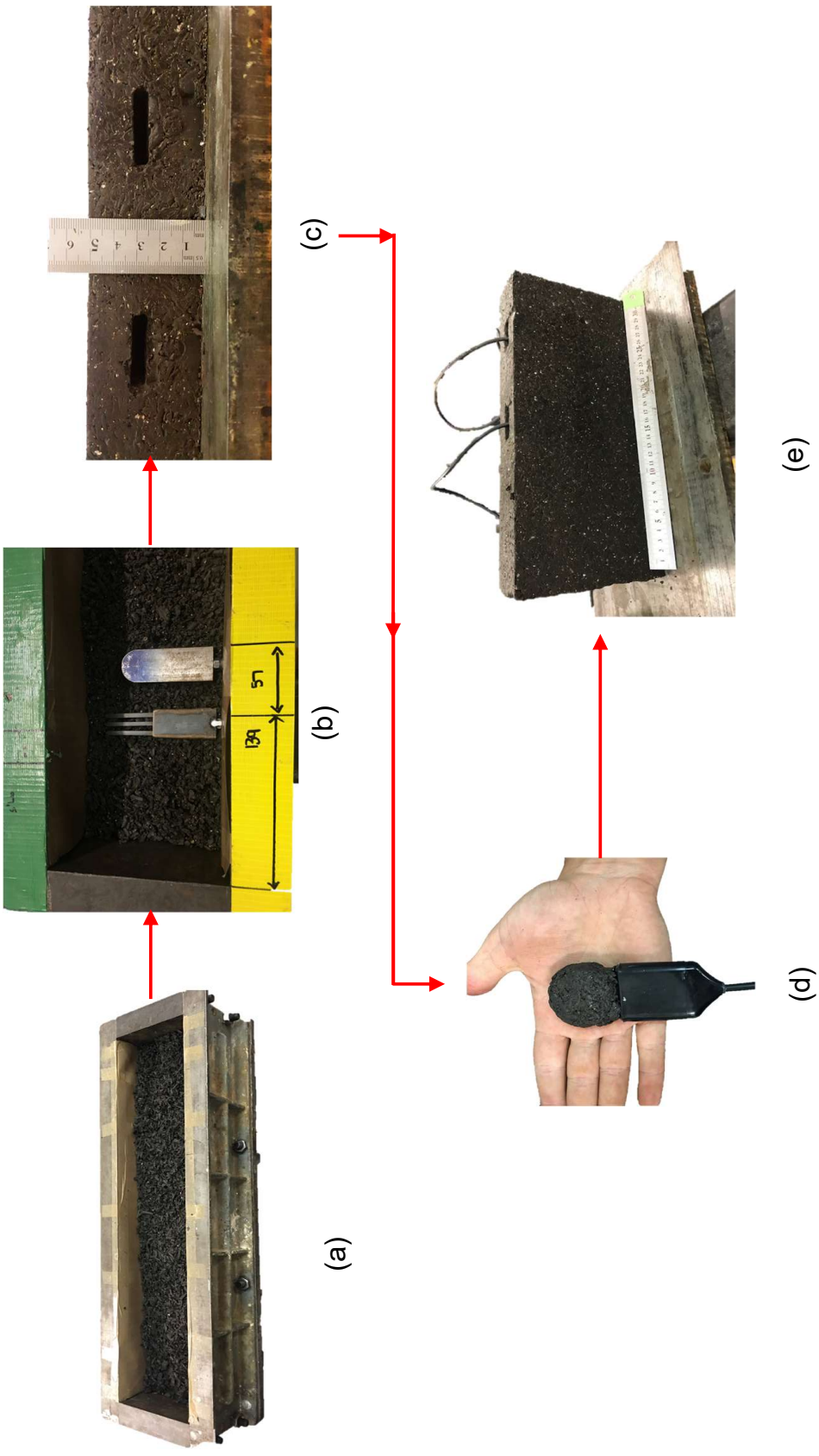

Figure 58: Flow diagram illustrating a) a half filled mould with clay gratings, b) placement of the sensor void formers at the desired positions, c) voids in slab after removal of spacers, d) moulded clay around suction sensor and e) moisture content and suction sensor installed in the clay slab

To investigate the performance of these factors, two sensors were installed in the same clay slab, one of which was installed 'wet' and the other installed 'dry'. The wet sensor was allowed to soak in water until the measured suction was 9 kPa (this is the reported lower end of the capacity of the sensor (Metergroup, 2017*a*; Tripathy et al., 2016)). Clay gratings were subsequently moulded around the sensor as prescribed in the manufacturer's user manual. For the dry sensor, the ceramic discs were removed and placed in an oven to dry at 60 °C. This was to ensure that the ceramics were dried out completely, such that they did not start the process of hydraulic equilibration on a scanning curve (discussed in Section 2.2). Once removing the ceramics from the oven, the sensor was reassembled and, similar to the first sensor, clay gratings were moulded around the ceramics. The two sensors were subsequently inserted into the slab, backfilled with clay and Whatman No. 42 filter papers were placed on the surface of the slab. This entire set-up was then tightly wrapped in clingfilm and aluminium foil as suggested by Heymann & Clayton (1999) and kept in a temperature-controlled room 22 °C ± 1 °C. The results for this test are included in Figure 59.

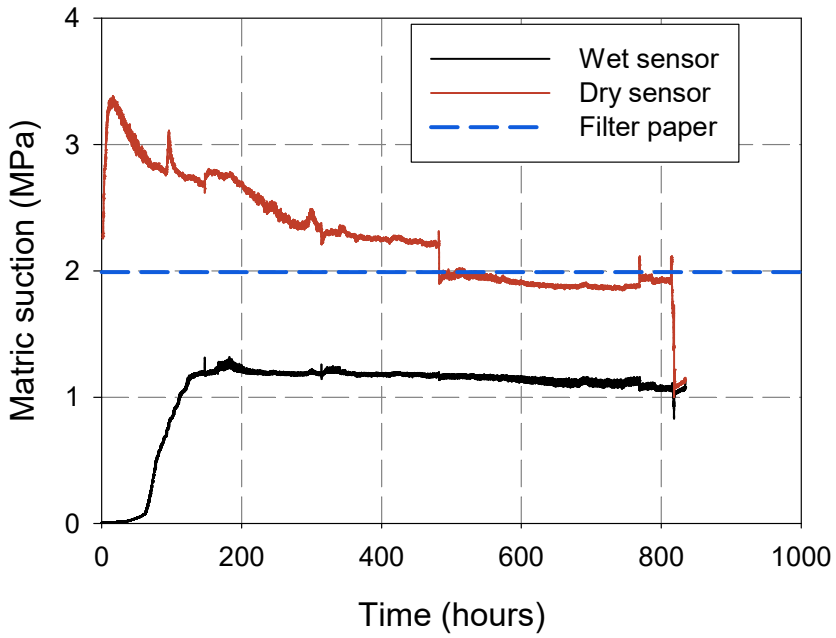

Figure 59: Suction measurements of two clay slabs installed in wet and dry states

The results presented in Figure 59 illustrate the equilibration time required for the two sensors, as well as the measured filter paper reading. The first surprising aspect of this result is that the sensor installed dry measured an initial suction of around 2 MPa before rapidly rising to approximately 3 MPa. This initial value falls well below the upper measurement limit of the instrument, quoted by the manufacturer to be 100 MPa at the time the sensor was purchased. This peculiarity could be attributed to moisture being absorbed by the ceramic discs after

removal from the oven. However, since the manufacturer has subsequently revised the capacity of this sensor to 2 MPa, it is possible that this seemingly low reading is simply a result of the limitations of the instrument. From Figure 59 it can also be seen that the sensor installed in a wet state equilibrated more rapidly. This result is contrary to what was found by Tripathy et al. (2016). However, the reason for the discrepancy is difficult to isolate since it could have arisen from any number of factors, e.g. differences in materials tested, soil structure, preparation procedures of the dry sensor, etc.

If the filter paper reading is considered a true reflection of the magnitude of suction, then it could be argued that by the end of testing the dry sensor provided a more accurate measurement of matric suction. However, it can clearly be seen that the measurements of the sensor installed dry were particularly erratic. For this reason, not much confidence can be placed on the accuracy of the final reading. The final finding from this test is that after equilibration, differences in the measured suction value were approximately 1 MPa, depending on the state of the sensor upon installation. This discrepancy can be attributed to the hysteretic properties of the ceramic discs. As discussed in Section 2.2, soils exhibit hysteretic behaviour in response to wetting and drying. It is therefore plausible to assume that the porous discs used in this sensor would illustrate a similar behaviour.

An alternative approach taken to sensor preparation was to allow an initially dry sensor to be wetted up to the anticipated matric suction of the clay used for centrifuge modelling (measured by the filter paper method to be $\approx$2 MPa). Preliminary experimentation with the sensor revealed that this could not be accomplished by simply submerging the sensor in water. Doing so has the effect of reducing the measured suction almost instantaneously from several megapascals to 9 kPa. For this reason, the rate at which the sensor was wetted up needed to be reduced significantly. This was achieved by placing a sensor with oven dried ceramics in a sealed chamber, partially filled with distilled water. Over time, through vapour transfer, the moisture content of the ceramics increased, resulting in a reduction of matric suction. Once the measured value of matric suction was approximately 2 MPa, clay gratings were moulded around the sensor and it was sealed until being inserted into the slab for centrifuge modelling. Figure 60 presents the results of this pre-equilibration process prior to moulding clay around the ceramics. This approach to sensor preparation was utilised for all centrifuge tests presented where suction was measured in-flight.

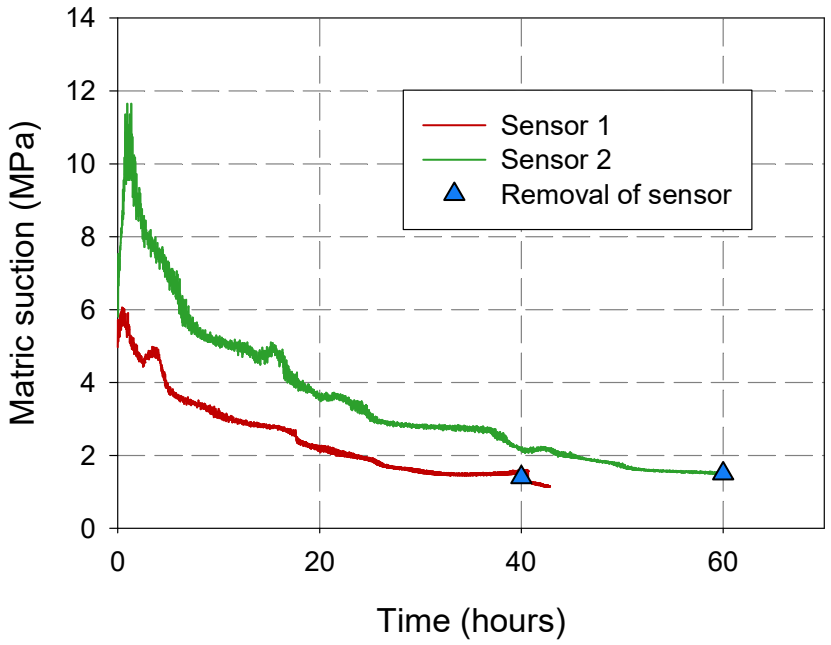

Figure 60: Equilibration of suction sensors through vapour transfer from a dry state

5.4.3 Pile pull-out tests

The results of the pile pull-out tests were presented by Smit et al. (2019). However, a brief description of the test is provided here with a detailed model layout illustrated in Figure 61. As for all tests described in this study, the pile pull-out tests consisted of five 50 mm thick statically compacted clay slabs, separated by layers of geotextile. Four scaled bored piles were installed into the clay profile by augering a 20 mm diameter hole to the required depth and filling the holes with a rapid hardening grout. Characterisation of this grout as well as a comparison with concrete scaled for centrifuge modelling purposes, as developed by Louw et al. (in review) are provided in Section 5.6. The edge-to-edge spacing of the piles was approximately 2.5 pile diameters (47 mm), with a spacing of the edge piles from the perforated plates of approximately 3 pile diameters (57 mm). A 4 mm mild steel threaded rod was then placed in the centre of each pile which was allowed to cure for approximately 14 hours before testing. No moisture or suction sensors were included in this test due to limited space.

All four piles were connected to a single frame which was lifted during the test using an actuator. To simplify the schematic, neither the frame nor the actuator has been included. On each pile, independent measurements of load and displacement were taken using load cells and linear variable differential transformers (LVDTs) respectively. To control the sequence in which each pile was pulled, an adjustable connection manufactured from square tubing was

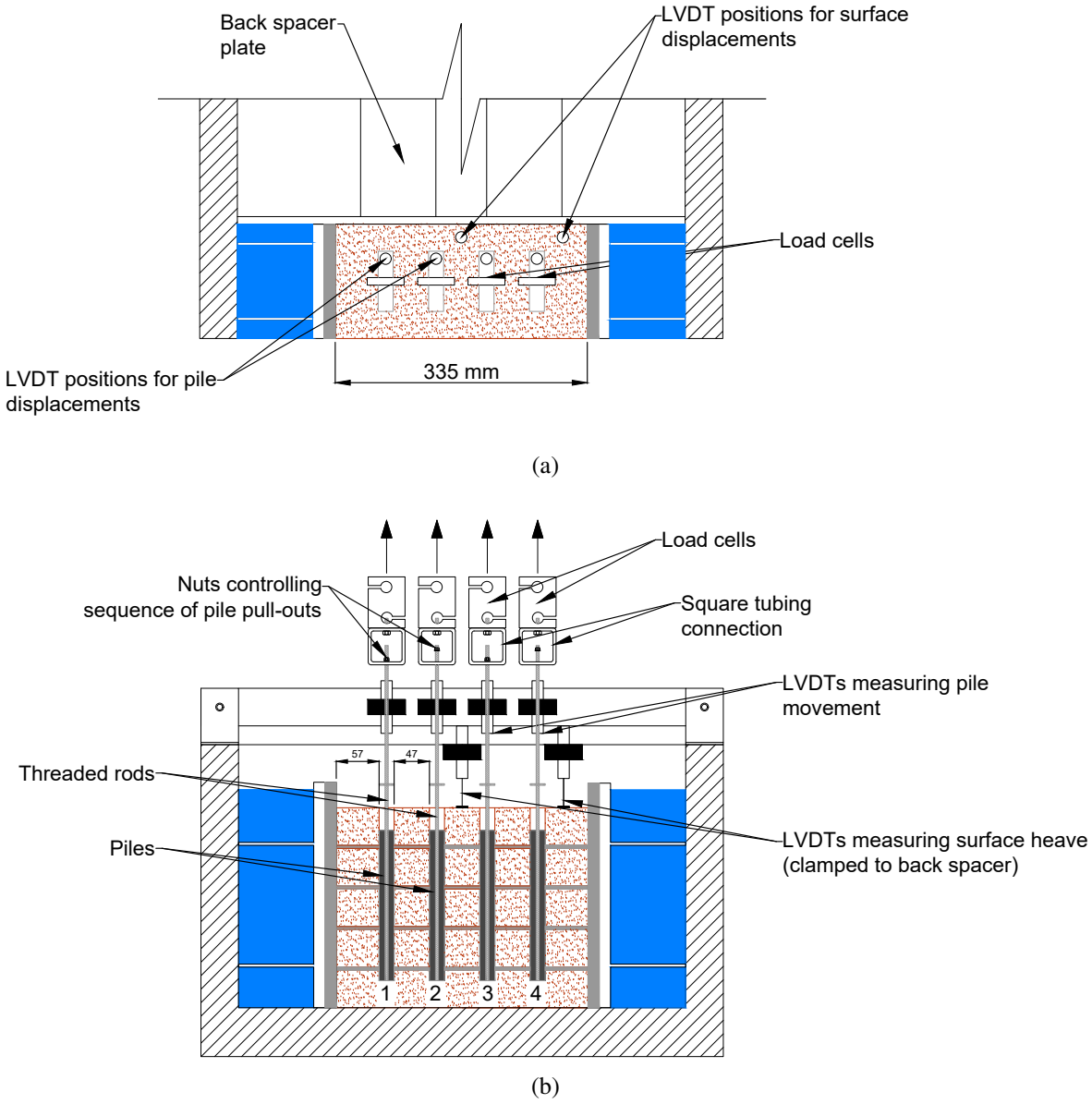

Figure 61: View of pile pull-out test from: (a) the top and (b) the front

utilised. This connection was bolted at the top to a load cell, with the threaded rod slotting into a hole through the bottom of the connection. By strategically positioning a nut and washer at certain heights on each threaded rod, the sequence at which each pile was pulled out could be controlled. A close-up schematic of this connection is provided in Figure 62.

Once the model had reached a centrifugal acceleration of 30 g, Piles 1 and 3 were pulled out at the in-situ moisture content of the clay (≈30% gravimetric). Note the lower positioning of the nuts on these piles in Figure 62. The model was then inundated with water and surface swell was monitored until the average of the two surface LVDTs measured the targeted swell. At this stage, the remaining two piles were pulled out of the profile.

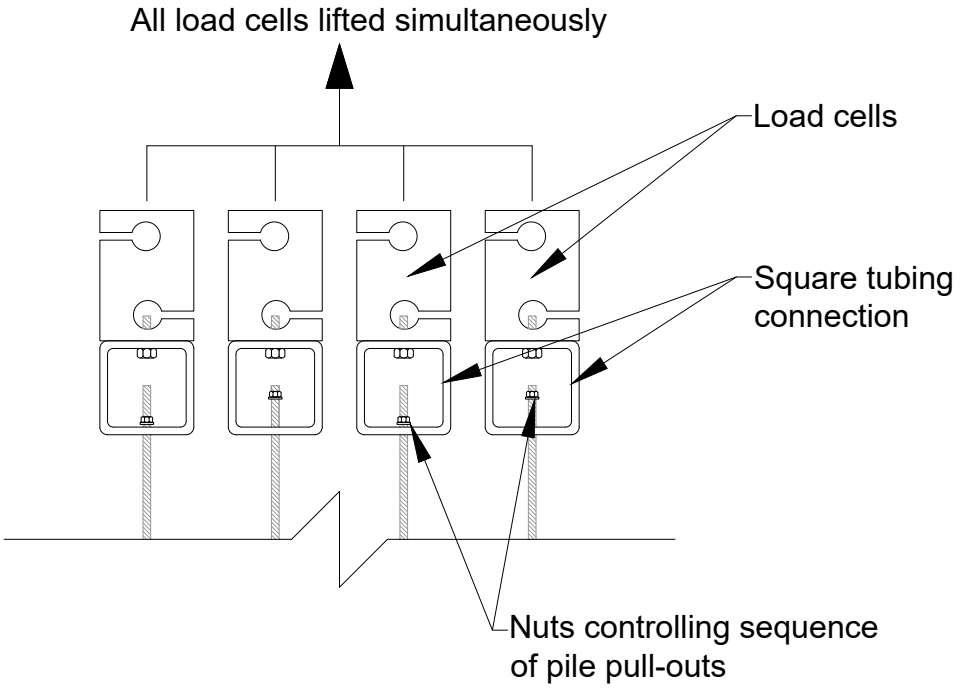

Figure 62: Connection between load cell and threaded rods

5.4.4 Plug pull-out test (in-situ moisture conditions)

While the pile pull-out tests presented in the previous section provide an indication of average shaft friction along the full length of the pile, they give no information on the variation in shaft resistance (pull-out capacity) with depth. Since the effective stress in the clay will vary from the surface to the base of the profile, a series of plug pull-out tests were conducted to quantify any effect on pull-out capacity with depth. The aim of this particular test was to determine the pull-out capacity of 4 short length piles at different depths under in-situ moisture conditions ($w_{ave} = 33\%$). The layout of this test was almost precisely the same as the pile pull-out test discussed in the previous section, with only two notable differences. Firstly, the piles (plugs) were approximately 30 mm rather than 200 mm long. This test also included moisture and suction sensors at specific positions. An illustration of this test set-up is provided in Figure 63.

While the primary aim of this test was to measure pull-out capacities under in-situ moisture conditions, the same plugs were pulled out a second time after achieving the targeted swell.

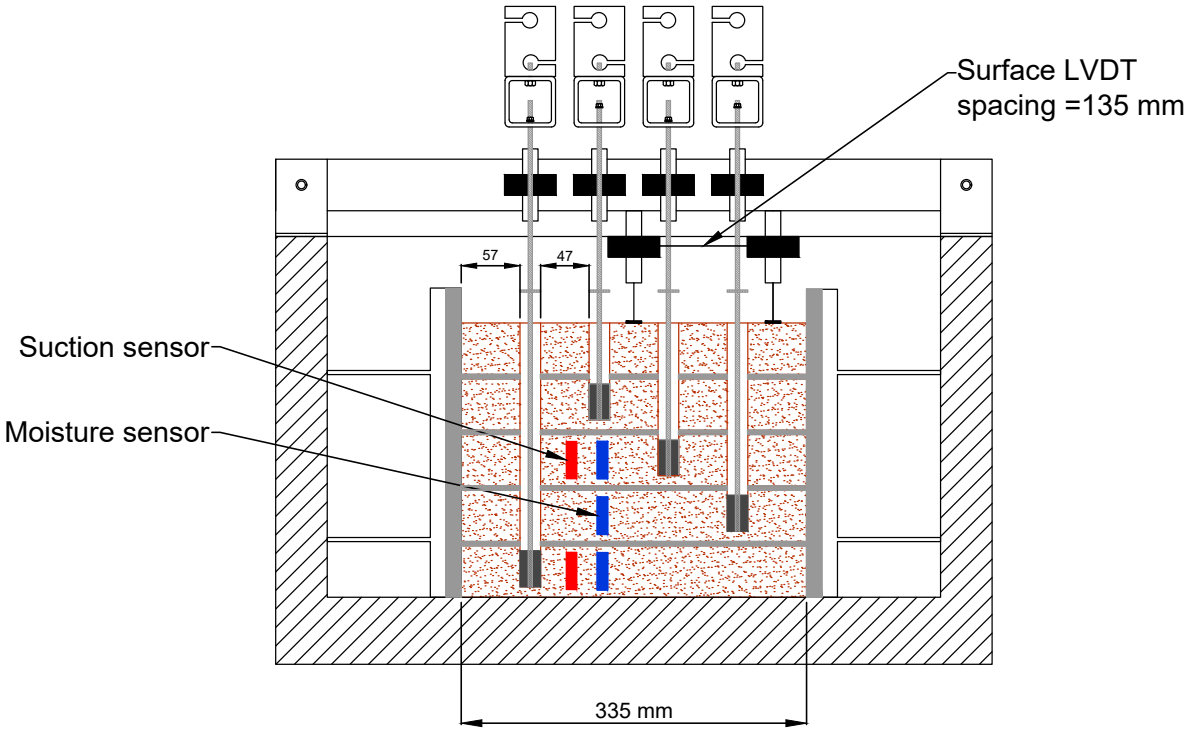

Figure 63: Test layout for plug pull-out tests under in situ moisture conditions

5.4.5 Plug pull-out tests (swelled state with unsupported holes)

For the second set of plug pull-out tests, plugs were only lifted after the model had been flooded and the profile had reached the targeted swell. This test layout was identical to that of the previous test presented in Figure 63. One notable aspect of this test is that the augered holes were unsupported above the plug. This meant that when the profile was flooded, the clay was free to swell closed behind the plug. While observations illustrated that the clay which swelled behind the plug had softened significantly and was of a low unit weight, it was still felt that the test should be repeated with supported holes. Doing so would highlight whether the material swelling behind the plugs had any effect on the measured pull-out capacity.

5.4.6 Plug pull-out tests (swelled state with supported holes)

To support the augered holes behind the plug, an aluminium tube was placed into the hole until it made contact with the short length pile and subsequently pulled back 5 mm. Results

from the previous pull-out tests revealed that a gap of 5 mm was more than sufficient for peak friction of the plugs to be mobilised. To ensure that this spacing was maintained even during the swell process, a 'clamp' was utilised around the pile at the clay surface. This ensured that when the clay swelled, the spacing between the aluminium tubing and the top of the pile was maintained to at least 5 mm. A schematic of the set-up used for this 'supported hole' set-up has been provided in Figure 64. A photograph of the portion above the clay surface is illustrated in Figure 65.

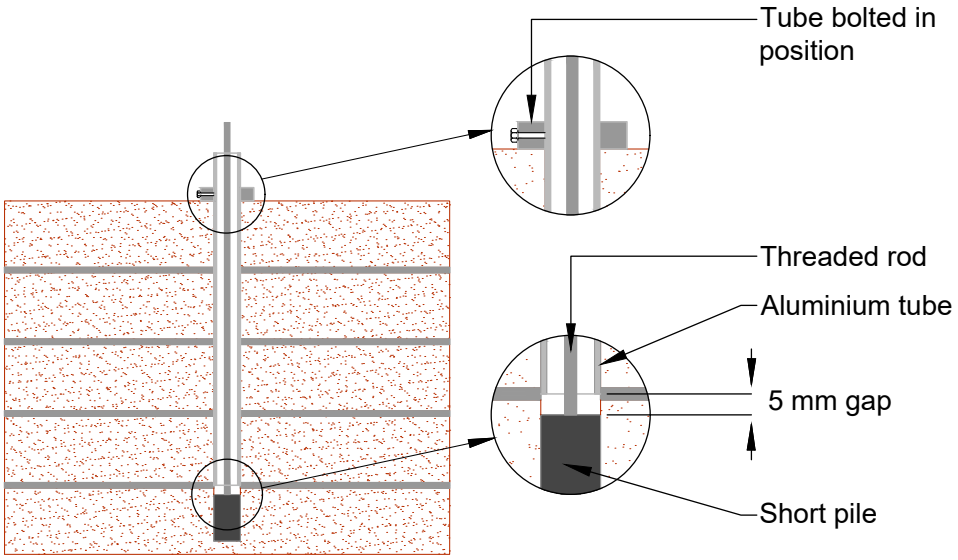

Figure 64: Set-up implemented to support augered holes

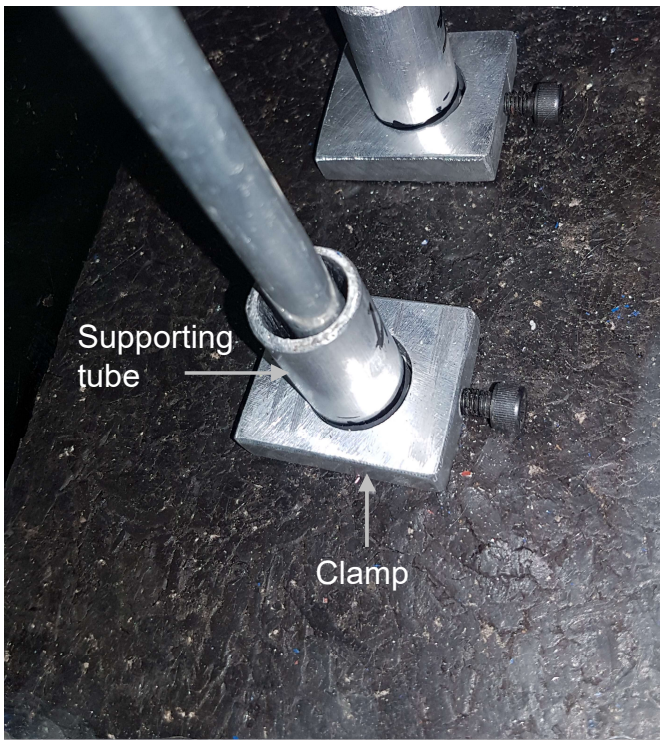

Figure 65: Photograph of supported hole set-up

5.4.7 Instrumented pile test

As mentioned in Section 3.5.3, literature by Blight (1984*a*) and Elsharief (2012) reported conflicting results on the shaft resistance of piles in expansive clays. While Blight (1984*a*) reported an increase in pull-out capacity after allowing swell to occur, Elsharief (2012) observed a decrease in shaft resistance following compressive pile load tests. A possible explanation for these discrepancies is that the pull-out capacity of piles in swelling clays is largely governed by two conflicting mechanisms. While the swelling process can increase lateral pressure against the pile shaft resulting in an increase in pull-out capacity, changes in lateral pressure will be accompanied by softening of the clay which will act to reduce it. The pull-out tests presented thus far measure the consequence of these two phenomena rather than any of the two mechanisms themselves. The aim of the instrumented pile test was to use an aluminium tubular pile (anchored at its base), instrumented with lateral load cells which could be used to measure changes in lateral pressure during swell. The outer diameter of the pile was 19.05 mm and it was placed within a latex membrane before being installed into an augured hole with a 20 mm diameter. Similarly, by performing cone penetration tests before and after allowing swell to occur, an indication of soil softening could be obtained. The details of the design and calibration

of both the cone penetrometer and the lateral load cells are provided in Sections 5.5.2 and 5.5.3 respectively. A layout of the instrumented pile test is provided in Figure 66.

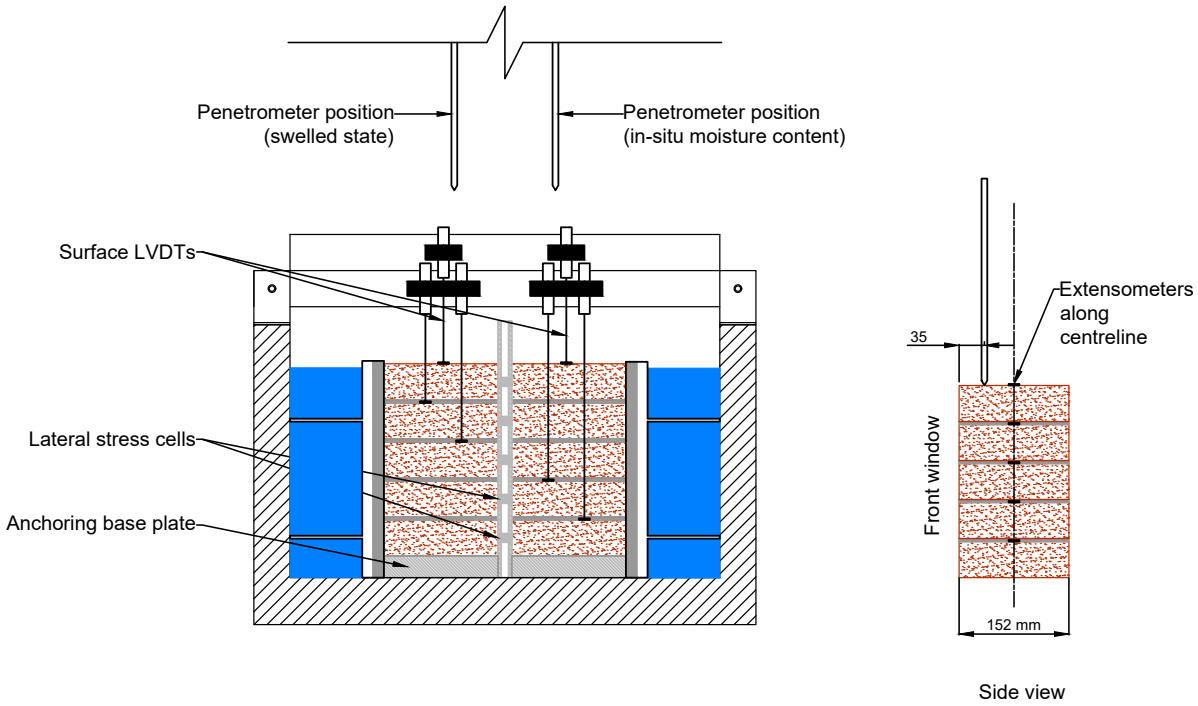

Figure 66: Layout for instrumented pile test

5.5 Development of equipment used

For all testing mentioned this far, specialised equipment needed to be designed, manufactured and calibrated for purpose. The sections that follow describe the design and calibration (where applicable) of the equipment used for the experimental work described thus far.

5.5.1 Static compaction set-ups used

In a geotechnical engineering laboratory, many compaction methods can be implemented. A popular technique which has been shown to provide consistency between samples in terms of density is the static compaction set-up (Booth, 1976; Shackel, 1970). The principle of the technique is that one or two plungers are allowed to slide into a split mould, compressing material between them (from either one or both sides). The final dimensions of the sample are controlled by limiting the travel of the plunger(s) when contact is made between their flanges and the mould itself. In the case where the sample is compacted from both ends, the weight of the mould is initially supported by split collars/spacers which are removed during compression.

Various aspects of this method have been investigated over the years. For example, when two plungers are used it was generally assumed that both plungers seated against the mould at the same time, producing the highest density in the centre of the sample. Shackel (1970) illustrated that this was in fact not the case and that the conventional method described above usually results in one piston seating home first, resulting in higher densities towards the end of the sample where the plunger seated last. Shackel (1970) improved upon this method with the development of the "floating mould" approach whereby the travel of the plungers is controlled by an external rig. In this research, Shackel (1970) highlighted that this approach significantly reduced density variations. However, this improvement was only seen for samples with height to diameter (h/d) ratios of 2/1. When samples with an h/d ratio of 0.625 were investigated, there was no significant benefit to using the "floating mould" approach.

In contrast to the findings of Shackel (1970), Whitman et al. (1960) found that static compaction from both ends did produce the highest density in the centre of the sample. However, Whitman et al. (1960) did come to similar conclusions on the effect of h/d ratios, stating that reducing this ratio to approximately 0.5 was enough to reduce density variations to "very low values". Furthermore, tests done by Whitman et al. (1960) on samples with an h/d ratio of less than 1 were all compacted from one end. Recognising the benefit of the conventional static compaction technique as described at the beginning of this section, variations of this approach have been commonly used, particularly when preparing oedometer samples where the h/d ratio is substantially low (Al Haj, 2013; Booth, 1976; Colmenares, 2002; Manca et al., 2016; Monroy, 2005; Monroy et al., 2015).

For this study, two static compaction approaches were used for the preparation of oedometer and centrifuge samples respectively. Both approaches have been described in the following sections.

Oedometer static compaction set-up

The compaction set-up utilised for the preparation of oedometer samples is illustrated in Figure 67. The set-up incorporated a mould split into an upper and lower half. The mould was machined such that an oedometer ring could fit into the centre, allowing soil to be compacted from both ends, ultimately reaching its final position in the oedometer ring. As suggested by Whitman et al. (1960) and Shackel (1970), the mould was lubricated prior to compaction. After compaction, the oedometer ring along with the sample could be removed and placed in the oedometer for testing, without the need for any further sample trimming. To reduce rebound of a sample after compaction, Shackel (1970) suggested that maintaining load for a period

of 2 minutes was sufficient. While this finding may be soil specific, a detailed investigation of this aspect for the clay used was outside the scope of this study. It was therefore decided that the load would be maintained on the sample for a period of 5 minutes after compaction. Observations of the sample post-compaction revealed that this period was sufficient to make rebound negligible. Figure 68 illustrates a photograph of the compaction set-up as well as the resulting sample.

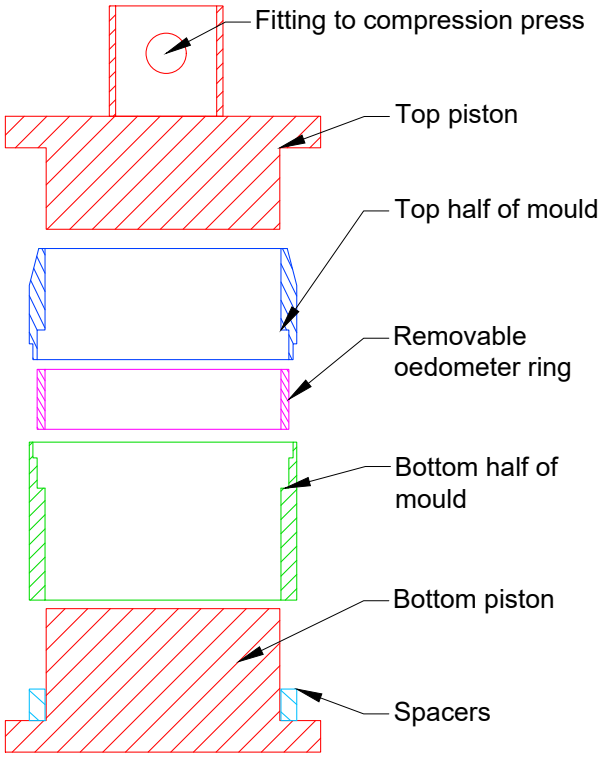

Figure 67: Static compaction set-up for preparation of oedometer samples

(a) (b)

Figure 68: Photographs of the a) static compaction set-up and b) the resulting sample

Static compaction for centifuge slabs

For the clay slabs used for centrifuge testing, compaction took place from one end only. The internal dimensions of the mould were $710 \times 152 \times 152$ mm. The inside of the mould was lined with Teflon. A channel section was used to press evenly onto the clay gratings. Two I-beam sections were positioned on top of the channel section to act as spacers, on top of which was a 20 mm thick plate which limited the travel of the hydraulically controlled piston. On top of the 20 mm plate was a thicker 30 mm section put in position to limit deflections (bending) of the set-up which would have resulted in non-uniform compaction along the length of the clay slab. Figure 69 illustrates a schematic cross-sectional view of the set-up at the end of compaction, with the final 30 mm thick slab indicated. Figure 70 provides a photograph of the set-up just prior to compaction.

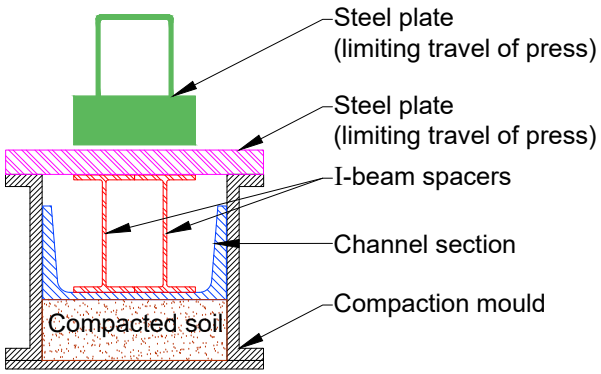

Figure 69: Cross section of the final position of the static compaction set-up described

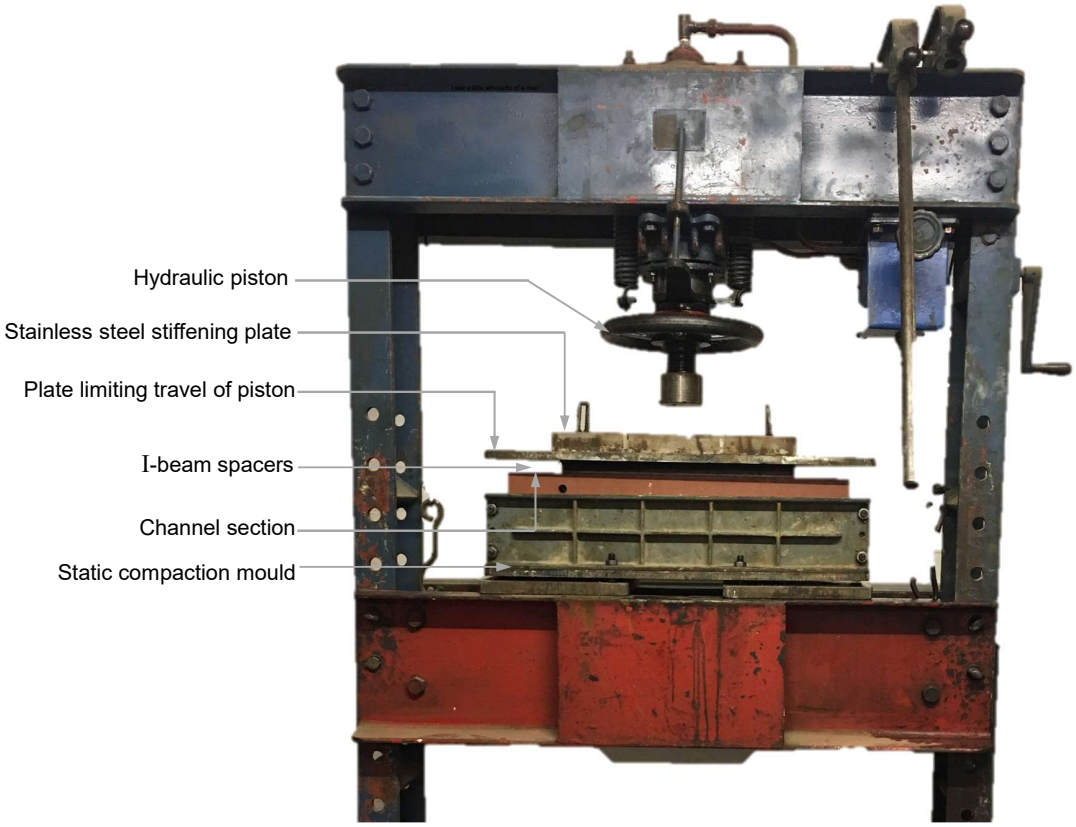

Figure 70: Photograph of the compaction set-up prior to compaction

5.5.2 Design and calibration of the cone penetrometer used in-flight

As centrifuge modelling has become increasingly popular in the geotechnical research community, the use of miniature cone penetrometer tests (CPTs) has been well recognised. The benefit of measuring penetration resistance in-flight has two main benefits, namely, to check uniformity and repeatability of the specimen and, perhaps more ambitiously, to obtain an absolute value

of in-flight soil strength (Bolton et al., 1999). The majority of the development of miniature CPTs for centrifuge testing has been done for saturated sandy material (Bolton et al., 1999; Kim et al., 2014; Zhou et al., 2014). Similarly, correlations between penetration resistance and undrained shear strength have been generally established for such materials. In this research project, the use of CPTs were to check repeatability in soil preparation procedures and to get a qualitative indication of the softening of the expansive soil profile post-swell.

Typically, miniature penetrometer designs incorporate measurement instrumentation behind the penetrometer tip to measure tip resistance. Doing so requires this instrumentation to be adequately shielded from any normal forces it may be subjected to as the penetrometer is pushed through a soil profile. Additionally, where water is involved, this instrumentation needs to be made watertight. These precautions become especially difficult to implement when designing a penetrometer for use in the geotechnical centrifuge, owing simply to the small size of the instrument. Research by Carey et al. (2014) overcame this difficulty by incorporating a load cell at the back of the penetrometer to measure tip resistance. The approach taken by Carey et al. (2014) was utilised for this study. The penetrometer used consisted of a 5 mm diameter inner rod, shielded by an 8 mm (outer diameter) tube with a 60° conical tip. Any shaft resistance mobilised on the outer tube was designed to thrust against an aluminium block which housed the load cell. The inner rod would then transfer load to a 2 kN HBM load cell housed inside the aluminium block. The penetrometer tip was designed to be replaceable in case of damage. Apart from the aluminium load cell 'block', the rest of the penetrometer was manufactured from stainless steel. A detailed schematic of the penetrometer used in this study is provided in Figure 71.

The purpose of the O-ring positioned just behind the penetrometer tip was to avoid soil from entering between the rod and outer shaft. When the tip was screwed into the inner rod it was done in such a way as to just make contact with the shaft (not to compress the O-ring). Care was taken to do this such that no significant portion of tip resistance would be transferred through the O-ring, to the outer tube and ultimately not be measured by the load cell.

As can be seen in the schematic provided in Figure 71, another O-ring was placed over the inner rod at a distance of 226 mm behind the tip. The purpose of this O-ring was to centre the rod within the outer tube. Upon assembly, this O-ring was lubricated before inserting it inside the tubing. A calibration of the fully assembled penetrometer was performed using a dead-load system. The rig used for this purpose is illustrated in Figure 72. The results of the calibration are presented in Figure 73. The error plotted on the secondary vertical axis is the difference in

the applied load to what was measured by the pre-calibrated load cell expressed as a percentage of the applied load.

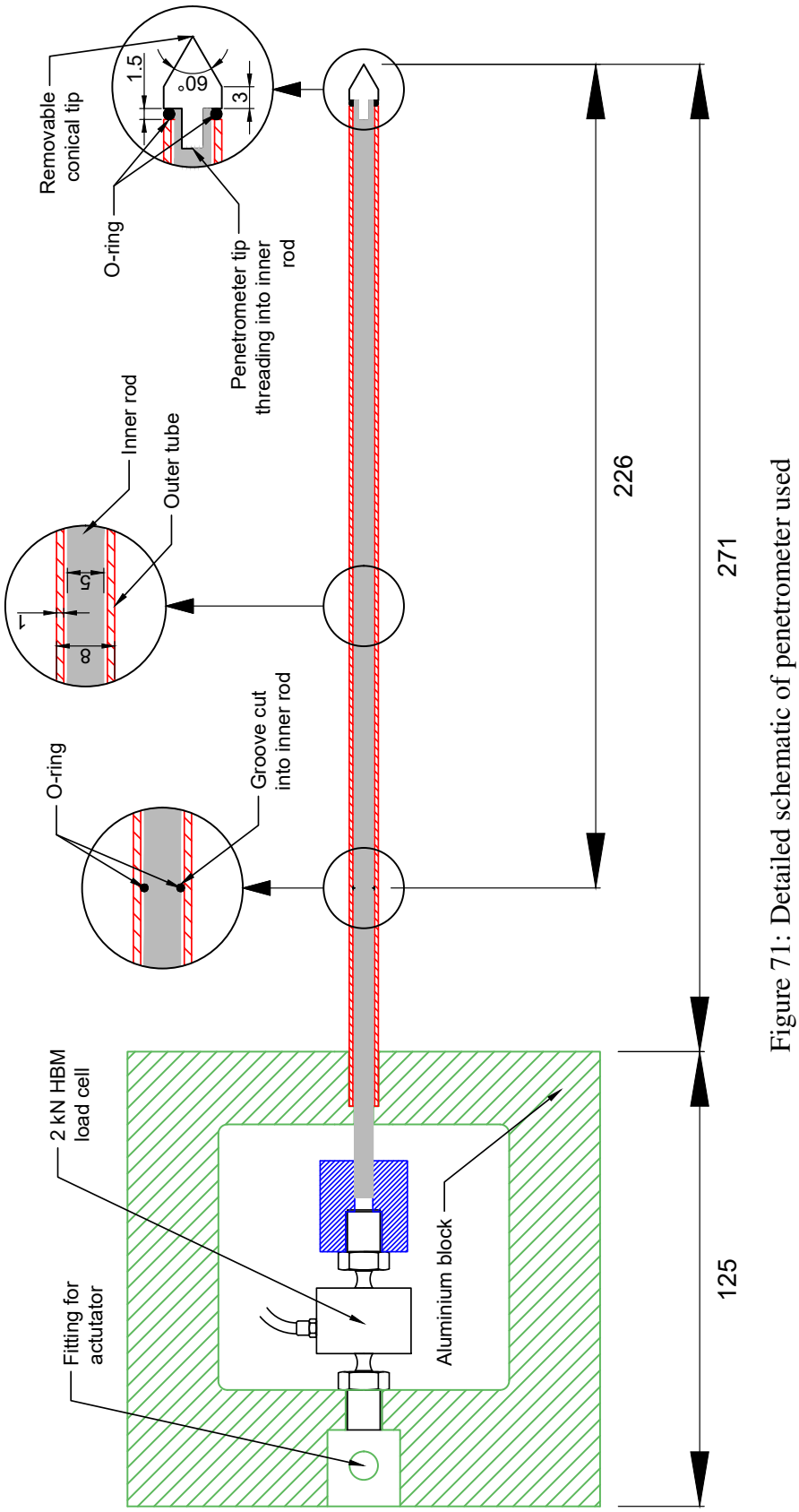

Figure 71: Detailed schematic of penetrometer used

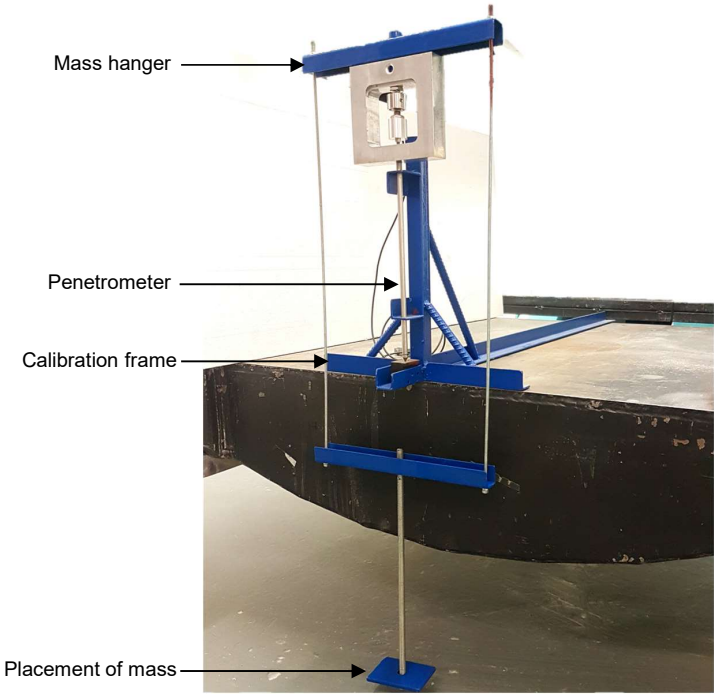

Figure 72: Pentrometer calibration set-up

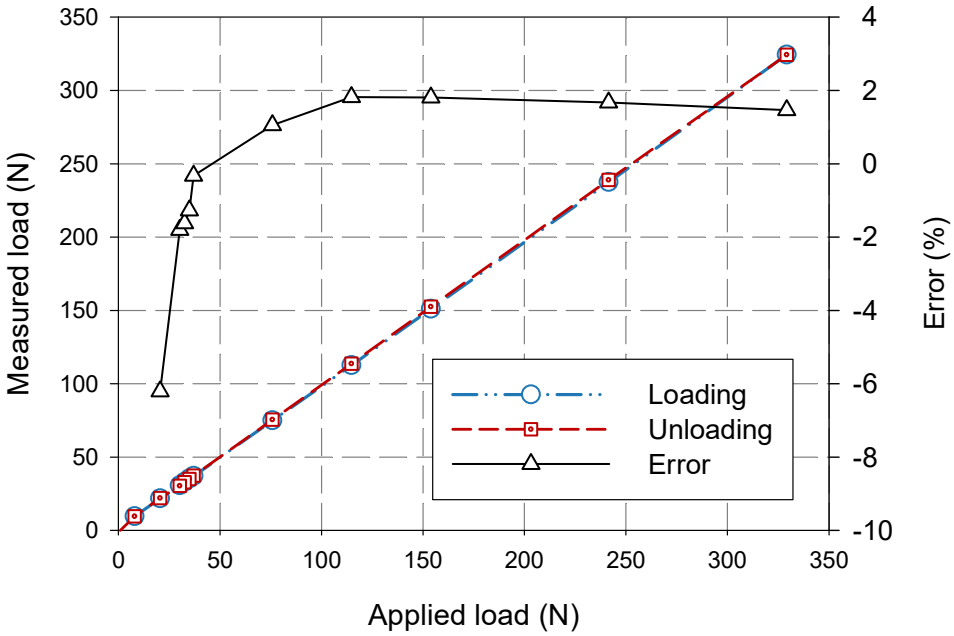

Figure 73: Penetrometer calibration results

From Figure 73 it can be seen that maximum error was recorded at around 25 N applied load. However, after initial bedding the measured error stabilised at approximately 1.5%. Since

the anticipated working range of the instrument is between 125 – 250 N, the error in this range was deemed acceptable.

5.5.3 Design and calibration of lateral load cells for instrumented pile test

For the instrumented pile test, the lateral load cells used were based on the design proposed by Jacobsz (2002). The load cells were manufactured from aluminium using a process referred to as electrical discharge machining (EDM) or "wire cutting", as it is more commonly referred. As shown in Figure 74, the load cells comprised of two rounded surfaces and an inner web measuring 0.3 mm in thickness. This web was instrumented on either side with 1 kΩ strain gauges and wired into a full-Wheatstone bridge configuration. Once strain gauges were attached to the load cell, half of it was slotted into the corresponding hole on the aluminium pile. Lead wires were then fed through the top of the tube (pile) and soldering took place with the load cells halfway into the slot. Once all 5 load cells had been inserted in the pile, the tube was filled with a dielectric gel and left to cure. The purpose of the dielectric gel was primarily to insulate the electronics from any moisture ingress. Furthermore, it helped keep the load cells in position. After installation of the load cells, the rounded surfaces fitted flush with the outer diameter of the pile. Figure 75 illustrates the final pile with the positions of the lateral stress cells highlighted.

Figure 74: Un-instrumented lateral load cells

Calibration of the pile was performed using air-pressure in an airtight vessel. The pile was placed inside a latex membrane before being placed in this vessel to ensure that the applied air pressure only acted on the external surface of the pile. It should be noted that when the pile was used in testing, the latex membrane remained over the pile such that the readings could be consistent with the calibration.

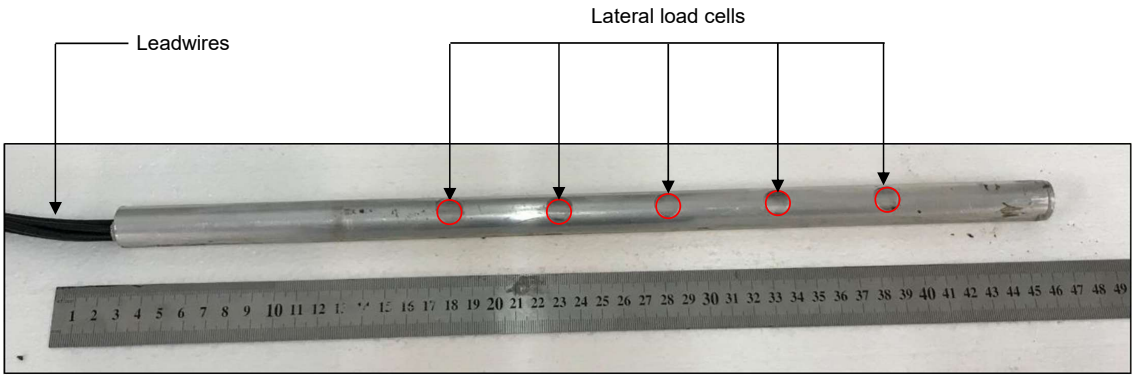

Figure 75: Final assembled pile

Prior to calibration, cycles of air-pressure between 0 – 500 kPa were performed to 'exercise' the cells to relieve any residual stresses imparted during the manufacturing process. Once stress cell responses and measurements became sharp and stable, two calibrations were performed. The first calibration was performed at 1 g with the second being performed at 30 g. While loading and unloading cycles were performed, negligible hysteresis was observed. The results presented in Figure 76 and Figure 77 therefore present the loading calibrations performed at 1 and 30 g respectively. The calibration coefficients for the two calibrations have been provide in Table 13.

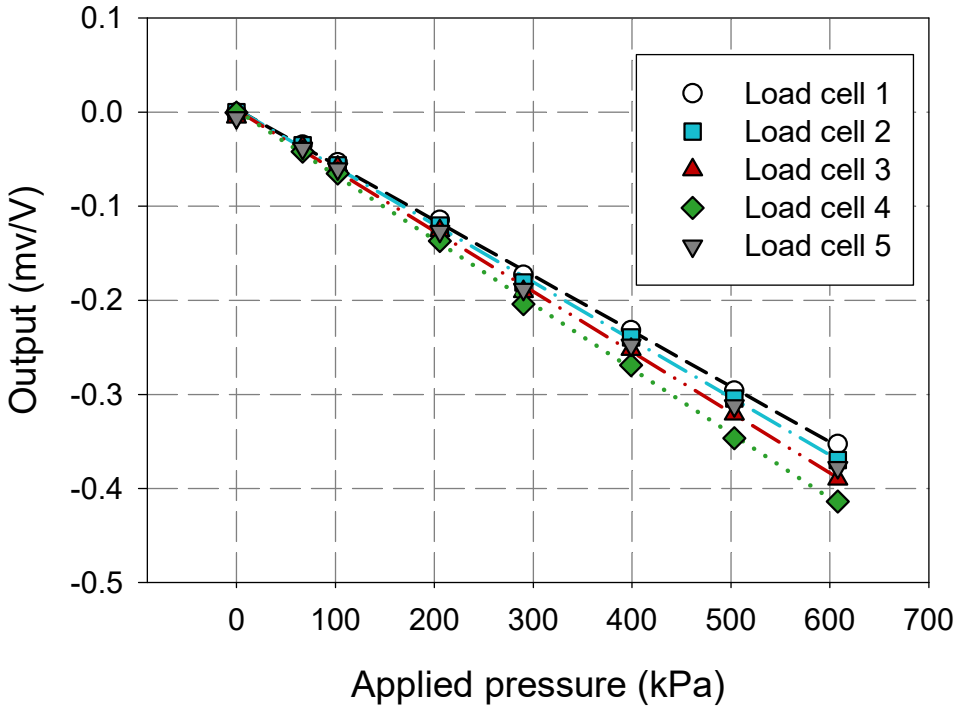

Figure 76: Calibration of instrumented pile at 1 g

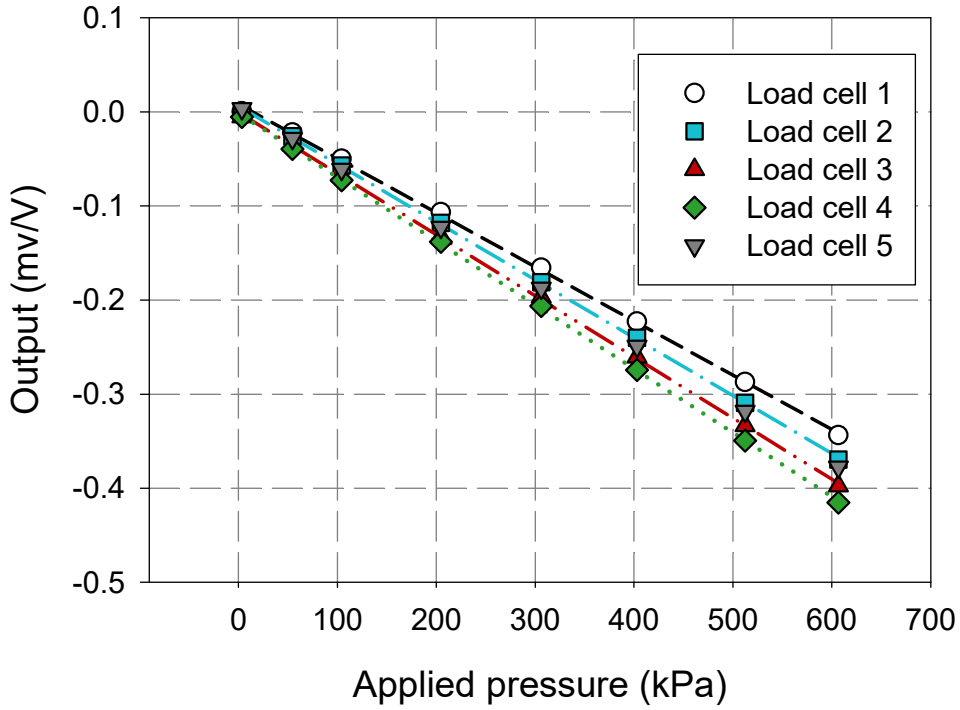

Figure 77: Calibration of instrumented pile at 30 *g*

Table 13: Calibration coefficients for instrumented pile

	Calibration coefficient (mV/V/kPa)	
	1 *g*	30 *g*
Load cell 1	-0.0005897	-0.0005760
Load cell 2	-0.0006129	-0.0006153
Load cell 3	-0.0006429	-0.0006503
Load cell 4	-0.0006874	-0.0006786
Load cell 5	-0.0006202	-0.0006321

5.6 Characterisation of rapid hardening grout

For the pull-out tests presented in this study it was desired that the piles and plugs be manufactured from a substance similar to that of concrete, as would be used in practice. The disadvantage of using conventional concrete is the curing period (typically 28 days or 7 days for rapid hardening cement). Since the piles were to represent bored piles and be cast in place, this long curing period could have resulted in substantial losses of moisture within the clay, ultimately changing its properties. For this reason, the use of rapid hardening grout was explored since this material could cure adequately overnight. Compressive, tensile and Young's

modulus tests were performed in accordance with the relevant concrete testing standards (BS EN 12390–13, 2013; BS EN 12390–3, 2019; BS EN 12390–6, 2009). These results were compared to a scaled concrete mix, designed for use in centrifuge modelling. The details and development of this mix design have been provided by Louw et al. (in review).

The rapid hardening grout is a commercially available powdered substance, commonly used for anchoring bolts (Rockset). This material was prepared by mixing the dry powder with water and allowing it to cure for a period of approximately 14 hours before testing. The ratio of water to grout mixed was 0.47 by mass. Details of the preparation procedure for the concrete mix have been provided by Louw et al. (in review) however, it should be noted that the curing period of these samples was 28 days. The results of this testing are provided in Table 14.

Table 14: Comparison of material properties for rapid hardening grout and scaled concrete

	Grout	Scaled concrete
Compressive strength (MPa)	35.87	35.83
Indirect tensile strength (MPa)	2.30	3.05
Young's modules (GPa)	11.90	20.53

While both the compressive and tensile strengths measured are almost identical for the two materials, it can be seen that the Young's modulus of the rapid hardening grout was approximately half that of the scaled concrete. However, the effect of the 4 mm threaded rod used in the centrifuge model which was cast into the rapid hardening grout needs to be considered. This can be done by accounting for axial stiffness which is equivalent to Young's modulus multiplied by the section's cross-sectional area (EA). By accounting for axial stiffness, it can be seen that the ratio of axial stiffness of the model pile to that of a concrete pile with 2% steel reinforcing ($EA_{model}/EA_{concrete}$) is equal to approximately 0.8. This comparison of axial stiffnesses was deemed sufficiently close real, full-scale applications.

CHAPTER 6

RESULTS - ELEMENT TESTING

The first results presented in this section are those of a one-dimensional consolidation test performed on a clay sample reconstituted at 1.1 times the soil's liquid limit (w_L). The purpose of this test was to determine the clay's intrinsic properties within the framework outlined by Burland (1990). Following from these results, a series of wetting after load tests (ASTM D4546–14, 2014) are presented as swell percentage versus time (initial sample details for all oedometer tests are presented in Table 11). The final achieved swell values from these tests are then presented in the form of a soaking under load curve, which affords the opportunity for the compressed and undisturbed samples to be compared. The properties of interest in this comparison are swell potential at various applied stresses, as well as the swelling pressure of the clay. After all samples were allowed to undergo swell, they were one-dimensionally consolidated until reaching their initial volumes and then unloaded entirely. These tests made it possible to obtain a second estimate on swell magnitude and swell pressure using a different approach. By following the 'swell followed by consolidation' method as discussed in Section 3.3.1, a further check of the predicted swell pressure as well as the swell magnitude at various applied stresses was obtained.

By comparing the consolidation tests of the compacted and undisturbed samples with that of the reconstituted specimen, a variety of soil properties were investigated. The first was that of soil structure. Using the concepts of permissible stress states and structure permitted space as proposed by Leroueil & Vaughan (1990), the effect of the sample preparation procedure on the structure of the soil was investigated. The section goes on to discuss the effect of swell on the yield stress of a soil. This phenomenon is presented and discussed within the extended framework for the behaviour of expansive soils (BExM) presented in Section 3.2.2.

The final section of this chapter presents the results of primary drying and wetting curves, as well as their associated shrinkage curves. The data presented in this section is based on the samples which underwent swell, consolidation and complete unloading. Comparisons of the water retention and shrinkage behaviour for the compressed, undisturbed and reconstituted samples are presented in this section.

It should be noted that throughout this chapter, samples are labelled according to the vertical stress applied during the wetting after loading tests, referred to as their 'soaking stress'. In cases where comparisons are made on the same figure between the undisturbed and compacted samples, the prefix of "U" and "C" are used for the undisturbed and statically compacted fissured samples respectively, i.e. the undisturbed sample allowed to swell under a soaking stress of 12.5 kPa has been labelled "U - 12.5 kPa". This labelling sequence has been employed throughout this chapter for all element testing performed.

6.1 Determination of intrinsic clay properties

Burland (1990) proposed a framework whereby the 'intrinsic properties' of a clay could be determined. Intrinsic properties are those determined from a sample which has been reconstituted at a water content of between w_L and $1.5 \cdot w_L$ without air or oven drying. The sample is then consolidated, preferably under one-dimensional conditions (Burland, 1990). The results of a one-dimensional consolidation test performed on the clay used in this study are presented in Figure 78. This sample was prepared at $1.1 \cdot w_L$.

Apart from the conventional consolidation data presented in Figure 78 a), other fundamental parameters are presented in Figure 78 b) – d) such as the coefficient of volume compressibility (m_v), the coefficient of consolidation (c_v) and the saturated hydraulic conductivity of the clay (k_{sat}). All of which help in providing a more comprehensive characterisation of the material tested.

The term 'intrinsic' is used to describe the results of one-dimensional consolidation tests on reconstituted specimens, since these properties are inherent to the soil and independent of its natural state (Burland, 1990). The framework developed by Burland (1990) is defined in terms of the intrinsic void ratios, e^*_{100} and e^*_{1000}, the void ratios at vertical effective stresses of 100 and 1000 kPa respectively and the intrinsic compression index, $C^*_c = e^*_{100} - e^*_{1000}$. Burland (1990) found that the relationship between these two parameters and e_L, the void ratio at the liquid limit of the clay were reasonably well-defined. Al Haj & Standing (2015) reproduced the plot presented by Burland (1990) with the results of two Sudanese expansive clays superimposed

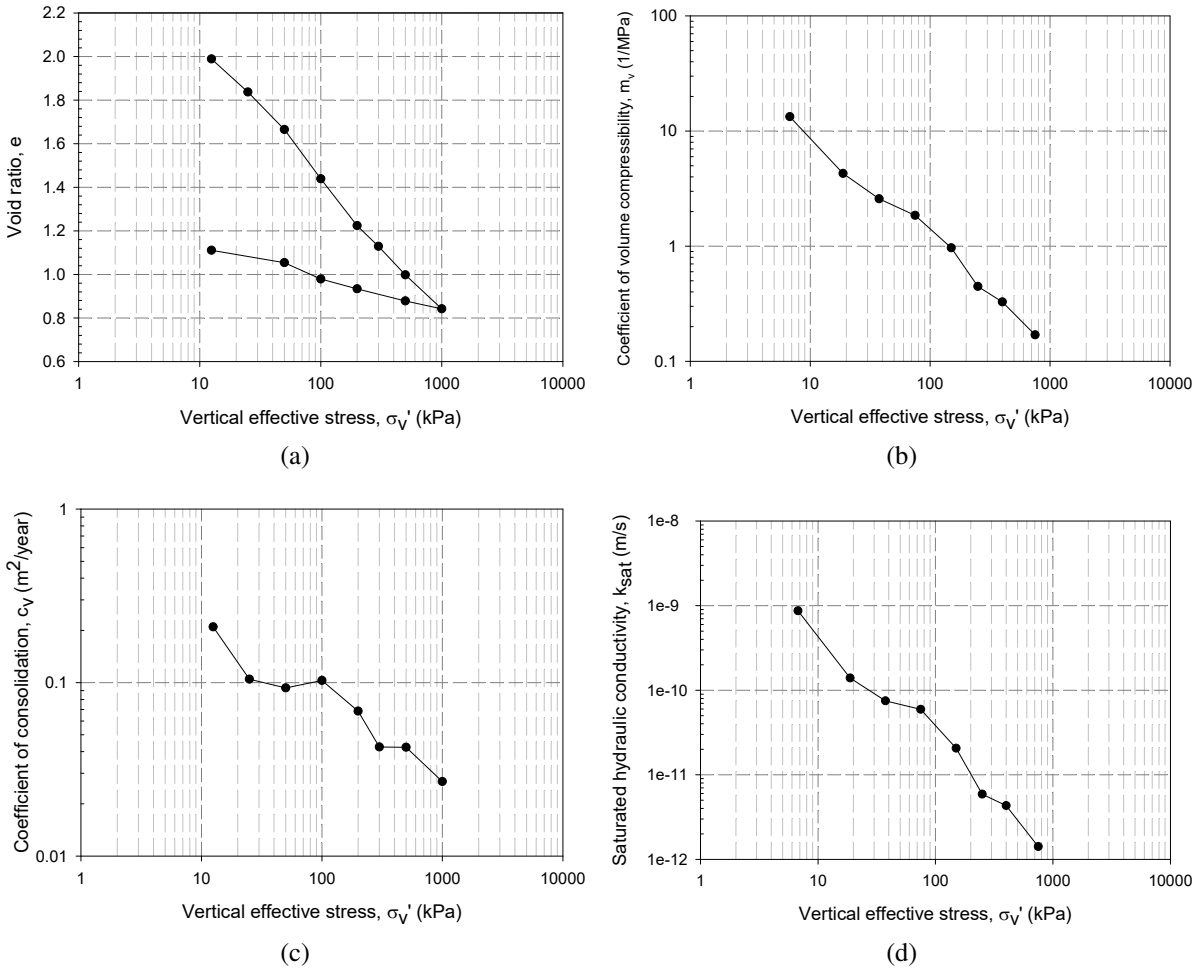

Figure 78: One-dimensional consolidation test results of a sample prepared at $1.1 \cdot w_L$ illustrating the relationship between σ'_v and a) e, b) m_v, c) c_v and d) k_{sat}

onto the original dataset. The intrinsic properties of the South African clay used in this study have been added to the dataset provided by Al Haj & Standing (2015) in Figure 79. The solid lines in Figure 79 are the empirical relationships established by Burland (1990) while the broken lines present the work of Nagaraj & Srinivasa Murthy (1986) who established a relationship between the ratio e/e_L and σ'_v based on considerations of physical chemistry (Burland, 1990).

The results presented in Figure 79 illustrate that the intrinsic properties of the clay used for this study fall within the data range illustrated. This provides confidence in the consolidation test performed on the reconstituted specimen, which is later used as a benchmark test to evaluate various other properties of the clay used in this study. The intrinsic void ratio at 100 kPa (e^*_{100})

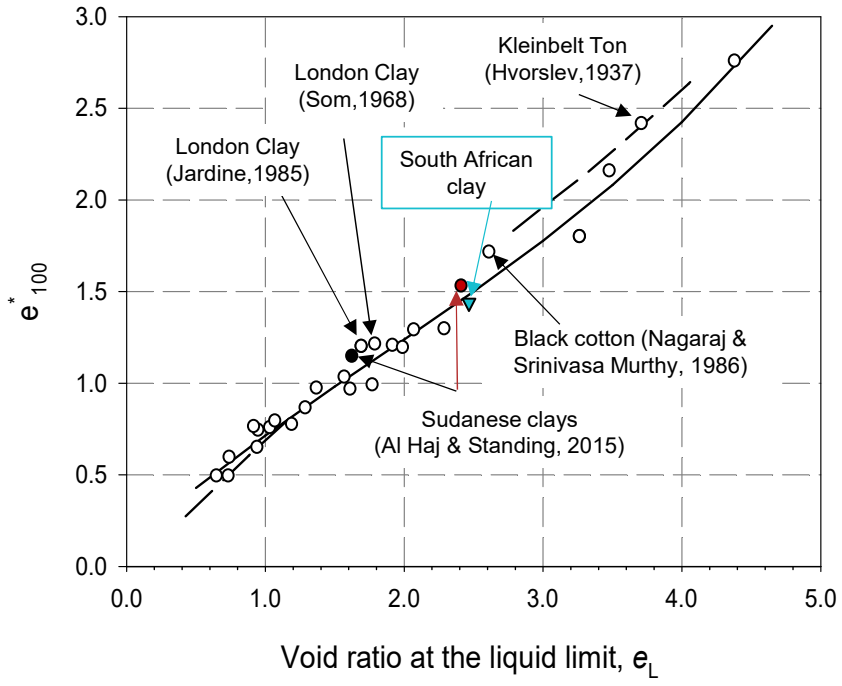

(a)

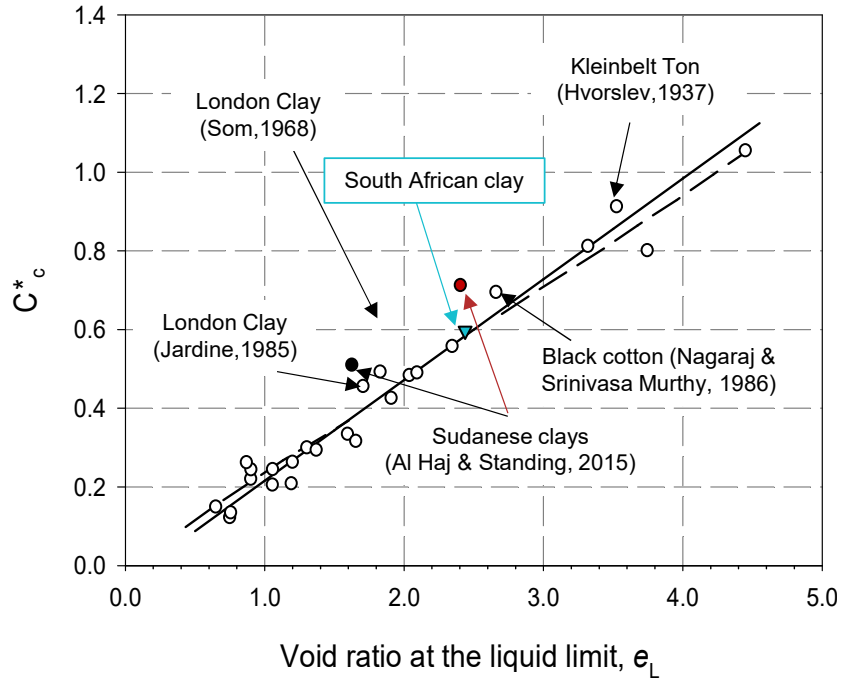

(b)

Figure 79: Relationships between e_L and the intrinsic parameters a) e^*_{100} and b) C^*_c (after Al Haj & Standing, 2015)

of the South African clay evaluated in this study compare relatively well with one of the Sudanese clays investigated by Al Haj & Standing (2015), denoted by a solid red circle in Figure 79. Al Haj & Standing (2015) did however note that the value of C_C^* plotted slightly above previously recorded dataset. This led to the suggestion that the testing of more tropical soils could indicate whether this finding was representative of some general trend. While the South African clay presented in this study plotted closer to the prediction of Burland (1990), this finding does not disprove the presence of a general trend for tropical soils plotting above it. According to the Köppen climate classification system, areas in the vicinity of Sudan and South Sudan are classified as "tropical moist" regions (Category A), whereas those in South Africa tend more towards drier, sub-tropical climates (Categories B and C) (Haut & Toll, 2012). The formation of these clays is therefore likely to have taken place under notably different conditions.

Following the characterisation of the intrinsic properties of the clays studied, a series of swell under load tests were conducted on both the compacted fissured material and undisturbed samples respectively. The results of these tests are presented in the following section.

6.2 Swell under load tests

As described in Section 5.3.1, swell under load or, *wetting after loading tests* were performed to determine the amount of swell that could be expected at various depths throughout the clay profile. The results of swell versus time for the compacted and undisturbed material have been presented in Figure 80 and Figure 81 respectively. Figure 82 presents a comparison of the swell results for the undisturbed and compacted material in the form of a 'soaking under load' curve.

On the swell versus time plots presented in Figure 80 and Figure 81, it can be seen that a constant value of volumetric strain was achieved by the end of testing. The final amount of strain seen in these two figures was subsequently plotted on Figure 82 as discrete points. Linear regression curves were then fitted through the data for compacted and undisturbed samples respectively. All three of the preceding figures illustrate the effect of soaking stress on the magnitude of volumetric strain. At low soaking stresses, samples experienced relatively high values of swell which decreased as the soaking stress increased. This reduction in swell was observed until the soaking stress resulted in compression of the sample.

From Figure 82 there are a few data points which do not conform to the general trends observed. For example, the undisturbed specimens tested at soaking stresses of 200 and 300 kPa respectively seem to deviate slightly from the overall trend. Considering that these

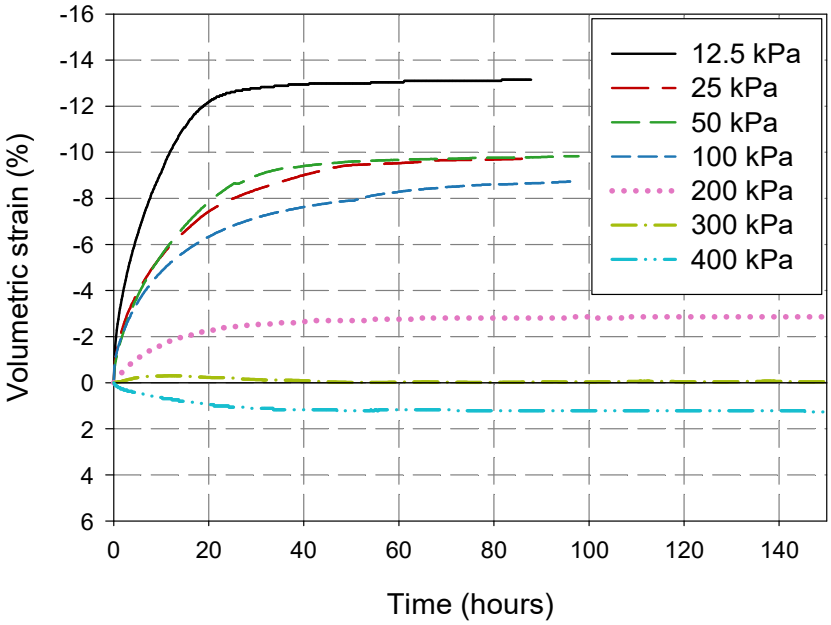

Figure 80: Swell versus time under constant vertical stress (compacted samples)

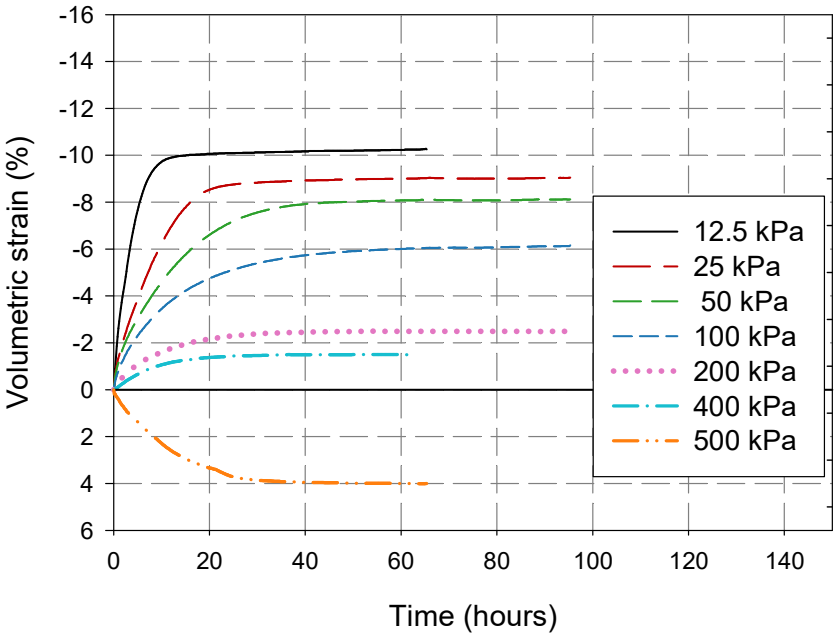

Figure 81: Swell versus time under constant vertical stress (undisturbed samples)

were 'undisturbed' samples it is difficult to distinguish which of these points is the outlier, i.e. whether the sample at 300 kPa swelled more than expected, the sample at 200 kPa swelled less than expected, or possibly a combination of both. What is known is that both samples had

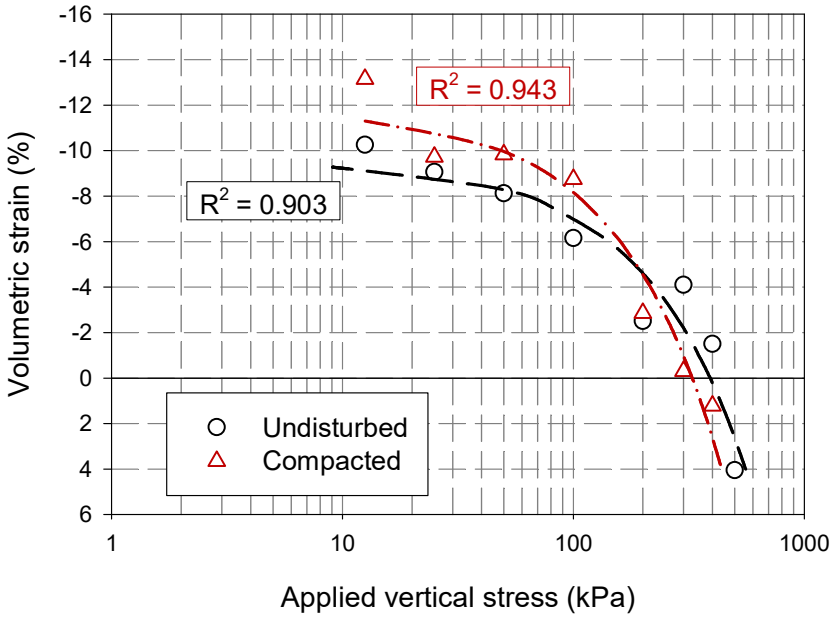

Figure 82: Soaking under load curves for compacted and undisturbed samples

similar initial moisture contents and void ratios. For completeness, the results of both samples have been included in the dataset.

Similarly, the compacted samples at soaking stresses of 25, 50 and 100 kPa appear to have swelled to approximately the same value, deviating slightly from the predicted regression curve. While stricter control was had over the compacted specimens, it should be noted that in its natural state, this soil comprises a clay matrix, interspersed with calcrete nodules. By observation it was noted that the grating process employed in the sample preparation procedure did remove some of these non-expansive nodules, thus slightly changing the overall mineralogical composition of a given sample. It is therefore possible that this change in composition might have affected the swell potential of the prepared samples by varying amounts.

Despite these outliers, the soaking under load curves presented in Figure 82 highlight how the statically compacted samples illustrated similar swell characteristics to the undisturbed specimens. Not only was the magnitude of swell achieved at all soaking stresses similar for the compacted and undisturbed samples, but the swell pressure also remained relatively unchanged. Using the regression curves plotted in Figure 82, the stress required to achieve 0% volumetric change was 329 and 392 kPa for the compacted and undisturbed specimens respectively. While perhaps counterintuitive, this finding is one which has been observed in the literature. In

studying the effects of fabric on the swelling characteristics of highly plastic clays, Armstrong & Zornberg (2017) concluded that soil fabric did not affect the magnitude of swell for laboratory prepared specimens. Furthermore, Brackley (1983) reported "no difference between swell of undisturbed and remoulded samples at similar densities and moisture contents". Brackley (1983) attributed this finding to the fact that highly expansive soils tend to have a remoulded structure in-situ. Given that swelling clays will, over a geological time frame, undergo many cycles of swelling and shrinking, Brackley's explanation is plausible.

Recognising this explanation, the findings of this study and of those reported, it would appear that changes in structure/fabric induced in the laboratory by grating and compaction, have minimal effect on the observed swell characteristics, provided that moisture contents and densities are consistent. This finding provided confidence that the preparation procedure employed in this study was adequate and would produce realistic swell properties when used for centrifuge testing.

After undergoing swell under various applied vertical stresses, the samples presented were subjected to one-dimensional consolidation tests. These consolidation tests were performed to investigate a range of soil parameters. The first of which was to provide a check on the swell pressure and potential at various applied stresses using the swell followed by consolidation approach. The results of these tests are presented in the following section.

6.3 Swell followed by consolidation

In addition to the soaking under load curve presented in the previous section, Section 3.3.1 discussed how a 'swell followed by consolidation' test could be performed to determine the same parameters (i.e. the magnitude of swell at various applied stresses as well as the swell pressure). This section presents the results obtained from the loading portion of the consolidation tests conducted on samples which underwent swell at a soaking stress of 12.5 kPa. The loading curves for both the compacted and undisturbed specimens are presented in Figure 83 a). In Figure 83 b) the same results have been superimposed onto the soaking under load curve presented earlier in Figure 82. This super-imposition allows for a comparison of swell magnitude and pressure predicted by the two test methods.

From Figure 83 a) it can be seen that the loading curves reach a volumetric strain of 0% at a swell pressure of 260 and 300 kPa for the undisturbed and compacted samples respectively. These values, while slightly lower than that predicted by the soaking under load curve, do compare well with the former approach. Figure 83 b) illustrates how the two methods predict

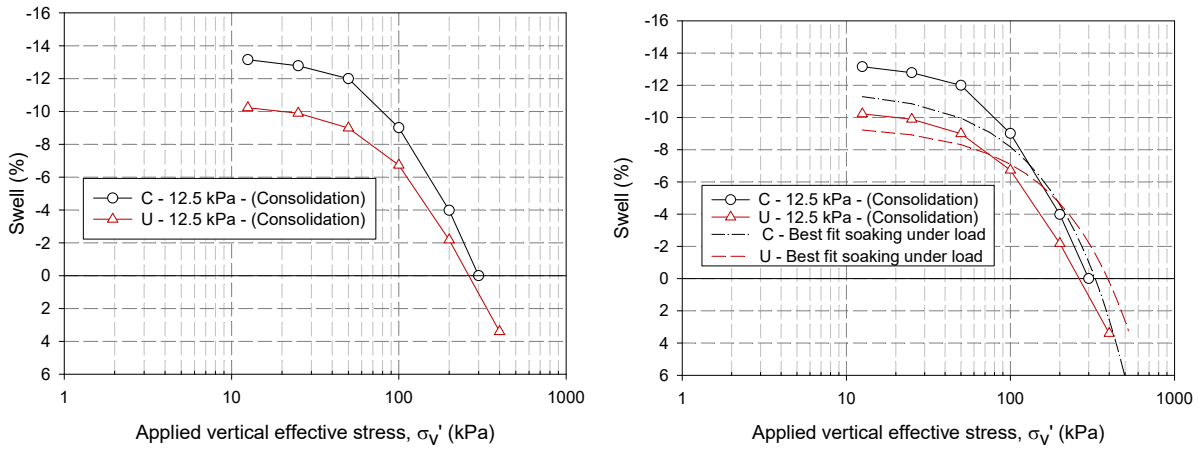

Figure 83: The results of a) consolidation tests and b) consolidation tests superimposed onto the soaking under load curve

similar values of swell potential across the range of vertical effective stresses. However, it cannot be categorically stated that one method consistently predicts higher or lower values over the stress range considered. At lower stresses, the swell followed by consolidation test predicts a higher swell potential, while at higher stresses the opposite is true. The highest difference in volumetric change predicted within the stress range considered was for the undisturbed specimens at a vertical effective stress of 400 kPa. The discrepancy at this stress was approximately 3%.

These results illustrate that despite the limitations of the aforementioned testing methods discussed in Section 3.3, for the soil tested in this study, the two approaches produce consistent results. Over and above the validity of the two testing approaches, the results achieved further illustrate that the sample preparation procedure employed managed to retain key properties of the expansive clay.

In addition to the samples soaked under stresses of 12.5 kPa, the rest of the specimens were also consolidated and unloaded to further characterise the material used. As is a common theme within the element testing results presented, these characterisations were necessary to determine whether the sample preparation procedure employed produced a material which was representative of field conditions, such that the results obtained from centrifuge testing could be meaningful.

6.4 One-dimensional consolidation tests

The following section presents the results of the one-dimensional consolidation tests of both the compacted and undisturbed specimens illustrated in Figure 84 and Figure 85 respectively. These consolidation tests were performed after samples were allowed to swell under an applied vertical stress as discussed in Section 6.2. The stresses referred to in the legend of these figures denote the stress under which they were allowed to swell (i.e. soaking stress). Figure 84 and Figure 85 have also included the results of the consolidation test performed on the specimen reconstituted at 1.1 times the soil's liquid limit. This result provides a benchmark against which the other tests can be compared. Furthermore, Figure 86 has been included to compare the compression and expansion indices of the compacted and undisturbed specimens. Also included in Figure 86, for the sake of comparison, are the compression and expansion indices of the reconstituted specimen. Since the value of 'soaking stress' is not applicable to this test, these values have merely been indicated as constant, horizontal dashed-dot lines, being denoted with a prefix "R" in the legend.

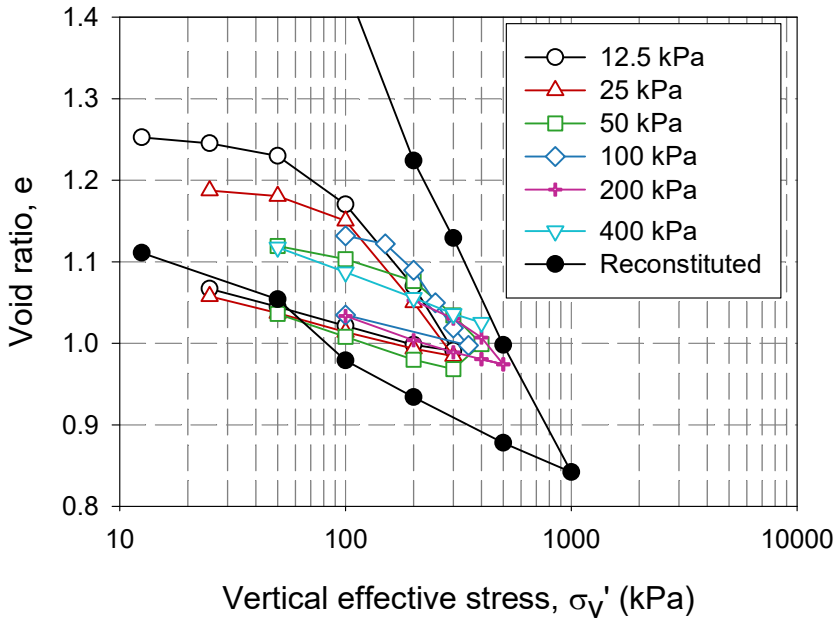

Figure 84: One-dimensional consolidation tests performed on compacted specimens following swell under a constant applied load

Perhaps the simplest parameter to discuss is that of the compression and expansion indices (C_c and C_e respectively). Figure 86 illustrates that there is little difference between the compacted and undisturbed specimens within the stress range considered, with slightly greater discrepancies observed for the compression indices. Another aspect which can be investigated

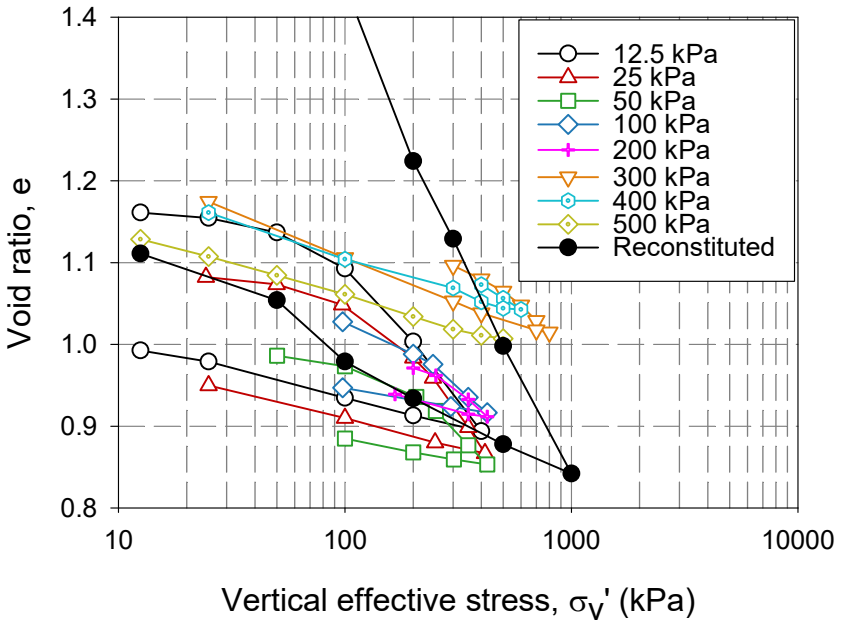

Figure 85: One-dimensional consolidation tests performed on undisturbed specimens following swell under a constant applied load

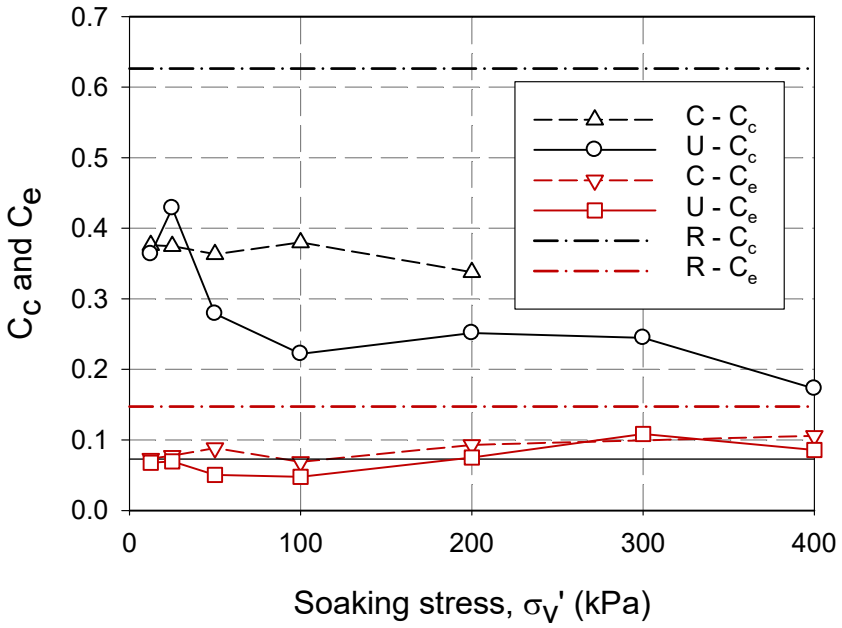

Figure 86: Compression and expansion indices of compacted and undisturbed specimens

is the relationship between the indices and soaking stress. Al Haj & Standing (2015) observed that while C_e was essentially independent of soaking stress, C_c reduced as soaking stress increased. For the material tested in this study, a similar relationship can be observed for the

undisturbed samples. Since the swell pressure of the compacted material was achieved for the soaking under load test at 300 kPa, further consolidation tests were not performed. As a result, it cannot be concluded from the data whether the same decrease in C_c with soaking stress would be observed. However, if the above parameters are investigated considering the mechanisms of soil structure, it is expected that a similar trend would hold for the compacted samples. Leroueil & Vaughan (1990) presented a study on the effect of structure in natural soils and weak rocks. While the term structure is used throughout their study, Yong & Warkentin (1975) defined structure as the combination of fabric (geometrical arrangement of particles) and bonding (due to cementation and physico-chemical interactions). While "fabric" and "structure" are often terms that are used interchangeably, Toll & Rahman (2010) illustrated that it is valuable to differentiate between the effects of 'fabric' and 'bonding', particularly in unsaturated soils. The author recognises the usefulness in differentiating between these two aspects. However, since the term "structure" is used throughout the publication by Leroueil & Vaughan (1990), this term has been used in the discussion that follows.

Leroueil & Vaughan (1990) demonstrated how structured soils exhibited a stiffer response than that of destructured soils, up until the point of yielding. In their publication, yielding (or loss of structure) was described as taking place due to compression, shear or swelling. It was also stated how structure is not removed instantaneously, but requires substantial post-yield strain. On this basis, Leroueil & Vaughan (1990) stated that it may be more logical to consider structure as a function of strain or strain energy.

With the effects of structure borne in mind, compression and expansion indices of swelling clays tested in this study, as well as those by Al Haj & Standing (2015) can be further discussed. Firstly, it can be stated that a soil with structure (or bonding) will be less compressible than the same material without structure. A reduction of C_c with soaking stress is therefore unsurprising. Such a trend is to be expected since an increase in soaking stress would have reduced volumetric strain due to *swell* to a greater extent, thus preserving structure. It is however important to note that this trend may not be applicable for samples soaked under stresses which far exceed the swell pressure of the soil. For such cases, samples may well undergo significant *compressive* volumetric strains which would also potentially destroy soil structure. In such a case, destroying structure would dictate that the value of C_c would begin to rise again. However, samples loaded to such high stresses would essentially be statically compacted to a large degree, thereby reducing compressibility. Due to the interplay between these two conflicting mechanisms, it is possible that C_c may reduce with soaking stress up to a point and then remain constant. However, this statement is by no means conclusive and would require further research.

The expansion index C_e, being independent of soaking stress, may also be interpreted within the framework of soil structure. Since the samples in this study and those by Al Haj & Standing (2015) followed the same testing sequence, i.e. swell under load, consolidation and unloading, structure could have been destroyed by swell-induced strains, compression-induced strains or a combination of both. It is therefore reasonable to assume that as a general rule, expansion indices should be independent of soaking stress, provided the samples have undergone this sequence of testing.

In comparison to the reconstituted sample, it can be seen that the compacted and undisturbed specimens were less compressible. This could be indicative of some degree of structure in the compacted and undisturbed samples. The expansion index of the reconstituted sample is however only slightly larger than the other samples. This finding supports the hypothesis that a testing sequence which involves swell, consolidation and unloading provides ample opportunity for soil structure to be destroyed.

6.4.1 Investigation of soil structure

Having introduced the concept of soil structure in the previous section, the following section focusses on a comparison between the compacted and undisturbed samples. Specifically, it aims to address any effects on structural changes which may have been induced in the laboratory preparation of the compacted samples. Drawing on the observations made by Leroueil & Vaughan (1990), Figure 87 illustrates the behaviour that may be expected of a soil with and without structure.

Firstly, Figure 87 illustrates the results of a reconstituted specimen. Consolidation of such a specimen would result in a straight diagonal line separating possible and impossible stress states on the left and right respectively. If an overconsolidated, unstructured soil is subjected to a one-dimensional consolidation test, the case illustrated in Figure 87 a) would be expected. With an increase in load, the void ratio would reduce at a rate dictated by C_e until the normal consolidation line (NCL) of the reconstituted specimen was reached. After this point, the specimen would follow the same trajectory as the reconstituted sample. However, the study conducted by Leroueil & Vaughan (1990) illustrated that a sample could exist in seemingly 'impossible' states if the soil was structured. In their publication Leroueil & Vaughan (1990) defined this region as structure permitted space as illustrated in Figure 87 b). Such a soil can exist in structure permitted space until such point that the structure is destroyed, after which the stress path will converge with, and follow the NCL defined by the reconstituted specimen.

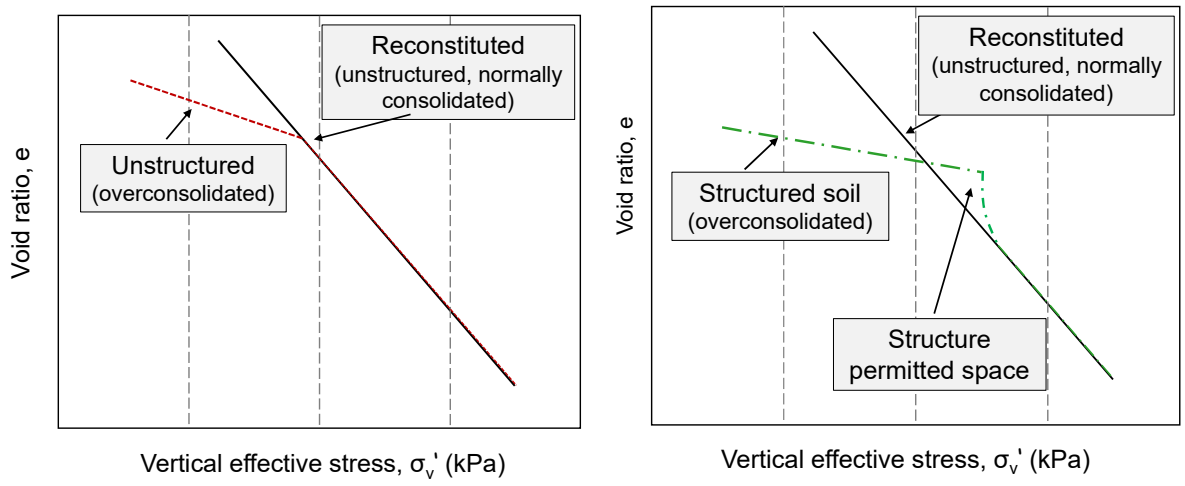

Figure 87: One dimensional consolidation of a) an unstructured and b) a structured soil

Figure 84 presents the results of consolidation tests conducted on the compacted samples after being allowed to swell under various soaking stresses. One important factor to note from this figure, is that all samples lie within permissible stress states. While they do not converge with the NCL of the reconstituted sample, a possible reason for this is that they were not loaded to sufficiently high stresses. Figure 85 illustrates consolidation tests performed on undisturbed samples. From this result, it can be seen that while most samples lie within permissible stress states, those inundated under soaking stresses of 300 and 400 kPa exist in structure permitted space. Such a result is consistent with the proposition put forth by Leroueil & Vaughan (1990) that structure should be considered a function of strain. The two samples which plotted in structure permitted space were also the two samples which experienced the least amount of volumetric strain during the swell under load tests (see Figure 80 and Figure 81).

Upon inspection of the consolidation tests and compression and swelling indices (Figure 84, Figure 85 and Figure 86 respectively) it appears that at low stresses, the swelling process had approximately the same effect on structural changes as the sample preparation procedure. Considering that the maximum vertical stress for all centrifuge testing conducted in this study was in the order of 130 kPa, such a result provides confidence that the laboratory compacted samples used in centrifuge modelling were representative of field conditions.

6.4.2 Investigation of yield stresses

The consolidation results presented in Figure 84 and Figure 85 illustrate different yield stresses for the various samples. Changes in yield stress for a given material can be attributed to two factors. Firstly, variation in the initial void ratio during a consolidation test will produce different yield stresses. However, as proposed by Gens & Alonso (1992), macroscopic volumetric change (i.e. swell) can result in softening of the clay. This was illustrated as movement of the LC yield curve in Figure 25. To investigate the reduction in yield stresses due to swell, two procedures were implemented. Firstly, the yield stress of each test was determined using the conventional Cassagrande (1936) approach. This yield stress accounts for the effects of softening due to swell. To determine the yield stress of a given sample, had it not undergone swell, a straight line was drawn from the initial void ratio at a slope of C_e to the normal consolidation line of the reconstituted sample. The intersection of this line with the NCL of the reconstituted sample was taken as the predicted yield stress of the sample in the absence of swell induced softening and soil structure. To illustrate this approach, consider Figure 88 which highlights the two yield stresses for sample C - 12.5 kPa. In Figure 88, σ_{vy1} represents the yield stress observed after swell, while σ_{yv2} represents the predicted yield stress in the absence of swell. This procedure was carried out for all samples tested and the results are presented in Figure 89 and Figure 90 for the compacted and undisturbed samples respectively.

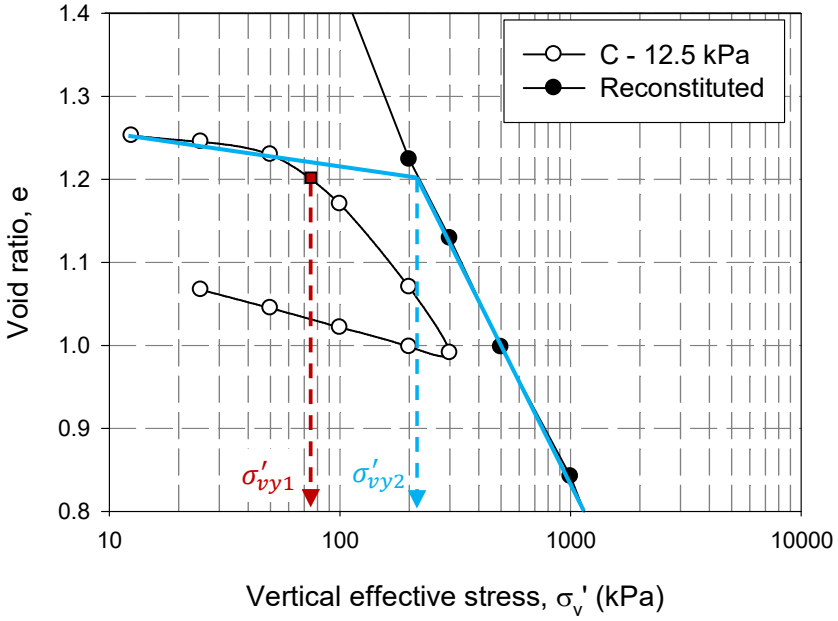

Figure 88: Reduction in yield stress due to swell

From Figure 89 and Figure 90 there are several trends which can be observed. The first and perhaps most obvious is that swell does produce a reduction in yield stress. Defining

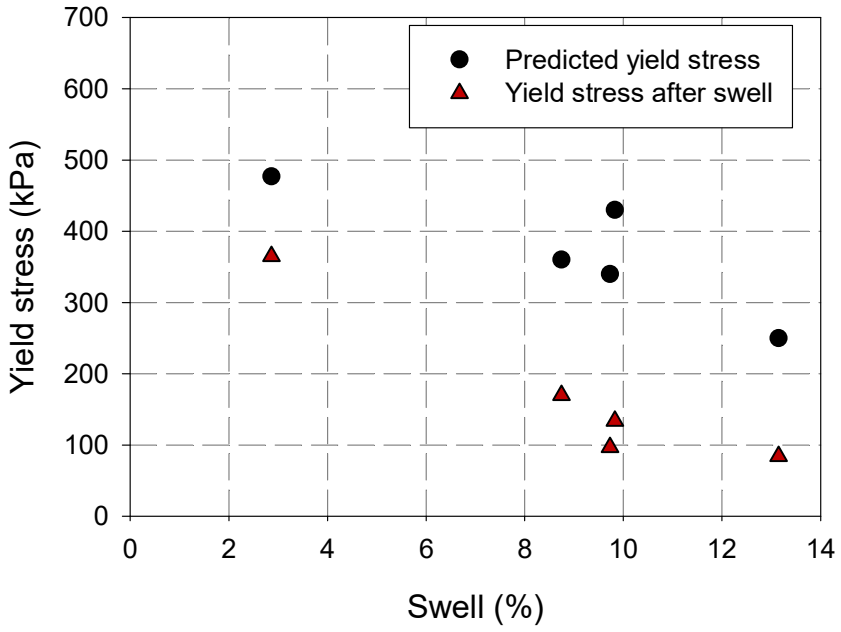

Figure 89: Reduction in yield stress due to swell for compacted specimens

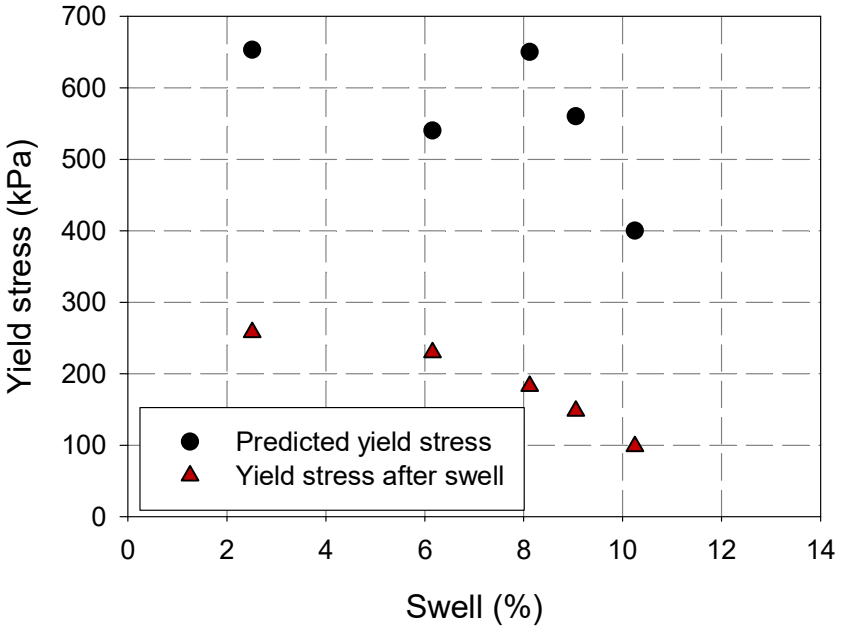

Figure 90: Reduction in yield stress due to swell for undisturbed specimens

a quantitative relationship between the reduction in yield stress and magnitude of swell is more troublesome. For the undisturbed samples presented in Figure 90, there appears to be an inconsistency in the predicted yield stress in the absence of swell. This occurs in the data points corresponding to approximately 6 and 8% swell. These two data points presented as

outliers in the soaking under load curve (Figure 82) and possible explanations for these results were discussed earlier (Section 6.2). Whatever the source of error for these two points, their initial void ratio at the start of consolidation would have affected the predicted yield stress, thus producing the peculiar result in Figure 90. Being 'undisturbed' specimens, variability in their initial properties (e.g. presence of calcrete nodules described previously) introduces a degree of uncertainty when quantifying the reduction in yield stress brought about by swell.

For the compacted samples, much stricter control was possible over the initial sample conditions, and so deducing trends from the data in Figure 89 is arguably more reliable. From Figure 89 it appears that there is initially a large drop in yield stress at low magnitudes of swell. From approximately 8% swell, the yield stress appears to remain constant. This result would point towards a non-linear relationship between post-swell yield stress and swell magnitude. Such a relationship is plausible since it implies a limiting value to which yield stress can be reduced due to swell.

Another aspect which can be investigated regarding the observed yield stresses is the coupling between micro and macrostructural swelling proposed by Gens & Alonso (1992). This coupling is illustrated graphically in Figure 26, where the horizontal axis represents the ratio of net mean stress to yield stress, and the vertical axis presents the ratio of macrostructural volumetric strain to microstructural strain. While microstructural strains were not measured in this study, all other parameters were, and so a qualitative comparison can be made of the observed behaviour and that conceptualised by Gens & Alonso (1992). Figure 91 a) presents the conceptual relationship proposed by Gens & Alonso (1992) with Figure 91 b) illustrating the experimental results obtained in this study.

From Figure 91 it can be seen that the measured trends are similar to that predicted by Gens & Alonso (1992). This result is useful since it illustrates how some behavioural aspects of swelling clays can be captured without knowledge of the microstuctural strains.

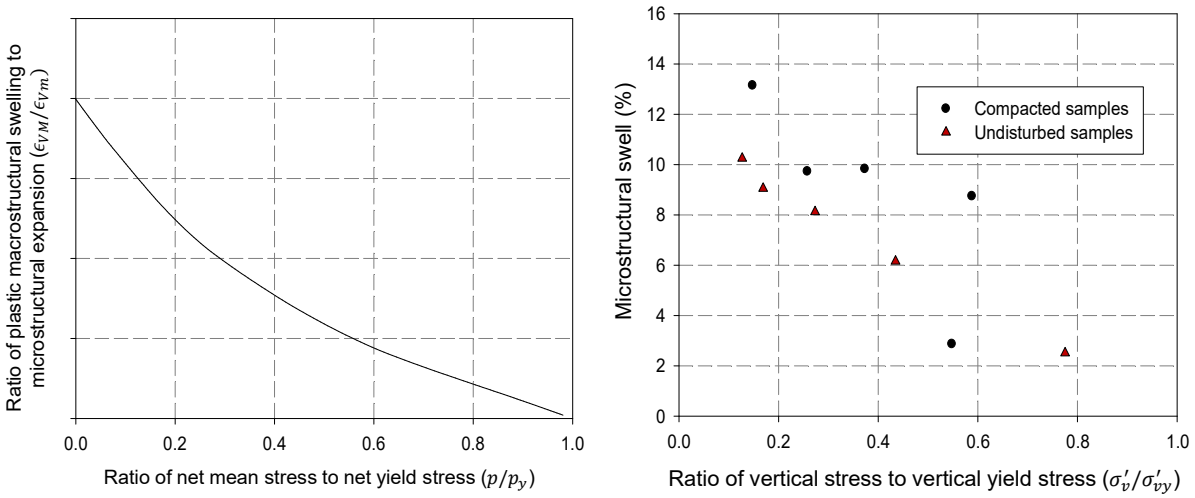

(a) (b)

Figure 91: Relationship between micro and macrostructural levels presented as a) a theoretical framework after Gens & Alonso, (1992) and b) experimental results

6.5 Soil water retention behaviour

Following the one-dimensional consolidation tests presented in the previous section, samples were unloaded entirely with free access to water, and allowed to rebound until volume changes became negligible. This step was to eliminate, as far as possible, any suction induced by the unloading process. After unloading, samples were removed from the oedometer apparatus and trimmed down to a size of approximately 37 mm and 9.5 mm in diameter and height respectively. Primary drying and wetting curves were then measured for all samples, with volumetric changes being recorded.

The following section presents the results of soil water retention curves (SWRCs), as well as shrinkage curves for both the compacted, undisturbed and reconstituted specimens. Data is presented as gravimetric moisture content versus suction and degree of saturation versus total suction. Shrinkage curves in terms of gravimetric moisture content are also provided and the section is concluded with a comparison of the best fit curves for the compacted, undisturbed and reconstituted specimens. The stresses indicated in each legend refer to the soaking stresses of the samples. Figure 92 and Figure 93 illustrate the soil water retention characteristics for compacted and undisturbed specimens respectively. The 'best fit' curves illustrated were derived using the Fredlund & Xing (1994) approach. The rationale behind using the Fredlund & Xing (1994) fit rather than more typical formulations (e.g. Van Genuchten (1980)) is that it incorporates a bounding value of 10^6 kPa at 0% water content. This value is supported by

thermodynamic considerations where it can be seen that as relative humidity is reduced to zero, suction approaches a value of 10^6 kPa.

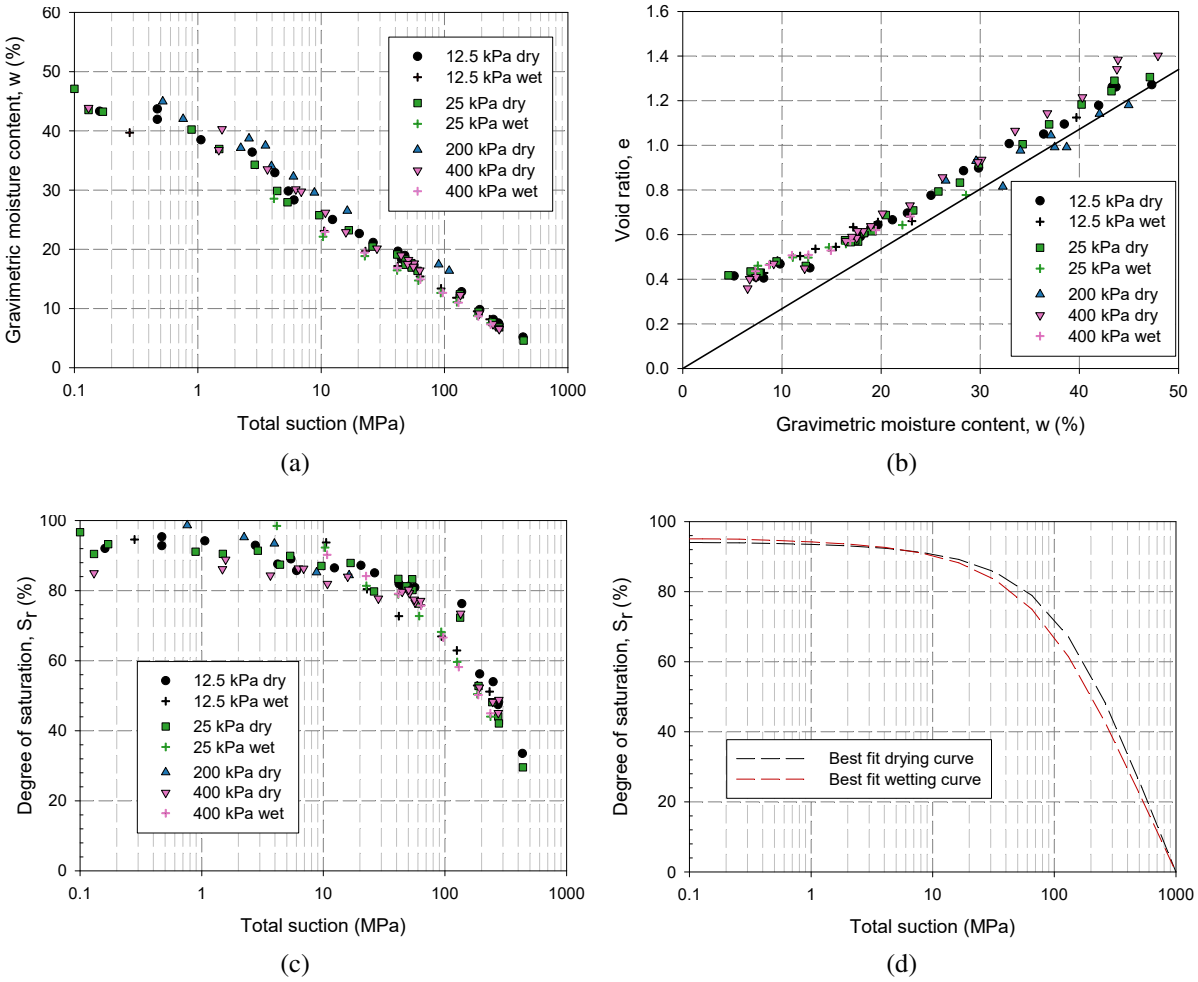

Figure 92: Soil water retention characteristics for compacted samples illustrating the a) gravimetric water content SWRC, b) shrinkage curve, c) degree of saturation SWRC and d) best fit primary drying and wetting curves

From Figure 92 it can be seen that the data follows a narrow band, with little differences being observed between samples allowed to swell at various soaking stresses. This is perhaps unsurprising since all samples were loaded to approximately the same stress and unloaded entirely. Since the expansion indices of the samples were seen to be essentially equivalent, the void ratios of the samples at the end of the unloading phase were similar, and as a result, so were the starting void ratios for the samples presented in Figure 92. Another useful point to emphasise from the data presented in Figure 92 is that little hysteresis was observed in both the saturation versus suction plot, as well as the void ratio versus gravimetric moisture

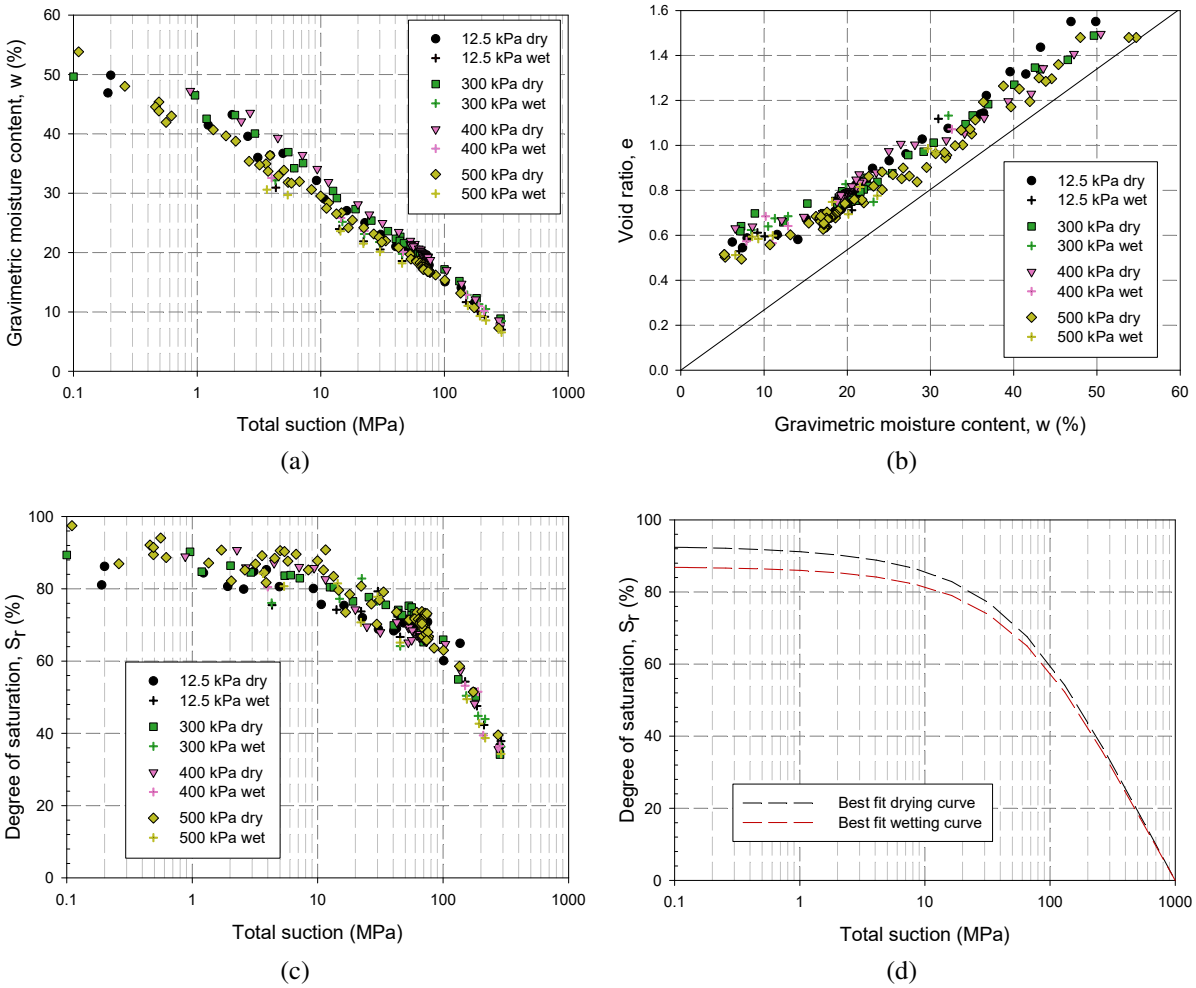

Figure 93: Soil water retention characteristics for undisturbed samples illustrating the a) gravimetric water content SWRC, b) shrinkage curve, c) degree of saturation SWRC and d) best fit primary drying and wetting curves

content result. This illustrates how the magnitude of suction is independent of whether the sample was wetted or dried to a particular point. Furthermore, it highlights that wetting/drying induced volumetric strains appear to be reversible. A study by Liu et al. (2020) presented the results of repeated wetting and drying cycled on a low-plasticity clay. In this study it was observed that initially, an accumulation of large irreversible shrinkage occurs. However, it was noted that the amount of shrinkage decayed significantly with an increase in the number of wetting/drying cycles and that after the third cycle, behaviour became almost repeatable. As mentioned previously, Brackley (1983) attributed the similarity of swell characteristics between undisturbed and laboratory compacted samples to the fact that expansive clays occur in a remoulded state in-situ. Having undergone many wetting and drying and swelling and

shrinkage cycles over geological time, the lack of hysteric behaviour observed in Figure 92 is consistent with the findings of Liu et al. (2020) and Al Haj & Standing (2016). In addition to the cycles occurring over a geological time frame, all samples presented in Figure 92 and Figure 93 underwent an initial wetting path along a scanning curve during the wetting under load test to a point of zero suction.

The results for the testing of undisturbed samples illustrate a wider band than that of the compacted samples. They are however similar in shape and do not differ significantly in the magnitudes of suction measured. Differences between samples tested which were swelled at different soaking stresses do not appear to follow any general trend, i.e. soaking stresses and the suction at a particular value of saturation are not proportional. Nevertheless, the wider band of data observed for the undisturbed specimens is not surprising since more repeatability is expected between various specimens prepared in a laboratory and 'undisturbed' samples. Furthermore, apart from creating a more closely fissured sample, grating of material in the preparation of compacted samples removed much of the calcrete nodules which were originally present in the material. This creates a difference in both the structure and mineralogy of compacted and undisturbed specimens which could conceivably become more pronounced in smaller sample sizes. The accuracy of the suction measurement should also be considered when viewing this data. The dewpoint hygrometer used (WP4-C) has a reported accuracy of 50 kPa between 0 and 5 MPa total suction, and 1% of the measured value between 5 and 300 MPa (Metergroup, 2017*b*).

The hysteretic behaviour in the saturation versus suction plot in Figure 93 d) appears to be slightly greater than what was observed for the compacted specimens. The shrinkage curves however illustrate no discernible differences between drying and wetting. This again illustrates that volumetric changes due to drying and wetting are reversible processes for the material tested, again being consistent with the explanation provided by Brackley (1983). Figure 94 illustrates a comparison of the best fit curves of the primary drying and wetting of the compacted, undisturbed and reconstituted samples respectively. SWRCs in terms of degree of saturation as well as shrinkage curves are presented.

From Figure 94 it can be seen that the general shape of the various curves are similar. It can however be seen that the undisturbed samples plot noticeably below the compacted and reconstituted specimens in Figure 94 a). This can be explained quite simply by the higher void ratios for the undisturbed samples in Figure 94 b). The hysteretic behaviour between wetting and drying cycles for the undisturbed samples in Figure 94 a) appear to be slightly greater than the laboratory prepared samples. This can be attributed to the higher void ratio attained at

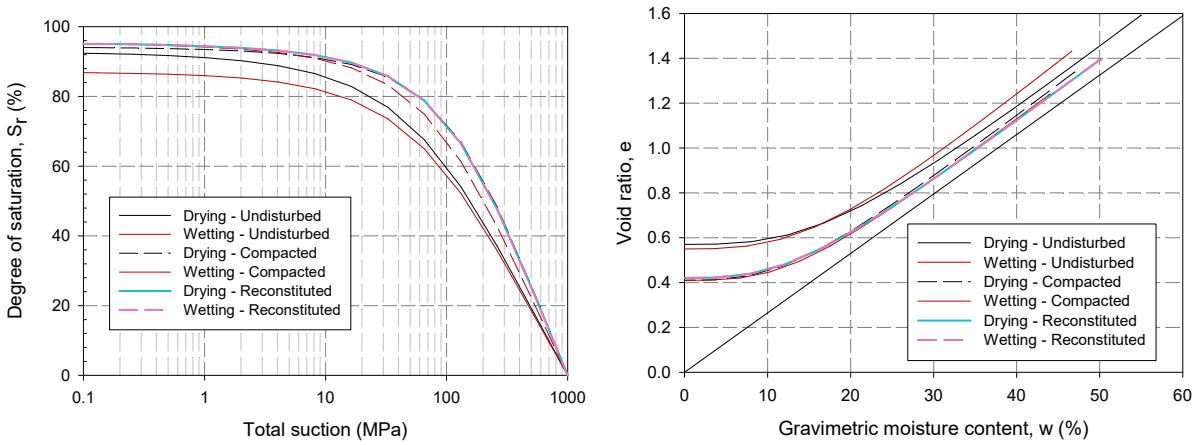

(a) (b)

Figure 94: Comparison of best fit curves for a) the SWRC and b) the shrinkage curve

the end of wetting for these samples. The higher void ratio at the end of the wetting process would have reduced the measured degree of saturation in Figure 94 a) where more hysteresis is observed.

CHAPTER 7

RESULTS - CENTRIFUGE TESTING

The following section presents the results of various centrifuge tests undertaken for this study. Details for initial soil properties are provided in Table 12. As mentioned in Section 5.4, Greenfield Test 1 and the Pile pull-out test was presented by Gaspar et al. (2019*b*) and Smit et al. (2019) respectively. The results of these tests are not discussed in detail in this thesis however, the key results from these tests are as follows:

- Greenfield Test 1
  - The clay preparation procedure employed, allowed for a magnitude of swell representative of field conditions to be achieved within a relatively short time frame in the geotechnical centrifuge.
- Pile pull-out test
  - For full length piles, shaft capacity reduced after allowing swell to occur.
  - Pull-out tests conducted after swell exhibited a less stiff response than those conducted at the soil's natural moisture content.
  - During pull-out tests, failure occurred within the clay, rather than along the pile/clay interface. This was a result which was not sufficiently emphasised in the original publication, but one which could potentially simplify numerical simulations.

The remainder of this section presents the results of the other tests listed in Section 5.4. Beginning with an improved Greenfield test, the section discusses factors such as magnitude of

swell versus time, and the variation of swell across the width of the profile. The variation and validity in suction measurements are also discussed for the Greenfield Test. The penetration resistance of this test was provided in Figure 53 and shown to be consistent in all slabs prior to swell, with a significant reduction in resistance post-swell.

The results of the three plug pull-out tests are initially presented separately, followed by a comparison of all three tests. The aim of these discussions is not only to investigate comparisons of shaft capacities pre and post swell, but also to look at variation in shaft resistance with depth. Following the pull-out tests, the results of the instrumented pile test which measured the development of lateral stresses during a swelling process are presented. The penetration test record for this test was illustrated in Figure 53 confirming consistency in the preparation of the clay slabs throughout the clay profile, as well as a consistent reduction in penetration resistance at the targeted swell. This section is concluded with a discussion on the development of swell throughout the modelled profile from Greenfield Test 2 and the Instrumented pile test. The measured swell profiles are then compared with the swell predicted by Van der Merwe (1964) as well as the results of the swell under load tests presented in Section 6.2.

7.1 Greenfield test 2

In contrast to the test presented by Gaspar et al. (2019*b*), this greenfield test measured only 335 mm in width and contained additional instrumentation such as:

- Multiple LVDTs to measure surface swell.
- Measurement of penetration resistance.
- Measurement of water content and soil suction in-flight.

Figure 95 illustrates the swell observed in each clay slab as well as the variation in surface swell across the width of the model. In Figure 95 a) the slope change observed at around 45 hours was due to an overnight drop in water level below the surface of the clay profile. The water level was promptly topped up at this point and swell proceeded. It should also be noted that in this figure, Slab 5 corresponds to the top slab and Slab 1 to the bottom slab. In Figure 95 b) the positions of the surface LVDTs have been indicated at the top of the graph.

Figure 95 a) illustrates that while the swell in the top slab reached an equilibrium state at around 60 hours, all slabs beneath it, subjected to higher overburden stresses continued to show

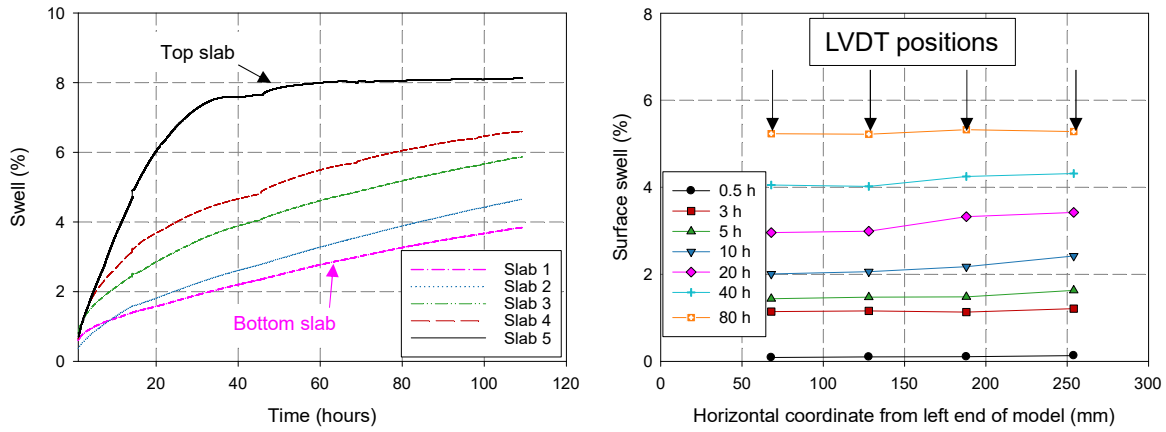

Figure 95: Figures illustrating a) swell versus time for every layer in the model and b) the variation in surface swell along the width of the model

a slow increase in swell with time. Figure 95 b) illustrates that there was very little variation in surface swell across the width of the profile. Due to the uniform heave across the width of the model, boundary effects were considered insignificant.

While the results presented in Figure 95 extend for a period of approximately 110 hours, the targeted swell was in fact achieved much sooner. Figure 96 illustrates how the targeted swell (predicted by Van der Merwe (1964) for a clay of very high potential expansiveness) was achieved at approximately 10 hours. The 10 hours required to achieve the targeted swell equates to 375 days at prototype scale if the scaling laws proposed by Caicedo et al. (2006) are applied. The implications of this are that, were a full-scale test to be conducted, the profile would need to be flooded for over a year before soil-structure interaction testing could be conducted at the targeted swell. This result alone illustrates the significance of the preparation procedure developed in this study, i.e. development of closely fissured clay slabs separated by layers of geotextile. Compared to the centrifuge tests, an equivalent full-scale test would be uneconomical and time consuming. Even recognising the nuances that exist with regard to the interpretation of centrifuge tests compared to full-scale tests, this highlights the advantages of centrifuge modelling.

Figure 96 also highlights how swell originally occurs at a relatively fast rate, but begins to slow down after approximately 20 hours. It is also worth noting that after the 120 hour period, swell within the profile had not reached a point of equilibrium and could well have achieved greater magnitudes of swell. Figure 97 illustrates a comparison of the swell profile

predicted by Van der Merwe (1964) for a clay of *very high potential expansiveness* to the measurements taken on each slab. This figure also highlights how the general shape of the swell profile predicted by Van der Merwe (1964) is similar to that measured in this centrifuge study. Another aspect investigated in this test is the reduction in matric suction as the model was flooded with water. Figure 98 illustrates the measured scanning curves in the middle and bottom clay layers of the centrifuge model.

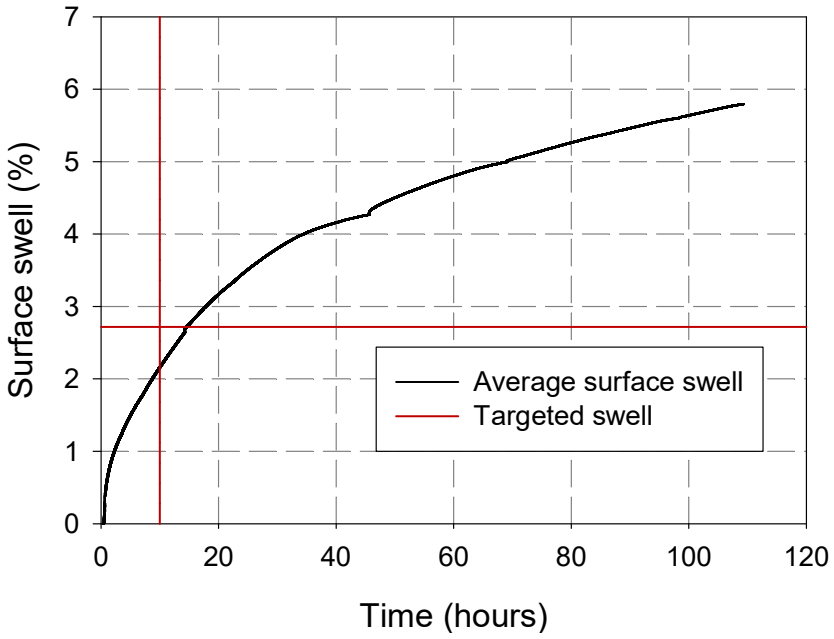

Figure 96: Average measured surface swell

Figure 98 presents the results of two scanning curves measured in different layers of the clay profile. It should be noted that for the volumetric measurements used to calculate the degree of saturation, it has been assumed that the only change in volume was due to swell in the vertical direction. In reality however, some swell will have occurred in the other two dimensions. The results presented in Figure 98 should therefore only be regarded as a qualitative illustration of the scanning curves followed. From Figure 98 it can be seen that the measured scanning curve for the middle layer follows a gradual reduction in suction as moisture content is increased. There is a slight discrepancy in the initial measured values of matric suction between the filter paper and the fixed-matrix porous sensor which measured 3 and 2 MPa respectively. The accumulation of data points at a degree of saturation of approximately 90% is not typical of measured soil water retention behaviour, but rather seems to be due to the limitation of the instrumentation having a lower capacity of 9 kPa (Metergroup, 2017*a*)[3]. The result presented

[3]This is the date when the sensor was purchased and the "Teros 21 integrator guide" downloaded. No date is however mentioned in this documentation.

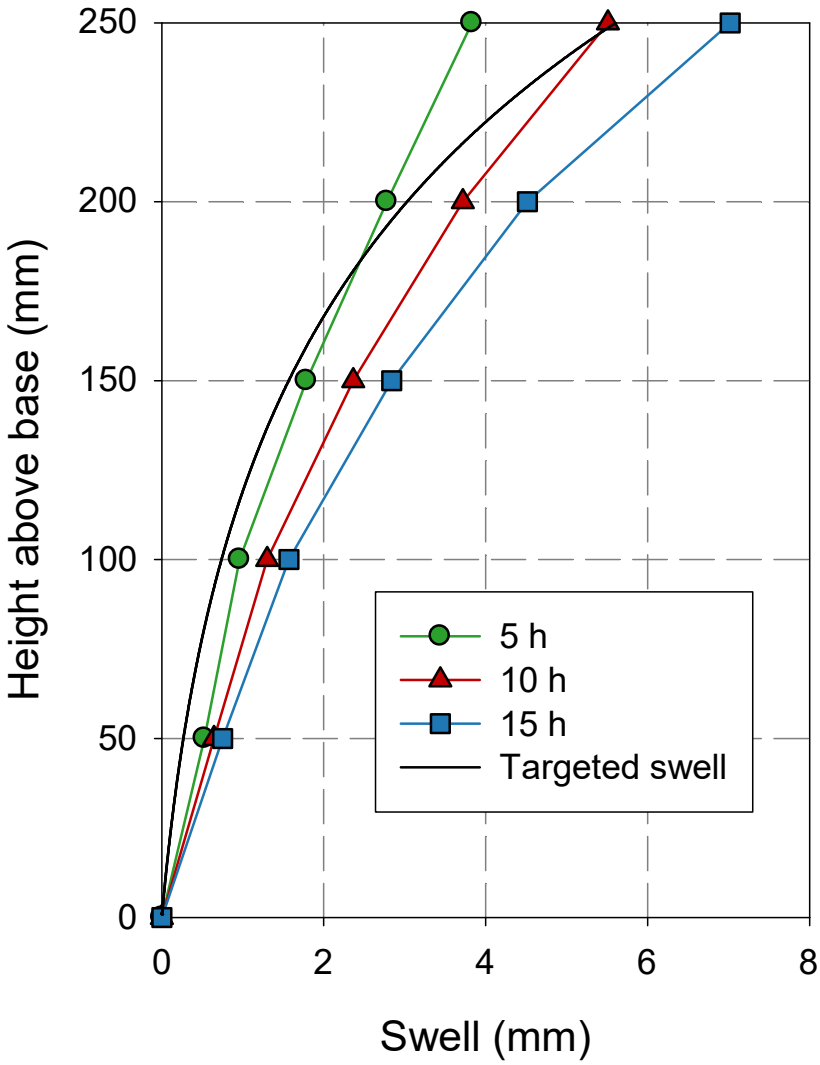

Figure 97: Measured versus predicted swell profile

for the bottom layer illustrates that, upon inundation, the measured value of suction dropped almost instantaneously, reaching a final recorded value of approximately 8 kPa. The logging rate used in this test was 1 reading per minute. This indicates that within a period of 3 minutes, moisture had flowed through the fissures of the profile and wetted the suction sensor to a point where it was reading its lowest possible value of suction. Of all the testing conducted in this study, eight attempts were made to measure changes in moisture content and suction in the geotechnical centrifuge. Of all these tests, the result presented in Figure 98 for the middle layer was the only result which illustrated a relatively gradual reduction in suction. For all remaining tests, even when logging rates were increased to 1 Hz, a dramatic drop in suction was observed as the water level in the model rose past the level of the sensor, in some cases reducing from

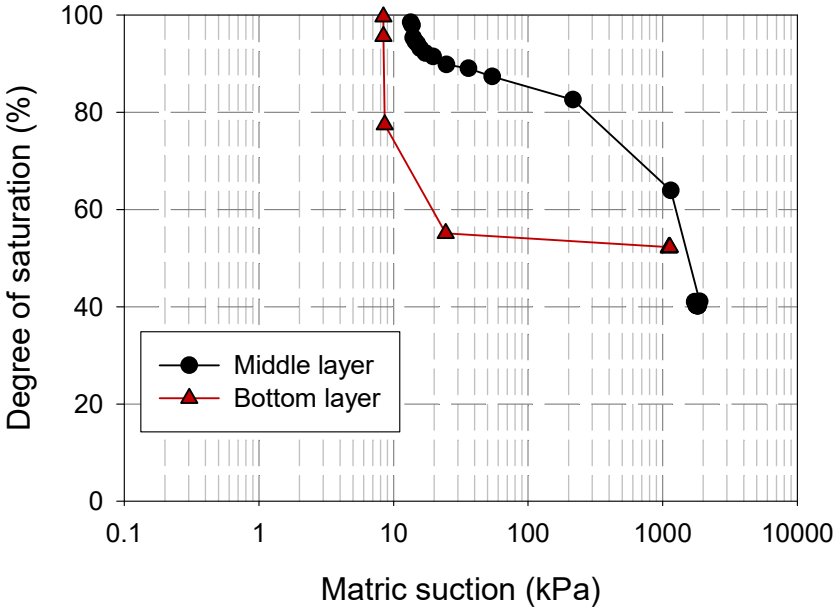

Figure 98: Scanning wetting curves for the middle and bottom clay layer of the centrifuge model

approximately 3 MPa to 9 kPa in one second. Such a result indicates that measuring matric suction in a fissured profile is troublesome since flow paths exist which allow moisture to flow directly to the sensor. This produced the dramatic drop in measured matric suction illustrated in Figure 98 for the bottom layer.

The above circumstance relates well to the question of what a 'representative' value of suction is for a fissured profile (see discussion on Figure 37). Given the rapid reduction in suction observed in the various tests presented in this study, a conceptual mechanism for the wetting of an expansive fissured profile is provided in Figure 99. In Figure 99, a representative mass of fissured clay is presented at different stages of wetting. The mass presented within this figure represents a relatively small volume of soil within an expansive profile, and so it is assumed that the confining pressure of surrounding soil would have suppressed the expansion of this representative mass. No volumetric changes of the representative mass are therefore presented. It should also be noted that there are some instances in an expansive soil profile where the fissures are not "air-filled" as is illustrated in Figure 99, but can be closed due to high overburden stresses. Closed fissures may be more typical deeper within a clay profile.

In Figure 99 a), the profile consists of a number of intact clay masses, separated by air-filled fissures. As the soil is initially wetted, the surfaces of the various intact masses of clay may rapidly reduce to a point of zero suction. This is illustrated conceptually in Figure 99 b) where

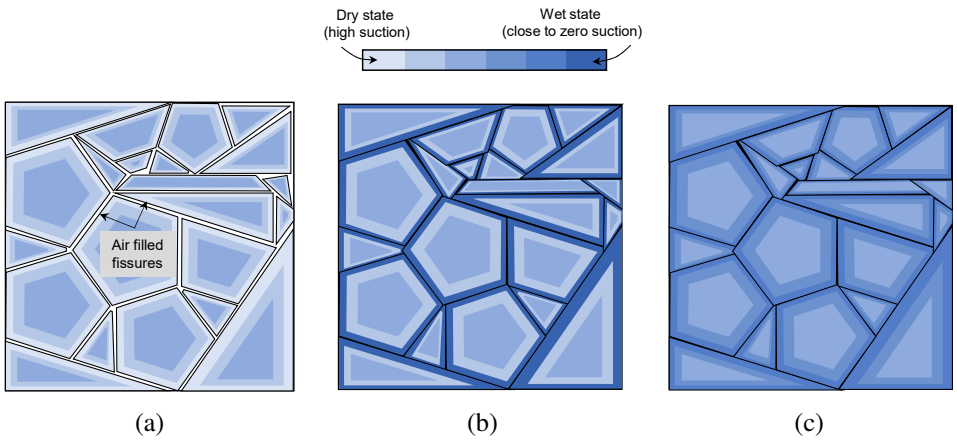

Figure 99: Wetting process of an expansive fissured profile illustrating a) the natural ('dry') state of the clay mass, b) the clay mass after initial wetting and closure of fissures and c) some time after closer of fissures where intact masses of clay tend towards an equilibrium value of suction

the outer regions of the clay masses correspond to the contour for a 'wet state'. Quantitatively this is represented by the result in Figure 98 for the bottom layer. As the fissures swell closed, the hydraulic conductivity of the entire soil mass will drop significantly (Figure 99 b)). Following closure of the fissures and a drop in hydraulic conductivity, matric suction on the outer portions of the intact masses of clay will tend towards a point of equilibrium with the centres of these masses. This is illustrated in Figure 99 c) where the colour contours of the inner and outer portions of the clay masses tend towards a point of equilibrium. By examining the infiltration process described in this section, it may be more accurate to state that two scaling laws are applicable when modelling a fissured clay. Initially, as water flows through the macro-fissures of the profile, the scaling law for seepage velocity is applicable and time should be scaled by N (where N is the model scaling factor). Once the fissures swell closed, the scaling law for a diffusion process proposed by Caicedo et al. (2006) becomes applicable and time should be scaled by N^2.

The result of the penetration test (CPT) performed (illustrated in Figure 53) supports the proposed mechanism. At the targeted level of swell, apart from the top layer, all subsequent slabs illustrated higher penetration resistances at their centre (between 3.5 – 4 MPa) than at their edges (approximately 2 MPa). If the top slab is considered, the penetration resistance had reduced to a value of almost zero.

Examining the CPT results more closely, qualitative interpretations can be made as to the likely stress paths undergone by the soil during swell. If it is recognised that the shear strength of unsaturated soils is both a function of suction and net stress (Alonso et al., 1990; Bishop, 1959; Fredlund & Morgenstern, 1977), it then becomes a point of interest as to what the relative contributions of these two mechanisms were. Considering the initial values of matric suction and maximum total stress (3 MPa and $\approx$ 130 kPa respectively), it can be seen that the initial suction in any given model was an order of magnitude larger than the net stress. It can therefore be reasonably assumed that suction was the dominating mechanism contributing to shear strength, and that the net stress component was almost negligible. At the time that the CPT was performed, the top slab had reached approximately 63% of its ultimate value of swell. After about 60 hours, negligible volumetric changes were observed in this slab. Such a trend is typical of that observed for swell under load tests performed in the oedometer (see Section 3.3.2) where the sample is typically referred to as reaching a point of "zero suction" (Schreiner, 1988*b*).

Considering that the top slab had not quite reached steady state at the time the CPT was performed, it cannot be stated that suction had completely reduced to zero. However, since the CPT result illustrates that the slab had close to no shear strength, it is likely that a relatively large proportion of suction had been lost. This is in contrast to the remaining four slabs in the centrifuge model which had markedly higher (but consistent) values of penetration resistance. While the top slab was free to swell in the vertical direction, the swell of subsequent slabs was restricted due to overburden stress. Figure 95 also illustrates that even after the test was completed, the rate of swell in these clay slabs had not approached a state of negligible volumetric change. The consistency in the penetration resistances of these slabs indicate that suction within the bottom four slabs was likely reduced by approximately the same amount.

The reduction in suction cannot be quantified by the change in degree of saturation using the SWRC presented in Figure 92 d). While void ratios can be calculated from only the change in height for oedometer tests where lateral expansion is restricted, the same is not true of the centrifuge models presented. Despite best efforts to perfectly restrict volumetric changes along the depth and width of a given model, swell did occur in these dimensions for all slabs (by varying degrees) and so calculations of void ratio would not be accurate. In light of the discussion presented above, the likely stress paths undergone by the various slabs are presented in Figure 100, using the BExM framework discussed in Section 3.2.2.

Within the BExM framework, the upper layer will have experienced a larger degree of softening during the swell process. This is predominantly due to the large reduction in suction

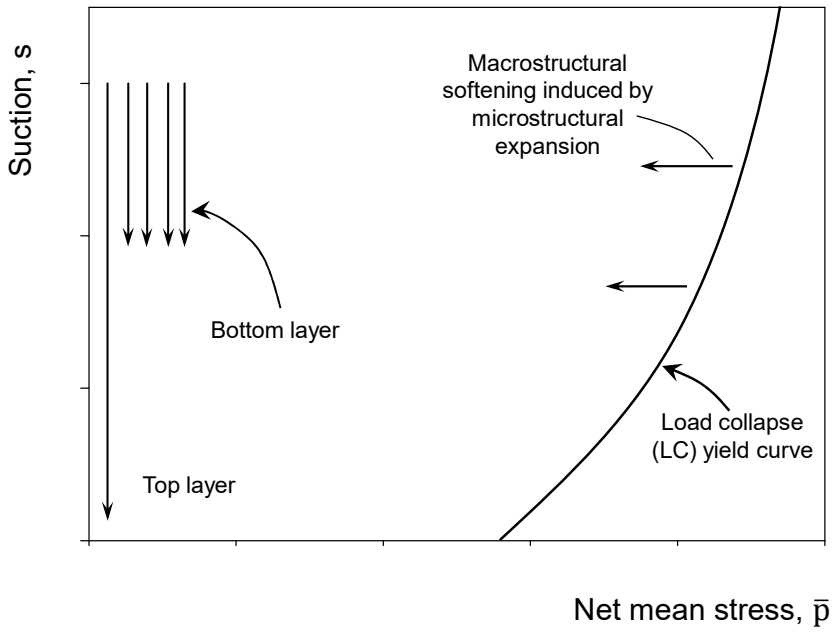

Figure 100: Qualitative illustration of the stress paths undergone for the various clay slabs during swell

experienced by this layer, and to a far lesser extent, its greater distance from the LC yield curve. Furthermore, within the BExM framework, Figure 100 would predict a larger magnitude of swell for the top layer which can again be explained by its large reduction in suction and proximity of its stress state from the LC yield curve. This is reflected in the swell measurements presented in Figure 95.

7.2 Pull-out tests

The results presented by Smit et al. (2019) revealed that the pull-out (shaft) capacity reduced after allowing swell to occur for *full length piles*. The aim of the plug (short pile) pull-out tests was to investigate the dependency of confinement (overburden) stress on the pull-out capacity of short piles. To investigate this, plugs were installed in the various layers and pulled out prior to, and after the targeted swell had been achieved. As mentioned previously, a series of plug pull-out tests were carried out during this study. This section aims to discuss them all separately and conclude with a section on the comparison between tests.

7.2.1 Pull-out (in-situ moisture conditions)

The aim of this series of pull-out tests was to investigate the pull-out capacity of piles prior to swell, i.e. at the soil's in-situ moisture content. The model layout is provided in Figure 63. After obtaining the pull-out capacity of the plugs prior to swell, the model was flooded to allow the targeted swell to be reached. Once reached, the plugs were pulled a second time. Figure 101 illustrates shaft friction versus plug displacement during the pull-out tests, prior to and after swell.

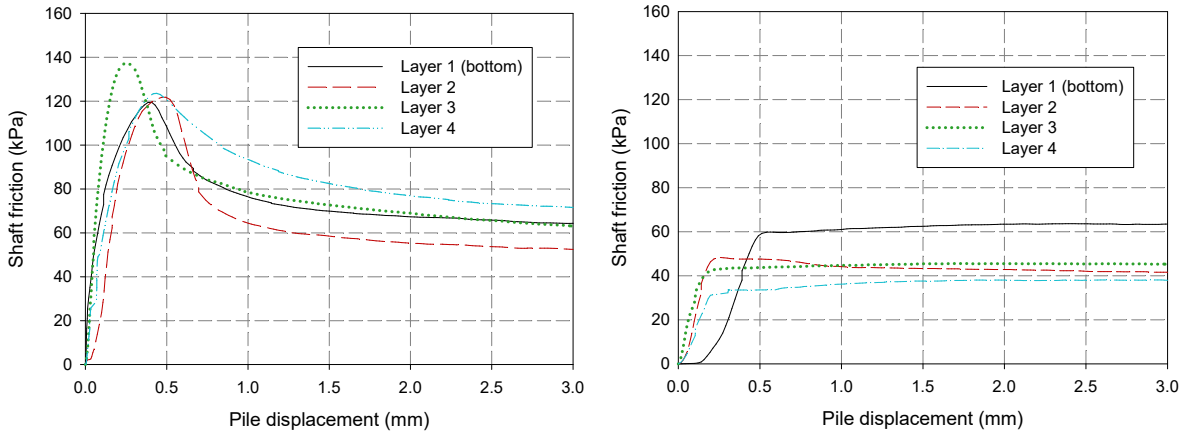

Figure 101: Shaft friction versus pile displacement at a) the soils in-situ moisture content and b) after swell had occurred

From Figure 101 a) it can be seen that peak shaft friction was achieved at approximately 0.4 mm displacement for all plugs except that in Layer 3, which appeared to reach its peak at approximately 0.1 mm. The peak shaft friction achieved seems independent of depth within the model and thus of confining pressure (consistent with a fully undrained response). Three of the piles consistently reached a peak shaft friction of approximately 120 kPa, with the plug in Layer 3 again being the outlier with a peak shaft friction of close to 140 kPa. In spite of the plug in Layer 3 exhibiting a slightly different response, all plugs appear to have produced consistent results.

Figure 101 b) presents the pull-out results for the same plugs after the targeted swell had been reached. In this figure, no peak is observed, but rather all piles seem to reach a certain value of shaft friction and then remain constant. Since this figure presents the results of piles which were previously pulled out of the soil, one might expect that the maximum shaft friction attained with any further "pulling" would be equivalent to the residual value observed in Figure 101 a). This is a sensible argument considering that a failure plane would have already

been established during the first pull-out test. However, upon closer inspection, it can be seen that there are some discrepancies between the maximum values of shaft friction attained in Figure 101 b) and the values of residual friction observed in Figure 101 a). These discrepancies can be attributed to the softening that occurs during the swell process.

The largest difference is for the plug in Layer 4. This is the plug that was the 'highest' in the profile and as a result had the lowest confining stress of all four plugs. The smallest discrepancy was for the plug in Layer 1, at the bottom of the model (experiencing the highest confining stress). The result in Figure 101 can be interpreted within the BExM framework by considering the degree to which swell-induced softening occurred. For this interpretation, Figure 100 is useful as it indicates how the highest and lowest plugs in the profile would have experienced the most and the least swell-induced softening respectively along their predefined failure planes.

7.2.2 Plug pull-out tests (swelled state with unsupported holes)

The results presented in this section are for a plug pull-out test with an identical layout to that presented in the previous section. However, for this test, plugs were only pulled out of the clay once the targeted swell had been achieved. Furthermore, augered holes behind the short length piles were left unsupported, allowing material to swell behind the plugs. Figure 102 illustrates the results of this pull-out test along with the pull-out tests conducted at the soil's natural moisture content discussed in the previous section (Figure 101 a).

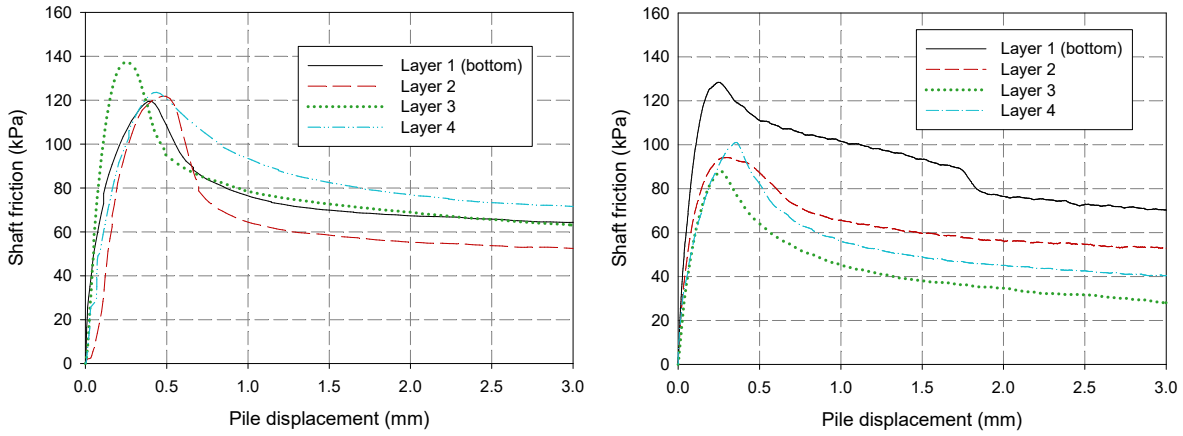

Figure 102: Results of pile pull-out tests at a) the soil's natural moisture content and b) after achieving the targeted swell

In the study conducted on full-length piles by Smit et al. (2019), it was found that the pull-out (shaft) capacity reduced by approximately 50%. Similarly, the results presented in Figure 102 show a reduction in shaft resistance for all layers, except Layer 1 (at the bottom of the model). Considering that vertical swell of this layer was restricted the most due to overburden stresses, it is intuitive that the lateral swell-induced pressure would be the highest for this pile. This increase in lateral pressure resulted in an increase in the measured shaft resistance.

Smit et al. (2019) reported a reduction in the stiffness of the response in full-length piles pulled out after allowing swell to occur. While Smit et al. (2019) were able to provide a conclusion in this regard, it should be borne in mind that the study presented by Smit et al. (2019) considered full length piles. For such testing, any imperfections along the pile length are less pronounced when observing the *average* stiffness of the pull-out test along the *full length* of a pile. Conversely, a short length pile is far more susceptible to minor imperfections along the pile/soil interface, and so calculated stiffnesses resulted in severely scattered results. For the short length piles reported in this study, it is therefore not possible to definitively conclude on any trend regarding the stiffnesses of pull-out responses for piles at various depths.

Figure 103 illustrates a typical example of a plug just after being removed from the model. From this photo it can be seen that during a pull-out test, failure occurs within the clay rather than along the pile/soil interface as may be expected for a perfectly smooth (e.g. aluminium) pile. This finding is in agreement with what was observed by Smit et al. (2019).

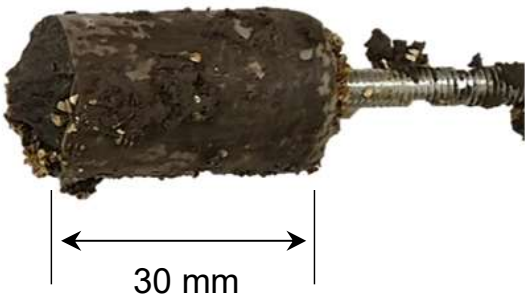

Figure 103: Photograph of short pile after pull-out test

7.2.3 Plug pull-out tests (swelled state with supported holes)

The final pull-out test was conducted with the same layout as the previous two tests, with the exception of the fact that the holes behind the plugs were supported with aluminium tubes. This test was performed to determine to what degree (if any) the clay which swelled behind the

plugs affected the measured pull-out (shaft) capacities. Figure 104 presents the results of the two pull-out tests conducted after swell with and without supported holes.

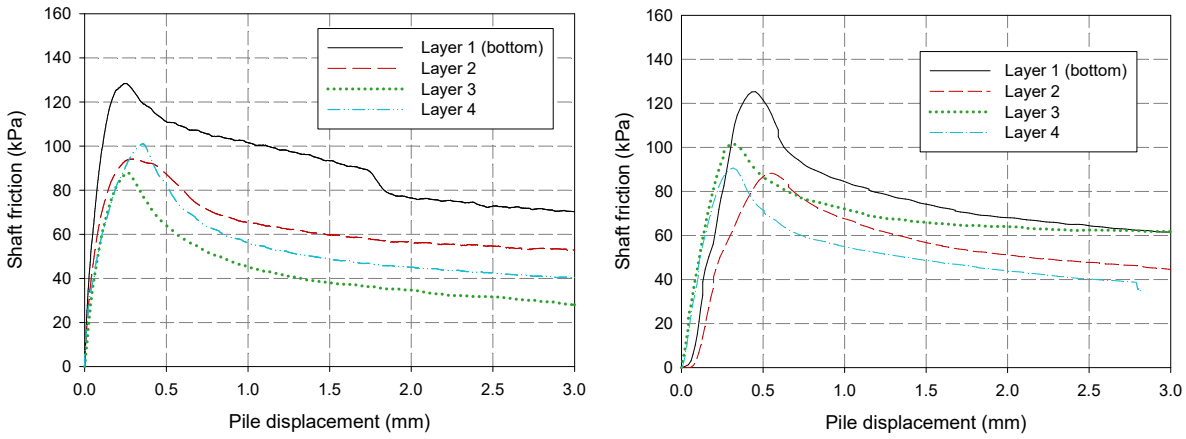

Figure 104: Plug pull-out tests conducted after achieving the targeted swell for a) unsupported holes and b) supported holes

The result presented in Figure 104 illustrates that the soil swelling behind the plugs for the test with unsupported holes had a negligible effect on the measured peak shaft friction. This can be attributed to the fact that the soil which was allowed to swell behind the plug had softened significantly. The phenomenon of swell-induced softening is included within the BExM framework. It should however be emphasised that the softening which occurred behind the plugs, occurred to a greater extent in the top slab (as discussed in Section 7.1) since it was allowed to swell more in the vertical direction due to the reduced overburden stress experienced by this slab. It is therefore likely that this clay had close to zero shear strength as is indicative by the penetration resistance measured for the top slab after swell. While the clay which swelled behind the plug had a negligible effect on the pull-out capacity of the various plugs, Figure 104 illustrates that it did affect the stiffness of the process with lower stiffnesses being observed for the tests conducted with supported holes.

Figure 105 presents the results of peak friction (i.e. pull-out capacity) for the various pull-out tests conducted. On the primary vertical axis (left) the overburden stress has been calculated from the initial unit weight of the various slabs. It is recognised that this value will have changed throughout the swell process but this would not change the observed trend. The secondary vertical axis (right) illustrates the position of the plug as the height above the base of the model.

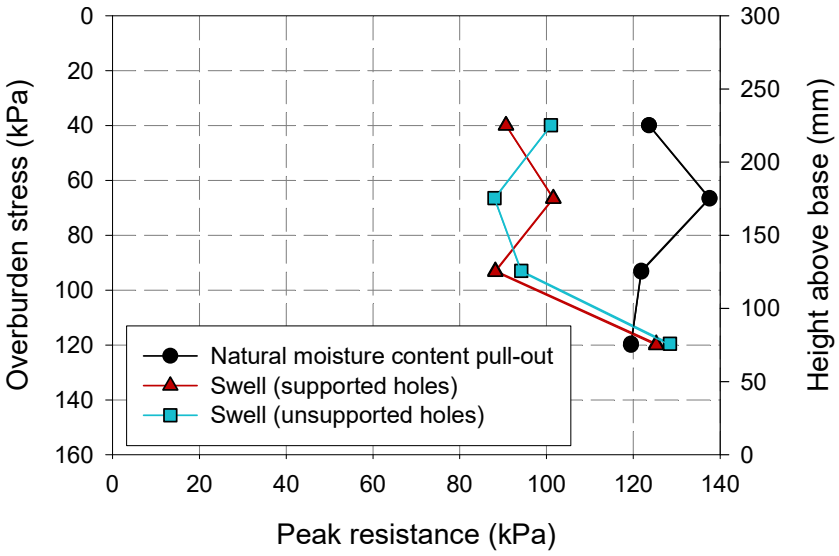

Figure 105: Comparison of pull-out capacities for the various pull-out tests conducted

The results in Figure 105 illustrate that in general, there is a reduction in pull-out capacity of piles after allowing swell to occur. However, at high confining/overburden stresses, pull-out capacity may increase locally since the restriction of vertical swell results in an increase in lateral pressure. Figure 105 also illustrates good repeatability in test results for piles pulled out after achieving targeted swell.

For the pull-out tests presented in this section, consideration has been given to swell induced softening and the development of lateral swelling pressure at depth where swell is restricted to some degree. However, the pull-out tests conducted present the consequence of these conflicting mechanisms. The test presented in the following section aims to address the changes in lateral pressure during swell by analysing the results of a centrifuge test performed with an aluminium pile, instrumented for this purpose.

7.2.4 Instrumented pile test

The results presented in this section are for a centrifuge test conducted with an aluminium pile (anchored at its base) instrumented such that it could measure changes in lateral swell pressure acting on the pile shaft. The test layout was presented in Figure 66. For the discussion presented on the greenfield test, it was highlighted that measurements of suction throughout the swell process could not be accurately measured. As a result, only qualitative interpretations of the likely stress paths were possible. For the test presented in this section, there were additional factors which made quantitative analyses troublesome. These issues include:

- Some movement of slabs during centrifuge acceleration causing bending moments within the pile which would have affected stress measurements in each layer.
- Since the augured hole was slightly larger than the pile itself (approximately 0.5 mm larger), some swell will have had to occur before contact was made with the pile. As noted by Fourie (1991) (and discussed in Section 35), allowing a certain degree of strain can significantly reduce swell-induced pressures.
- Considering that not all slabs were cut perfectly to the same dimension along their width, different amounts of volumetric swell would have occurred in each slab. This fact is related to the previous point and likely accounts for the relatively low stresses measured throughout this test.
- Finally, during installation of the pile, some disturbance of the adjacent soil will have occurred and movement of the various load cells within the piles could have moved.

For the reasons mentioned above, the analysis that follows will be qualitative and aims to address the trends observed. As a first check on the quality of readings obtained from the load cells, the measured pressures were compared to the hydrostatic pressure of water as the box was flooded. After acceleration of the centrifuge, water was introduced from the bottom of the model, until the surface of the water was approximately 10 mm above the surface of the top clay slab. Figure 106 illustrates the response in measured lateral pressures during flooding of the box. Starting with the bottom load cell, lateral stresses increased in the subsequent slabs as the water level rose past the corresponding load cell. The solid lines presented in Figure 106 illustrate the measured lateral pressures, the broken lines indicate the calculated hydrostatic pressure based on the position of each load cell, and the solid markers represent the point at which the water level had reached its final position above the model surface. Figure 107 summarises the comparison of measured lateral stresses with the known hydrostatic pressure in the centrifuge model. From Figures 106 and 107, it can be seen that the measured lateral stresses correlate well with the corresponding hydrostatic pressures. The biggest discrepancy however, is observed in the measurement of the top load cell which measures approximately half of what would be expected. This could possibly be attributed to movement of this load cell within the pile during installation or spin-up.

The results presented in Figure 108 represent changes in lateral pressure due to swell. Data in this figure was zeroed after the model was flooded, and so the hydrostatic water pressure is not accounted for. The general trend observed for all cells is that an increase in lateral pressure occurs relatively early in the test, followed by a drop in pressure. This agrees with the

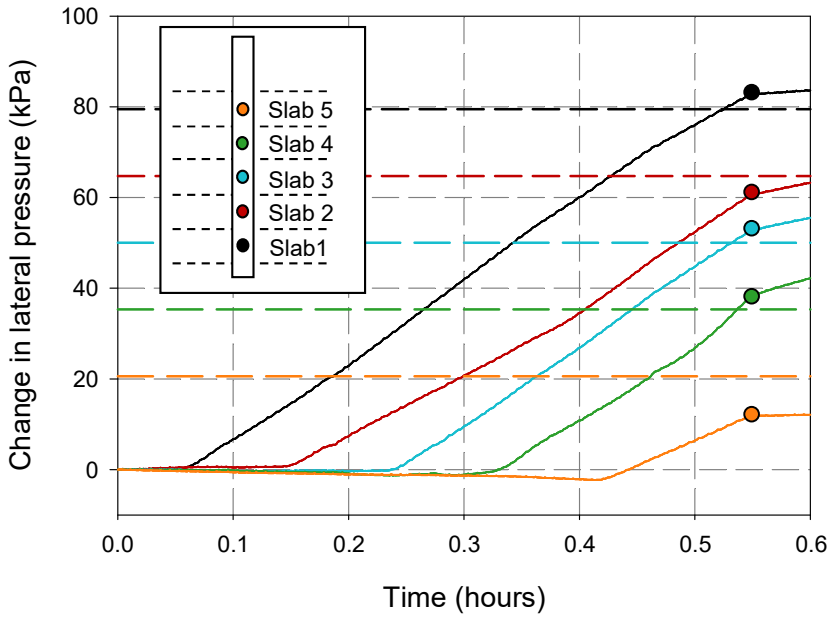

Figure 106: Measurement of lateral pressures during flooding of the centrifuge model

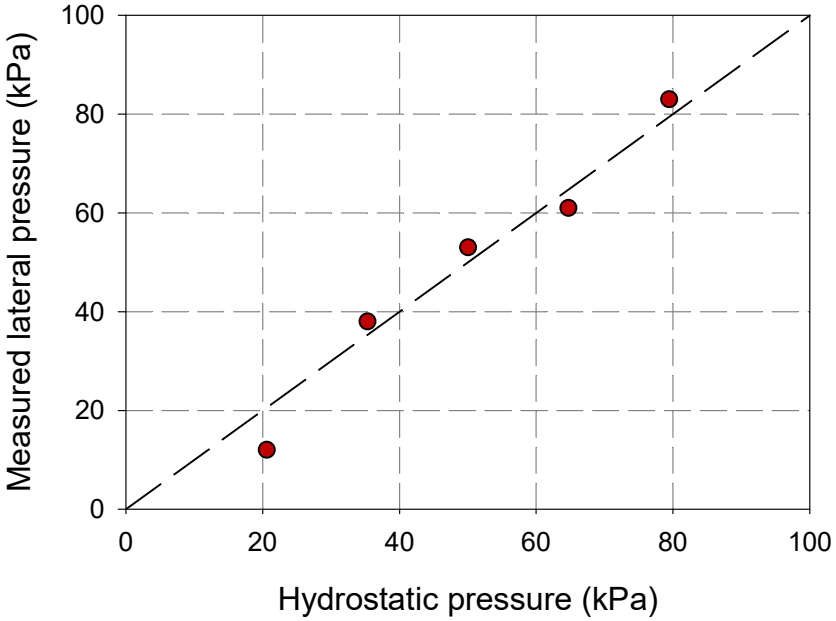

Figure 107: Comparison of measured lateral pressures with known hydrostatic water pressures

results of Schreiner & Burland (1991) of an oedometer test with lateral stress measurements (Figure 33). It also agrees with the findings of Robertson & Wagener (1975) who observed that the maximum swell induced lateral pressure occurred before complete wetting was achieved.

A closer analysis of the dataset reveals that the top slab initially experienced a slight reduction in lateral pressure, followed by an increase to approximately 20 kPa, which then reduced to zero (i.e. the initial pressure at the start of testing). The initial drop in pressure or 'lag' before observing a pressure increase can be attributed to the fact that the aluminium pile was pushed through the augured hole from the top of the profile. Doing so would have disturbed the soil in the top slab (creating a larger gap between the pile and augured hole) and could also have moved the load cell within the pile. Whatever the reason for this discrepancy, it appears that after approximately 0.5% average surface swell, readings in this load cell tended to stabilise and conform to the trends observed for all subsequent load cells.

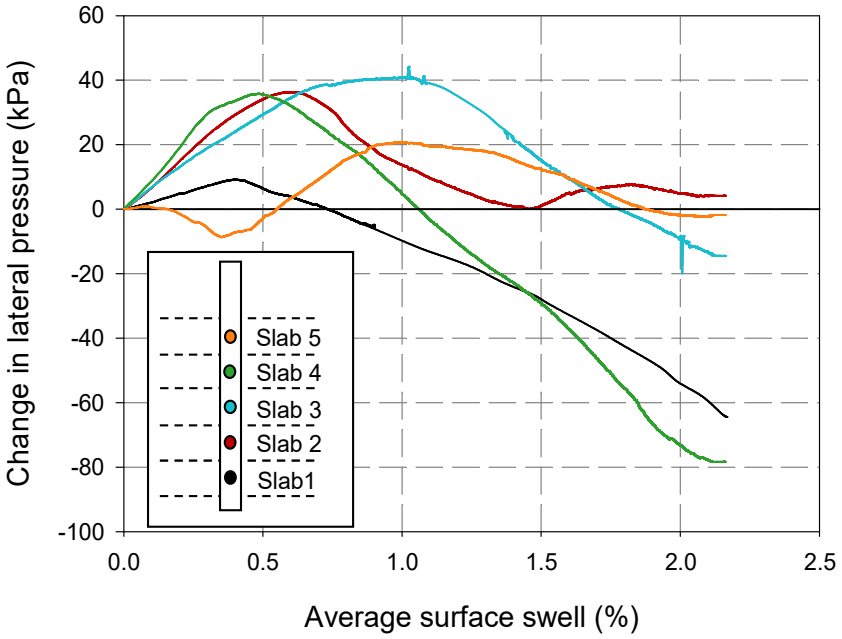

Figure 108: Change in lateral pressure due to swell

Another feature of the results presented in Figure 108 is that the measured pressures are relatively low. Schreiner & Burland (1991) observed that lateral stresses during a swell process can be far greater than the applied vertical stress. This relationship was not observed in this centrifuge model. However, the findings of Fourie (1991) highlighted how, by allowing a finite amount of swell, the observed swell induced pressure can be significantly reduced. Considering that the augured hole had to be slightly larger than the instrumented pile to allow installation, swell would have occurred before the clay made contact with the pile. During installation, this hole could have been enlarged further. Another source of error which may have contributed to the relatively low measured stresses is that not all clay slabs would have fitted perfectly within the boundaries of the model. An exaggerated illustration of the imperfections described in this paragraph is provided in Figure 109. Since the top and bottom load cell exhibit markedly

different behaviour in Figure 108, it is likely that these slabs were affected most by the pile installation process.

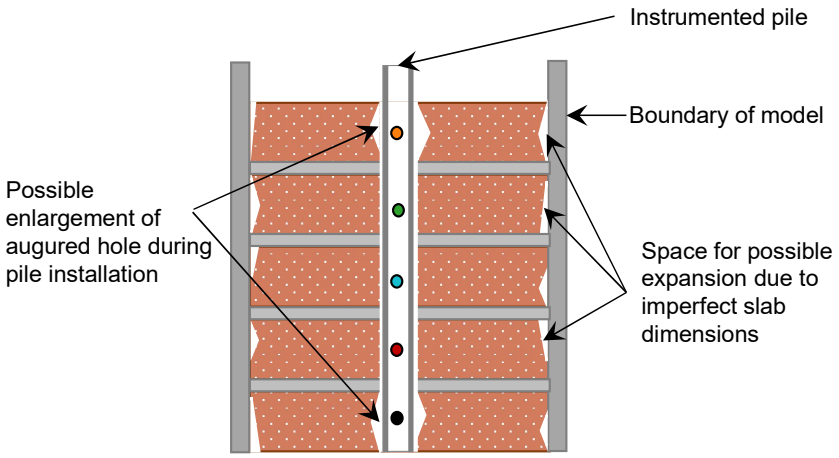

Figure 109: Exaggerated imperfections of the instrumented pile model

Despite the imperfections highlighted above which preclude rigorous quantitative analyses, there is a prevailing trend. At all depths, the maximum swell-induced pressure occurred relatively early in the test (at relatively low values of swell). This corresponds to the findings of Schreiner & Burland (1987) with sophisticated oedometer testing, as well as by Robertson & Wagener (1975) for full-scale testing for the design of abutment walls. The results in Figure 108 also provide an explanation as to the discrepancy between studies performed by Elsharief et al. (2007) and Blight (1984*a*) who found a reduction and increase in peak shaft friction respectively after wetting. Elsharief et al. (2007) attributed the reduction in capacity to the loss of shear strength in the surrounding clay due to wetting (i.e. softening). Blight (1984*a*) attributed the increase in capacity to an increase in lateral pressure, induced by the swell process.

However, neither study reported the amount of surface heave that had occurred when the tests were performed. While no details were provided by Elsharief et al. (2007) as to how the profile was wetted, the study reported that flooding occurred for a period of two months. This is significantly longer than the 3 to 4 week wetting period reported by Blight (1984*a*). This difference in wetting period along with Figure 108 highlight an important factor regarding the shaft capacity of piles in swelling clays. While an increase in swell induced lateral pressure may be the dominant mechanism for lower values of swell, softening tends to dominate if larger magnitudes of swell are permitted. It is therefore crucial that any tests which aim to investigate the shaft capacity of a pile after swell has occurred should be considered together with the anticipated magnitude of swell. By not considering the magnitude of anticipated

swell, it cannot be stated whether softening or increases in lateral pressure will dominate the behaviour of the pile.

7.2.5 Swell profile measurements

This section presents a comparison of the measured swell profile in Greenfield Test 2 and the Instrumented pile test. It also includes predictions made by the swell under load curve determined from oedometer testing and the swell profile predicted by Van der Merwe (1964) for a clay of *very high potential expansiveness*. Figure 110 presents these comparisons.

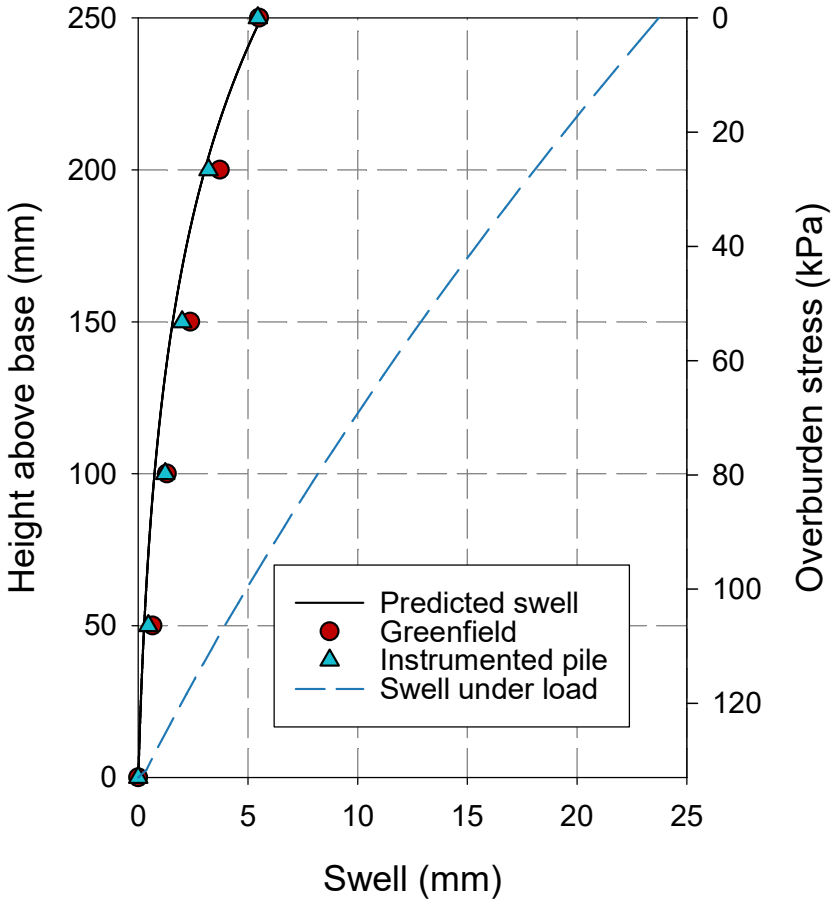

Figure 110: Comparison of predicted and measured swell

From Figure 110 there are several conclusions which can be drawn. Firstly, it can be seen that the measured swell profile in both centrifuge tests presented are remarkably similar. Furthermore, the time to achieve the targeted swell in the Greenfield and Instrumented pile test were also similar (10 and 12 hours respectively). This is an indication of a high degree of repeatability for the centrifuge modelling conducted in this study.

Another conclusion which is perhaps of more practical relevance is that the measured profiles in both tests follow *trends* similar to what was predicted by the empirical prediction method. There is however, a caveat to this observation which necessitates emphasis. In presenting the heave results for the Greenfield test, Figure 95 illustrated that levels of swell far greater than that predicted by the empirical heave approach (achieved in 10 hours) is possible given enough time and availability of water. The discussion that follows is therefore specifically focussed to address the non-linearity of the relationship between heave and overburden stress observed from centrifuge testing, which is in contrast to the linear relationship measured using swell under load testing of this study, and that which has been observed by other researchers as mentioned in Section 3.3.2. It is proposed that this discrepancy is attributed to the rate of infiltration into the clay, which will differ from the top to the bottom of the profile.

Firstly, it should be noted that the rate of infiltration, or hydraulic conductivity of the soil mass is dependent on the soil's fabric (Romero & Simms, 2008), void ratio, and its degree of saturation. Figure 78 which presented the results of a one-dimensional consolidation test illustrates how the saturated hydraulic conductivity of a soil can reduce by several orders of magnitude as the void ratio decreases. Similarly, a reduction in suction (or increase in degree of saturation) will increase the hydraulic conductivity (Fredlund, 2018; Lu & Likos, 2004). These two mechanisms occur simultaneously in an expansive clay. However, since swell (or changes in void ratio) are suppressed deeper in the profile, the increase in hydraulic conductivity will occur at a slower rate for an element of soil deep in the profile, in comparison to one which is close to the surface. As a result, swell at the bottom of the profile will not only be restricted by overburden pressures, but significantly delayed owing to the lower hydraulic conductivity of these elements.

To illustrate this concept, consider Figure 111 and Figure 112 which describe the changes in hydraulic conductivity for an element of soil close to the surface, and deep in the profile respectively. In both figures, the three rectangles at the top illustrate expansion of a soil element. Each element is labelled t_1, t_2 and t_3. These labels represent the progression of time with t_1 representing the instant at which the entire profile is given access to water and t_3 represents an arbitrary point in time after allowing swell to occur. The instances represented by t_1, t_2 and t_3 represent the same point in time in both figures. The two graphs presented in each figure describe the effect of a reduction in suction and an increase in void ratio on increasing the hydraulic conductivity. The suction-hydraulic conductivity relationship presented is that proposed by Fredlund (2018) which results from the mathematical integration of the soil water retention curve (SWRC). It should be noted that the data points presented in Figure 111, which illustrate the effect of void ratio on hydraulic conductivity, are taken from the consolidation test

performed on a reconstituted sample as presented previously. These data points do not present a swell process but simply aim to illustrate that the saturated hydraulic conductivity of a soil will increase significantly as its void ratio increases. In each figure, an initial stage is illustrated whereby an increase in moisture content results in the closure of fissures (Path AB). This process has a significant effect on the macro fabric, and is assumed to occur relatively quickly in the infiltration process. It is also assumed that the macro suction of the soil mass remains relatively unchanged as fissures swell closed (i.e. the suction of the soil mass in Figure 99 b) is similar to that in Figure 99 a)).

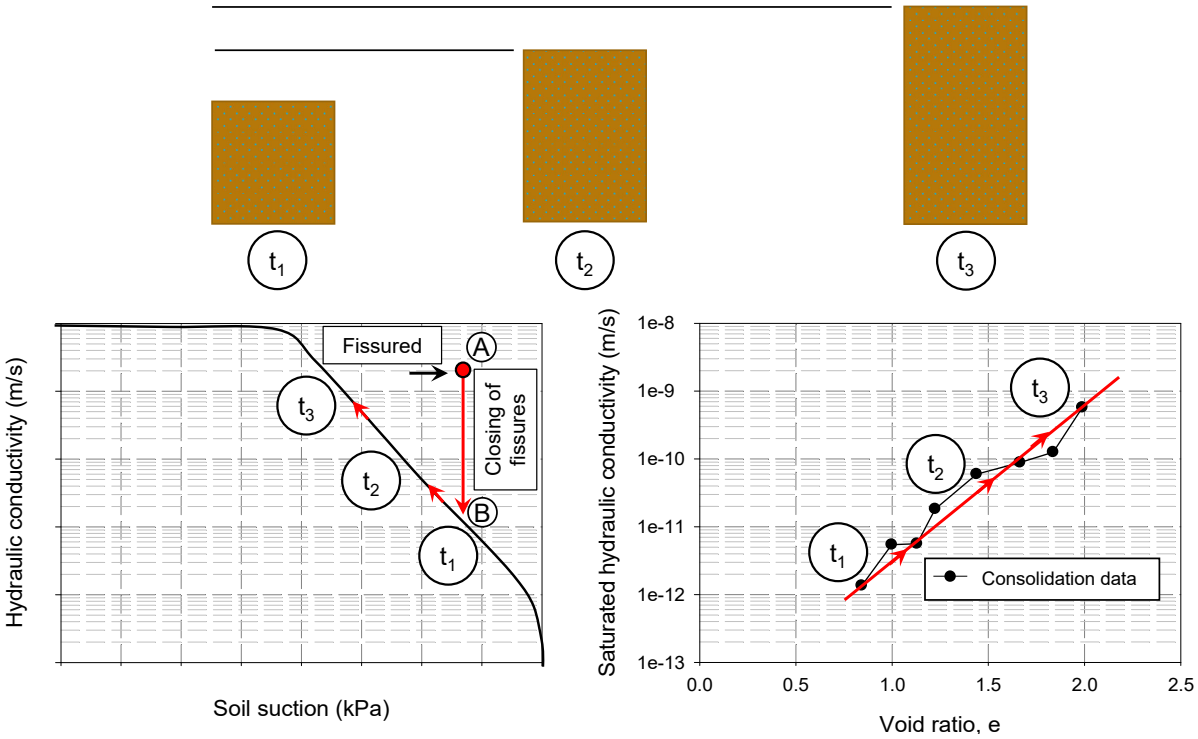

Figure 111: Development of swell for an element of soil close to the surface of the profile

The conceptualisation of this infiltration process illustrates that, given an indefinite availability of water, an element of soil close to the surface will achieve the level of swell predicted by the swell under load tests first. In contrast, an element of soil deeper in the profile may take significantly longer to achieve the magnitude of swell predicted by oedometer testing. In presenting the results of Greenfield test 2, it was observed that swell in the top slab only became negligible at approximately 60 hours (equivalent to 6 years in prototype scale), while the swell in subsequent layers were still steadily increasing after 110 hours (over 11 years at prototype scale).

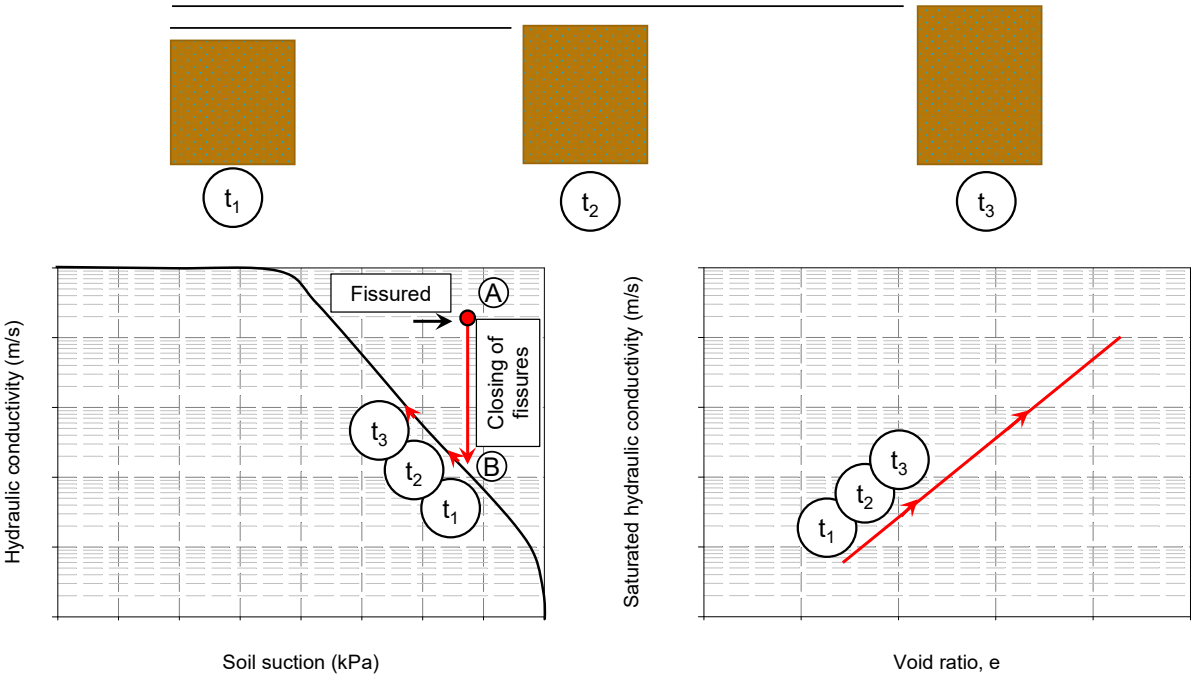

Figure 112: Development of swell for an element deep within the soil profile

Recognising the mechanisms described in this section, observations of heave in the field should tend towards the predictions made by swell under load tests, given sufficient time and availability to water. Conventional swell under load tests can therefore be regarded as *indicator tests* that provide the upper limit of swell which is theoretically possible (given specific initial soil conditions).

CHAPTER 8

CONCLUSIONS AND RECOMMENDATIONS

The introduction to this study highlighted the significant economic implications related to damage caused by swelling clays. Due to these implications and their widespread occurrence worldwide, extensive research studies were conducted, predominantly between the 1950s and early 1990s as illustrated in the literature review of this thesis. While research on expansive clays has certainly continued since the 1990s, the technological advancements made in the past three decades can be further exploited to gain a better understanding of this problem soil. The aim of this study was to use element testing, in conjunction with centrifuge modelling to investigate factors affecting the behaviour of piled foundations in swelling clays.

The section that follows highlights the conclusions which can be drawn from the study performed. The recommendations which follow from these conclusions have been divided into two sections. The first provides areas for further research. The latter section on recommendations is aimed at bridging the gap between research and practice, a dominant theme of the 2017 Terzaghi Oration (Day, 2017). This part of the recommendations culminated as a combination of the conclusions made in this study, and communications between geotechnical practitioners in South Africa, as well as with commercial laboratories in the country.

8.1 Conclusions

From the element testing and centrifuge modelling performed in this study, the following conclusions can be drawn.

8.1.1 Dependence of swell induced lateral pressure on swell magnitude

In an expansive clay, the magnitude of lateral swell pressure against a structure will increase initially but will begin to decrease if a significant amount of swell is allowed.

During a swell process, there are two mechanisms which need to be considered, namely, a change in pressure against the structure and soil softening which occurs as a result of the reduction in suction. It was found that increases in swell pressure are the dominant mechanism during initial swell. However, if the magnitude of swell continues to relatively large values, softening tends to dominate, which results in a reduction in swell pressure and therefore, in pile shaft capacity.

8.1.2 Dependence of pile shaft friction on depth within the profile

For a given magnitude of swell, shaft capacity in clay layers close to the soil surface illustrate a reduction in capacity, while increases in shaft resistance were observed at depth. These changes in capacity are made with reference to the shaft capacity of the pile at the soil's natural moisture content, i.e. before swell.

For this study, all pull-out tests were conducted at the soil's natural moisture content (i.e. with no swell occurring) and after allowing a relatively large amount of swell to occur (i.e. that predicted by Van der Merwe (1964) for a clay of *very high potential expansiveness*). These tests revealed that while decreases in shaft resistance were observed in the upper layers of the profile, increases in pull-out capacity were measured for short piles cast deep within the profile. Since swell in the bottom layers is restricted, an increase in pull-out capacity can be attributed to the development of lateral swell induced pressures.

8.1.3 Swell in the geotechnical centrifuge

A significant amount of swell can be achieved in the geotechnical centrifuge using the sample preparation procedure employed in this study.

By creating a scaled, closely fissured clay profile incorporating layers of geotextile separating consecutive clay layers, a significant amount of swell (that predicted by Van der Merwe (1964) for a clay of *very high potential expansiveness*) was achieved within approximately

11 hours in all centrifuge tests presented. By applying the scaling laws proposed by Caicedo et al. (2006), an equivalent full-scale test would require 413 days of constant flooding before the soil-structure interaction testing presented in this study could be performed. Assuming it would be possible to flood an expansive clay profile for this period of time at full-scale, such a test would be very costly. The model setup developed in this study therefore highlights the significant advantages which are possible with the centrifuge modelling of expansive clays.

The swell profile measured in the geotechnical centrifuge closely matches that predicted by Van der Merwe (1964) for a clay of *very high potential expansiveness.*

The significance of this conclusion is that the measured swell along the profile depth is *non-linear*. Such a trend is observed for most empirical prediction models (many of which have been validated by field observations) but does not agree with the linear relationship measured by the oedometer testing of this study and by previous researchers (see Section 3.3.2). This is due to the fact that conventional oedometer tests bring a soil sample to a point of zero suction, and is therefore an indication of the maximum magnitude of swell possible at a given overburden stress. In field applications, while moisture ingress may reduce suction to zero for soil close to the surface, elements of soil deeper in the profile will require a constant supply of water for an indefinite period of time for suction to be reduced to zero.

8.1.4 Swell-induced softening

There is a marked reduction in yield stress (as determined from one-dimensional consolidation tests) for samples which have been allowed to swell.

For samples compacted in the laboratory at their in-situ moisture content, the reduction in yield stress continues until approximately 8% swell, after which no significant reduction takes place. For undisturbed specimens, there appeared to be no magnitude of swell above which the reduction in yield stress became negligible. A conclusive statement as to the relationship between swell magnitude and reduction in yield stress cannot however be made from this study, owing to the relatively small number of samples tested.

8.1.5 Comparison of undisturbed and laboratory prepared specimens

Samples prepared by static compaction at their in-situ moisture content showed almost identical swell properties (i.e. swell magnitude and swell pressure) when compared to

undisturbed samples. Their water retention properties during wetting and drying cycles also appear to be virtually equivalent.

Both the soaking under load curve and the 'swell followed by consolidation' approach illustrated that statically compacted and undisturbed samples illustrate almost identical swell properties (i.e. magnitude of swell at a given overburden stress and the swell pressure). This supports the findings of Brackley (1983) and Armstrong & Zornberg (2017). This finding adds to the plausibility of the mechanism hypothesised by Brackley (1983) that highly expansive clays tend to have a remoulded structure in-situ, owing to the large number of swelling/shrinking and wetting/drying cycles that swelling clays undergo during their geological lifetime. Processing of this type of material that occurs in the laboratory therefore appears to have little effect on the soil's swell properties.

Strong similarities were also observed for the soil water retention behaviour for the various samples. While more hydraulic hysteresis was observed for undisturbed samples than for compacted and reconstituted specimens, general relationships and trends remained similar. This finding is again consistent with the hypothesis proposed by Brackley (1983).

The findings of this study illustrate that for a swelling clay, by the time the material has been sampled from a site and brought to a laboratory, it has already undergone numerous wetting and drying cycles. When such a soil is prepared for testing in the laboratory, provided it has not been oven dried or had its structure destroyed, any further wetting and drying will simply be a continuation of what has occurred over geological time in-situ. Lack of hysteretic behaviour in measured suction upon wetting and drying is thus unsurprising and supporting of studies conducted by Liu et al. (2020) and Al Haj & Standing (2016), who observed little hysteretic behaviour after the third wetting/drying cycle.

8.1.6 Investigation of soil structure

Remoulding and compaction of soil specimens in the laboratory appear to have as much an effect on destroying soil structure as the swelling process does.

This conclusion comes from the finding that all samples tested (disturbed or undisturbed) exist in permissible stress states for most of the tests conducted. It is only when volumetric strains are suppressed (due to applied overburden stresses) that specimens tend to exist in structure (or bond) permitted space. This is in line with the proposition by Leroueil & Vaughan (1990) that structure should be considered a function of strain.

8.1.7 Intrinsic clay properties

The intrinsic properties (discussed in Section 6.1) determined from a one-dimensional consolidation test on a sample reconstituted at $1.1 \cdot w_L$ conform well to the framework proposed by Burland (1990).

Such a conclusion is valuable since it provides confidence in the experimental data gained from such a test, which, as was shown in this study, can be used as a benchmark to evaluate various soil properties. Aspects evaluated in this study include the investigation on the effect of soil structure as well as on the reduction in yield stress due to swell. Another useful aspect of this conclusion is perhaps that it further illustrates the ability of the framework put forth by Burland (1990) to predict the behaviour of clays which have formed under climatic conditions which are arguably different from the bulk of the data on which the framework was based. This provides further confidence that the framework put forth by Burland (1990) can reliably predict *intrinsic clay properties*.

8.2 Recommendations for further research

Based on the conclusions made in this study, a number of recommendations are proposed. In the sections that follow, recommendations for further research are provided. In some cases, recommendations have been accompanied by proposed testing programmes. However, a conceptualised experimental programme is unlikely to foresee practical difficulties which are inevitable for any experimental work. The suggested testing sequences presented are therefore 'simplified' frameworks which can be altered to address whichever practical difficulties arise during their implementation.

8.2.1 Investigation of swell-induced softening

While this study clearly observed a reduction in the soil's yield stress after swell, a relatively small number of samples were tested. For this reason, a quantitative correlation between the reduction in yield stress and the percentage swell could not be established. By following the testing sequence presented in this study, as well as the interpretations detailed in Section 6.4.2 for a larger number of samples, a possible quantitative correlation could be derived. Such a study could be repeated for laboratory compacted soils and undisturbed samples collected from within or below the active zone in a clay profile.

8.2.2 Undisturbed and laboratory prepared specimens

In this study it was found that undisturbed samples and those prepared in the laboratory by static compaction at the soil's in-situ moisture content illustrated similar expansive properties (i.e. swell pressure and magnitude of swell). This is in agreement with studies conducted by Brackley (1983) and Armstrong & Zornberg (2017). Brackley (1983) hypothesised a mechanism which could lead to this very observation by stating that highly expansive clays occur in a remoulded state in-situ, due to the numerous swelling/shrinking and wetting/drying cycles undergone during their geological lifetime. This hypothesis is one which can be investigated experimentally. If the mechanism described by Brackley (1983) is correct, expansive clays sampled at a depth below the active zone would possess different swell properties than samples prepared in the laboratory, or indeed with undisturbed samples collected from within the active zone. This expected behaviour should hold, provided initial void ratios and moisture contents remained the same for the compared samples. In this case the term "active zone" is used to denote the depth to which seasonal swelling/shrinking has occurred. To investigate the mechanism proposed by Brackley (1983), the following testing sequence is recommended:

1. Perform a site investigation and determine the depth to which the relevant profile contains an expansive mineralogy.
2. Determine the clay's swell pressure (using any or all of the methods described in Section 3.3) to provide an indication of the active zone.
3. Compare swell properties of samples collected from above and below the depth corresponding to the swell pressure determined in Step 2.

It should be noted that samples collected beneath the active zone should possess a similar mineralogical composition as the samples collected from within the active zone for test results to be comparable. The geological origin of the material throughout the profile considered should also be the same (e.g. transported, residual, etc). Such a testing sequence would therefore require a relatively deep expansive profile. From the proposed testing sequence it is suggested that the soil's swell pressure be used as an indication of the active zone. This is preferable to monitoring seasonal moisture fluctuations for two reasons. Firstly, the latter approach is both time consuming and significantly more costly than evaluating a soil's swell pressure. More importantly, however, even if seasonal moisture fluctuations were to occur at depths greater than what is suggested by the clay's swell pressure, it will not have undergone

the 'remoulding' process described by Brackley (1983) as they are unlikely to have undergone the swelling/shrinking cycles which occurred within the active zone.

8.2.3 Using soil structure as an estimate of the active zone

In this study it was found that samples which underwent negligible volumetric changes upon inundation could exist in structure (or bond) permitted space whereas samples which had undergone significant swell did not. It is therefore proposed that investigation of an expansive clay's structure be used as an estimate of the active zone. To perform this investigation, the following testing sequence would need to be implemented.

1. Perform a one-dimensional consolidation test on a reconstituted specimen as per the recommendations by Burland (1990).
2. A site investigation should be conducted to determine the depth to which the clay's mineralogy is of an expansive nature.
3. Undisturbed samples should be collected throughout the profile where an expansive mineralogy is present.
4. The swell pressure of the clay should be determined.
5. Samples collected throughout the profile should be one-dimensionally consolidated to determine whether they venture into structure permitted space.

   There is however one important aspect of this testing sequence which is that the swell pressure should be applied to all samples prior to inundation in the oedometer. This is to ensure that the samples do not undergo significant volumetric strains during the inundation process. If strains are kept as close to zero as possible, soil structure should *in principle* not be destroyed.

The expectation of such a testing sequence would result in specimens collected from within the active zone existing in permissible stress states, with those beneath the active zone venturing into structure permitted space.

The hypothesis behind this proposed testing sequence is that the structure of soils within the active zone will have been destroyed by seasonal swelling and shrinking cycles, whereas soil sampled below the active zone will retain some soil structure.

8.2.4 Continued determination of intrinsic clay properties

The first finding of this study was that the clay's intrinsic parameters (see Section 6.1) determined for the material tested, conformed well to the framework proposed by Burland (1990). It is recommended that the determination of such properties should be standard practice for any research performed on clays (expansive or otherwise). In doing so, researchers can add to the validity of the proposed framework for a variety of clays or highlight any of its shortcomings. An example of a possible shortcoming was highlighted by Al Haj & Standing (2015) who illustrated that the value of C_c^* plotted slightly above predictions made by the framework. Al Haj & Standing (2015) recommended that further work be conducted on tropical soils to determine whether this was indicative of an underlying trend. Considering the usefulness of evaluating a particular clay in the context of its intrinsic properties, such a recommendation will be useful for further research on clays.

8.3 Recommendations to industry

As stated at the beginning of this chapter, the section that follows combines the findings of this study and communication with geotechnical practitioners and commercial laboratories in South Africa. The first finding of these communications was that the terminology used to refer to various testing methods differed between academic publications and commercial laboratories. Furthermore, it was found that in some instances the same test name was used by different laboratories, despite different testing methodologies being used. As a result, the first part of this section aims to distinguish between the various tests and summarise the applicability of the various stress paths followed by the different testing procedures. The chapter summarises the general approach to foundation design on swelling clays, as reported by the various respondents. Comments are then presented on the current standard practices, considering the findings of this study. Suggestions which are more specific to piled foundations are also highlighted. Finally, concluding remarks are provided on the information discussed in the chapter.

8.3.1 Commercially available swell testing

The aim of this section is to distinguish between the various testing methodologies currently available to industry. The terminology used in this section to define the various tests are those which are generally used by the research community and has been used throughout this thesis. Relevant testing standards have also been provided for each approach. Figures have been provided to each corresponding method to highlight the stress paths undergone.

1. Swell followed by consolidation (see Figure 113)
   Relevant standard: *loading after wetting* tests (ASTM D4546–14, 2014)
   A sample is placed inside the oedometer (typically at its in-situ moisture content) and a nominal stress is applied (usually in the order of 5 kPa). This is represented by Point A in Figure 113. The sample is then inundated until the magnitude of volumetric change becomes negligible (Path AB). After the swelling stage, the sample is consolidated in the conventional manner until such point that its initial volume is reached (Path BC).
   Swell properties measured:

   - The magnitude of swell under various applied stresses
   - Swell pressure (pressure required to prevent swell)

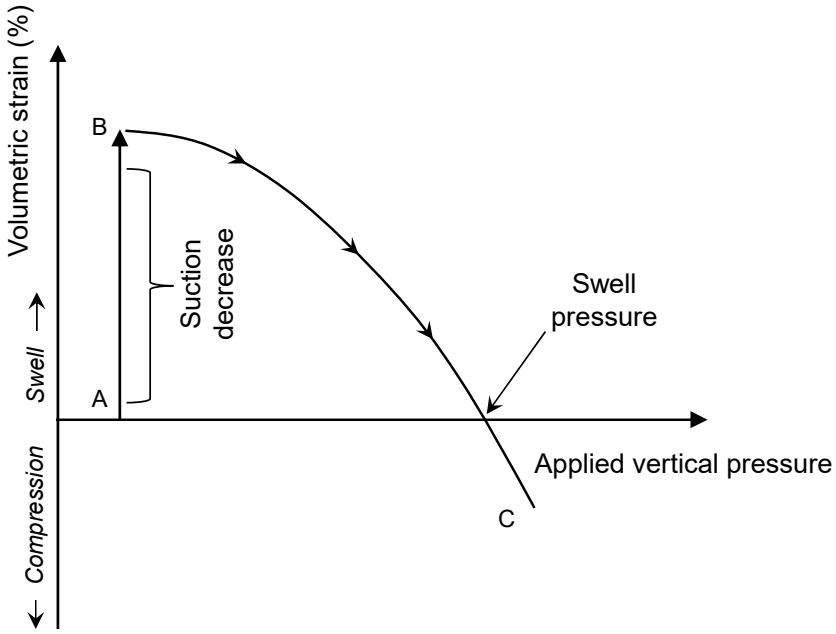

Figure 113: Swell followed by consolidation test

2. Swell under constant load
   Relevant standard: *wetting after loading* tests (ASTM D4546–14, 2014)
   A sample is placed in the oedometer at its in-situ moisture content. A predetermined vertical pressure is applied to the sample (based on expected foundation loadings) and the sample is then inundated with water and allowed to swell under that stress.
   Swell properties which can be measured:

   - If the test is performed once, only an estimate of heave at the applied stress can be estimated (Figure 114 a)).

- If the test is repeated with different applied vertical stresses, the swell pressure can be interpolated from the results (Figure 114 b)).

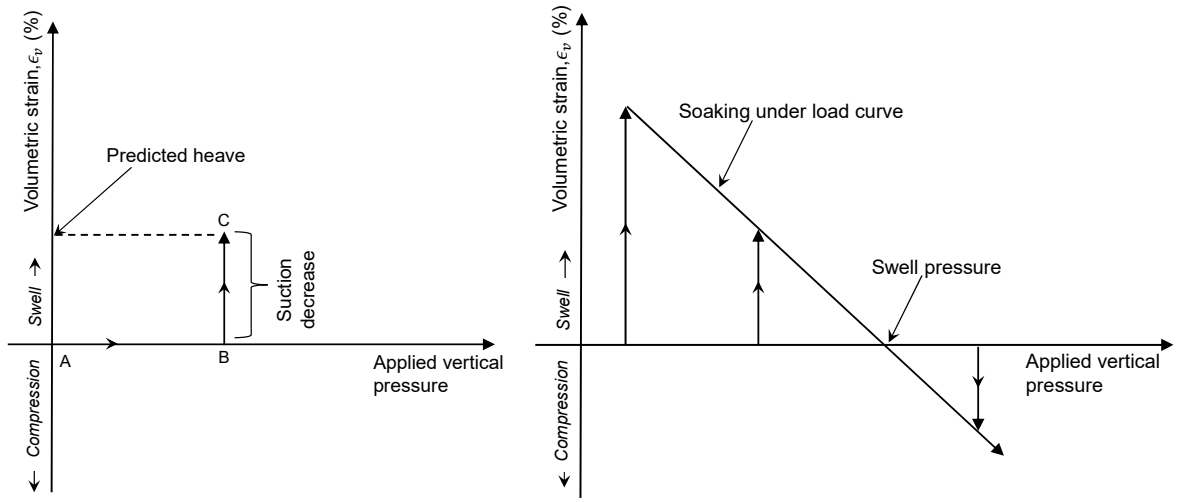

Figure 114: Swell under constant load test performed under a) one applied stress and b) multiple applied stresses

3. Constant volume swell test
   Relevant standard: BS 1377–8: 1990 (1990) Clause 4.3
   A sample is placed in the oedometer and inundated. The volume is then kept constant by one of two approaches:

   - The top cap of the oedometer is placed in contact with a stiff load cell. The load cell measures the pressure which develops throughout the swell process. This approach is more typically used by the research community. (Figure 115 a)).
   - Incrementally increasing the stress on the sample until equilibrium is reached. This approach correlates to that described by BS 1377–8: 1990 (1990) Clause 4.3 (Figure 115 b)).

   Swell properties which can be measured:

   - Swell pressure
   - The magnitude of swell can theoretically be estimated from this test if the sample is allowed to swell by removing all vertical confinement after reaching equilibrium

(see Section 3.3.3). This approach is described by BS 1377–8: 1990 (1990) Clause 4.4.

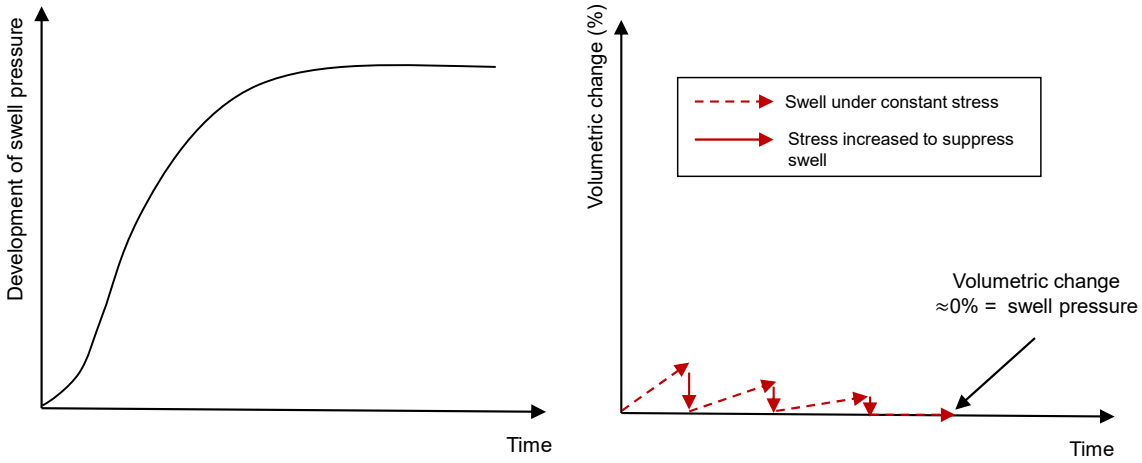

(a) (b)

Figure 115: Constant volume swell test where volume is restrained by a) stiff load cell in contact with top cap and b) by incrementally increasing applied vertical stress

It should be noted that while the terminology used to define each test in this section is *generally* utilised by researchers, *slight* nuances in these test names do exist in academic publications. The intention of outlining the tests above is therefore not to state the exact name which should be used to refer to each test, but rather to make it possible to distinguish between them. While these tests can all theoretically measure the same properties, each follows different stress paths and so differences in the measured property may exist between tests.

In discussing the validity of the stress paths followed by the various approaches listed, Schreiner & Burland (1991) highlighted that the "swell under constant load" test is generally the stress path which is most applicable to common construction sequences. This stress path will be applicable for a case where the structure is built at the soil's natural moisture content, with changes in moisture content occurring after the structure is built. Schreiner & Burland (1991) also stated how the "swell followed by consolidation" approach is applicable if the profile is "pre-wetted" before construction. Finally, it was stated that the "constant volume" approach does not represent any typical construction sequences and would only be applicable where the profile is wetted up under restraint.

While the results reported by various tests can differ due to the different stress paths undergone, it is important to emphasise that *all* of the above tests are simply *indicators* of the

upper limits of swell or swell pressure for a specific set of initial properties (e.g. moisture content and void ratio). This is a consequence of samples in such tests being reduced to a state of zero suction.

It should be noted that while the upper limits of swell predicted by oedometer testing were not achieved in the centrifuge tests of this study, it is still possible that such limits can be reached in extreme circumstances. To support this statement, the effect of soil fabric cannot be overstated. The clay tested in this study had a fabric type predominantly consisting of a continuous clay matrix (Figure 22 a)). As such, it has an extremely low saturated hydraulic conductivity ranging from 10^{-9} to 10^{-12} m/s depending on void ratio. For a comparatively 'open' fabric consisting of more sand or silt particles (Figure 22 b)), the soil's hydraulic conductivity may be significantly higher, making the oedometer swell predictions more achievable in a practical time frame.

8.3.2 Design on swelling clays

This section presents the responses of various practising geotechnical engineers and aims to add some insights which were obtained throughout this study. Recognising the challenges in geotechnical engineering in a developing country (Day, 2017), the question presented to industry was directed to address the type of laboratory testing that is generally utilised to guide foundation design. More specifically, it was of interest to gain an indication of the perception of the more basic indicator testing (Atterberg limits, grading analyses and shrinkage limits) versus the seemingly more rigorous testing offered by the various oedometer options. The section begins by addressing the responses from industry professionals and then provides some insights on the pull-out (shaft) capacity of piled foundations in swelling clays.

While the various responses obtained from the survey, highlighted different aspects to the design of foundations on swelling clays, a consistent theme could however be identified. The general approach to the design of foundations on swelling clays in South Africa can be summarised as follows:

- Determine Atterberg limits, linear shrinkage and grading analyses.
  - These results provide a good *first estimate* of swell potential. However, it is sometimes the only laboratory testing conducted which is used together with empirical approaches as a criterion for design.

- *Swell followed by consolidation* tests are preferred to the indicator testing mentioned above, but are less commonly used. Reasoning for not doing such testing can be attributed to the added cost, but also due to the fact that soil heave may not be a governing aspect in design.
- *Swell under load* tests are sometimes performed whereby a predetermined stress (accounting for structural loading and any fill material) is applied prior to the swelling process.

The majority of respondents however highlighted the complexity of this soil type, emphasising limitations of the various laboratory testing offered. Exceptions to the general approach outlined above were presented by various respondents whereby the importance of initial void ratio and moisture content was emphasised and tested for, such that more rigorous empirical approaches could be utilised (e.g. Brackley (1975*a*)). Furthermore, one respondent stressed the importance of mineralogy, stating that indicator testing (Atterberg limits, linear shrinkage and grading analyses) can be misleading in this regard and not capture features that a swell under load test will, if carried out correctly. By merely considering the notorious difficulty of quantifying the clay fraction in a grading analysis (Stott et al., 2016) it can be seen that there may be limitations to only using the indicator testing mentioned above. Recognising "common practice" in the field of geotechnical engineering and the findings of this study, the following statements can be made:

- Empirical approaches such as Van der Merwe (1964), Jones (2017) and Brackley (1975*a*) predict a *trend* which is consistent with the centrifuge modelling conducted in this study.
- The three empirical approaches mentioned above were chosen out of the 5 presented in Section 3.4.6 and are preferred for the following reasons.
  - The approach presented by Weston (1980) is heavily dependent on the liquid limit of the soil. Small differences in this soil parameter can therefore result in substantial changes in the predicted heave. Such an approach should therefore be used cautiously. This limitation was discussed by Gaspar (2019).
  - In principle, the approach presented by Brackley (1980) is attractive since it accounts for soil suction which is a driving mechanism in the swelling of clays. It is however recognised that suction measurement is not readily available to practitioners. If measurement of suction is possible, the question of what a 'representative'

value of suction is still remains to be settled. While this concept was not investigated in this study, possible errors in heave prediction may result, depending on where the suction measurement is taken. If the measurement is taken on the outer portion of a specimen, which is likely to be drier than its centre, a dramatically high heave prediction may result. Conversely, suction measured on the inner (wetter) portion of a specimen may underpredict heave. Use of suction measurement to predict field heave therefore remains an area for further research.

  - Having mentioned the role of suction in swelling clays, it is important to emphasise that a soil with a high degree of saturation can still sustain high magnitudes of suction. From the various site investigations undertaken in this study, the average degree of saturation of this soil was approximately 93% (see Table 7). According to the soil water retention curve measured for undisturbed specimens, over a megapascal of suction is possible at this degree of saturation (see Figure 93).

- All commercially available oedometer testing relies on bringing the soil sample to a point of zero suction. As a result, any oedometer testing performed will predict the *upper limit* of heave or swell pressure (for a given initial void ratio and moisture content). The unavoidable seasonable variability in these initial soil parameters introduce another layer of complexity to the applicable testing methods. Such a result may however be desirable in cases where foundation movements are critical to design.

- The probability of a material reaching a point of zero suction is not one which can be addressed with a universally applicable answer. In the discussions had, factors were highlighted which can affect the likelihood of this occurrence, namely mineralogy, vegetation, etc. However, a factor which was not mentioned was that of soil fabric. While the effect of fabric is fairly widely acknowledged in the context of collapsible soils, it is also one which should be considered for swelling clays. The Extended Barcelona Basic Model (BExM) (Gens & Alonso, 1992) which provides a constitutive framework for expansive clays, recognises different fabric types in its formulation. Figure 116 highlights the two fabric types (for a more comprehensive review see Section 3.2.2).

  Fabric type A is representative of that tested in this study. In the centrifuge tests conducted, it was found that the point at which volumetric change became negligible (typically referred to as the point of zero suction in swell under load tests) was only achieved in the top clay layer (equivalent to 1.5 m at full scale). Furthermore, if the appropriate scaling laws are utilised, the equivalent time at full scale to achieve this magnitude of swell would equate to over 6 years of flooding. Such a situation may

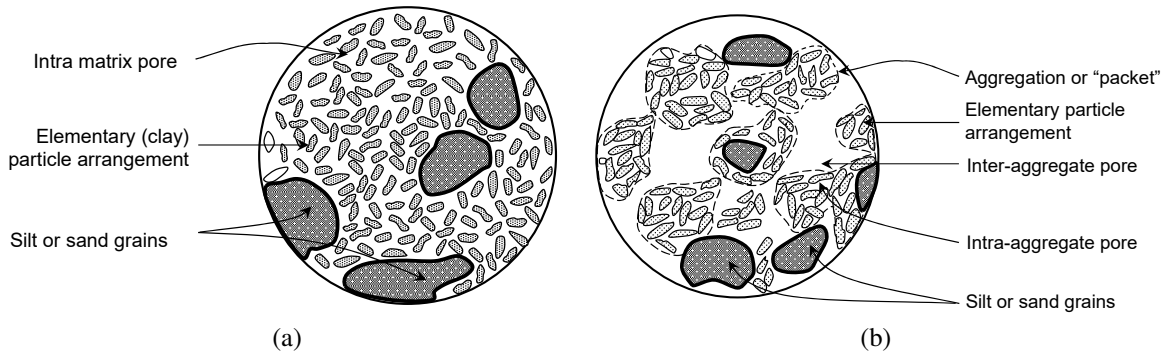

Figure 116: Fabric types for an expansive clay illustrating a) a microfabric predominantly consisting of a continuous matrix of elementary clay particles and b) a microfabric consisting of a number of 'packets' of elementary clay particles (after Gens & Alonso, 1992)

reasonably be regarded as unlikely, however, it cannot be stated that the same would apply for the comparatively open fabric illustrated by Fabric B. Additionally, a fabric type that is not dominated by a clay matrix but has a greater proportion of sand or silt particles will have a higher hydraulic conductivity, making the state of 'zero suction' more achievable in a shorter time frame.

The main purpose of the centrifuge modelling conducted in this study was to investigate the variation of pile pull-out (shaft) friction throughout a swelling process. It was found that shaft friction in swelling clays is governed by two counteracting mechanisms, namely lateral swell-induced pressure and soil softening. The overriding findings from this study on this principle are listed below.

- An increase in lateral pressure occurs initially (at relatively low values of swell) but is followed by a reduction in lateral pressure over time (at relatively high magnitudes of swell). The mechanism governing the reduction in lateral pressures can be attributed to the fact that over time, soil softening tends to dominate shaft capacity.
  - The implications of this finding are that if site testing is to be conducted to determine the shaft capacity after swell, the magnitude of swell at which the tests are performed must be specified. If the test is performed relatively early in the swell process, an increase in shaft capacity is likely to be measured. Conversely, a reduction in shaft capacity will likely be measured if the test is performed relatively late in the swell process.

- The second key finding of this study is that local increases in shaft capacity can be measured deeper in the profile, where confinement due to overburden stresses restrict swell in the vertical direction. For such cases, restriction of vertical swell can lead to an increase in lateral pressure against a pile at depth.
  - If shaft capacity is to be measured on short length piles (plugs), the position of the pile is important. Plugs installed close to the soil surface may experience a reduction in shaft capacity after the profile is wetted, while piles installed deeper may experience an increase in shaft capacity.

8.3.3 Concluding remarks

The purpose of this section was to interpret standard practice and testing methodologies available to industry, using insights gained from the more sophisticated testing methods offered by research institutions. The intention is that the concepts outlined can, together with the experience and judgement of practitioners, add to the understanding and practical dealings with this problem soil.

REFERENCES

Aitchison, G. D. (1960), Relationships of moisture stress and effective stress functions in unsaturated soils, *in* 'Conference on Pore Pressure and Suction in Soils', Butterworths, London.

Al Haj, K. (2013), Mechanical response of two plastic clay soils from Sudan, PhD thesis, Imperial College, University of London.

Al Haj, K. M. A. & Standing, J. R. (2015), 'Mechanical properties of two expansive clay soils from Sudan', *Géotechnique* **65**(4), 258–273.

Al Haj, K. M. A. & Standing, J. R. (2016), 'Soil water retention curves representing two tropical clay soils from Sudan', *Géotechnique* **66**(1), 71–84.

Alonso, E. E., Gens, A. & Josa, A. (1990), 'A constitutive model for partially saturated soils', *Géotechnique* **40**(3), 405–430.

Alonso, E. E., Vaunat, J. & Gens, A. (1999), 'Modelling the mechanical behaviour of expansive clays', *Engineering Geology* **54**, 173–183.

Armstrong, C. P. & Zornberg, J. G. (2017), Effect of Fabric on the Swelling Characteristics of Highly Plastic Clays, *in* '2nd Pan–American Conference on Unsaturated Soils', Dallas, Texas, pp. 28–37.

ASTM D4318–17e1 (2017), Standard Test Methods for Liquid Limit, Plastic Limit, and Plasticity Index of Soils, Technical report, ASTM International, West Conshohocken, P. A.

ASTM D4546–14 (2014), Standard Test Method for One-Dimensional Swell or Collapse of Soils, Technical report, ASTM International, West Conshohocken, P. A.

ASTM D5298–16 (2016), Standard Test Method for Measurement of Soil Potential (Suction) Using Filter Paper, Technical report, ASTM International, West Conshohocken, P. A.

ASTM D6836–16 (2016), Standard Test Methods for Determination of the Soil Water Characteristic Curve for Desorption Using Hanging Column, Pressure Extractor, Chilled Mirror Hygrometer, or Centrifuge, Technical report, ASTM International, West Conshohocken, P. A.

Atkinson, J. H. & Bransby, P. L. (1978), *The mechanics of soils. An introduction to critical state soils mechanics*, London : McGraw-Hill.

Bishop, A. W. (1959), The principle of effective stress, *in* 'Teknick Ukeblad', Vol. 39, pp. 859–863.

Bishop, A. W., Alpan, I., Blight, G. E. & Donald, I. B. (1960), Factors controlling the shear strength of partially saturated cohesive soils, *in* 'Proceedings and Discussion of the ASCE Research Conference on Shear Strength of Cohesive Soils', University of Colorado, Boulder, pp. 503–532 and 1027–1042.

Bishop, A. W. & Blight, G. E. (1963), 'Some aspects of effective stress in saturated and partly saturated soils', *Géotechnique* .

Blight, G. E. (1984*a*), Power Station Foundations in Deep Expansive Soil Power Station Foundations in Deep Expansive Soil, *in* 'First International Conference on Case Histories in Geotechnical Engineering', Missouri, pp. 77–86.

Blight, G. E. (1984*b*), Uplift Forces Measured in Piles in Expansive Clay, *in* 'Fifth International Conference on Expansive Soils', Adelaide, South Australia, pp. 240–244.

Bolt, G. H. (1956), 'Physico–Chemical Analysis of the Compressibility of Pure Clays', *Géotechnique* **4**(2), 86–93.

Bolton, M. D., Gui, M. W., Garnier, J., Corte, J. F., Bagge, G., Laue, J. & Renzi, R. (1999), 'Centrifuge cone penetration tests in sand', *Géotechnique* **49**(4), 543–552.

Bolzon, G., Schrefler, B. A. & Zienkiewicz, O. C. (1996), 'Elastoplastic soil constitutive laws generalized to partially saturated states', *Géotechnique* **46**(2), 279–289.

Booth, A. R. (1976), 'Compaction and Preparation of Soil Specimens for Oedometer Testing', *ASTM STP 599* pp. 216–228.

Brackley, I. J. A. (1975*a*), The interrelationship of the factors affecting heave of an expansive unsaturated soil, PhD thesis, University of Natal, Durban, South Africa.

Brackley, I. J. A. (1980), Prediction of soil heave from suction measuerments, *in* 'Proceedings of the 7th Regional Conference for Africa on Soil Mechanics and Foundation Engineering', Vol. 1, Accra, Ghana, pp. 159–166.

Brackley, I. J. A. (1983), The effects of density, moisture content and loading swelling of clays, Technical report, NHBRI.

Brackley, I. J. A. B. (1975*b*), A model of unsaturated clay structure and its application to swell behaviour, *in* 'Proceedings of the 6th African Regional Conference on Soil Mechanics and Foundation Engineering', Vol. 1, pp. 65–70.

Brackley, I. J. A. & Sanders, P. J. (1992), 'In situ measurement of total natural horizontal stresses in an expansive clay', *Géotechnique* **42**(3), 443–451.

BS 1377–8: 1990 (1990), Methods of test for soils for civil engineering purposes (Part 5), Technical report, British Standards Intisutuion.

BS EN 12390–13 (2013), Testing hardened concrete. Determination of secant modulus of elasticity in compression, Technical report, British Standards Institution.

BS EN 12390–3 (2019), Testing hardened concrete. Compressive strength of test specimens, Technical report, British Standards Institution.

BS EN 12390–6 (2009), Testing hardened concrete. Tensile splitting strength of test specimens, Technical report, British Standards Institution.

Burland, J. B. (1965), Some aspects of the mechanical behaviour of partly saturated soil, *in* 'Moisture equilibria and moisture changes in soils beneath covered areas; a symposium in print.', Butterworths, Guildford, pp. 270–278.

Burland, J. B. (1990), 'On the compressibility and shear strength of natural clays (30th Rankine Lecture)', *Géotechnique* **40**(3), 329–378.

Byrne, G., Chang, N. & Raju, V. (2019), *A Guide to Practical Geotechnical Engineering in Africa*, fifth Edition edn, FRANKI A KELLER COMPANY.

Caenn, R., Darley, H. C. H. & Gray, G. R. (2017), *Composition and Properties of Drilling and Completion Fluids*, Elsevier, chapter Chapter 4 Clay Mineralogy and the Colloid Chemistry of Drilling Fluids, pp. 93–134.

Caicedo, B., Medina, C. & Cacique, A. (2006), Validation of time scale factor of expansive soils in centrifuge modeling, *in* 'International Conference on Physical Modelling in Geotechnics 06', pp. 273–277.

Carey, T., Gavras, B., Kutter, B., Haigh, S. K., Madabushi, S. P. G., Okamura, M., Kim, D. S. Ueda, K., Hung, Y. G., Zhou, Y. G., Liu, K., Chen, Y. M., Zeghal, M., Abdoun, T., Escoffier, S. & Manzari, M. (2014), A new shared miniature cone penetrometer for centrifuge testing, *in* 'Proceedings of the 9th International conference on Physical Modelling in Geotechnics'.

Cassagrande, A. (1936), Determination of the preconsolidation load and its practical significance, *in* 'Proceedingsof the International Conference on Soil Mechanics and Foundation Engineering', Vol. 3, Cambridge, MA, Harvard University, pp. 60–64.

Chandler, R. J. & Gutierrez, C. I. (1986), 'The filter paper methodof suction measurement', *Géotechnique* **36**(2), 265–268.

Chapman, D. L. (1913), 'A contribution to the theory of electro–capillarity', *Philosophical magazine* **25**, 475–481.

Charlie, W. A., Osman, M. A. & Elfatih, M. A. (1985), 'Construction on expansive soils in Sudan', *Journal of Construction Engineering and Managemnet* **110**(3), 359–374.

Chen, T., Zhou, C., Wang, G., Liu, E. & Dai, F. (2017), 'Centrifuge Model Test on Unsaturated Expansive Soil Slopes with Cyclic Wetting–Drying and Inundation at the Slope Toe', *International Journal of Civil Engineering* .

Clayton, C. R. I., Matthews, M. C. & Simons, N. E. (1995), *Site investigation*, Oxford Wiley-Blackwell.

Collins, K. (1984), Characterisation of expansive soil microfabric, *in* 'Proceedings of the 5th International Conference on Expansive Soils', Adelaide, pp. 37–43.

Colmenares, J. E. (2002), Suction and volume changes of compacted sand–bentonite mixtures, PhD thesis, Imperial College, University of London.

Croney, D., Coleman, J. D. & Black, W. P. M. (1958), Movement and distribution of water in soil in relation to highway design and performance, *in* 'Proceedings of the Thirty-Seventh Annual Meeting of the Highway Research Board'.

Day, P. (2017), Challenges and shortcomings in geotechnical engineering practice in the context of a developing country (Terzaghi Oration), *in* 'Proceedings of the 19th International Conference on Soil Mechanics and Geotechnical Engineering', Seoul, pp. 11–34.

Day, P. (2020), 'Personal communication'.

Day, P. W. (2013), A contribution to the advancement of geotechnical engineering in South Africa, PhD thesis, Stellenbosch University.

Delage, P., Vicol, T. & Suraj de Silva, G. P. R. (1992), Suction controlled testing of non saturated soils with an osmotic consolidometer, *in* 'Proceedings of the 7th Iinternational Conference on Expansive Soils', Dallas, pp. 206–211.

Dhowian, A. W. (1990), 'Field performance of expansive shale formation', *Journal of King Abdulaziz University (Engineering Sciences)* **2**, 165–182.

Dineen, K. (1997), The influence of soil suction on compressibility and swelling, PhD thesis, Imperial College, University of London.

Dineen, K. & Burland, J. B. (1995), A new approach to osmotically controlled oedometer testing, *in* E. E. Alonso & P. Delage, eds, 'Unsaturated Soils: Proceedings of the 1st International Conference on Unsaturated Soils', pp. 459–465.

Dudley, J. H. (1970), 'Review of Collapsing Soils', *Journal of the Soil Mechanics and Foundations Division – ASCE* **96**(3), 925–947.

Elsharief, A. (2012), Foundations on Expansive Soils, Sudan Experience, *in* 'Graduate School Conference, on Basic Sciences and Engineering, University of Khartoum'.

Elsharief, A. M., Ahmed, E. O. & Mohamedzein, Y. E. A. (2007), Guidelines for the Design of Bored Concrete Piles in Expansive Soils of Sudan, *in* 'Graduate School Conference, on Basic Sciences and Engineering, University of Khartoum'.

Ferrari, A., Manca, D. & Laloui, L. (2018), Hydro-chemo-mechanical behavior of a sand/bentonite mixture upon wetting paths, *in* 'Proceedings of the 7th International Conference on Unsaturtaed Soils', Hong Kong.

Fleming, K., Weltman, A., Randolph, M. & Elson, K. (2009), *Piling Engineering*, third edn, Taylor & Francis.

Fourie, A. B. (1991), Lateral swelling pressure developed in an active clay, *in* G. E. Blight, A. B. Fourie, I. Luker, D. J. Mouton & R. J. Scheurenberg, eds, 'Geotechnics in the African Environment', Vol. 1, Balkema, Rotterdam, Maseru, Lesotho, pp. 267–274.

Fredlund, D. G. (1983), Prediction of ground movements in swelling clays, *in* '31st Annual Soil Mechanics and Found Engineering Conference', University of Minnesota, Minneapolis.

Fredlund, D. G. (1996), The emergence of unsaturated soil mechanics, *in* 'The Fourth Spencer Buchanan Lecture'.

Fredlund, D. G. (2000), The implementation of unsaturated soil mechanics into geotechnical engineering, *in* 'The R.M. Hardy Lecture'.

Fredlund, D. G. (2018), Role of the soil–water characteristic curve in unsaturated soil mechanics, *in* 'The 7th International Conference on Unsaturated Soils', Hong Kong.

Fredlund, D. G. (2019), Determination of unsaturated soil property functions for engineering practice-17th Jennings Lecture, *in* 'The 17th African Regional Conference on Soil Mechanics and Geotechnical Engineering'.

Fredlund, D. G. & Morgenstern, N. R. (1977), 'Stress State Variables for Saturated and Unsaturated Soils', *Journal of Geotechnical Engineering Division* **103**, 447–466.

Fredlund, D. G. & Rahardjo, H. (1993), *Soil Mechanics for Unsaturated Soils*, John Wiley & Sons, Inc.

Fredlund, D. G., Rahardjo, H. & Fredlund, M. D. (2012), *Unsaturated Soil Mechanics in Engineering Practice*, John Wiley & Sons, INC.

Fredlund, D. G. & Xing, A. (1994), 'Equations for the soil-water characteristic curve', *Canadian Geotechnical Journal* **31**(6), 521–532.

Gardner, R. (1937), 'A method of measuring the capillary tension of soil moisture over a widemoisture range', *Soil Science* **43**(4), 227–284.

Gaspar, T. A. V. (2019), A comparison of swell prediction methods to centrifuge testing, *in* '7th African Young Geotechnical Engineers Conference'.

Gaspar, T. A. V., Jacobsz, S. W., Schultz-Poblete, M. V. & Toll, D. G. (2019*a*), Measurement of the soil water retention curve: practical considerations, *in* 'Proceedings of the 17th African Regional Conference on Soil Mechanics and Geotechnical Engineering', Cape Town, South Africa.

Gaspar, T. A. V., Jacobsz, S. W., Smit, G. & Osman, A. S. (2019*b*), An expansive clay for centrifuge modelling, *in* 'XVII European Conference on Soil Mechanics and Geotechnical Engineering', Reykjavik, Iceland.

Gens, A. (2007), 'Soil - environment interactions in geotechnical engineering (47th Rankine Lecture)', *Géotechnique* **60**(1), 3–74.

Gens, A. & Alonso, E. E. (1992), 'A framework for the behaviour of unsaturated expansive clays', *Canadian Geotechnical Journal* **29**(6), 1013–1032.

Gens, A., Vallejan, B., Sanchez, M., Imbert, C., Villars, M. V. & Van Geet, M. (2011), 'Hydromechanical behaviour of a heterogeneous compacted soil: experimental observations and modelling', *Géotechnique* **61**(5), 367–386.

Ghiadistri, G. M., Potts, D. M., Zdravković, L. & Tsiampousi, A. (2018), A new double structure model for expansive clays, *in* 'Proceedings of the 7th International Conference on Unsaturtaed Soils', Hong Kong.

Gouy, G. (1910), 'Sur la constitution de la charge electrique à la surace d'un électrolyte', *Physique* **9**, 457–468.

Gouy, G. (1917), 'Sur la fonction electrocapilaire', *Annales de Physique (Paris)* **Série 9**(7), 129–184.

Gu, X. W., Zhang, W. M. & Xu, G. U. (2010), Earth pressure at rest of expansive soil against retaining wall, *in* S. Springman, J. Laue & L. Seward, eds, 'Proceedings of the 7th International Conference on Physical Modelling in Geotechnics (ICPMG 2010)', Zurich, Switzerland, pp. 443–448.

Hamblin, A. P. (1981), 'Filter paper method for the routine measurementof field water potential', *Journal of Hydrology* **53**, 355–360.

Haut, B. B. K. & Toll, D. G. (2012), Introduction, *in* B. B. K. Huat, D. G. Toll & A. Prasad, eds, 'Handbook of Tropical Residual Soils Engineering', Taylor & Francis, chapter 1, pp. 2–20.

Heymann, G. & Clayton, C. R. I. (1999), Block sampling of soil: Some practical considerations, *in* G. R. Wardle, G. E. Blight & A. Fourie, eds, 'Geotechnics for Developing Africa', Balkema/Rotterdam/Brookfield, Durban, pp. 331–339.

Hoek, E. (2020), 'Personal communication'.

Hofmann, U., Endell, K. & Wilm, O. (1933), 'Kristalstructur und quellung von motmorillonit', *Z. Krist* .

Holtz, G. W. & Gibbs, H. J. (1956), 'Engineering Properties of Expansive Clays', *Transactions of the American Society of Civil Engineers* **121**(1), 641–663.

Holtz, R. D. & Kovacs, W. D. (1981), *An Introduction to Geotechnical Engineering*, Prentice–Hall, Inc.

Hvorslev, M. J. (1937), Uber die Festigkeitseigenschaften Gestorter Bindiger Boden, PhD thesis, Ingeniorvidenskabelige Skrifter.

Jacobsz, S. W. (2002), The effects of tunnelling on piled foundations, PhD thesis, University of Cambridge September.

Jacobsz, S. W. (2018), Low-cost tensiometers for geotechnical applications, *in* 'Proceedings 9th International Conference on Physical Modelling in Geotechnics', Boca Raton, FL: CRC Press, London, pp. 305–310.

Jacobsz, S. W. (2019), 'TUKS tensiometer measures to –1.7 Mega Pascal', *Civil Engineering* **27**(1), 24–26.

Jacobsz, S. W. & Day, P. (2008), 'Are we getting what we pay for from geotechnical engineering laboratories?', *Civil Engineering* pp. 8–11.

Jacobsz, S. W., Kearsley, E. P. & Kock, J. H. L. (2014), The geotechnical centrifuge facility at the University of Pretoria, *in* C. Gaudin & D. White, eds, 'Physical modelling in Geotechnics: Proceedings 8th ICPMG', CRC Press, pp. 169–174.

Jardine, R. J. (1985), Investigation of pile–soil behaviour with special reference to the foundations of offshore structures, PhD thesis, Imperial College, London.

Jennings, J. E. B. (1957), Discussion on M. S. Youssef's Paper, *in* 'Proceedings of the 4th International Conference on Soil Mechanics and Foundation Engineering'.

Jennings, J. E. B. & Burland, J. (1962), 'Limitations to the use of effective stresses in partly saturated soils', *Géotechnique* **12**(2), 125–144.

Jennings, J. E. B., Firth, R. A., Ralph, T. K. & Nagar, N. (1973), An improved method for predicting heave using the oedometer test, *in* 'Proceedings of the 3rd International Conference on Expansive Soils', Vol. 2, Haifa, pp. 149–154.

Jennings, J. E. B. & Knight, H. (1975), A guide to construction on or with materials exhibiting additional settlement due to 'collapse' of grain structure, *in* 'Proceedings of the 6th Regional C for Africa on Soil Mechanics & Foundatin Engineering', Durban, pp. 99–105.

Jennings, J. E. B. & Knight, K. (1957), The Prediction of Total Heave from the Double Oedometer Test, *in* 'First Symposium on Expansive Clays', Vol. 1, pp. 285–291.

Jennings, J. E. & Kerrich, J. E. (1962), 'The heaving of buildings and the associated economic consequences with particular reference to the Orange Free State Goldfields', *The Civil Engineer in South Africa* **4**(11), 221–248.

Jones, D. E. & Holtz, W. G. (1973), 'Expansive soils-The hidden disaster', *Civil Engineering, ASCE* **43**(8), 49–51.

Jones, G. (2017), 'An empirical preliminary prediction of heave', *Journal of the South African Institution of Civil Engineering* **59**(4), 64–66.

Jones, G. A., Meintjes, H. A. C. Aucamp, J. P. & Dutchman, J. R. (2016), A case study of heave due to flooding, *in* 'Proceedings of the 1st Southern African Geotechnical Conference', Sun City, pp. 221–228.

Jones, H. E. & Kohnke, H. (1952), The influence of soil moisture tension on vapour movement of soil water, *in* 'Proc. Soil Science Soc. America', pp. 245–248.

Jones, L. D. & Jefferson, I. (2012), *Expansive clays*, ICE Publishing, chapter 5, pp. 413–441.

Josa, A., Alonso, E. E., Lloret, A. & Gens, A. (1987), Stress – strain behaviour of partially saturated soils, *in* 'Proceedings of the 9th European Conference on Soil Mechanics and Foundation Engineering', Dublin, pp. 561–564.

Justo, J. L., Delgado, A. & Ruiz, J. (1984), The Influence of Stress-path in Collapse-swelling of Soils at the Laboratory, *in* 'Fifth International Conference on Expansive Soils', Adelaide, South Australia.

Karagoly, Y., Tripathy, S., Cleall, P. J. & Mahdi, T. (2018), Suction measurements by a fixed-matrix porous ceramic disc sensor, *in* 'The 7th International Conference on Unsaturated Soils'.

Kassif, G. & Zeitlen, J. G. (1962), 'Behavior of Pipes Buried in Expansive Clays', *Journal of the Soil Mechanics and Foundations Division* **88**(2), 466–148.

Katti, R., Bhangale, E. S. & Moza, K. K. (1983), Lateral pressure in expansive soil with and without a cohesive non-swelling soil layer : application to earth pressures on cross drainage structures in canals and key walls in dams. Part 1, Technical report, Central Board of Irrigation and Power.

Khalili, N. & Khabbaz, M. H. (1998), 'A unique relationship for χ for the determination of shear strength of unsaturated soils', *Géotechnique* **48**(5), 681–688.

Kim, J. H., Kim, H. Y., Lee, Y. W., Choo, D. S. & Kim, D. J. (2014), Miniature cone tip resistance on silty sand in centrifuge model tests, *in* 'Proceedings of the 8th International conference on Physical Modelling in Geotechnics', Australia, Perth.

Kim, T. & Hwang, C. (2003), 'Modeling of tensile strength on moist granular earth material at low water content', *Engineering Geology* **69**(3–4), 233–244.

Kjellander, R. (1991), Electrostatic ion-ion correlation forces, a possible mechanism for restricted calcium–clay swelling, *in* 'Proceedings, NATO Advanced Research Workshop on Clay Swelling and Expansive Soils', Cornell, Ithaca, N. Y.

Knappet, J. A. & Craig, R. F. (2012), *Craig's Soil Mechanics*, Spoon Press an imprint of Taylor & Francis.

Komornik, A. & Zeitlen, J. G. (1965), An Apparatus for Measuring Lateral Soil Swelling Pressure in the Laboratory, *in* 'Proceedings of the 6th International Conference of Soil Mechanics and Foundation Engineering', Vol. 1, Montreal, Canada, pp. 278–281.

Laporte, S., Siemens, G. A. & Beddoe, R. A. (2018), Physical modelling of roads in expansive clay subjected towetting–drying cycles, *in* A. McNamara, S. Divall, R. Goodey, N. Taylor, S. Stallebrass & J. Panchal, eds, 'Proceedings of the 9th International Conference on Physical Modelling in Geotechnics (ICPMG 2018)', London, United Kingdom, pp. 175–178.

Leroueil, S. & Vaughan, P. R. (1990), 'The general and congruent effects of structure in natural soils and weak rocks', *Géotechnique* **41**(2), 281–284.

Li, J., Cameron, D. & Ren, G. (2014), 'Case study and back analysis of a residential building damaged by expansive soils', *Computers and Geotechnics* **56**, 89–99.

Liu, G., Toll, D. G., Kong, L. & Asquith, J. D. (2020), 'Matric Suction and Volume Characteristics of Compacted Clay Soil under Drying and Wetting Cycles', *Geotechnical Testing Journal* **43**(2), 464–479.

Liu, Y. & Vanapalli, S. K. (2007), 'Influence of Lateral Swelling Pressure on the Geotechnical Infrastructure in Expansive Soils', *Journal of Geotechnical and Geoenvironmental Engineering ASCE* **143**(6), 1–19.

Lourenço, S. D. N., Gallipoli, D., Toll, D. G. & Evans, F. D. (2006), 'Development of a commercial tensiometer for tri-axial testing of unsaturated soils', *Geotechnical Special Publication, 147. American Society of Civil Engineers* pp. 1875–1886.

Louw, H., Kearsley, E. P. & Jacobsz, S. W. (in review), 'Modelling horizontally loaded piles in a geotechnical centrifuge', *International Journal of Physical Modelling in Geotechnics* .

Low, P. F. (1980), 'Soil Science Society of America Journal', *The swelling of clay. 11. Montmorillonites* **44**, 667–676.

Lu, N. & Likos, W. (2004), *Unsaturated soil mechanics*, John Wiley & Sons, Inc., Hoboken, New Jersey.

Madabhushi, G. (2015), *Centrifuge Modelling for Civil Engineers*, Taylor & Francis Group.

Manca, D., Ferrari, A. & Laloui, L. (2016), 'Fabric evolution and the related swelling behaviour ofa sand/bentonite mixture upon hydro-chemo-mechanical loadings', *Géotechnique* **66**(1), 41–57.

Mantikos, V., Tsiampousi, A. & Standing, J. R. (2018), Swelling behaviour of an expansive clay at high suction, *in* 'Proceedings of the 7th International Conference on Unsaturtaed Soils', Hong Kong.

McGown, A. & Collins, K. (1975), The microfabrics of some expansive and collapsing soils, *in* 'Proceedings of the 5th Pan–American Conference on Soil Mechanics and Foundation Engineering', Vol. 1, Buenos Aires, pp. 323–332.

Meintjes, H. A. C. (1991), A case history on heaving clay: Colinda Primary School, *in* G. E. Blight, A. B. Fourie, I. Luker, D. J. Mouton & R. J. Scheurenberg, eds, 'Geotechnics in the African Environment', Balkema, Rotterdam, Maseru, Lesotho, pp. 99–104.

Meintjes, H. A. C. & Pellissier, J. P. (1994), An experimental pile in deep residual expansive clay, *in* 'Proceedings of the 13th International Conference on Soil Mechanics and Foundations Engineering', New Dehli, India, pp. 487–492.

Metergroup (2017*a*), 'Teros 21. user manual'.

Metergroup (2017*b*), 'WP4C Dew Point PotentiaMeterOperator's Manual'.

Miao, L., Wang, F., Cui, Y. & Shi, S. B. (2012), Hydraulic characteristics, strength of cyclic wetting-drying and constitutive model of expansive soils, *in* 'Proceedings of the 4th International Conference on Problematic Soils', Wuhan, China, pp. 303–322.

Mitchell, J. K. (1976), *Fundamentals of soil behaviour*, John Wiley & Sons, Inc.

Mitchell, J. K. & Soga, K. (2005), *Fundementals of soil behaviour*, John Wiley & Sons.

Monroy, R. (2005), The Influence of Load and Suction Changes one the Volumetric Behaviour of Compacted London Clay, PhD thesis, Imperial College, University of London.

Monroy, R., Zdravkovic, L. & Ridley, A. M. (2015), 'Mechanical behaviour of unsaturated expansive clay under K_0 conditions', *Engineering Geology* **197**.

Morin, W. (1971), Properties of African tropical black clay soils, *in* 'Proceedings of the 5th regional conference for Africa on soil mechanics and foundation engineering', Vol. 2 of *1*, Angola, pp. 46–54.

Moses, A. M. (2008), Mineralogy, Chemistry and Pedological Investigations of the Maandaagshoek 254 kt's Palygorskite deposit: Implication on the Genesis and Industrial Application, Technical report, University of Pretoria.

Nagaraj, T. S. & Srinivasa Murthy, B. R. (1986), 'A critical reappraisal of compression index equations', *Géotechnique* **36**(1), 27–32.

Nelson, J. D. & Miller, D. J. (1992), *Problems and Practice in Foundation and Pavement Engineering*, John Wiley & Sons.

Nelson, J. D., Reichler, D. K. & Cumbers, J. M. (2006), Parameters for heave prediction by oedometer tests, *in* 'Proceedings of the 4th International Conference on Unsaturated Soils', Carefree, Arizona, pp. 951–961.

Offer, Z. & Blight, G. E. (1985), 'Measurement of Swelling Pressure in the Laboratory and In Situ', *Transporation Research Record* (1032), 15–22.

Olson, R. E. & Mesri, G. (1970), 'Mechanisms controlling the compressibility of clay', *ASCE Journal of the Soil Mechanics and Foundations Division* **96(SM6)**, 1863–1878.

Pellissier, J. P. (1991), Piles in deep residual clays, *in* G. E. Blight, A. B. Fourie, I. Luker, D. J. Mouton & R. J. Scheurenberg, eds, 'Geotechnics in the African Environment', Balkema, Rotterdam, Maseru, Lesotho, pp. 31–39.

Pellissier, J. P. (1997), A raft design method for swelling clay, *in* 'Proceedings of the 14th International Conference on Soil Mechanics and Foundations Engineering', Hamberg, Germany, pp. 863–869.

Plaisted, M. D. & Zornberg, J. G. (2010), Testing of an expansive clay in a centrifuge permeameter, *in* S. Springman, J. Laue & L. Seward, eds, 'Proceedings of the 7th International Conference on Physical Modelling in Geotechnics (ICPMG 2010)', Zurich, Switzerland, pp. 1477–1481.

Plaisted, M. D. & Zornberg, J. G. (2011), Testing of Expansive Clays in a Centrifuge Permeameter, *in* 'Pan–Am CGS Geotechnical Conference'.

Poorooshasb, H. B. & Roscoe, K. H. (1961), The correlation of the results of shear tests with varying decrees of dilatation, *in* 'Proceedings of the 5th International Conference on Soil Mechanics and Foundation Engineering', Paris, pp. 297–304.

Puppala, A. J. & Cerato, A. B. (2009), 'Heave Distress Problems in Chemically Treated Sulfate–Laden Materials', *GeoStrata* **10**(2), 28–32.

Radcliffe, D. & Šimůnek, J. (2010), *Soil Physics with HYDRUS: Modelling and Applications*, Taylor & Francis.

Richards, B. G. & Kurzeme, M. (1973), 'Observations of earth pressure on a retaining wall at the Gouger street Mail Exchange', *Australian Geomechanics Journal* **G3**(N1), 21–26.

Robertson, A. & Wagener, F. (1975), Lateral swelling pressures in active clay, *in* 'Proceedings of the 6th African Regional Conference on Soil Mechanics and Foundation Engineering', Vol. 1, Durban, pp. 107–114.

Romero, E. & Simms, P. H. (2008), 'Microstructure investigation in unsaturated soils: A review with special attention to contribution of mercury intrusion porosimetry and environmental scanning electron microscopy', *Geotechnical and Geological Engineering* pp. 705—-727.

Roscoe, K. H. & Burland, J. B. (1968), On the generalized stress–strain behavior of wet clay, *in* 'Engineering Plasticity', Cambridge University Press, Cambridge, England, pp. 535–609.

Roscoe, K. H. & Poorooshasb, H. B. (1963), 'A theoretical and experimental study of strains in triaxial compression tests on normally consolidated clays.', *Géotechnique* **13**(1), 12–38.

Roscoe, K. H., Schofield, A. N. & Wroth, C. P. (1958), 'On The Yielding of Soils', *Géotechnique* **8**(1), 22–53.

Roscoe, K. H., Schofield, M. A. & Thurairaj, A. (1965), 'Yielding of Clays in States Wetter Than Critical', *Géotechnique* **13**(3), 211–240.

Rust, E., Heymann, G. & Gary, J. (2005), 'Collapse potential of partly saturated sandy soils from Mozal, Mozambique', *Journal of the South African Intitution of Civil Engineering* **47**(1), 8–14.

Sánchez, M., Gens, A., Guimarães, L. & Olivella, S. (2005), 'A double structure generalized plasticity model for expansive materials', *International journal for numerical and analytical methods in geomechanics* **29**, 751–787.

Schnaid, F. & Haut, B. B. K. (2012), ampling and testing of tropical residual soils, *in* B. B. K. Huat, D. G. Toll & A. Prasad, eds, 'Handbook of Tropical Residual Soils Engineering', Taylor & Francis, chapter 3 S, pp. 67–115.

Schofield, A. N. (1980), 'Cambridge Geotechnical Centrifuge Operations (20th Rankine Lecture)', *Géotechnique* **30**(3), 227–268.

Schofield, A. & Wroth, P. (1968), *Critical State Soil Mechanics*, McGraw Hill.

Schreiner, D. & Burland, J. B. (1987), Stress Paths during Swelling of Compacted Soils under Controlled Suction, *in* 'Proceedings of the 6th International Conference on Expansive Soils', New Dehli, India, pp. 155—159.

Schreiner, H. D. (1988*a*), The use of predictive methods in expansive soil engineering, *in* '9th Regional Conference for Africa on Soil Mechanics and Foundation Engineering', Lagos, pp. 135–141.

Schreiner, H. D. (1988*b*), Volume Change of Compacted Highly Plastic African Clays, PhD thesis, Imperial College London.

Schreiner, H. D. & Burland, J. B. (1991), A comparison of three swell test procedures, *in* G. E. Blight, A. B. Fourie, I. Luker, D. J. Mouton & R. J. Scheurenberg, eds, 'Geotechnics in the African Environment', Balkema, Rotterdam, Maseru, Lesotho, pp. 259–266.

Schubert, H. (1975), 'Tensile Strength of Agglomerates', *Powder Technology* **11**(4), 107–119.

Schwartz, K. (1985), 'Problem Soils in South Africa – State of the Art', *The Civil Engineer in South Africa* **27**(7).

Shackel, B. (1970), 'The compaction of uniform, replicate soil specimens', *Australian Road Research Board* **4**(5), 12–31.

Smit, G., Gaspar, T. A. V., Jacobsz, S. W. & Osman, A. S. (2019), Centrifuge modelling of pile pull-out tests in expansive soil, *in* 'XVII European Conference on Soil Mechanics and Geotechnical Engineering', Reykjavik, Iceland.

Som, N. N. (1968), The effects of stress path on the deformation and consolidation of London Clay, PhD thesis, Imperial College, London.

Sophocleous, M. (2010), 'Understanding and explaining surface tension and capillarity: an introduction to fundamental physics for water professionals.', *Hydrogeology Journal* **18**(4), 811–821.

Sparks, D. & Pigeon, T. (2011), 'Simplifying expansion of clays', *Civil Engineering* pp. 30–36.

Sridharan, A. & Jayadeva, M. S. (1982), 'Double layer theory and compressibility of clays', *Géotechnique* **32**, 133–144.

Sridharan, A., Rao, A. S. & Puvvadi, V. S. (1986), 'Swelling Pressure of Clays', *Geotechnical Testing Journal* **9**(1), 24–33.

Sridharan, A. & Rao, G. V. (1973), 'Mechanisms controlling volume change of saturated clays and the role of the effective stress concept', *Géotechnique* .

Standing, J. R. (2012), 'The Development of Unsaturated Soil Mechanics at Imperial College, London', *Geotechnical Engineering Journal of the SEAGS & AGSSEA* **43**(1).

Stott, P. R., Monye, P. K. & Theron, E. (2016), Assessment of reliability of the hydrometer by examination of sediment, *in* S. W. Jacobsz, ed., 'Proceedings of the first Southern African Geotechnical Conference', Sun City, South Africa, pp. 281–286.

Sullivan, R. A. & McClelland, B. (1969), Predicting Heave of Buildings on Unsaturated Clay, *in* 'Proceedings of the 2_{nd} International Conference on Expansive Soils', Texas A&M University Press,, College Station, pp. 404–420.

Templer, C. F. (1957), Notes on the Design of Structures Founded on Heaving Soil, *in* 'First Symposium on Expansive Clays', pp. 387–392.

Terzaghi, K. (1936), The shearing resistance of saturated soil and the angle between the planes of shear., *in* 'Proceedings of the First International Conference for Soil Mechanics and Foundation Engineering', Harvard, Massachusetts, pp. 313–359.

Thorne, C. P. (1984), 'Strength assessment and stability analyses for fissured clays', *Géotechnique* **34**(3), 305–322.

Toll, D. G. (2012), The behaviour of unsaturated soil, *in* B. B. K. Huat, D. G. Toll & A. Prasad, eds, 'Handbook of Tropical Residual Soils Engineering', Taylor & Francis, chapter 4, pp. 119–145.

Toll, D. G., Fraser, A., Asquith, J., Hassan, A., Liu, G., Lourenço, J., Mendes, J., Noguchi, P., Osinki, P. & Stirling, R. (2015), Tensiometer techniques for determining soil water retention curves, *in* 'Asia-Pacific Conference on Unsaturated Soil', Guilin, China.

Toll, D. G. & Rahman, Z. A. (2010), Engineering Behaviour of Unsaturated Structured Soils, *in* '3rd International Conference on PROBLEMATIC SOILS', Adelaide, Australia.

Tripathy, S., Al-Khyat, S., Cleall, P. J., Baille, W. & Schanz, T. (2016), 'Soil Suction Measurement of Unsaturated Soils with a Sensor Using Fixed-Matrix Porous Ceramic Discs', *Indian Geotechnical Journal* **46**(3), 252–260.

Tripathy, S., Sridharan, A. & Schanz, T. (2004), 'Swelling pressures of compacted bentonites from diffuse double layer theory', *Canadian Geotechnical Journal* **41**(3), 437–450.

Van der Merwe, D. (1964), 'The prediction of heave from the plasticity index and percentage clay fraction of soils', *The Civil Engineer* pp. 103–107.

Van Genuchten, M. T. (1980), 'A closed-form equation for predicting the hydraulic conductivity of unsaturated soils.', *Soil Science Society of America Journal* **4**, 892–898.

Vanapalli, S. (2012), 'A state-of-the art review of 1-D heave prediction methods for expansive soils', *International Journal of Geotechnical Engineering* **6**, 15–41.

Verwey, E. J. W. & Overbeek, J. T. (1948), *Theory of the Stability of Lyophobic Colloids*, Elsevier, New York.

Weston, D. J. (1980), Expansive roadbed treatment for Southern Africa, *in* 'Proceedings of the 3rd International Research and Engineering Conference on Expansive Clays', Vol. 1, Denver, CO, pp. 339–360.

Whitman, R. V., Roberts, J. E. & Man, S. (1960), One Dimensional Compression and Wave Velocity Tests, and Responses of Soil to Dynamic Loads, Report 4, Publ. 106, Technical report, Soil Engineering Division, Department of Civil and Sanitary Engineering, Massachusetts Institute of Technology.

Williams, A. A. B. (1991), The extraordinary effect of chemical heaving and its effect on buildings and roads, *in* G. E. Blight, A. B. Fourie, I. Luker, D. J. Mouton & R. J. Scheurenberg, eds, 'Geotechnics in the African Environment', Balkema, Rotterdam, Maseru, Lesotho, pp. 91–98.

Williams, A. A. B., Pidgeon, J. T. & Day, P. W. (1985), 'Problem Soils in South Africa - State of the Art', *The Civil Engineer* **27**(7).

Ye, W. M., Zhang, Z., Wang, Q. & Chen, Y. G. (2018), Investigation on the swelling pressure of compacted gmz01 bentonitepellets/powder mixtures, *in* 'Proceedings of the 7th International Conference on Unsaturtaed Soils', Hong Kong.

Yong, R. N., Japp, R. D. & How, G. (1971), Shear strength of partially saturated clays, *in* 'Proceedings, 4th Asian Regional Conference on Soil Mechanics and Foundations Engineering', Vol. 2, pp. 183–187.

Yong, R. N., Sadana, M. L. & Gohl, W. B. (1984), A particle interaction model for assessment of swelling of an expansive soil, *in* 'Proceedings of the 5th International Conference on Expansive Soils', Adelaide, pp. 183–187.

Yong, R. N. & Warkentin, B. P. (1975), *Soil Properties and Behavior*, Elsevier.

Zhou, Y. G., Liang, T., Chen, Y. M. amd Ling, D. S., Kong, L. G., Shamoto, Y. & Ishikawa, A. (2014), A two–dimensional miniature cone penetration test system for centrifuge modelling, *in* 'Proceedings of the 8th International conference on Physical Modelling in Geotechnics', Australia, Perth.

Zornberg, J. G. & McCartney, J. S. (2010), 'Centrifuge Permeameter for Unsaturated Soils.I: Theoretical Basis and Experimental Developments', *Journal of Geotechnical and Environmental Engineering* **136**(8), 1051–1063.